IEA ADVANCED SOLAR ENERGY SYSTEMS

INTERNATIONAL ENERGY AGENCY
Solar Heating & Cooling Programme

Dynamic Testing of Active Solar Heating Systems

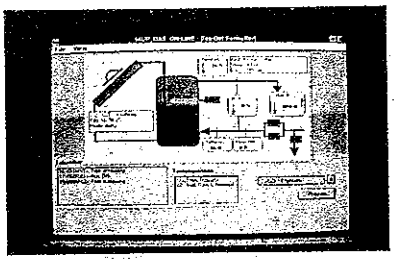

Final Report of the Task 14
Dynamic Component and
System Testing Subtask

Volume A
Dynamic Collector Testing
Component Testing and System Simulation of Small Solar Heating Systems
In Situ Testing of Large Solar Heating Systems

IEA Report no. T.14.DCST.1A

Dynamic Testing of Active Solar Heating Systems

Final Report of the Task 14 Dynamic Component and System Testing Subtask

Volume A

Dynamic Collector Testing

Component Testing and System Simulation of Small Solar Heating Systems

In Situ Testing of Large Solar Heating Systems

Summaries by:
Per Isakson
Thomas Pauschinger
Bengt Perers

Edited by:
Huib Visser
Thomas Pauschinger

April 1997

INTERNATIONAL ENERGY AGENCY
Solar Heating & Cooling Programme

The DCST Subtask Final Report "Dynamic Testing of Active Solar Heating Systems" consists of two Volumes which are distributed together. This Volume A has IEA no. T14.DCST.1.A.

The report is available under number 96-BBI-R0876/526.6.3573 from:

TNO Building and Construction Research
P.O. Box 49, NL-2600 AA Delft
The Netherlands

The cost of the two Volumes amounts to approximately US$60.- excl. VAT and mailing costs.

Information on the status and availability of the standards and matching software tools mentioned in this report can be obtained from:

Secretariat ISO / TC 180
Standards Australia
c/o Mr. M. Maffuci
1 The Crescent, Homebush 2140 NSW
Australia

and:

Secretarial CEN / TC 312
Centre for Renewable Energy Sources
c/o Mrs. E. Nicolinacou
19th km Marathonos Ave
GR-19009 Pikermi
Greece

CONTENTS OF VOLUME A OF THE DCST SUBTASK FINAL REPORT

EXECUTIVE SUMMARY

Objectives and scope

Dynamic testing has grown into a sound method for performance characterization of solar energy components and systems. The power of dynamic data processing was demonstrated before for solar domestic hot water systems. Now, further experience has been gained for solar collectors and heat stores, both small and large in size, for outdoor laboratory tests and in situ measurements. Data processing been evaluated and test procedures for reliable and accurate performance characterization, including prediction, have been designed. This report describes experiences of the participants in the Subtask on Dynamic Component and System Testing (DCST) within Task 14 of the International Energy Agency's Solar Heating and Cooling Programme.

Work was carried out in three Groups:

I. on Dynamic Collector Testing (DCT);

II. on Dynamic System Testing (DST) of solar domestic hot water (DHW) systems;

III. (a) on Component Testing and System Simulation (CTSS) of small solar heating systems and
(b) on in situ testing of large solar heating systems.

The work of these Groups constitutes the scientific basis for the present status in ISO and CEN standardization on solar energy components and systems.

General features of dynamic testing and measuring

Dynamic fitting is the inversion of dynamic simulation: simulation yields the component or system output using given model parameters, whereas dynamic fitting provides the model parameters from the measured component or system output.

The several dynamic fitting procedures, investigated by the DCST participants, all feature a black box approach in which a so-called parameter identification technique is combined with an appropriate mathematical model of the solar energy component or system. Measured output behaviour of the component or system is compared with the corresponding calculated quantity from the model. The calculated output depends on the model parameters. In an iterative optimization procedure, the deviation between calculated and measured output is minimized through adaptation of the parameter values. After dynamic fitting, the same mathematical model is commonly used for long term performance calculations for reference meteorological and load conditions.

Since no stationary test conditions have to be obtained, the measuring procedure, especially outdoor, can be shorter and less expensive. Since effects for the all day performance are taken into account, characterization can be more complete as well. Moreover, identical models for parameter identification and simulation give more accurate long term performance predictions compared to model calculations based on specifications determined from stationary tests. However, accurate and reliable characterization requires variability of component or system input sufficiently tuned into the model parameters.

Activities, results and recommendations of Group I on dynamic collector testing

Work in Group I involved investigation of various solar collector models and parameter identification techniques as well as design of a dynamic collector test procedure for outdoor laboratory testing. Main goal of the work was to investigate the extension of the present stationary ISO test standard to non-stationary testing using normal meteorological and operating conditions. Second order collector properties can be taken into account in this way so that a much wider range of collector types can be characterized accurately.

Three collector models were developed and evaluated. For one model, correction terms for diffuse irradiation, wind velocity, sky temperature, wind dependency of the zero loss collector efficiency, and possible piping heat loss were added to the terms of the stationary ISO standard, which already includes zero loss efficiency, temperature dependent heat loss coefficient, incident angle dependency of the zero loss efficiency and effective heat capacity of the collector. Local heat loss and thermal capacity have been incorporated in the other two models so that low flow collectors can be characterized more accurately. For parameter identification, both the Marquardt-Levenberg solution method has been used and a special version of the multiple linear regression method.

The test procedure includes steps up and down in collector inlet temperature together with requirements on solar irradiation and wind velocity. In order to fulfil the requirement of backwards compatibility to stationary testing, however, the most advanced possibility with rapidly varying inlet temperature has been left out so that both stationary and dynamic properties can be derived from the same test. As no continuous good weather is needed, the dynamic collector test takes only about two weeks for the average mid-European climate, which is half the time of the full stationary test. In spite of the shorter testing time, a much more complete and realistic characterization of the collector is derived.

Experimental results from dynamic collector testing show that different models and parameter identification methods show very small differences for routine testing. However, standard ISO testing has been combined now with determination of incident angle modifier and heat capacity in one single, shorter test. Moreover, a much wider range of collectors, from unglazed swimming pool collectors to concentrating collectors for high temperature applications, can be handled correctly by dynamic testing in comparison to the stationary methods needed for these varieties. Scientific work on the dynamic collector test method has finished and the method has partly been validated. Further thorough validation of the DCT method is still needed for standardization purposes.

Activities, results and recommendations of Group II on dynamic testing of solar DHW systems

Activities of Group II focused on the development and evaluation of an outdoor laboratory test procedure for small solar DHW systems including further assessment of data processing using the so-called model P. This general model contains four parameters for main characterization of solar collector and heat store, and five more parameters describe system behaviour in more detail. The procedure forces the solar DHW system to be tested in its most important system states in order to obtain accurate

parameters and annual performance prediction.

Tests were carried out for solar DHW systems with spectral selective flat plate collectors, forced circulation in the collector loop and an electric element for auxiliary heating. The tests revealed accurate and reproducible results, both in identified parameters and annual performance calculations. Further investigations on solar pre-heat and solar plus supplementary systems were performed based on simulated test data. Results confirmed the power of the DST method for a wide range of factory-made systems. Preliminary boundaries of the method were determined to be the temperature dependency of the heat loss coefficient and incident angle dependency of the zero loss efficiency of the collector.

Main recommendations for standardization activities are further determination of the application range for the DST method as well as additional experimental validation.

Activities, results and recommendations of Group III on component testing and system simulation

Participants in Group III contributed to CTSS with scientific developments and investigations on heat store testing, development of a test concept to translate component testing into performance predictions for the whole system and experimental validation of the reliability and accuracy of the whole method.

Two heat store models, i.e. a multi-port and a plug flow model, have been developed and evaluated for data processing and simulation. A special indoor test procedure has been created for inducing physical effects for accurate determination of heat store characteristics from measurements of flow rates and inlet and outlet temperatures for thermal charge and discharge. Parameters include effective heat capacity, heat loss rate, heat transfer rate of heat exchangers, possible auxiliary volume, thermal stratification and vertical thermal conduction. The method, applied on twelve heat stores, yielded reliable and reproducible results.

The CTSS procedure supports thermal performance characterization of custom-built solar energy systems, and consists of four steps, (1) dynamic testing of the solar collector, heat store and controller components, (2) check of the whole system by inspection of the various components including interconnections and documentation, (3) modelling of the whole system for the relevant system configuration, and if no validated system model is available, then (4) validation by a whole system test. Component testing followed by system simulation features flexibility, both in exchanging components and in application in a large range of custom built system types, including systems for combined hot water and space heating. The CTSS method was successfully performed in practice for eleven quite different solar DHW systems. Success was also confirmed by comparison with results from DST tests on these systems.

Standardization requires further validation of the heat store test method for other store designs, refinement of the CTSS procedure to strict guidelines and extension of the scope to other system configurations such as for combined solar DHW and space heating.

Activities, results and recommendations of Group III on in situ measuring

Group IIIb focused on in situ testing for commissioning of new large scale solar water heating plants and continuous monitoring of plants in operation. The goal of the work was to apply and further develop dynamic procedures for on site testing of these systems. The method used parallels the CTSS method. The main difference is that all measured data are acquired during regular operation of the plant. Participants carried out a number of studies, mainly concentrating on the collector array. They all used data sequences of several months or longer and cross-predicted the long term performance with models fitted to monthly sequences or shorter. The time resolution of the data varied from a few minutes, which was used in most studies, to one hour, and even one day. The latter was used together with a simple regression model. One single study covered the complete procedure and predicted the yearly gain of the solar heating system.

The precision achieved in the cross-predictions of the collector array output agrees well in all of the studies. The extreme figures are ± 3% and ± 7%. This agreement is remarkable considering the large variation both with respect to models and measurements. The single study on a complete system indicates that an inaccuracy only slightly larger is possible for a complete system test. The group concludes that an in situ performance test based on the dynamic testing technique is feasible, and that an overall inaccuracy better than ± 6% is within reach for the predicted long term solar collector output.

The group recommends that the work be continued with the objective to develop an in situ test procedure for large custom built solar heating systems based on the dynamic testing technique. The cost of applying the test on a routine basis should be a major consideration.

Overview of the DCST Subtask Final Report

The results of the participants activities have been presented in two Volumes of the DCST Subtask Final Report "Dynamic Testing of Active Solar Heating Systems". Both Volumes contain a note on the IEA and the DCST Group followed by summaries of the coordinated work. Further Annexes in both Volumes present a collection of papers of the DCST Subtask participants embodying the findings of dynamic testing and measuring of solar energy components and systems in more detail. Report summaries, prepared by the coordinators of the various Groups, describe the general experience of the DCST Subtask. Participants are responsible for the contents of the papers in the Annexes. Although references have been made to the participants contributions, summaries can be understood without reading the papers.

Volume A describes the investigations, results and recommendations of Group I on dynamic collector testing as well as Group III on CTSS for small solar heating systems and in situ measuring for large systems. Experiences of the Group II participants on dynamic testing of solar DHW systems have been presented in Volume B.

INTRODUCTION TO THE INTERNATIONAL ENERGY AGENCY AND THE DYNAMIC COMPONENT AND SYSTEM TESTING GROUP

The International Energy Agency

The International Energy Agency (IEA), located in Paris, was founded in 1974 as an autonomous body within the framework of the Organization for Economic Cooperation and Development (OECD) to coordinate the energy policies of its members. The 23 member countries seek to create the conditions in which the energy sectors of their economies can make the fullest possible contribution to sustainable economic development and the well-being of their people and the environment.

The policy goals of the IEA include diversity, efficiency and flexibility within the energy sector, the ability to respond promptly and flexibly to energy emergencies, the environmentally sustainable provision and use of energy, more environmentally-acceptable energy sources, improved energy efficiency, research, development and market deployment of new and improved energy technologies, and cooperation among all energy market participants.

These goals are addressed in part through a program of collaboration in research, development and demonstration of new energy technologies consisting of about 40 Implementing Agreements. The IEA's R&D activities are headed by the Committee on Energy Research and Technology (CERT) which is supported by a small Secretariat staff in Paris. In addition, four Working Parties (in Conservation, Fossil Fuels, Renewable Energy and Fusion) are charged with monitoring the various collaborative agreements, identifying new areas for cooperation and advising the CERT on policy matters.

The Solar Heating and Cooling Programme

The Solar Heating and Cooling Programme was one of the first IEA collaborative R&D agreements to be established. Since 1977, its participants have been conducting a variety of joint projects in active and passive solar and photovoltaic technologies, primarily for building applications. The present twenty members are:

Australia	France	Norway
Austria	Germany	Spain
Belgium	Greece	Sweden
Canada	Italy	Switzerland
Denmark	Japan	Turkey
European Commission	The Netherlands	United Kingdom
Finland	New Zealand	United States

The overall Programme is monitored by an Executive Committee consisting of one representative from each of the member countries. The leadership and management of the individual research projects, or Tasks, are the responsibility of Operating Agents. A total of 22 Tasks have been undertaken since the beginning of the Solar Heating and Cooling Programme of which the first 14 have been completed so

far. These tasks and their respective Operating Agents are:

Task 1 : Investigation of the Performance of Solar Heating and Cooling Systems - Denmark
Task 2 : Coordination of Research and Development on Solar Heating and Cooling - Japan
Task 3 : Performance Testing of Solar Collectors - Germany/United Kingdom
Task 4 : Development of an Insolation Handbook and Instrumentation Package - United States
Task 5 : Use of Existing Meteorological Information for Solar Energy Application - Sweden
Task 6 : Solar Systems Using Evacuated Collectors - United States
Task 7 : Central Solar Heating Plants with Seasonal Storage - Sweden
Task 8 : Passive and Hybrid Solar Low Energy Buildings - United States
Task 9 : Solar Radiation and Pyranometry Studies - Canada/Germany
Task 10 : Material Research and Development - Japan
Task 11 : Passive and Hybrid Solar Commercial Buildings - Switzerland
Task 12 : Building Energy Analysis and Design Tools for Solar Applications - United States
Task 13 : Advanced Solar Low Energy Buildings - Norway
Task 14 : Advanced Active Solar Systems - Canada
Task 15 : Not initiated
Task 16 : Photovoltaics in Buildings - Germany
Task 17 : Measuring and Modelling Spectral Radiation - Germany
Task 18 : Advanced Glazing Materials - United Kingdom
Task 19 : Solar Air Systems - Switzerland
Task 20 : Solar Energy in Building Renovation - Sweden
Task 21 : Daylighting in Buildings - Denmark
Task 22 : Building Energy Analysis Tools - USA

Task 14 on Advanced Active Solar Systems

Task 14 was initiated to advance the State-of-the-Art in active solar energy systems. Many features developed during the few years before the start of the Task, when used alone or in combination, had the potential to significantly improve the performance of these systems. It was the objective of Task 14 to analyze, design, evaluate and, in some cases, construct and monitor a number of different systems incorporating one or more of these features.

The work of the Task was divided into three Working Groups, based on the type of systems studied, and one Subtask dealing with dynamic testing. The goal of the Working Groups and the Subtask was to facilitate interaction between participants with similar projects. Participants were able to identify and address issues of common interest, exchange knowledge and experience and coordinate collaborative activities.

Domestic Hot Water Systems - Working Group

The focus of this Working Group was the development of advanced DHW systems using the "low flow" concept. Participating countries contributed expertise related to different system components. The

collaborative work in the Task brought this expertise together to allow participants from each country to design systems which show a significant cost/performance improvement (as high as 45%) over systems on the market in their respective countries when the Task began.

Air Systems - Working Group

Task work concentrated on further development of a commercially available concept for the preheating of ventilation air in industrial and commercial buildings. This concept is a specially designed cladding system to capture the air heated by solar radiation on the south wall of a building. Four projects, two in Canada, one in the USA and one in Germany, were constructed using a perforated version of the wall. The German project adapted the concept to preheat combustion air for a district heating plant. The practical work of these projects was complemented by theoretical work conducted at the University of Waterloo in Canada and the National Renewable Energy Laboratory (NREL) in the United States. Task work demonstrated that the cost/performance of the perforated wall is over 35% greater than earlier versions of the design.

Large Systems - Working Group

The Task also examined large scale heating systems involving temperatures under 200°C. Five large systems were studied. They were all very different but each represented important applications of active solar systems. District heating, the subject of the Swedish project, can be used in most IEA member countries to provide space and water heating for communities. The German project also involved district heating but with no storage. A tulip bulb drying installation in The Netherlands explored the staggered charging and discharging of long term storage, a strategy which may find many uses, especially in agricultural applications. Solar desalination, the subject of the Spanish project, has wide application in water starved areas of the world and could represent a major export opportunity for IEA countries. Industrial process heat was represented by a project in Switzerland. Since virtually all large systems are custom designed, cost/performance improvements for this Group was not a meaningful measure of achievement. Documentation of lessons learned is the most important product of the work.

Dynamic Component and System Testing - Subtask

Attention of the DCST Subtask was directed to research and development of dynamic test and measuring methods for characterization of solar energy components and systems on the level of long term performance prediction from short term measuring periods.

Task 14 activities began in 1989 and were completed in 1995. The following countries participated in this Task: Canada, Denmark, Germany, the Netherlands, Slovenia, Spain, Sweden, Switzerland and the United States. Canada provided the Operating Agent.

Subtask on Dynamic Component and System Testing

The Subtask on Dynamic Component and System Testing (DCST) was added to Task 14 in 1993 and provided a continuation and broadening of work completed earlier by the IEA Dynamic Systems Testing Group (DSTG). The DSTG established that dynamic fitting (or parameter identification) was

a suitable tool in processing laboratory tests and on site monitoring of solar DHW systems. Final DSTG results also included preliminary versions of test and measuring procedures for solar DHW systems.

In the DCST Subtask, work on definition of the dynamic laboratory test procedure for solar DHW systems was continued, and finally led to a Committee Draft for international standardization. Broadening of the work on dynamic fitting involved development of procedures for laboratory testing of solar collectors and heat stores and the data processing tools to match as well as investigation of in situ measurements from more locations. Work was carried out in three Groups:

I. Dynamic Collector Testing (DCT);

II. Dynamic System Testing (DST) of solar DHW systems;

III. (a) Component Testing and System Simulation (CTSS) of small solar heating systems and
(b) In Situ Testing of large solar heating systems.

Participants in the DCST Subtask were:

Canada	S.J. Harrison	Queen's University Department of Mechanical Engineering Solar Calorimetry KINGSTON Ontario K7L 3N6
Denmark	J.E. Nielsen M. Bosanac	Danish Technological Institute Department for Energy Technology Solar Energy Laboratory P.O. Box 141 DK-2630 TAASTRUP
Germany	K. Vanoli R. Tepe	Institut für Solarenergieforschung Hameln-Emmerthal Am Ohrberg 1 D-31860 EMMERTHAL
Germany	W. Spirkl A. Brunotte	Universität München Sektion Physik Amalienstraβe 54/II D-80799 MÜNCHEN
Germany	J. Spehr	ZAE Bayern P.O. Box 440254 D-80751 MÜNCHEN
Germany	T. Pauschinger (leader WG IIIa) H. Drück	Universität Stuttgart Institut für Wärmetechnik Pfaffenwaldring 6 D-70550 STUTTGART
Netherlands	H. Visser (leader WG II, subst. coordinator) J. van der Linden	TNO Building and Construction Research Department of Indoor Environment, Building Physics and Systems P.O. Box 49 NL-2600 AA DELFT

Slovenia	C. Arkar	University of Ljubliana Faculty for Mechanical Engineering Murnikova 2 SL-61000 Ljubliana
Spain	C. Granados	Instituto Nacional de Tecnica Aerospacial Dpto. Energía Solar Campo experimental de El Arenosillo Ctra. Huelva-Matalascañas km 27.2 E-21130 MAZAGÓN HUELVA
Spain	J.I. Ajona	IER-CIEMAT Avda. Complutense 22 E-28040 MADRID
Sweden	B.O. Perers (leader WG I)	Vattenfall Utveckling AB c/o Miljökonsulterna P.O. Box 154 S-61124 NYKÖPING
Sweden	P. Isakson (leader WG IIIb)	Royal Institute of Technology Department of Building Services S-10044 STOCKHOLM
Switzerland	B. Lachal D. Cabrera	CUEPE Université Geneve 4 Chemin de Conches CH-1231 CONCHES GENEVE
Switzerland	N. Findlater	ITR Solarenergie Pruf- und Forschungsstelle Oberseestraβe 10 CH-8640 RAPPERSWIL
Switzerland	P. Bremer	SEDE SA 33 Rue du Midi CH-1800 VEVEY

Coordinator of the DCST Subtask was Mr. P. Bremer. His leadership was brought to a brutal end by his sudden illness and death. His enthusiasm and dedication to the work on dynamic fitting and the fine organization talents may be an inspiration for all those people working in the solar energy field.

The report on the DCST coordinated activities consists of two Volumes. Volume A describes the combined dynamic testing of components and system simulation for small solar heating systems as well as in situ measurements of large solar heating systems. Volume B presents the work on dynamic testing of solar DHW systems. Both Volumes contain summaries of the work carried out followed by a collection of papers contributed by DCST participants describing the experiences with dynamic testing and measuring in more detail.

SUMMARIES OF THE DCST COORDINATED ACTIVITIES:

- DYNAMIC COLLECTOR TESTING
- COMPONENT TESTING AND SYSTEM SIMULATION OF SMALL SOLAR HEATING SYSTEMS
- IN SITU TESTING OF LARGE SOLAR HEATING SYSTEMS

DYNAMIC COLLECTOR TESTING

Summary by Bengt Perers

This Section summarizes the activities of the DCST Subtask on dynamic collector testing. Goal of the work was the development of a dynamic test method as extension to the ISO 9806-1 standard for collector testing. The DCST Group contributed with development and analysis of collector models and dynamic fitting procedures and with the establishment of a dynamic test procedure.

1. Objective

The aim of the work within IEA SH&C Task 14 has been to give a scientific basis for an update of the present stationary collector test standard ISO 9806-1 to extend the test method also to non-stationary all day outdoor climate and operating conditions. Close connection to both CEN and ISO has been kept through the National Testing and Research institute, SP, in Sweden. The backwards compatibility to existing standards has turned out to be an important point to speed up the introduction of dynamic collector testing.

Some of the main advantages that are looked for are a shorter and less expensive outdoor test and at the same time a much more complete characterization of the collector in a single test procedure.

An important goal has been to also include annual performance prediction as an integral part of the method. The same collector model and identified parameters from the test should be possible to use in a simulation program for the extrapolation to the long term performance.

2. Scope

Dynamic testing is a rapidly expanding field with many new possibilities. The increasing availability of fast PC computers and advanced data loggers has made it possible to collect and use much more test data also from non-stationary outdoor conditions in a standard test.

The solar collector testing work within IEA Task 14 has been focused on models and methods that can be used to improve standard collector testing. Several collector models starting from the present stationary collector test standard ISO 9806-1 and different parameter identification methods have

been investigated. One of the main limitations in the method turned out to be the backwards compatibility to existing standards that finally decided what collector models presently could be chosen and recommended for standard testing.

3. Activities

3.1 Solar thermal collector models

There are a number of collector models that differ significantly in the individual sub-models of the collector to take into account different second or third order effects more accurately and also with the aim to model the collector output at very short time steps, low flow rates and steps in inlet temperature and flow.

Still all the collector models agree in the common general structure as zero loss efficiency, heat loss coefficient, and thermal capacitance correction. The collector models with the more advanced heat loss models need the iterative DF parameter identification program, whereas the extended ISO model with correction terms can be evaluated with standard Multiple Linear Regression.

There are three main collector models that have been used in this work. The extended ISO model, the MFC model and the Dyncoll model. For comparison, we start with the collector model options in ISO 9806-1.

The ISO 9806-1 collector model

For comparison, we start to describe the present stationary ISO model used in the standard ISO 9806-1. This model has been widely used both in testing and for simulation. The basic equation is a stationary model for near normal incident angle operation (the nomenclature is given in the next Section):

$$q_u = \quad F'(ta)_e\, G_b \; - \; F'U_0\, DT \; - \; F'U_1\, (DT)^2 \qquad (6.1)$$

The solar irradiance is denoted G_b to point out that only high insolation levels with low diffuse fraction are accepted in the test sequence. No correction for non-stationary conditions is made so very stable inlet and irradiation conditions are needed for each test point. Furthermore, it is assumed that the incident angle is normal so that incident angle effects can be neglected. This restricts the measuring time very much during normal weather conditions except for very sunny climates.

In the ISO 9806-1 standard, there are optional test procedures also for the determination of incident angle dependence of the zero loss efficiency and the effective thermal capacitance of the collector. The full instantaneous equation from all the options in the ISO standard can be written:

$$q_u = F'(ta)_e K_{tab}(q) G_b - F'U_0 DT - F'U_1 (DT)^2 - (mC)_e dT_m/dt \quad (6.2)$$

Note that this is a clear weather or indoor simulator model as the solar irradiation is treated as beam irradiation. No correction term for diffuse irradiation is proposed in the standard. In most simulation programs the solar irradiation is divided into beam and diffuse irradiation and a separate incident angle correction is added for diffuse irradiation. This correction term is often derived from the incident angle dependence for beam irradiation of the collector. Therefore a complete ISO test gives this information for standard simulation purposes but the cost would be much higher than one dynamic test giving all parameters at the same time.

The Extended ISO model

This model is basically the same as the ISO model but with some extra correction terms for diffuse irradiation, wind speed, sky temperature and wind dependence in the zero loss efficiency (e.g. unglazed rubber collectors). A correction term is also given if the inlet and outlet sensors cannot be mounted close enough to the collector. Such temperature losses should of course be avoided in laboratory testing. All the standard ISO and extended model parameters can be identified with Multiple Linear Regression as well as with DF (Dynamic Fitting Program). The sub-models in this equation have all been verified against measured data in other IEA SH&C activities as within IEA Task VI and Task III. They are also based on physics even if the detailed heat loss pattern of a solar collector is very complicated in detail mainly due to the convection heat flows. The extended ISO model reads:

$$q_u = F'(ta)_e K_{tab}(q) G_b + F'(ta)_e K_{tad} Gd - k_w G_{tot} w - F'U_0 DT - F'U_1 (DT)^2 - F'U_w DT w - F'U_{sky} DT_{sky} - (mC)_e dT_f/dt - U_p DT \quad (6.3)$$

q_u	= Collector array thermal output	[W/m^2]
$F'(ta)_e$	= Zero loss efficiency for direct irradiation at normal incidence	[-]
$K_{tab}(q)$	= Incident angle modifier for direct irradiation	[-]
K_{tad}	= Incident angle modifier for diffuse irradiation	[-]
G_{tot}	= Global irradiance onto the collector plane	[W/m^2]
G_b	= Direct irradiance onto the collector plane	[W/m^2]
G_d	= Diffuse irradiance onto the collector plane	[W/m^2]
$F'U_0$	= Heat loss coefficient at $(T_m - T_a) = 0$	[W/(m^{2}K)]

$F'U_l$	= Temperature dependence of the heat loss coefficient	[W/(m^{2}K^2)]
$F'U_w$	= Wind speed dependence of the heat loss coefficient	[Ws/(m^{3}K)]
$F'U_{sky}$	= Sky temperature dependence of the heat loss coefficient	[W/(m^{2}K)]
U_p	= Piping heat loss coefficient per m2 of collector area	[W/m^{2}K]
$(mC)_e$	= Effective thermal capacitance including piping for the collector array	[J/(m^{2}K)]
DT	= Temperature difference (T_m -T_a)	[K]
DT_{sky}	= Temperature difference (T_a-T_{sky})	[K]
w	= Wind speed near the collector	[m/s]
k_w	= Wind dependence in the zero loss efficiency	[s/m]
dT_f/dt	= Mean time derivative for the average fluid temperature T_m within the time step	[K/s]
T_m	= Mean fluid temperature in the collector (T_{in}+T_{out}) * 0.5	[°C]
T_a	= Ambient air temperature near the collector	[°C]
T_{sky}	= Effective broad band sky temperature	[°C]
q	= Incident angle for the direct solar irradiation onto the collector plane	[radians]

The MFC Matched Flow Collector model

The MFC Matched Flow Collector model has been developed by Per Isakson at KTH in Sweden. This model is very elaborated in the heat loss and thermal capacitance part. An elegant analytical solution has been found so that a distributed absorber model with local capacitance's and local U values that are temperature dependent can be handled without iterations within each time step. One of the main aims is to be able to model the heat losses more accurately at low flow conditions and rapid changes in inlet temperature when the temperature increase along the absorber flow path can be highly non-linear. Wind and sky temperature influence on the heat losses are also an option in the model. The optical part of the collector equation is prepared with a large number of standard options for the incident angle dependence. The model is written as a TRNSYS component and the model parameters are identified with the external model option in DF. Per Isakson has also written a special interface between the MFC model and DF to speed up the parameter identification and also document each run in a systematic way. A more detailed description can be found in the MFC manual (Isakson 1994).

The collector parameters used in the MFC model are similar but not exactly the same as in the ISO model. The MFC model is based on an integration of local temperatures in the collector while the ISO model uses the arithmetic mean temperature T_m between inlet and outlet of the collector. The differences and conversion between the parameter values have been investigated by Pierre Bremer and Per Isakson [Isakson 1995]. For normal test flow conditions, 0.02 kg/(m^{2}s), the ISO parameters can be used in the MFC model (or the opposite) without correction. Even at low flow conditions down to 1/6 of standard test flow, 0.0033 kg/(m^{2}s), the parameter values only differ by 0.3% which is less than the experimental uncertainty in test results. Only at 1/10 of normal test flow the parameters

differ by 1% due to the mathematical differences in the models. This is the lowest flow that can be used in practice as the temperature rise over the collector will be more than 60°C at high irradiation conditions. Of course also changes in the heat transfer rate inside the absorber fluid channels will have an influence at low flow conditions but this has similar influences for both models.

For simulation purposes, the MFC model has an advantage over the ISO model that it gives the outlet temperature of the collector without iterations. In the case of the ISO model, one or two iterations are needed to calculate a sufficiently accurate value of T_m in the ISO equation. This disadvantage for the ISO model is not a major problem as also other component models, as storages, need iterations in a system simulation.

The DF Dyncoll collector model

Dyncoll is a multinode collector model that is distributed together with the DF program. The absorber is divided into a number of nodes along the flow path similar to Per Isakson's model but in this case no analytical solution is used. The focus is also here to take into account the temperature distribution along the absorber flow path. The optical part of the collector equation is the same as the ISO collector model except that the incident angle dependence is described with the Ambrosetti equation and not the ASHRAE b_0 function. The parameter identification is done with Dyncoll as an external model. A more detailed description can be found in the DF manual delivered together with the program.

Finite difference and FFC Collector models for detailed simulation

Some limited work has also been done with more detailed models as a finite difference collector model and an FFC (Fast Fourier Transform) collector model. The aim was to produce synthetic test data and to investigate the effects of wind speed , sky temperature and thermal capacitance during a test with rapid changes in inlet temperature, flow rate and solar irradiation.

It was found that the back insulation of the collector gives a small additional very long time constant that none of the present collector models can take into account. By avoiding fast changes or having symmetrical steps up and down in inlet temperature in the test sequence, this small effect is taken care of. This effect was also recognized when evaluating experimental data from the ISFH indoor test.

3.2 Parameter identification methods

Two different parameter identification methods have been used within IEA Task 14. They have different application ranges and advantages.

The DF parameter identification method

An iterative search method using the DF program package, specially developed for this purpose. The freedom in the collector model is very large. The identification method takes a significant time due to the iterative process and theoretically there is also a possibility that the globally best parameter set is not found. This is addressed in the program algorithm by making many new searches from different starting points and choosing the best parameter set. In practice, this has not shown to be a problem with the more recent versions of the program.

Of course also the systematic but at the same uncorrelated variation of the input parameters is a very important condition to find accurate parameter values. Basically the DF program uses the iterative Levenberg Marquardt parameter identification method. This is a well known algorithm that can be programmed from for example numerical recipes in Pascal. But the DF program has been developed and improved during more than five years and is now a general purpose software package with a number of routines like pre-processing of data, plotting and long term prediction. The program can be bought from In Situ Software in Munich.

The Multiple Linear Regression method

This is a non-iterative very fast matrix method called Multiple Linear Regression MLR that is available in most standard program packages as LOTUS, EXCEL or more specialized statistical programs like MINITAB or SISS. Multiple Linear Regression is a generalization to a multidimensional space of standard Linear Regression used to fit a straight line to data in two dimensions.

Linear does only mean that the model has to be written as a sum of terms with the parameters p_n as a multiplier in front of the terms. For example: $Yout = p_0 + p_1*f(x_1,x_2) + p_2*g(x_1, x_3, x_4) + p_3*h(x_2, x_5)$. The sub models f(x..) g(x..) and h(x..) in each term can be non-linear.

A special case of MLR has also been tested which makes it possible to identify the variation of a parameter between different subsets of the database. This has made it possible to identify for example the zero loss efficiency angle by angle without the need to have an equation. The derived IAM results can be used directly in TRNSYS, WATSUN or MINSUN. It has also been found that the heat loss factor can be identified in successive ranges of DT. The latest development is the extension of MLR to identification of two axis IAM values that solves the problem of testing collectors with special optical designs as for Honeycomb glazings, CPC reflectors or round glazings or absorbers.

3.3 Test sequence design

During the work within IEA Task 14 it has become more and more evident that the uncorrelated variation of the different influencing variables as for example solar irradiation, inlet temperature and incident angle is very important to give accurate parameter values and further on long term prediction results. This is much more important than the choice of collector model and parameter identification method. Even with the most advanced parameter identification method accurate parameter values cannot be achieved with data that has not enough variability.

A test sequence has therefore been designed to give the required variability in a short testing time. Due to the requirement of backwards compatibility to stationary testing the most advanced possibilities with rapidly varying inlet temperature have to be left out so that both stationary and dynamic data can be derived from the same test sequence. Figure 3.1 shows a graphical representation of the different test sequences as different boxes.

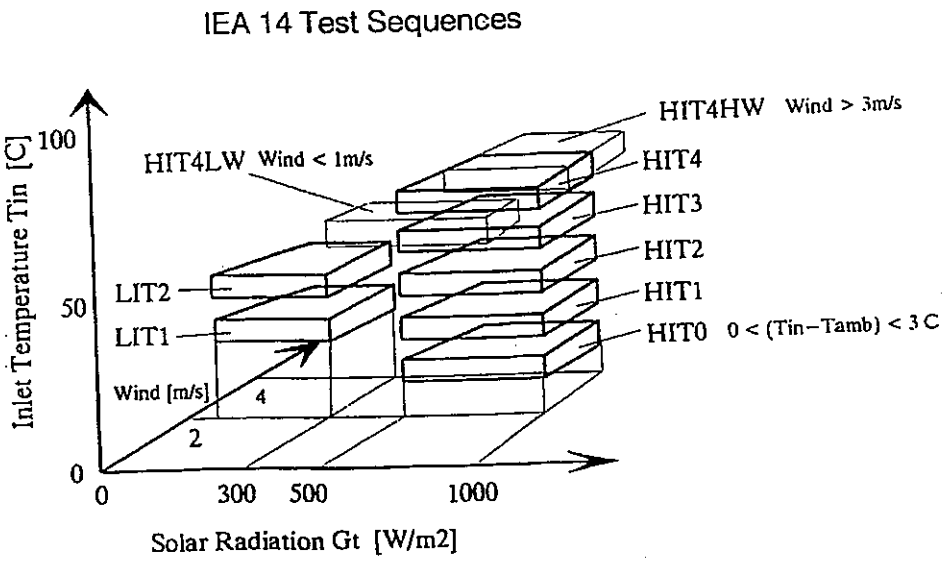

Figure 3.1: The test sequences proposed to derive reliable results from outdoor dynamic testing.

The exact duration of the test is determined by the weather and cannot be predicted exactly. In practice it has turned out that the dynamic test normally takes about half the time of a stationary test, 2 weeks, instead of 1 month in the middle European climate.

3.4 Check of measured data

A check of the measured data is needed both to identify problems with the measurements but also to determine whether enough data is available for an accurate parameter identification. As mentioned

above the weather determines when enough data is available; this has to be determined from test to test.

Check for errors in the measured data

A very efficient check of errors in the data can be made by using a preliminary guessed parameter set for the test object as input to the collector model. By plotting the measured collector output against this preliminary expected output, errors both in the collector operation and the measurement system can be detected as outliers from the expected relation. This method is very efficient as all relevant measured quantities are used intensively in the model and measured output.

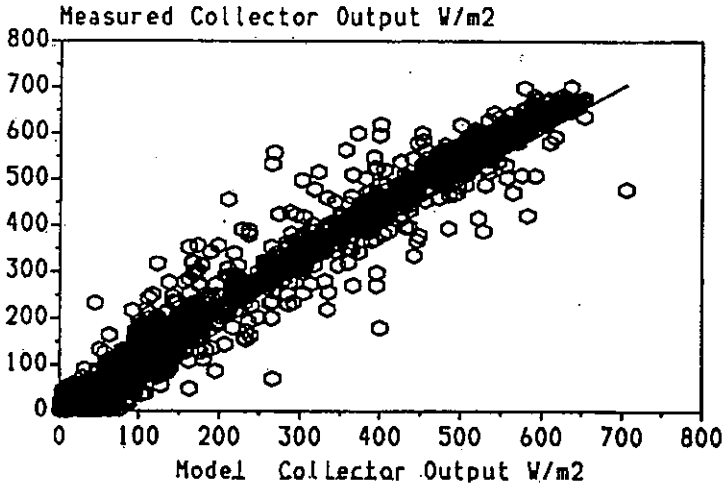

Figure 4.1: A data check diagram to identify errors in the data base. This can also be done on-line if a PC is connected to the measurement system. In this case there was an intermittent problem in the test equipment causing many outliers.

3.5 Experimental results from indoor and outdoor testing

For routine testing purposes, it has turned out that the difference is very small between the different models and methods. The collector parameters that are common with the stationary ISO collector model also come out the same if a test is extended so that also stationary test points can be derived from the test period.

Therefore, the MLR method with a modification of the ISO (T_m) collector model used in the present stationary test standard is sufficient for a wide range of collectors and is presently used by the Swedish National Testing and Research Institute for routine collector testing. Correction terms are added for thermal capacitance, wind speed, thermal sky radiation etc. but basically the collector equation is the same as in the present ISO standard with $T_m = (T_{out} + T_{in}) * 0.5$ as the reference

Table 3.1: *Comparison of repeatability of collector parameters derived with stationary (DIN) and dynamic (DCT) testing for different test periods. Test data and results come from five months of measurements at ITW in Stuttgart, Germany.*

Test period number	Test method	Zero loss efficiency for the collector [-]	First order Heat loss coefficient [W/(m² K)]	Second Order Heat loss coefficient [W/(m² K²)]	Total Heat loss coefficient at DT=50°C [-]	Incident angle coefficient r [-]	Thermal capaci-tance of the collector [kJ/(m² K)]
Z1	DCT	0.771	3.945	0.009	4.4	0.3323	10.57
	DIN	0.764	3.567	0.014	4.27		
Z2	DCT	0.759	3.316	0.017	4.17	0.3452	9.73
	DIN	0.747	2.863	0.023	4.013		
Z3	DCT	0.768	4.022	0.01	4.52	0.3018	9.525
	DIN	0.763	3.73	0.013	4.38		
Z4	DCT	0.75	2.953	0.02	3.95	0.3189	7.644
	DIN	0.756	3.147	0.019	4.1		
Z5	DCT	0.76	3.22	0.018	4.12	0.3173	9.056
	DIN	0.753	3.66	0.012	4.26		

temperature. The separate test for incident angle modifiers and thermal capacitance in the present stationary standards can now be integrated into a single dynamic test.

The repeatability of the method has also been investigated at several test institutes to assure that the results are independent of the period when the test is done. Small variations in results were found but they were of the same size as with the present stationary method in spite of the very strict selection of data used for stationary evaluation. Table 3.1 shows results from a five month testing period at ITW in Stuttgart.

Also the stability in long term performance predictions has been checked by cross prediction. Test results from one test period were used to predict the energy output for an other test period. Table 3.2 shows reliable results within a few percent from the measured output.

3.6 Measurement specifications

A special document about measurement specifications has also been written to define a common basis for measurements under non-stationary conditions. An example of a special requirement is a high enough sampling frequency of the solar irradiation to give true mean values under variable irradiation conditions. The mounting and location of sensors is also more critical when using all day

Table 3.2: *Check of the accuracy in long term prediction based on short term testing for one period and extrapolation to an other period. Test data and results come from ITW in Stuttgart, Germany.*

Collector Parameters from test period number Zx:	Measured collector output for period Zy and calculated(extrapolated) collector output for the same period number Zy using parameters from an other period Zx but climate and operating conditions from period Zy: [W] The difference is given relative to the measured performance [%]				
	Z1	Z2	Z3	Z4	Z5
	Measured performance [W]				
	797	811	890	949	941
	Calculated (extrapolated) performance [W] and difference [%]				
Z1	799 ± 1.2 0.25 %	817 ± 1.4 0.74 %	882 ± 1.3 0.9 %	956 ± 1.4 0.74 %	934 ± 1.5 0.75 %
Z2	783 ± 0.95 1.76 %	812 ± 0.91 0.12 %	874 ± 0.84 1.8 %	939 ± 1 1.05 %	924 ± 0.96 1.8 %
Z3	803 ± 2.5 0.75 %	818 ± 2.1 0.86 %	884 ± 1.7 0.67 %	952 ± 1.8 0.32 %	929 ± 1.4 1.3 %
Z4	802 ± 1.5 0.63 %	837 ± 1.8 1.97 %	894 ± 1.5 0.45 %	953 ± 1.2 0.42 %	940 ± 1.3 0.10 %
Z5	802 ± 1.6 0.63 %	833 ± 1.8 2.77 %	893 ± 1.5 0.34 %	954 ± 1.1 0.53 %	938 ± 1.2 0.30 %

data. The extra requirements are easily met with professional equipment available today and will also improve the accuracy of standard stationary testing.

3.7 Standardization

A proposal to ISO about dynamic collector testing has been given by the Swedish National Testing and Research Institute. The proposal has been accepted as a work item within ISO. The next step will be a proposal for a test procedure that will be written by the same institution in close co-operation with the IEA Task 14 experts.

The same procedure is now going on within the European standardization organization CEN and a draft test proposal is ready and a validation of the proposed method by national testing institutes is the next step.

Both proposals are put up as extension to the present ISO 9806-1 standard and not a separate new standard to speed up the process and also due to the fact that the test equipment and procedure are the same in many respects.

4. Conclusions and recommendations

The main advantages with dynamic collector testing are a shorter and less expensive outdoor test and at the same time a much more complete characterization of the solar collector in a single test procedure.

Important effects for the all day performance as for example influence of diffuse fraction, incident angle, flow rate, wind speed, thermal sky radiation and thermal capacitance are taken into account.

The more complete characterization of the collector also leads to less restrictions on the collector designs that can be tested and a wider range of collectors will be covered in the same dynamic test method.

All common collector designs from unglazed swimming pool collectors to concentrating high temperature collectors can now be tested with the same method. A validation of this wide range is still needed for standardization purposes, but on a research level the method already has been verified for this range.

The method also includes long term performance prediction as an integral part of the method. The same collector model and identified parameters from the test are used in a simulation program for the extrapolation to the long term performance. This minimizes the error in long term performance prediction.

Only minor changes and refinements in the test equipment are required. By using all day data a much more complete characterization of the collector can be derived in the one short test as one does not have to wait for stationary clear sky conditions to get useful test data.

To give representative long term results the test sequence has to be specified so that a full variability in all important normal operating conditions are encountered during the test. This is done similar to the present stationary standard by a systematic variation of the inlet temperature to the collector within the design range of the collector.

It has been found that the back insulation of the collector gives a small additional long time constant that none of the present collector models take into account. By avoiding step changes or having symmetrical steps up and down in inlet temperature in the test sequence this small effect is taken care of.

The experiences from IEA Task 14 is now being forwarded to the collector testing groups within ISO and CEN. ISO has accepted dynamic collector testing as a work item. A test proposal has been sent to CEN.

Acknowledgements

Funding from National Research Organizations is gratefully acknowledged. Important contributions to this IEA work have come from the Kingston University in Canada, ITR-SPF and SEDE SA in Switzerland, the München University, ITW and ISFH in Germany, TNO in the Netherlands, DTI in Denmark, and SP, the Royal Institute of Technology and the Vattenfall Älvkarleby Laboratory in Sweden.

References

This reference list only contains internal reports and working documents produced within IEA Task 14.

[1] Data Requirement Specification for IEA SH&C Task 14 Sub Task DCST Collector Testing Group 1, B. Perers et al., VUAB, Sweden.

[2] Dynamic Fitting of Matched Flow Collector Model to outdoor Test Data, P.Isakson, KTH, Sweden, Ueli Frei and Nigel Findlater, ITR, Switzerland, July 1992.

[3] Matched Flow Collector Model. Progress Report, P.Isakson, KTH, Sweden, January 1993.

[4] Influence of Variations in Wind Speed and Long Wave Sky Radiation on the Performance of Solar Collectors, B. Perers, VUAB, Sweden.

[5] Relations between Dynamic Fit Parameters and ISO Collector second order Linear Regression Equation, P. Isakson, P. Bremer and N. Findlater.

[6] MFC 1.0β Matched Flow Collector Model for Simulation and Testing, Users Manual, P. Isakson, KTH, Sweden, August 1993.

[7] MFC_DF 1.1β An External Model to DF, Based on the Matched Flow Collector Model, Users Manual, P. Isakson, KTH, Sweden, March 1994.

[8] Review of Non-Stationary Collector Test Data, Evaluation Procedures, Th. Pauschinger, Th. Held, ITW, Germany, 1993.

[9] Procedure for Testing Solar Collectors under Non-Stationary Conditions, Th. Pauschinger, ITW, Germany, B. Perers, VUAB, Sweden.

[10] Progress Report June 1994, Dynamic Solar Collector Testing in Sweden, B. Perers, VUAB, Sweden, 12 June 1994.

[11] Comparison of Flat Plate Collector Performance Parameters Obtained with the Standard ISO Test Procedure and Dynamic Collector Testing, Th. Pauschinger, ITW, Germany.

[12] Fitting the MFC Model to Data generated with the FFC Model, P. Isakson, KTH, Sweden.

[13] A Flat Plate Collector Model in the Frequency Domain, P. Isakson, KTH, Sweden.

[14] Dynamic Test of Two Collectors, M. Bosanac and J.E. Nielsen, DTI, Denmark.

[15] Comparison of Collector Parameters from an In Stationary and a Steady State Collector Test, G. Rockdorf and Th. Barkmann, ISFH, Germany.

[16] Dynamic Collector Testing, Group 1, Final Report from IEA Task 14, First Draft, B. Perers, Th. Pauschinger, M. Bosanac, G. Rockdorf, P. Bremer et al., February 1995.

[17] Dynamic Collector Testing - Final report from IEA SH&C Programme Task 14 DCST Subtask, Group I, B. Perers, Th. Pauschinger, M. Bosanac, G. Rockdorf, P. Bremer et al., 1996. Also included in Annex A of the present report.

PERFORMANCE TEST METHOD FOR SOLAR HEATING SYSTEMS BY MEANS OF COMPONENT TESTING AND WHOLE SYSTEM SIMULATION

Summary by Thomas Pauschinger

This Section summarizes the contribution of the DCST Subtask to a performance test method for solar heating systems by means of component testing and whole system simulation. The goal is the development of this test method for solar heating systems for hot water preparation and/or space heating and to establish a corresponding international test standard. The DCST group contributed to this work with scientific developments and investigations on the field of storage testing, the development of a test concept and the validation of the whole method by experimental tests.

1. Introduction

Several performance test methods for solar heating systems have been established as international standards or drafts within the international standard ISO 9459 (Part 1, Part 2, Part 3 and Part 5). All of these test methods are based on a *test of the whole system*, carried out either as indoor or outdoor test. This means the system is installed as a whole on a test stand for the necessary measurements.

Alternatively to these whole system test methods, a test method by means of *component testing and whole system simulation* is proposed. Instead of the test of the whole system, the system components, namely the collector, the store and the controller are experimentally tested. The performance prediction is then carried out by a computer simulation of the whole system, using a modular computer program such as TRNSYS [1]. In the following, this method is called CTSS method, standing for *Component Testing - System Simulation*. Figure 1 shows the structure of the CTSS method.

The development of the CTSS method is motivated by several needs on the market and advantages over the whole system tests:

- The CTSS method is flexible with respect to exchanging and combining of the system components. A large part of the solar heating systems on the market are not offered in fixed sizes. This means components can be alternatively chosen from an assortment of a company and can be combined in different sizes. The components can also be assembled in different system configurations, e.g. to a system for domestic hot water preparation only or a system for combined domestic hot water preparation and space heating. For these types of systems, a whole system test

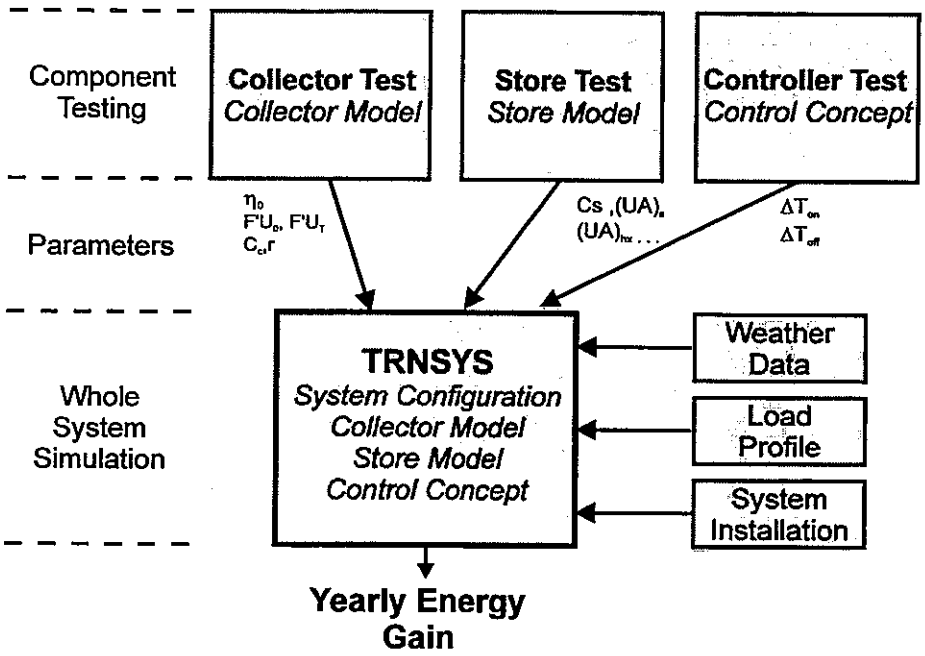

Figure 1: *Procedure for testing solar heating systems with the CTSS method*

method would require the installation of all possible combinations and configurations on the test stand. Thus, cost for testing would be high. With the CTSS method only, the components are experimentally tested. The performance prediction for the whole system is performed with validated computer programs. Thus, the CTSS method allows for more flexibility and cheaper testing.

- The CTSS method gives more insight in the thermal behaviour of the system components.
- The CTSS method is currently the only test method that makes testing of systems for combined hot water preparation and space heating possible.

The need for a CTSS method was recognized already a long time ago. However, none of the developments has been internationally harmonized and has reached the level of an internationally accepted test standard so far. The International Standardization Organization ISO has reserved Part 4 of ISO 9459 for a CTSS method. Recent activities in the European Committee for Standardization CEN, based on the work of the DCST group, head for an appropriate test standard.

2. Goals of the DCST Group work

The DCST Group originated in the IEA Dynamic Systems Testing Group (DSTG) [2]. During the work of the DSTG, experience was gained on the field of modern methods for testing and simulating

solar heating systems. Especially the numerical method of parameter identification was introduced for these purposes.

With this background, the goal of the DCST Group was to contribute to the development and validation of the CTSS method by extending the application of these modern methods on component testing of collectors and stores and the synthesis of the component test results to a long term performance prediction for the whole system. The results shall form the scientific base for an international development of a test standard for the CTSS method as foreseen by the ISO technical committee ISO/TC 180 and now also adopted by the CEN technical committee CEN/TC 312.

The necessities identified for the development of the CTSS method were:

- A performance test method for stores of solar heating systems, which makes it possible to simulate the behaviour of the store in the whole system is needed. Of special interest is the application of the parameter identification method on store testing.
- The definition of a test procedure for the CTSS method.
- The reliability and accuracy of the method must be proved by experimental validation.

The development of an advanced collector test method was treated in Group I. No work has been carried out in the field of controller testing.

Important contributions to this work items has come from LMU in Munich and ITW in Stuttgart. Results from Group I dealing with Dynamic Collector Testing were an important input to the CTSS method. The experiences gained from theoretical and experimental work were lively exchanged with the experts of Group II working on Dynamic System Testing and the experts of Group III working on in situ measurements of solar heating systems.

3. Development of a test method for hot water stores

Testing of stores for solar heating systems as integral part of the CTSS method requires, that the test method delivers all relevant data for a dynamic simulation of the thermal behaviour of the store. Experience from many years of testing solar heating systems showed, that the accuracy of simulation results crucially depends on the compatibility of the test method and the simulation program. Dynamic testing as it was introduced with Dynamic System Testing and Dynamic Collector Testing opens the possibility to ensure a maximum compatibility between testing and simulation. This is reached by evaluating test data with parameter identification methods with appropriate numerical models and using then the same models with the obtained parameters for simulation. Thus, the same principle was chosen for testing stores for solar heating systems.

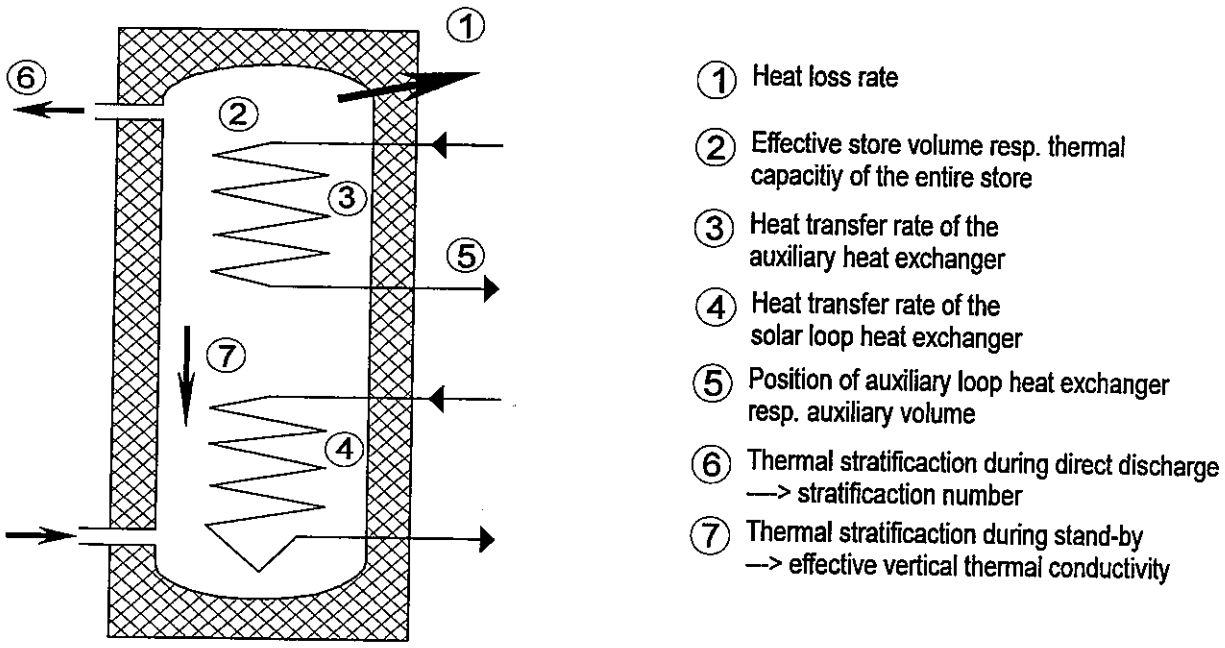

Figure 2: Thermal parameters of a store for solar heating systems

The goal of the DCST Group was to develop a store test method based on dynamic testing and to deliver the scientific base for a store test standard. Following work was carried out:

- Development of a store model for testing and simulation.
- Definition of a test procedure for store testing.
- Experimental investigations on the applicability of the store test method.

Two models, the Multiport Model [3] and a Plug-Flow Model [4] were developed. Both were implemented as parameterized models in the simulation program TRNSYS so that they can be used for the process of parameter identification with the computer program DF [5].

Measuring data are gained during tests, where the store is connected to a testing stand located in a laboratory with controlled ambient temperature. The testing stand consists of a charge and a discharge loop, which enables the thermal charging and discharging of the store according to well defined test sequences. During these tests, the volume flow rates, all inlet and outlet temperatures of the store and the ambient temperature are measured and registered continuously. No measurements inside the storage are necessary.

Special test sequences were designed in order to stimulate the physical effects to be identified. The complete specifications for these test sequences can be found in [6].

The basic store parameters that can be identified by this method are shown in Figure 2. Parameters can be added or omitted depending on the store design.

The store test method was up to now applied on 12 different stores. For several stores, repeated tests were carried out in order to show the reproducibility of the test results.

In [7], a very good reproducibility and accuracy of the test results are obtained for two different types of stores. For both stores a long term performance prediction was carried out using a standard solar heating system and the results obtained from the repeated store tests. In all cases, the deviation of the solar fraction remained below ± 0.01 (1 % absolute).

Further, the test method was applied on data gained during a whole system test of a solar heating system according to ISO 9459, Part 5 with additional sensors at the store's in- and outlets. Also with this so called InSys test, a good agreement with the results from a separate storage test was obtained for the single parameters and the result of the long term performance prediction, where the deviation of the solar fraction remained below ± 0.01. InSys testing of stores could significantly reduce testing cost.

In [4], results from *detail tests* (only singular parameters result from a single test sequence) and *integrated tests* (a complete parameter set is identified from one test sequence) are compared.

The results of all these investigations show that the method of *dynamic testing* represents a powerful tool, also for testing stores for solar heating systems. The developed models and test procedure proved to be suitable for several types of stores.

The procedure as proposed by the DCST group [6] was adopted by the technical committees of ISO and CEN. It is currently developed further by a group of experts within CEN TC 312 [8].

4. Procedure for a CTSS method

Apart from the advantages of the CTSS method mentioned above, there are also several risks with regard to the reliability of the test results. Since only the components are tested by real measurements, typical system failures (e.g. wrong placed sensors) might remain unrecognized. Also the system model for the long term performance prediction might not represent the behaviour of the real system. A concept for the whole test procedure must take this facts into account and should comprise, beside the specifications for component tests and the whole system simulation, also additional steps to ensure a sufficient reliability and accuracy of the test results (e.g. validation of the system simulation models).

Following steps for the CTSS test procedure are proposed:

Step 1: The components collector, storage and controller are tested with a suitable test method.

Step 2: The function of the whole system is checked by inspecting all components and parts as well as the system documentation.

Step 3: The whole system is modelled using a simulation program for the relevant system configuration and the obtained component parameters. The yearly energy gain is predicted for reference conditions.

Step 4: If for the relevant system configuration no validated system simulation model is available, then the model used for step 3 shall be validated by a test of the whole system, a so-called validation test.

In [9] these steps are described more in detail. Reference is made to suitable test methods for the components (see Dynamic Collector Testing and the store test methods described in Section 3) and requirements on the whole system simulation are specified.

Following features of the test procedure are considered as important aspects for the reliability of the CTSS method:

- Very often the numerical models used in simulation programs are based on assumptions that are rarely or not known by the user of the program. The chosen input parameters, obtained from testing, might be entered in a wrong meaning leading to inaccurate results. The principle chosen for the CTSS method ensures a maximum compatibility by *requiring the same models for testing and simulation* (see Figure 1).
- A *function check* of the whole system is carried out as step 2 of the CTSS procedure, prior to the whole system simulation: all components and parts of the system as well as the system documentation are visually inspected with regard to typical system failures. Since in most cases the system is not installed as a whole, this step is important for detecting all failures that might not be recognized during the component tests.
- As step 4, the *validation of the system simulation model* for the system performance prediction is adopted as integral part of the test procedure. For the validation of the system simulation model, the system is installed and tested as a whole. The measured and simulated thermal behaviour of the system is compared. Deviations shall remain below a certain required value. Such a validation is required only for new system configurations (i.e. hydraulic and control concept). Once a program is validated for a certain system configuration it can be used for all systems with the same configuration.
- Both the CTSS method and the whole system test methods will serve for testing certain types of systems. In many cases, these methods will be used in parallel and must deliver comparable results. This was achieved by choosing the same *reference conditions* for the system installation (e.g. pipe length and insulation of the collector loop) and for the long term performance prediction (e.g. weather data, hot water load).

The procedure as proposed by the DCST Group was adopted by the technical committees of ISO and CEN. It is currently developed further by a group of experts within CEN TC 312 [8].

5. The CTSS method in practice

Within the work of the DCST Group experience with the CTSS method was gained with typical forced-circulation systems for hot water preparation [9]. Eleven systems were tested:

- seven conventional systems with flat-plate collector;
- two conventional systems with ETC;
- one system with flat-plate collector and a store with stratifier;
- one matched-flow system with concentrating ETC and external heat exchanger in the charge loop.

For these systems, a separate test of the collector, the storage and the controller has been carried out. The yearly energy gain was predicted using a validated system simulation model. In addition, each system was installed as a whole and tested according the DST method, so that a direct comparison is possible.

Figure 3 shows the test results for these eleven systems according the DST and the CTSS method.

In general the test results show a very good agreement. Apart from two exceptions, the deviation remains below ±0.03 for the solar fraction. The CTSS method consistently produces higher results. An analysis of this effect showed that the reason was the use of different heat transfer fluids for the

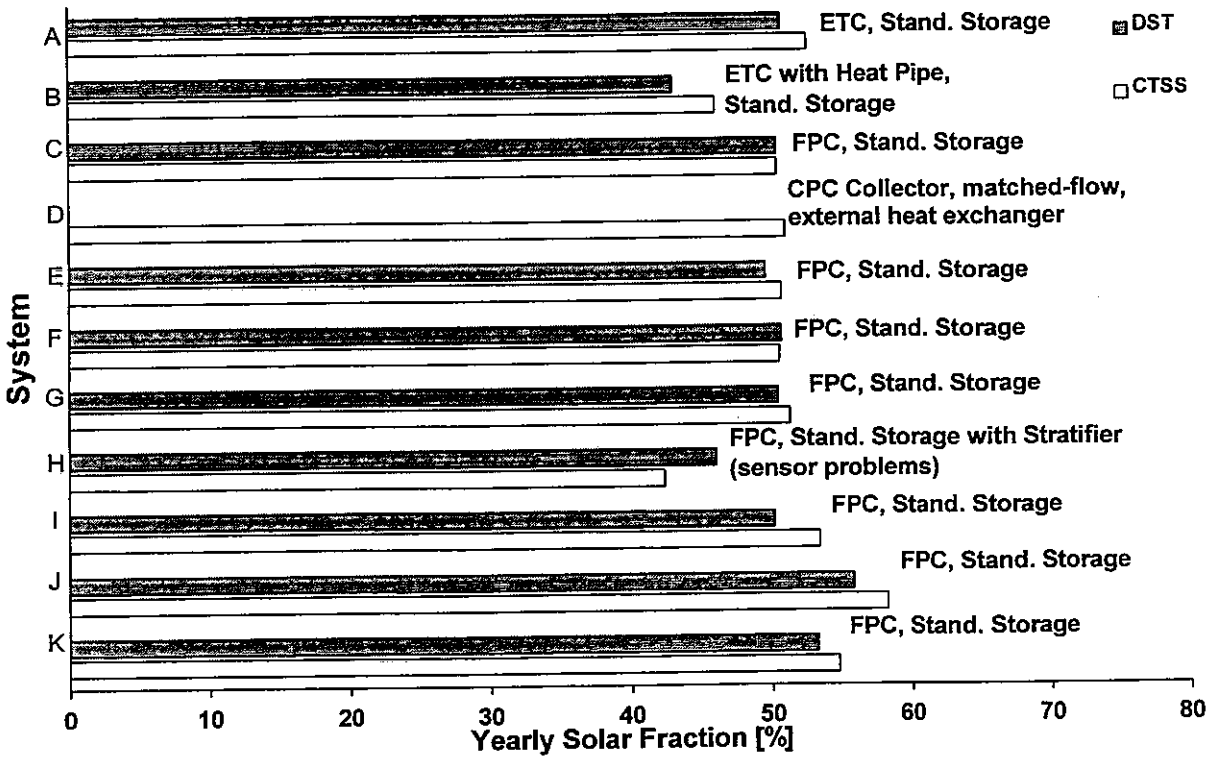

Figure 3: *Comparison of the test results for eleven solar heating systems according to the DST and the CTSS method*

component tests and the whole system tests. However, also the fact that the CTSS method assumes a 'perfect' installation between the components could contribute to this effect. In [9], the remaining deviations and the cases of system D and H are discussed in detail.

No experimental investigations were carried out for systems for combined domestic hot water preparation and space heating.

6. Conclusions and outlook

A large part of the solar heating systems for hot water preparation or combined hot water preparation and space heating is offered as components that are chosen from an assortment and combined to the whole system. For these systems, a component oriented test method, as the CTSS method, has several advantages over the whole system test methods.

The DCST Group contributed with scientific work to the development of the CTSS method. The results from this work are:

- a method for testing stores for solar heating systems and
- a test procedure for the CTSS method.

With experimental investigations, it was shown that both the store test method as well as the whole CTSS method deliver accurate and reliable results.

The studies show that both the CTSS method and the store test method, as proposed by the DCST Group, are feasible test methods for solar heating systems.

The newly developed store models are suitable for the purpose of parameter identification and simulation. The developed test sequences for the store test method lead to a good accuracy and reproducibility of the identified store parameters. If a long term performance prediction is carried out using a standard solar heating system and the results obtained from the store tests, in all cases, the deviation of the solar fraction remained below $\pm$ 0.01 for repeated tests of the same store. Those results were obtained for stores which are charged via one or two immersed heat exchangers and directly discharged. For other store types, modifications to the store model and the test sequences might be necessary.

A similar accuracy of test results was obtained for so-called InSys tests, where data are gained during a whole system test of a solar heating system with additional sensors at the store's in- and outlets. InSys testing of stores could significantly reduce testing cost. However, further investigations for this approach have to be carried out.

The results from the CTSS method are comparable with results from the DST method. In general, the agreement of the results of both methods can be expected to be better than ±0.03 for the solar fraction obtained from a long term performance prediction. The good agreement could be achieved by following several principals as outlined in Section 4. On the other hand, the method was only applied by one institute and only on a limited number of possible system types. Only systems for domestic hot water preparation were treated.

Principally, the combination of the two methods, firstly parameter identification in combination with component models for testing, and secondly system simulation using the same models, proved to be a powerful toolbox for performance testing of solar heating systems.

The proposals of the DCST Group were already adopted by the committees of ISO and CEN for the development of an international standard for the CTSS method. For the further development of the CTSS method and the support of the standardization work of ISO and CEN, following future activities are recommended:

- Further development and validation of the store test methods with respect to other store designs than treated within the work of the DCST group.
- A refinement of the proposed test procedure for the CTSS method towards a more strict guideline.
- An extension of the scope of the CTSS method to other system designs than treated within the work of the DCST group.
- An extensive treatment of solar heating systems for combined domestic hot water preparation and space heating.

A perspective for future scientific work is given by the promising results obtained from InSys testing, combined whole system and component tests.

References

[1] S.A. Klein et al.: TRNSYS, A Transient Simulation Program Version 14.1, University of Wisconsin, 1994.

[2] H. Visser, A.C. de Geus (editors): Dynamic Testing of Solar Domestic Hot Water Systems, Final Report of the IEA Dynamic Systems Testing Group, TNO Building and Construction Research, Delft, Netherlands, December 1992.

[3] H. Drück, Th. Pauschinger: Type 74 - MULTIPORT Storage Model for TRNSYS, Institut für Thermodynamik und Wärmetechnik, University of Stuttgart, 1994.

[4] A. Brunotte: A Model for Component Testing of Hot Water Storage Tanks, Sektion Physik, Ludwig-Maximilians-Universität München, 1995.

[5] Dynamic System Testing Program Manual Version 2.4α, ISS, Klein & Partners, Baadstr. 80, 80469 München, 1994.

[6] ISO 9459-4 (Working Draft): System performance characterization by means of component testing and whole system simulation, Annex A: Performance characterization of hot water storages for solar heating systems, Institut für Thermodynamik und Wärmetechnik, University of Stuttgart, 1995.

[7] H. Drück: Thermal Testing of Stores for Solar Domestic Hot Water Systems, Institut für Thermodynamik und Wärmetechnik, University of Stuttgart, 1995.

[8] CEN TC 312, WG 3: EN TC 312, Part 6; Thermal Systems and Components; Custom Built Systems, Test Methods for Small Systems (Working Draft), Institut für Thermodynamik und Wärmetechnik der Universität Stuttgart, October 1995.

[9] Th. Pauschinger: CTSS - A Component Oriented Test Method for Solar Heating Systems, Institut für Thermodynamik und Wärmetechnik, University of Stuttgart, 1995.

IN SITU TESTING OF LARGE SOLAR HEATING SYSTEMS

Summary by Per Isakson

This Section summarizes the work of the DCST Subtask on in situ testing of large solar heating systems. The aim is a short term test for long term system performance prediction.

1. Introduction

In situ tests of the thermal performance of large solar heating plants are required for commissioning of new plants and continuous monitoring of plants in operation. No normative test is available. However, within recent activities of the CEN technical committee CEN TC 312 a standard for a short term in situ test is drafted (EN TC 312, Part 7). Dynamic testing opens possibilities to devise powerful in situ tests of the thermal performance of solar heating systems.

Figure 1 outlines the data flow of the proposed in situ test. The main result of the test is a prediction of the annual solar energy utilized under reference conditions defined by a Test Reference Year (TRY) and a load profile. The test is based on parameterized component models, which are derived from physical insight. The component models are integrated into a system model using a modular simulation program, e.g., TRNSYS. The test comprises the following steps:

- Sequences of *measured data* from components and subsystems are acquired during regular operation.
- The component models are *calibrated* by fitting the models to data sequences. This step produces *fitted parameter values.*
- The component models together with the estimated parameter values are combined to a *system model.*
- A comparison between the simulated and the measured energy gain (and possibly other quantities) *validates* the system model.
- The *yearly energy gain* under reference conditions is *predicted* using the system model, a test reference year, and a specific load profile.

1.1 Requirement analysis

The test should fulfil requirements concerning cost, accuracy, ease of use, and the maximum period of time needed for monitoring. The in situ test will theoretically yield a very accurate prediction of the yearly energy gain given that

- The plant encounters a wide enough range of operation conditions during the test.
- The parameterized model together with an appropriate set of parameter values faithfully models the thermal behaviour of the plant for all relevant operation conditions.
- The monitoring system is accurate enough and data is sampled and recorded for all relevant quantities at a high enough frequency.

However, in practice these three items can seldom be fulfilled mainly because of the requirements regarding the cost:

- In large plants it is often both costly and difficult to perform specially designed experiments. Thus, it would be advantageous to base the test on data from regular operation. Furthermore, only with a good enough model the accuracy of the long term prediction would benefit from including non-typical operation conditions in the test.
- Accurate measurements during regular operation of large solar heating plants are expensive.
- The test must be based on generic component models, that is parameterized models that can be applied to fairly large classes of components. The cost, among other reasons, makes detailed dedicated models impossible. Furthermore, to be meaningful detailed models require extensive and thus expensive measuring programmes.

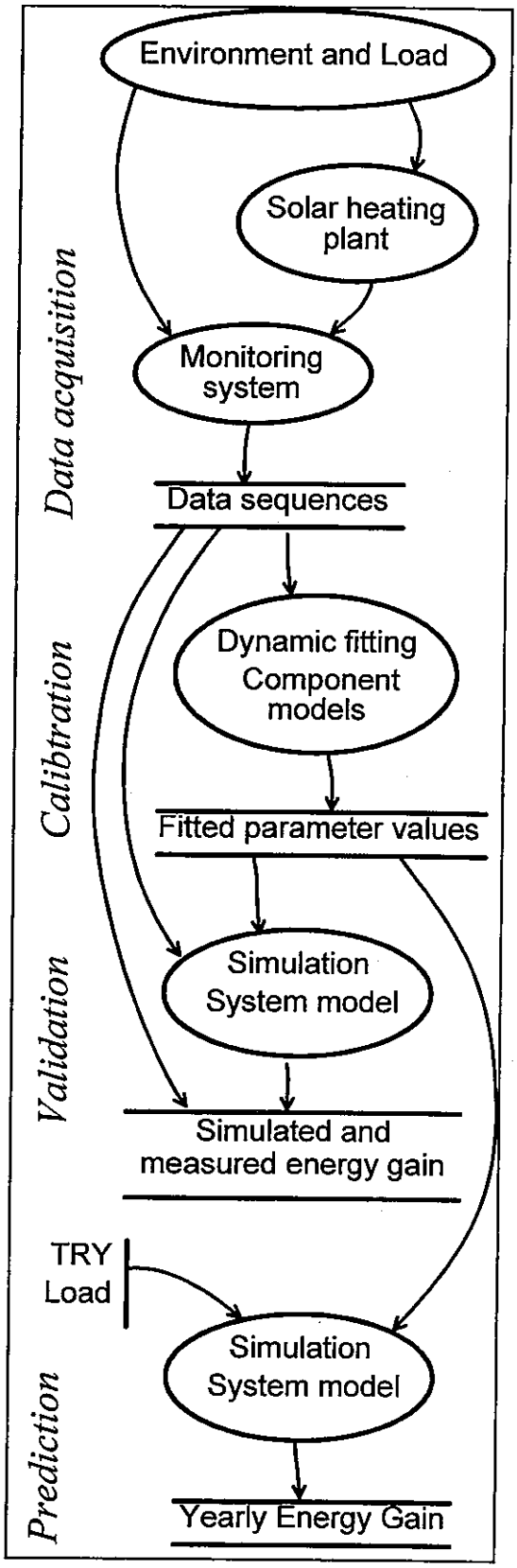

Figure 1: Data flow of the in situ test. The predicted yearly energy gain is the bottom line of the test.

Many sources contribute to the inaccuracy of the predicted yearly energy gain:

- The model error of the system model, which comprises the model errors of the calibrated component models, the model errors of other components and model errors due to simplified modelling of the interconnection of the components. The errors of the calibrated models are limited as long as the operation conditions do not deviate from those of their calibration.
- The errors in the estimated parameter values, which include contributions from errors in the measured data, lack of variation in the operation conditions of the calibration period, and the fitting method itself. Furthermore, the characteristics of components might change during the calibration period.
- "Errors" in the test reference year (TRY), and in the load profile, which are used in the prediction may both strongly affect the value of the predicted yearly energy gain. However, these two do not contribute to the inaccuracy of the test since they are given beforehand.

1.2 Goal

The objective put up for this work reads as follows: *Apply and further develop the dynamic testing methodology to test large SHW systems*. It is supposed to deliver: *Recommendations regarding experimental design, data analysis, modular simulation and validation of system models.*

2. Contributions

The following countries participated in this work: Denmark, Germany, Slovenia, Spain, Sweden and Switzerland. Six technical reports are presented in Annex C. Section 2.1 through 2.6 summarize these contributions.

2.1 In situ check of collector array performance

Miroslav Bosanac and Jan Eric Nielsen, Denmark, studied the possibility to perform a short term collector test attaining acceptable accuracy and repeatable results. They acquired accurate one-minute data during a six month period from a 60 m^2 collector array in regular operation. The measurements included the basic quantities, diffuse irradiance and wind velocity. The collector array was connected to a domestic hot water system and thus a fair variation was obtained in the collector working temperature. There was no shading between rows in the array.

They fitted an extended version of the dynamic collector model DynColl to data sequences from twelve selected periods each of five days. Next, they made twelve predictions of the energy gain for the six month period excluding the five day period used for fitting. These predictions did all agree within ±5% with the measured values, respectively.

2.2 Development of in situ test procedures for solar DHW systems

At ZAE, Germany, one applied in situ dynamic testing to eight solar DHW systems during the last three year period. The area of the collector ranges from 3 to 64 m^2 and the storage volume from 0.27 to 3.5 m^3. Accurate data were recorded at a high frequency for periods of one to three years. However, diffuse irradiance is not measured.

In one of those eight cases Justus Spehr evaluated a solar domestic hot water system comprising a 7.1 m^2 collector and a 0.50 m^3 storage. The yearly collector output and the average efficiency were 258 kWh/m^2, and 23%, respectively. The solar fraction of the yearly load was 59%. Especially in the summer the store reached high temperature values. He fitted the DynColl collector model (extended with adjoining pipes) to twenty monthly sequences of data (March through October) and predicted the collector output of the 1994 season. The predictions agree within ±3% with the measured value and the residuals do not depend on the season. Furthermore, he made a system model (TRNSYS) and simulated the performance of the entire system for the 1994 season. The agreements with measured values are excellent for a number of quantities including the solar fraction.

At ZAE the future cost of applying a complete test including a one month monitoring campaign was estimated to be in the range of 8,000 to 10,000 USD.

2.3 Development of the ISFH I/O - procedure and test in the project Solar District Heating Göttingen

Klaus Vanoli and Rainer Tepe, Germany, applied the ISFH I/O-Procedure both on-line and off-line in the evaluation of the collector array of the solar district heating plant at Göttingen. The collector comprises three roof-integrated arrays facing East, South and West, respectively. The total collector area is 785 m^2. The collector loop supplies heat directly to the return of the district heating network. The solar fraction is low. They acquired high quality data for each of the three arrays starting in April 1993. Five or ten minute data based on 10 second samples are recorded. However, the diffuse irradiance was not measured.

The primary purpose of the IFSH I/O-procedure is on-line fault detection at a low cost. It is based on the I/O-regression model that models daily values of the collector output as a function of daily values

of the global irradiation in the plane of the collector, and the average temperature difference between the collector fluid and ambient. They developed the IFSH I/O-controller that comprises a controller, a heat meter, and a fault detection algorithm based on the IFSH I/O-procedure. However, at Göttingen they implemented the procedure in the data acquisition system. The procedure also includes long term prediction and may be used for commissioning.

They fitted the I/O-regression model to data sequences of daily values of the three arrays (East, South and West) and of four different months, respectively (April, May and August 1993 and August 1994) resulting in twelve sets of parameter values. They used the irradiation while the collector was in operation rather than the total irradiation. Next, they made twelve long term predictions of the energy gain. The predictions spanned 15, 13, and 6 months for the South, West and East array, respectively. The months November through February were excluded. These predictions did all agree within ±6% with the measured values, respectively.

2.4 Dynamic in situ testing of a large solar system

Ciril Arkar et al., Slovenia, evaluated a nine years old solar DHW system, which includes a 57 m^2 collector and two 1.5 m^3 storage tanks. In summer time they realized a fairly complicated system configuration, whereas in winter time a simple pre-heat system configuration. They sampled every five second and stored half-minute data during draw-off and otherwise 10-minute data. Furthermore, they applied dynamic system testing based on the P-model (DST).

They attained large discrepancies between fitted and expected parameter values. They conclude that the P-model cannot satisfactory model a complicated solar DHW system.

2.5 Towards a performance test for large collector arrays

Per Isakson, Sweden, applied dynamic fitting to three years of data from a 5500 m^2 collector array in regular operation. The array is part of a central solar district heating plant, which also includes a 1100 m^3 storage, and conventional boilers. Some shading occurs between the rows in the array. The yearly solar energy gain, the average collector efficiency, and the solar fraction are 2.82 GJ/m^2, 26%, and 6%, respectively. The monthly solar fraction exhibits its largest value 61% in July 1991.

The experiment was not designed for dynamic fitting and thus the data exhibit some drawbacks. The measured data comprise hourly values based on two minute samples. The diffuse irradiance was not measured. The global irradiance and the ambient temperature were measured half a kilometre off the

array. The variation in the collector inlet temperature is small and the correlation between the measured quantities is large.

He fitted his MFCA model with one free parameter π^* (a linear combination of the zero loss efficiency and the collector U-value) to each of 23 monthly sequences of hourly data yielding 23 estimated values. Next, for each of these values, he predicted the energy collected during the 23 months. He repeated this for some variants of the MFCA model.

With the best model a third of the predicted values was within ±1% of the measured values, two thirds within ±3%, and all within ±6%. However, in this case the values of the collector parameters did take unreasonable values. Furthermore, there was a seasonal effect. The estimated values $\hat{\pi}^*$ of spring and autumn are larger than those of the summer.

2.6 In situ dynamic system test applied to a large solar domestic hot water system

Daniel Cabrera and Bernard Lachal, Switzerland, applied dynamic testing to a large solar domestic hot water system, comprising 200 m^2 of collector and 4 m^3 of storage. It serves 126 apartments. The collectors are mounted in four rows on a flat roof and thus some shading occurs between the rows. The total fluid volume of the collector loop is 1.6 m^3, a third of which is in the collectors. The hydraulic residence time of the entire loop is 10 minutes.

They acquired 6-minute data during the period September 1992 through August 1993. The quality of their data is high. The collector output and the average efficiency were 430 kWh/m^2 and 36%, respectively. The solar fraction of the yearly load was 27%.

They fitted the solar DHW system model, P-model (DST), to data sequences of each month resulting in twelve sets of parameter values. Then, they used these sets to predict the solar energy gain for the total period. The predicted values agreed to the measured values within ±7%. Their predictions exhibit a seasonal effect, the models fitted to the data of December and July yield the lowest predictions, and March and September the highest.

3. Discussion and conclusions

Our studies indicate that the in situ test outlined in Figure 1 is feasible. We have not encountered any major obstacles, that would hinder the development of such an in situ test. The promising results obtained both with system and component oriented dynamic tests support our general CTSS and DST conclusions. However, our work is focused on the collector array; only one participant has completed a study according to Figure 1. In this single case, the agreement between the predicted and the

measured yearly solar energy gain was excellent. Further work is needed to devise a specific test procedure.

Our work was *explorative*. Each participant has used a slightly different approach, different models, and his own data sequences. Several approaches and ideas have been tried, but the results are difficult to compare. However, almost all participants report on cross-predictions.

A *total inaccuracy* better than ±6% in the predicted yearly collector energy output appears to be possible at least in favourable cases. This Figure includes the measurement errors and the method error estimated by the cross-prediction. The discrepancies in the cross-predictions between predicted and measured long term solar energy gain all fall within a narrow range. The two extremes are ±3% and ±7%, respectively. Justus Spehr's studies (Section 2.2) indicate that an inaccuracy only slightly larger is possible for a system test. The system test done with the P-model (Section 2.6) points in the same direction.

The *cost* of applying an in situ test is an important aspect, especially since it is aimed at commissioning of one-of-a-kind systems; each plant must carry the cost of testing. Little information on costs is presented in the contributions. However, we have not encountered any problems that might increase the cost to apply the test. The IFSH I/O-procedure (Section 2.3) indicates a potential to considerably lower the cost compared to "research evaluations".

The need for *variability in the measured data* is pointed out in most reports on dynamic testing, so also in our contributions. Nevertheless, none of us has applied a specially designed experiment to improve the variability. A fair variability in data can be expected from solar DHW systems providing a high solar fraction of heat delivered to the load (Sections 2.1 and 2.2). On the other hand, as reported in Section 2.5, the variability may be very poor in the measured data of solar heating plants, where the solar fraction is small. However, that contribution indicates that the lack of variability might be circumvented by an appropriate parameterization of the model. The number of free parameters should be adapted to the variability of the data. Consequently we deem that measurements during regular operation will be adequate; specially designed experiments can be avoided.

A short *duration of the test* is important, because of the cost, and since a prompt result of a commissioning test is desirable. In most cases, we have fitted models to data sequences of one month, and in one case, five days. The latter resulted in somewhat larger inaccuracy. However, our studies and studies on short term outdoor collector tests suggest that a crucial factor beside the length is the blend of weather types represented in the sequence.

In most of our experiments we have recorded data with a high *time resolution*; in the range of one to six minutes. However, with fair success one test (Section 2.5) used hourly data and another (Section 2.3) used daily data from large collector arrays. The benefit of a high time resolution will

depend on the type of component, the model's performance at high frequencies, the characteristics of the driving signals, etc. However, we did not address the cost associated with a high recording rate.

A solar collector responds differently to beam and *diffuse* irradiance. Thus, to measure and model the two separately should improve the accuracy of the test. Nevertheless, the contribution summarized in Section 2.2 that did not measure the diffuse irradiance, reports a very high accuracy. Estimating the fraction diffuse might be an alternative to measuring. This was done in the contribution in Section 2.5, which concludes that no appropriate regression model is available to calculate the fraction diffuse based on the global irradiance in the collector plane.

Two of the contributions (Sections 2.5 and 2.6) report on a similar *seasonal effect*. Models fitted to summer data underpredict the yearly solar energy gain, whereas models fitted to spring and autumn data overpredict. In these two cases the collector arrays comprise several rows mounted on a horizontal surface. Shading between rows, which occurs only in these two, does probably contribute to this seasonal effect. It is important to know the fraction diffuse to correctly calculate the shading effect. Furthermore, this problem indicates the importance of long data sequences in the assessment of in situ testing procedures.

4. Recommendations

We recommend that the in situ tests for custom build solar heating systems are developed based on the dynamic testing technique. The cost of applying the test on a routine basis should be a major consideration. It is appropriate that this task is tackled in collaboration by an international group.

We deem the following subtasks to be appropriate:

- *Requirement analysis*. Which specific tests are needed? What accuracy is required? How large a cost to apply a test is acceptable in different situations? Different test might be required for small and large systems, for commissioning and performance verification on a regular basis, etc.
- *Analysis of the cost* to apply the tests. What are the marginal costs for extensions of a measuring program regarding various sensors, recording frequency, length in time, etc.? How does the cost depend on the type of software? The time aspect will probably have a large influence on the result. For example, the cost to operate on data will decrease over time as appropriate software becomes available.
- Compilation of a common *bank of measured data sequences*, the length of which are at least several months. Different tentative tests need to be assessed based on the same data sequences. Some suitable data have been acquired by participants in Task 14.

- Systematic evaluation of how *accuracy* depends on the factors that have a significant influence on the *cost* to apply the test.
- Devise and assess *storage tests* based on available storage models.
- Further assess the *collector array* tests and if needed make refinements. It is rather expensive to accurately measure *diffuse irradiation.* Moreover, in our current results we cannot see that it renders a real gain in the overall accuracy. Thus, it would be interesting to assess a new *regression model* that is based on the global irradiance in the plane of the collector. Furthermore, the model to calculate the shading between collector rows might need to be refined.
- Devise and assess full *system tests* according to Figure 1. The assessment should be based on available measured data. To study the influence of the time resolution in data, sequences with high resolution data should be reduced in steps to low resolution data giving several sequences from one test. A variety of methods should be assessed including the ISFH I/O-procedure.

ANNEX A: TECHNICAL PAPER ON DYNAMIC COLLECTOR TESTING

Dynamic Collector Testing - Final report from IEA Solar Heating and Cooling Programme Task 14, DCST Subtask, Group 1

Bengt Perers, Thomas Pauschinger, Miroslav Bosanac, Gunter Rockdorf, Pierre Bremer et al.

Summary

The work on dynamic collector testing within IEA Task 14 is based on previous work within IEA Task III Task VI and the DST working group. The aim is to give a scientific basis for an update of the present stationary collector test standard ISO 9806-1 in order to extend the method also to non-stationary all day weather and operating conditions.

One of the advantages is a shorter and less expensive outdoor test and at the same time a much more complete characterisation of the collector in a single test procedure. Important effects for the all day performance as for example influence of diffuse fraction, incidence angle, flowrate, wind speed, thermal sky radiation and thermal capacitance are taken into account.

The more complete characterisation of the collector also leads to less restrictions on the collector designs that can be tested, which means that a wider range of collectors can be covered by the dynamic test method.

The method also includes annual performance prediction as an integral part of the method. The same collector model and identified parameters from the test are used in a simulation programme for the extrapolation to the long-term performance. This minimises the error in long-term performance prediction.

Still to give a representative long-term result the test sequence has to be specified so that all important normal operating conditions are encountered during the test. This is done similar to the present stationary standard by a systematic variation of the inlet temperature to the collector within the design range of the collector. Only minor changes in the test equipment are required and by using all day data a much more complete characterisation of the collector can be derived in the one short test as one does not have to wait for stationary clear sky conditions to get useful test data.

The experiences from IEA Task 14 are now being forwarded to the collector testing groups within ISO and CEN. ISO has accepted dynamic collector testing as a work item and a draft standard has been sent to CEN.

TABLE OF CONTENTS

1 INTRODUCTION

The work presented here, on dynamic collector testing, are results from the IEA SH&C programme Task 14 subtasks DCST (Dynamic System Testing). The aim has been to give a scientific basis for an update of the present stationary collector test standard ISO 9806-1 in order to extend the method also to non-stationary all day climate and operating conditions.

One of the advantages is a shorter and less expensive outdoor test and at the same time a much more complete characterisation of the collector. Important effects for the all day performance as for example influence of diffuse fraction, incidence angle, flowrate, wind speed, thermal sky radiation and thermal capacitance are taken into account.

The method uses the same collector model and identified parameters from the test for the extrapolation to the long-term performance. This minimises the error in long-term performance prediction.

Still to give a representative long-term result the test sequence has to be specified so that all important normal operating conditions are encountered during the test. This is done similar to the present stationary standard by varying the inlet temperature to the collector within the design range of the collector.

Several collector models starting from the present stationary collector test standard ISO 9806-1 and different parameter identification methods has been investigated.

Important contributions to this IEA work has come from Kingston University in Canada, Rappersville in Switzerland, ITW in Stuttgart, ISFH in Hameln, TNO in the Netherlands, DTI in Denmark, SP in Sweden, The Royal Institute of Technology in Sweden and Vattenfall Utveckling AB in Sweden.

2 MEASUREMENT SPECIFICATIONS

This specification is based on the ISO 9806-1 collector test standard. The experiences so far from dynamic outdoor collector testing are added as well as **extra requirements for the IEA research work**. Hopefully some requirements can be relaxed for routine testing but this has to be verified first. Most of the extra requirements will also improve the accuracy and repeatability of stationary collector testing.

2.1 Measurement sensors

G001: Global solar radiation in the collector plane. Sampling interval max. 6 s. Integration of the signal is recommended. The detector plane should be parallel to

the collector plane within ±1°. East-west direction is most important. First class pyranometer type CM11 or Eppley PSP. Regular cleaning of the outer dome and checking for moisture inside are also important. This should be done between individual test sequences. The detector should be mounted on a metal plate or any other weather proof material that will not change shape due to moisture or temperature. A ventilator for the base and dome of the pyranometer can also be recommended.

G002: Diffuse solar radiation in the collector plane. Sampling interval max. 6 s. Integration of the signal is recommended. The detector plane should be parallel to the collector plane within ±2°. First class pyranometer. The shadow band should be adjusted at least once a week depending on the geometry of the sensor and shadow band. A table with the position of the shadow band is very useful. The adjustment can then be done at regular intervals independently of the weather.

The alignment of the pyranometers can be checked roughly by looking at the collector and detector plane from both sides. If the pyranometer is mounted on a sufficiently large metal plate, the tilt and orientation of the detector and collector can be compared and calculated by measuring the shadow length on the metal plate and collector glazing from a right angled object. Near solar noon the comparison is very easy. To check that the detector plane is parallel to the base plane the pyranometer can be rotated at stable sunshine in the morning or afternoon (high incidence angle). Look for variations in the reading.

T001: Ambient air temperature near the collector at mid height. Sampling interval max. 15 s. Careful radiation shielding is important and forced ventilation can be recommended. Accuracy ±0.2 °C. This is a very difficult and still important measurement. The placement of the sensor in the shadow behind a freestanding collector has shown to give good results if forced ventilation can not be applied.

T101: Inlet temperature to the collector. Sampling interval max. 15 s. Accuracy ±0.1 °C.

T102: Outlet temperature from the collector. Sampling interval max. 15 s. Accuracy ±0.1 °C. Should be matched with T101 to an accuracy in temperature difference of ±0.02 °C.

Note: T101 and T102 should be mounted as close to the collector as possible and in a pipe where the flow is rising to avoid air from being trapped at the sensor. The sensor should point downwards (but still upstream). A right angled bend or a special flow mixer should be placed just before the sensor to avoid any temperature stratification at the sensor location. The sensor should point against the flow direction. The sensor housing and nearby piping should be carefully insulated.

W100: Volumetric flow in the collector loop. A position at the inlet side of the collector after a deairation device is recommended. Pulse counter for integration. Sampling interval max. 15 s. Accuracy ±1 %. The temperature of the fluid in the flow meter should be known within 2 °C for the accurate calculation of the mass flow, se T103.

Note: A transparent tube or a rotameter near the flow meter W100 is very useful to check the fluid for air and contaminants. A pressure gauge placed near the inlet side of the pump is also recommended to assure that there is a safe over pressure in the whole collector loop. The pressure should be at minimum 1 bar for collectors with metal absorber piping or as high as possible taking into account manufacturer specifications for other materials as rubber or plastic. This overpressure will prevent air from entering the system at valves, bends or variations in cross section. The static head should be added/subtracted to this pressure if the collector is placed above or below the pressure gauge. **Appendix A** shows how the collectors can be connected in series to achieve equal mass flow to further improve the accuracy when comparing different collectors.

T103: Temperature of the fluid in the flow meter. T103 can be omitted if the temperature drop between the flow meter and collector inlet temperature sensor is less than 2 °C. Sampling interval max. 15 s. Accuracy ±1 °C.

V001: Wind speed near the collector front surface. The sensor should be tilted to measure the wind component parallel to the collector aperture, glass or absorber plane. Sampling interval max. 15 s. Integration of the signal is recommended. Accuracy ±0.5 m/s.

L001: Thermal radiation onto the collector plane, wavelength >3 μm. Pyrgeometer of type Eppley PIR. For the best accuracy the sensor should be both ventilated and shaded from beam solar radiation. Sampling interval max. 6 s. Integration of the signal is recommended. Accuracy ±5 %. Regular cleaning is important between the test sequences as e.g. fat and water on the dome will absorb thermal radiation and give too low readings.

V002: Wind direction. Preferably for the free wind. Sampling interval max. 15 s. Accuracy ±10 °C. Most important for unglazed collectors but it is also valuable to check the influence for glazed collectors.

F001: Relative humidity of the air. Close to the collector. Sampling interval max. 15 s. Most important for unglazed collectors. May be omitted for glazed collectors.

R001: Atmospheric precipitation. Integration of signal. Accuracy not critical but should be able to indicate when the collector glazing may be covered with rain or

snow. Can be replaced with frequent manual observations and notes in the log book.

It is recommended to also take into account the measurement specification in ISO 9806.

2.2 On-line calculations

DT100: Time derivative of the mean fluid temperature in the collector:

DT100 = (T_m new – T_m old) / (sampling interval for T101 and T102).

Note: Tm = (T101+T102)·0.5. Average for each storage interval [K/s].

As an alternative the instantaneous value of Tm or both T101 and T102 can be stored at the beginning or end of each storage interval so that the temperature change within the interval can be calculated afterwards.

P100: Thermal output power from the collector.

P100 = V100·ρ(T103)·C_p(Tm)·[T102-T101]; Tm = (T101+T102)·0.5;

T103 is the fluid temperature at the flow meter and can be replaced by T101 or T102 if the temperature difference is small. P100 may be calculated afterwards when evaluating the data if the flow in the collector loop, V100, is kept near constant within each storage interval.

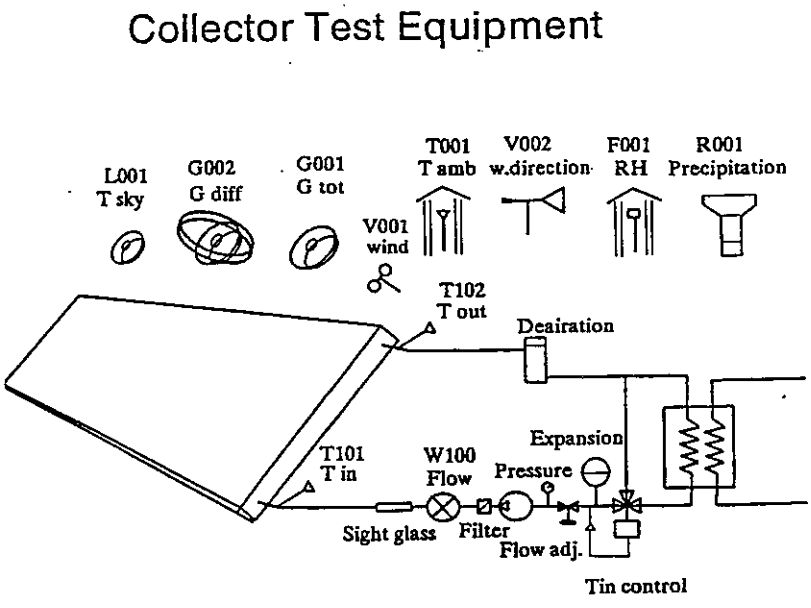

Figure 1: Measurement equipment for dynamic collector testing.

2.3 Calibration

All sensors should be calibrated at regular intervals, at least once a year. A movable extra pyranometer and temperature sensor can be very useful in checking the measurements. If these extra sensors are connected to separate calibrated instruments the whole chain of measurements including cabling, data logger and software can be checked without interrupting the measurements. Regular cleaning of the pyranometers and pyrgeometer and check of the desiccant (should be blue for silica gel), to avoid moisture inside, are very important. A ventilated ambient air temperature sensor should be checked for dust accumulation or spider web inside the air flow path. The temperature difference T102–T101 can be checked during the night if no heating or cooling takes place in the collector loop. The difference (T102–T101) should then be very small and correspond to the small heat losses to the surroundings. In this case a check of the ambient sensor will also be the result.

2.4 Manual measurements and observations

2.4.1 Mounting data

Tilt and azimuth of the collector should be known within $\pm 2°$. This can be checked at noon for example with a paper and a right angled object placed on the collector glazing. In case of a non-flat front surface, a large enough rigid metal plate can be placed on top of the collector aperture as basis for the shadow measurement. By marking the length of the shadow on the paper in the collector plane in N-S and E-W direction the absolute tilt and azimuth of the collector can be calculated based on the position of the sun.

The latitude and longitude of the test site and the location and height of objects along the horizon in front of the collector should be noted. Also surface materials in front of the collector. Even small shadowing or specularly reflecting surfaces in front of the collector can influence the pyranometer reading and give a different irradiation than the average in the collector plane. No visitors should be allowed to come close to the collector during testing for the same reason.

2.4.2 Collector area

Gross area, Aperture area and Absorber area as defined in ISO 9806-1. For evacuated tubular collectors IEA SH&C Task VI has proposed an aperture area definition independent of reflector design. Aperture area = Tube pitch · Number of tubes · Illuminated absorber length.

2.4.3 Log Book

Note everything of importance to the test, such as frost, rainwater, dust or dew on the collector glazing and pyranometers/pyrgeometer. Condensation of water on the inside of the collector glazing, dirt accumulation and material degradation.

Operating problems, deairation, low pressure and leakage/refilling of the collector loop, change of collectors, sensors, valves pumps and fluid in the collector loop. Adjustment of shadow band for G002. Cleaning of the pyranometers and pyrgeometer, status of desiccator (should be blue). Condense in the pyranometer domes.

When making these manual inspections it is essential not to shade the collector or sensors at any time. Make notes of the time if this can not be avoided.

2.4.4 Photographs

Documentation of the test with photographs of the test object, sensors and surroundings during the test.

2.5 Data format

2.5.1 Storage interval

At least hourly mean values should be stored. 10 minute storage interval is recommended as a compromise between high resolution and storage/memory requirement. Intervals shorter than 10 minutes are recommended for detailed evaluation of the thermal capacitance correction terms used in different collector models. For less than 10 minute mean values one has to keep in mind that the sampling rate and time constants of the sensors may have a significant influence on the results at non-stationary weather conditions. This needs further investigations. A comparison of collector parameters derived with 1 hour and 10 minute mean values has shown that the difference is very small for the same data set. In case of identification of the incidence angle dependence for collectors with special optics and for a better resolution for standard collectors the 10 minute option can be recommended. The variation range of the insolation can also be expected to be larger for 10 minute values which may shorten the testing time if the weather is favourable.

2.5.2 Data gaps

For the DF parameter identification method continuous data sequences without gaps are easier to evaluate even if gaps can be allowed.

The MLR identification method has no requirement on the sequence of data. Every observation, or set of mean values, is treated as a separate unit and gaps can be allowed without any problems. Most standard softwares for MLR also have the possibility to select data that fulfils certain criteria so that an automatic selection of acceptable data can be done before the parameter identification.

Still the evaluation will be much easier and reliable if data gaps can be avoided. Therefore changes and maintenance of the test equipment should be done preferably between the test sequences.

2.5.3 *Data format*

Each stored observation or data record should be written on one line together with day number and time of day. For the use of DF the time, "TIMES" = time in hours from the beginning of the test sequence, should be added. The same clock without daylight saving changes should be used throughout the year. The absolute accuracy in time should be better than 1 minute to give accurate calculations of incidence angles. Each measured quantity should be placed in a column separated by a blank for example. ASCII data format should be used with one extra decimal compared to the required accuracy. If possible a header in the file with identification and units of the data columns. Otherwise a separate description of the data should be given. Se example of the data file format below. The order of the columns is not critical.

DAY	TIME hours	T101 °C	T102 °C	W100 dm^3/s	T001 °C	G001 W/m^2	G002 W/m^2	V001 m/s	L001 W/m^2	DT100 K/s	P100 W	"TIMES" h
223	1300	56.23	63.24	0.0161	15.42	532.1	341.1	3.81	395.1	0.0023	300.1	0.167
223	1310	56.43	63.25	0.0161	15.51	522.1	343.1	1.81	393.1	0.0012	289.1	0.333
223	1320	56.63	63.34	0.0161	15.72	632.1	241.1	4.81	405.2	0.0534	250.3	0.500
223	1330	56.73	64.54	0.0162	15.32	332.1	310.1	2.81	407.1	0.0337	230.3	0.667

2.5.4 *Comments for exchange of data*

The data files should be accompanied with the information from manual observations noted in the logbook as specified above. Data from other collectors tested in parallel are very useful, especially if a reference collector is used. A well written log book is important for data exchange. To our experience measured data very often contains minor errors or problems like shading, too low resolution, frost, snow in the data etc. They can often be identified by checking the residuals. Before deleting data and rerunning the parameter identification it is essential to have either manual observations, a reference collector, or extra sensors that can verify and explain the strange results. Photographs of the test objects and test installation showing the environments and sensor locations is also very useful.

3 *TEST PROCEDURE*

To be able to identify the collector parameter accurately there must be a large enough variation of the measured quantities used in the collector model and connected to each parameter. It is assumed in this proposal that only the inlet temperature can be controlled systematically. All other parameters will be determined by the weather or fixed during the test. The test sequence is designed in such a way that also stationary test points according to the ISO 9806-1 standard can be derived from the test if the weather is clear and stable enough during each

subsequence. This requires that the inlet temperature is varied between stable inlet temperature levels. In general the dynamic test method does not need a stable inlet temperature, but in the present introduction phase the backwards compatibility is a great advantage to gain confidence in the results. In a further development of the test procedure a much shorter test will be possible if the requirement for stable inlet temperature levels can be relinquished. DTI in Denmark has made progress in his direction.

3.1.1 The present IEA Task 14 test procedure for evaluation of the dynamic test method

The whole test consists of several shorter test sequences. Hereby a test sequence is defined as a time period of continuous measuring of input and output quantities of the solar collector as specified in *Chapter 2*. For each test sequence limits of the mean values of the solar irradiance in the collector plane G_{tot} and the air velocity in collector plane w as well as range for the incidence angle are specified. The inlet temperature to the collector shall be kept constant (standard deviation <0.1 K) during one test sequence.

Five High Irradiance Tests (HIT0, HIT1, HIT2, HIT3, HIT4) are foreseen. If the wind speed is taken into account two additional tests (HIT4LW, HIT4HW) are to be applied. Two further sequences with low irradiance (LIT1, LIT2) are proposed but preliminary results show that these sequences will gain very little extra information and may be omitted. Provided that sufficient meteorological conditions are given during the test, the sequences will include data for steady state evaluation according to ISO 9806-1. *Figure 3.1* shows the distribution of the test sequences versus input quantities.

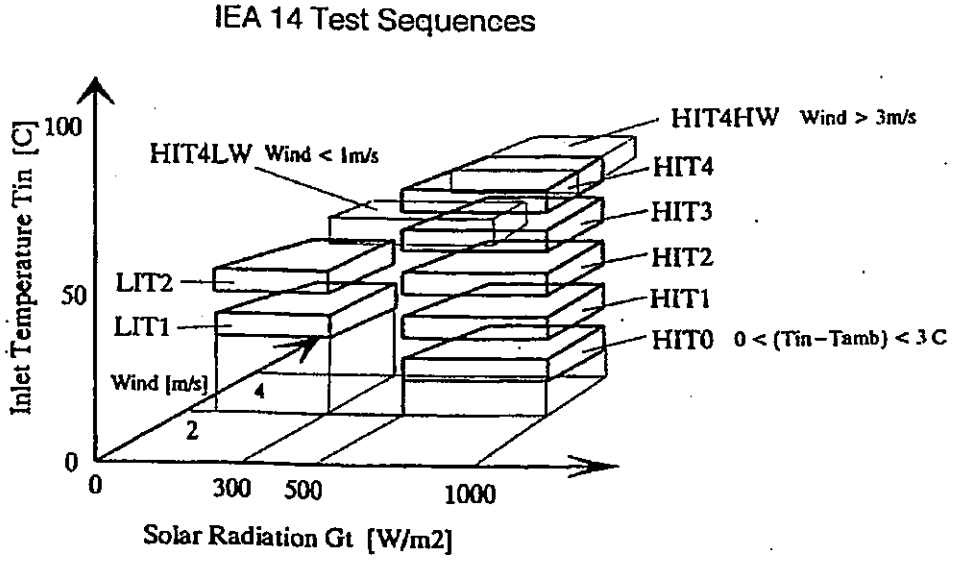

Figure 3.1 Distribution of the test sequences versus the input quantities.

3.1.2 *High irradiance tests*

The high irradiance test basically consists of 5 test sequences (HIT0, HIT1, HIT2, HIT3, HIT4). The subsequent requirements have to be fulfilled:

	HIT0	HIT1 ..... HIT4
Collector inlet temperature	SDEV(T_{in}) < 0.1K 0 < (T_{in}-T_a) < 3K	SDEV(T_{in}) < 0.1K $T_{in}1$....$T_{in}4$ spanning the operating range of the collector (according to ISO 9806-1 but $T_{in}1$ can be chosen higher)
Test Duration	Min 60 minutes	Weather dependent
Incidence Angle	θ < 30 ° during the whole sequence (depending on the type of collector)	θ has to cover the whole incidence angle range between 20 ° and 70 ° .
Mean Irradiance level	Mean(G001) > 500 W/m^2	Mean(G001) >500 W/m^2
Mean wind speed	2 m/s < w < 4 m/s	2 m/s < w < 4 m/s

If the wind speed is taken into account two additional test sequences with the requirements of HIT4 (highest temperature) but with (1) a mean wind speed of w <1 m/s (HIT4LW) and (2) a mean wind speed of w >3 m/s (HIT4HW) are applied.

3.1.3 *Low irradiance tests*

The two test sequences on low temperature levels Tin1 and Tin2 are repeated for low irradiance conditions (LIT1, LIT2), i.e. the same requirements as stated for HIT1 and HIT2 have to be fulfilled but with G001 < 300 W/m^2. The collector net heat output shall be positive during the whole sequence. ITW in Stuttgart has found that these sub sequences gain very little extra information and may be left out.

3.1.4 *Step changes*

To take into account the dynamic behaviour of the collector with respect to changes of the inlet temperature, the sequences can be linked together in a way that the ramp changes of the inlet temperature (from one temperature level to the other) are included. However, the total number of temperature changes to a higher temperature shall be equal to the total number of temperature changes to a lower temperature. It has been clearly shown that the long time-constant of for example the back insulation of a flat plate collector may give significant systematic errors if data from the temperature steps are used for parameter identification and the temperature steps only are upwards or downwards.

4 CHECK OF MEASURED DATA

A check of the measured data is needed both to identify problems with the measurements but also to determine if enough data is available for an accurate parameter identification.

4.1.1 Check for errors in the measured data

A very efficient check of the data can be made by using a preliminary guessed parameter set for the test object as input to the collector model. By plotting the measured collector output against this preliminary expected output, calculated with the model, errors in both the collector operation and the measurement system can be detected as outliners from the expected relation. This method is very efficient as all relevant measured quantities are used intensively in the model and measured output. Of course one has to make a reasonable guess of the collector parameters but this should be no problem except for completely new collector designs. This check can even be done on-line in the measurement system to get a fast feedback if something goes wrong. This has been used in many of the Swedish demonstration projects with good results since 1979. The different versions of the extended ISO model was used. An automatic check of the difference between the expected model output and measured collector output with an alarm limit could be a very useful tool for a data check during routine testing.

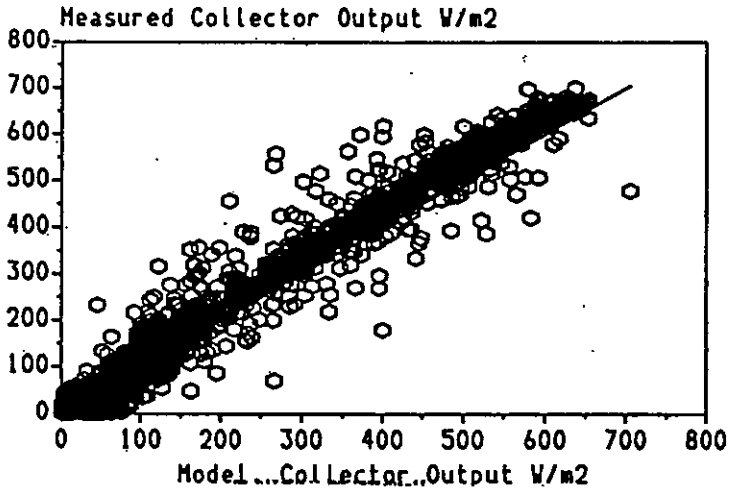

Figure 4.1: **Shows a data check diagram to identify errors in the data base. This can also be done on-line if a PC is connected to the measurement system. In this case there was an intermittent problem in the test equipment causing many outliers.**

4.1.2 *Check if enough data is available for parameter identification*

Before ending the test and beginning to identify the model parameters it is important to check that enough data is available and that there are no operating or measurement problems hidden in the data base. This should be done on a regular basis, for example each day.

Figure 4.2 gives two examples of diagrams that will give the most important information about the database. The two diagrams should be filled out with data points as much as possible and especially the outer areas should be represented to give a good parameter identification for the heat loss and zero loss efficiency and its dependence on incidence angle. Ideally all input parameters should be plotted against each other and against the output power. This check can be complemented with the cross correlation matrix. But the diagrams are much easier to interpret even if no absolute criteria can be derived from them.

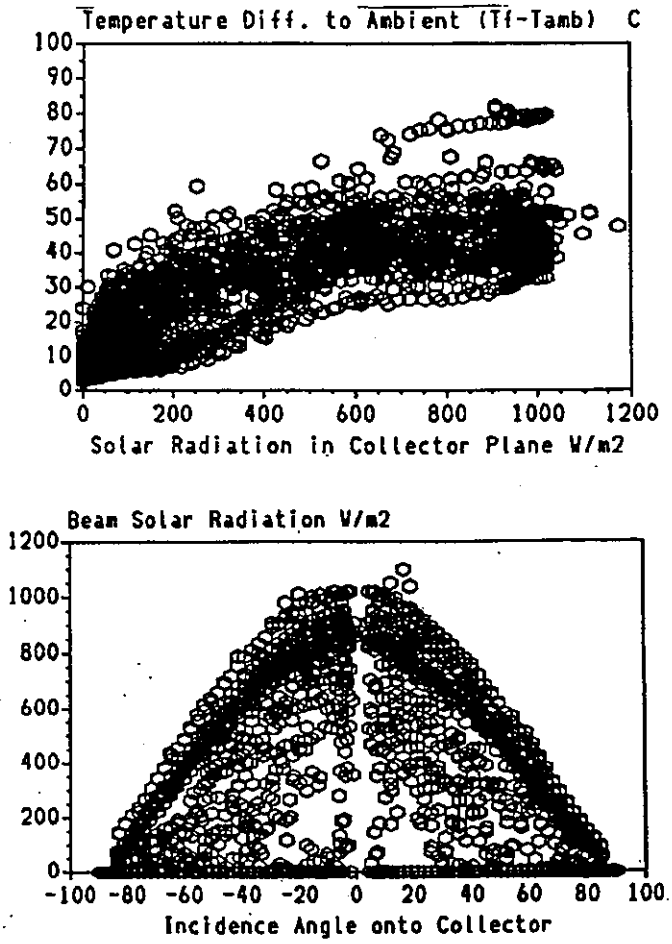

Figure 4.2: **Two examples of diagrams that will help to determine if enough data is available. The diagrams should be filled out with as much data points as possible. In the upper diagram some data is missing for low temperatures.**

5 PARAMETER IDENTIFICATION METHODS

Two different parameter identification methods has been used within IEA Task 14. They have different application ranges and advantages.

5.1.1 The DF parameter identification method

This is an iterative search method using the DF (Dynamic Fitting) program package specially developed for this purpose. The freedom in the collector model is very large. The iterative identification method takes a significant time and theoretically there is also a possibility that the globally best parameter set is not found. This is addressed in the programme algorithm by making many new searches from different starting points and choosing the best parameter set. In practice this has not shown to be a problem with the more recent versions of the programme.

Of course also the systematic but at the same uncorrelated variation of the input parameters is a very important condition to find accurate parameter values. Basically the DF programme uses the iterative Levenberg Marquardt parameter identification method. This is a well known algorithm that can be programmed from for example numerical recipes in Pascal. But the DF programme has been developed and improved during more than five years and is now a general- purpose software with a lot of routines like pre-processing of data, plotting and long term prediction. The programme can be bought from In Situ Software in Munich.

5.1.2 The Multiple Linear Regression method

This is a non iterative very fast matrix method called Multiple Linear Regression, MLR, that is available in most standard programme packages as LOTUS, EXCEL or more specialised statistical programmes like MINITAB or SISS. Multiple Linear Regression is a generalization of standard Linear Regression used to fit a straight line to data in two dimensions.

Linear does only mean that the model has to be written as a sum of terms with the parameters p_n as a multiplier in front of the terms. For example: $Y_{out} = p_0 + p_1 \cdot f(x_1,x_2) + p_2 \cdot g(x_1, x_3, x_4) + p_3 \cdot h(x_2, x_5)$. The sub models f(x..) g(x..) and h(x..) in each term can be non-linear.

A special case of MLR has also been tested that makes it possible to identify also non-linear characteristics. It is now possible to identify the different values of a parameter for different subsets of the database. This has made it possible to identify for example the parameter for zero loss efficiency angle by angle without the need to have an equation. See *figure 7.3a* and *b* and *7.4*. This is very useful for special collectors as ETC, CPC or unglazed collectors with round separate absorber tubes that can not be modelled with the standard IAM equations. In fact also the two-

axis IAM variation is possible to resolve from outdoor dynamic testing! The derived IAM results can be used directly in simulation programmes as TRNSYS WATSUN or MINSUN.

It has also been found that the heat loss parameter F'UL can be identified in successive ranges of ΔT. This overcomes the problem of a slight nonlinearity and the correlation between the ΔT and ΔT2 terms. The heat loss coefficient can also be modelled in this way for collectors with special heat loss effects as heat pipe collectors or other special designs. The use of night time measurements of the heat losses would also be possible to evaluate with MLR. This could shorten the testing time dramatically if one can correct for the small difference between day and night heat losses. This has only been tested a few times but with promising results. The key is to model the difference in day and night heat losses in a simple but accurate enough way.

6 *COLLECTOR MODELS*

There are a number of collector models that differ significantly in the individual sub models of the collector to take into account different second or third order effects more accurately and also with the aim to model the collector output at very short time steps and steps in inlet temperature and flow rate.

Still all the collector models agree in the common general structure in such aspects as zero loss efficiency, heat loss coefficient, and thermal capacitance correction. The collector models with the more advanced heat loss models need the iterative DF parameter identification programme. Whereas the extended ISO model with correction terms can be evaluated with standard Multiple Linear Regression.

As a basis for the discussion about the importance of different details in the collector models an elasticity analysis was made to investigate how important the different parts of the collector equation are. *Figure 6.1* shows the result. It can be seen that the optical or zero loss part of the collector equation has the largest influence on the annual performance. The heat losses comes only in second or third place depending on the operating temperature. This means that most important is to have an accurate modelling of the optics in the collector that determines the absorbed energy in the collector. If this is not properly modelled the heat loss part of the collector will be forced to include the optical model error as wrong or biased values for the heat loss parameters.

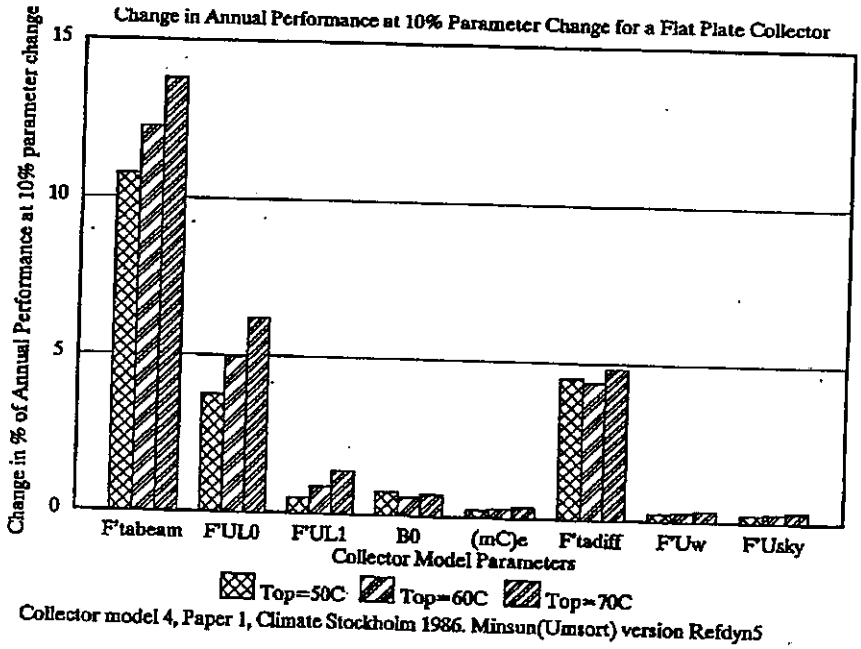

Figure 6.1: **Results from an elasticity analyse showing how much the annual collector output is varying for a 10% variation in the different collector parameters.**

6.1 Collector models for testing

There are three main collector models that has been used in this work The extended ISO model, the MFC model and the Dyncoll model. For comparison we start with the collector model options in ISO 9806-1.

6.1.1 The ISO 9806-1 model

This model has been widely used both in testing and for simulation. The basic equation is a stationary model for near normal incidence angle operation. The nomenclature is given in the next section.

$$q_U = F'(\tau\alpha)_e - F'U_0\Delta T - F'U_1(\Delta T)^2 \qquad [6.1]$$

The insolation is denoted G_b to point out that only high insolation levels are accepted in the test sequence with low diffuse fraction. No correction for non-stationary conditions is made, so very stable inlet and radiation conditions are needed for each test point. Furthermore it is assumed that the incidence angle is normal, (incident solar radiation perpendicular to the collector aperture area), so that incidence angle effects can be neglected. This restricts the measuring time very much during normal weather conditions except for very sunny climates.

There are in the ISO 9806-1 standard also optional test procedures for the determination of incidence angle dependence of the zero loss efficiency and the effective thermal capacitance of the collector. The full equation from all the options in the ISO standard can be written:

$$q_U = F'(\tau\alpha)_e K_{\tau\alpha b}(\theta)I_b - F'U_0\Delta T - F'U_1(\Delta T)^2 - (mC)_e dTm/dt \qquad [6.2]$$

Note that this is a clear weather or indoor simulator model as the solar radiation is treated as beam radiation. No correction term for diffuse radiation is proposed in the standard. In most simulation programmes the solar radiation is divided into beam and diffuse radiation and a separate incidence angle correction is added for diffuse radiation. This correction term, $K_{\tau\alpha d}$, is often derived by integrating over the incidence angle dependence for beam radiation of the collector. Therefore a complete ISO test gives this information for standard simulation purposes, but the cost would be much higher compared to a dynamic collector test giving all parameters at the same time.

6.1.2 The Extended ISO model

This model is basically the same as the ISO model but with some extra correction terms for diffuse radiation, wind speed, sky temperature and wind dependence in the zero loss efficiency (e.g. unglazed rubber collectors). A correction term is also given if the inlet and outlet sensors can not be mounted close enough to the collector. Such temperature losses should of course be avoided in laboratory testing. All the ISO and extended model parameters can be identified with MLR (Multiple Linear Regression) as well as with DF (Dynamic Fitting). The sub models in this equation have all been verified against measured data in other IEA SH&C activities, as within IEA Task VI and Task III. They are also based on physics, even if the detailed heat loss pattern of a solar collector is very complicated and has to be handled with correlation models, mainly due to the mix of natural and forced convection heat flows.

$$q_U = F'(\tau\alpha)_e K_{\tau\alpha b}(\theta) G_b + F'(\tau\alpha)_e K_{\tau\alpha d} G_d - k_w G_{tot} w - F'U_0\Delta T - F'U_1(\Delta T)^2 - F'U_w\Delta T w - F'U_{sky}\Delta T_{sky} - (mC)_e dT_f/dt - U_p\Delta T \qquad [6.3]$$

q_u	=	Collector array thermal output	[W/m^2]
$F'(\tau\alpha)_e$	=	Zero loss efficiency for direct radiation at normal incidence.	[-]
$K_{\tau\alpha b}(\theta)$	=	Incidence angle modifier for direct radiation	[-]
$K_{\tau\alpha d}$	=	Incidence angle modifier for diffuse radiation	[-]
G_{tot}	=	Global radiation onto the collector plane (G001 in meas. sp.)	[W/m^2]
G_b	=	Direct radiation onto the collector plane	[W/m^2]
G_d	=	Diffuse radiation onto the collector plane (G002 in meas. sp.)	[W/m^2]
$F'U_0$	=	Heat loss coefficient at $(T_m - T_a)=0$	[W/(m^2·K)]
$F'U_1$	=	Temperature dependence of the heat loss coeff.	[W/(m^2·K^2)]
$F'U_w$	=	Wind speed dependence of the heat loss coeff.	[Ws/(m^3·K)]

$F'U_{sky}$	=	Sky temperature dependence of the heat loss coeff.	[W/(m^2·K)]
U_p	=	Piping heat loss coefficient per m^2 of coll.	[W/m^2·K]
$(mC)_e$	=	Effective thermal capacitance including piping for the collector array.	[J/(m^2·K)]
ΔT	=	Temperature difference (T_m -T_a)	[°C]
ΔT_{sky}	=	Temperature difference (T_a -T_{sky})	[°C]
w	=	Wind speed near the collector	[m/s]
k_w	=	Wind dependence in the zero loss efficiency	[s/m]
dT_f/dt	=	Mean time derivative for the average fluid temperature T_m within the time step.	[K/s]
T_m	=	Mean fluid temperature in the collector (T_{in}+T_{out})·0.5	[°C]
T_a	=	Ambient air temperature near the collector	[°C]
T_{sky}	=	Effective broadband sky temperature	[°C]
θ	=	Incidence angle for the direct solar radiation onto the collector plane	[radians]

6.1.3 The MFC Matched Flow Collector model

The MFC Matched Flow Collector model has been developed by *Per Isakson* at the Royal Institute of Technology, KTH, in Sweden. This model is very elaborated in the heat loss and thermal capacitance part. An elegant analytical solution has been derived so that a distributed absorber model in which the temperature dependency of both local capacitances and local UL values can be handled without iterations within each time step. One of the main aims is to be able to model the heat losses more accurately at low flow conditions and rapid changes in inlet temperature when the temperature increase along the absorber flow path can be highly non-linear. Wind and sky temperature influence on the heat losses are also options in the model. The optical part of the collector equation is prepared with a large number of standard options for the incidence angle dependence. The model is written as a TRNSYS component and the model parameters are identified with the external model option in DF. Per Isakson has also written a special interface between the MFC model and DF to speed up the parameter identification and also document each run in a systematic way. A more detailed description can be found in the MFC manual [Isakson 1994] and the PhD Thesis [Isakson 1995].

The collector parameters used in the MFC model are similar but not exactly the same as in the ISO model. The MFC model is based on an integration of local temperatures in the collector while the ISO model uses the aritmetic mean temperature Tm between inlet and outlet of the collector. The differences and conversion between the parameter values have been investigated by Pierre Bremer and Per Isakson [Isakson 1995]. For normal flow conditions, 0.02 kg/(s*m2), the ISO parameters can be used in the MFC model (or the opposite) without correction. Even at low flow conditions down to 1/6 of standard test flow, 0.0033 kg/(s*m2), the parameter values only differ by 0.3% which is less than the experimental uncertainty in test results. Only at 1/10 of normal test flow the parameters differ by 1% due to the mathematical differences in the models. This is the lowest flow that can be used in practice as the temperature rise over the

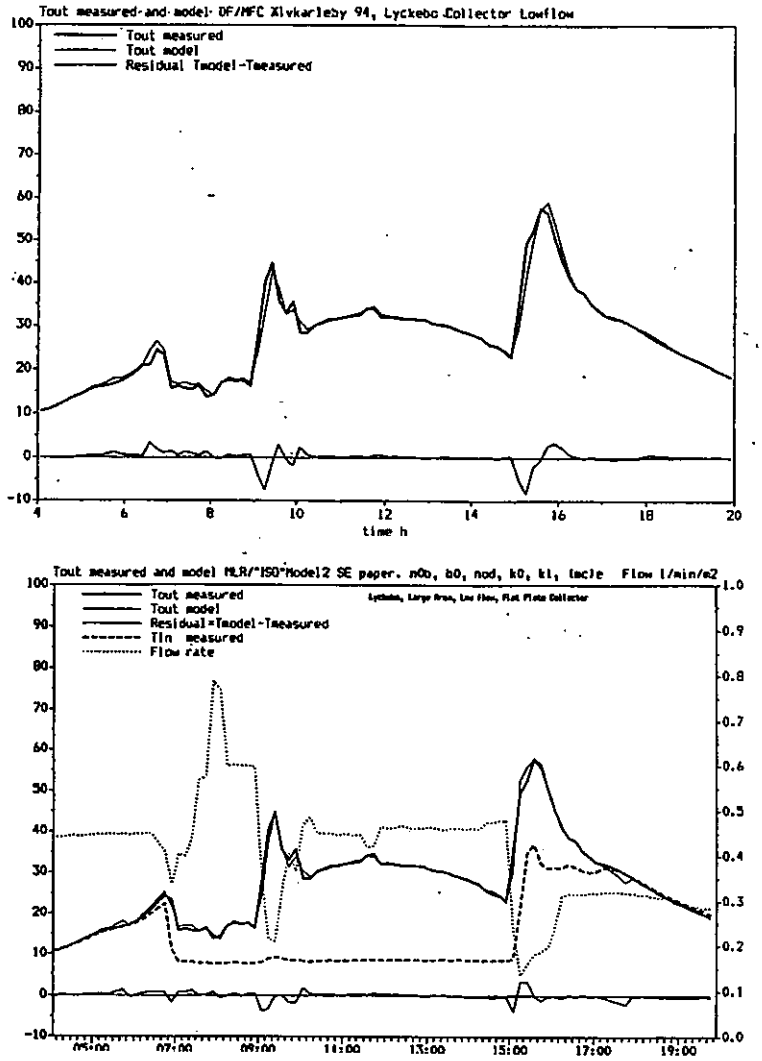

Figure 7.1 a-b: The upper diagram is the MFC model with parameters identified with DF. The lower diagram is the "ISO" Tm based model with corrections and parameters identified with MLR.

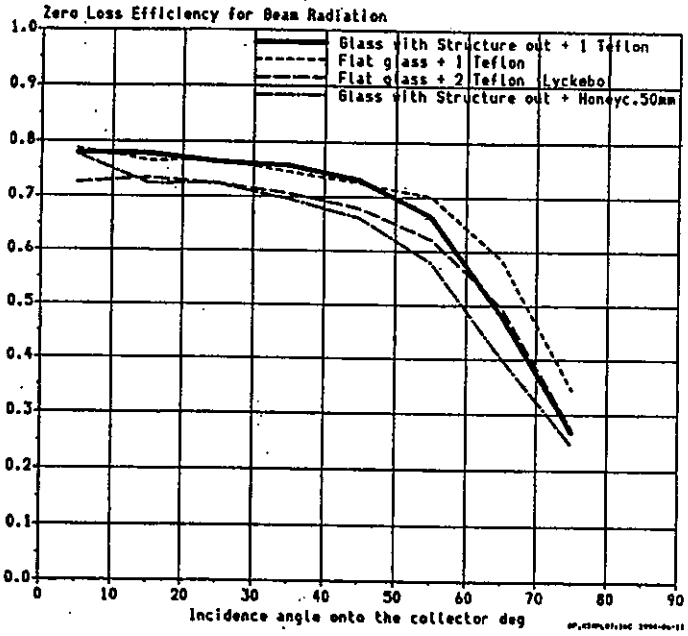

Figure 7.3: **Incidence angle curves for a number of different collectors identified with the extended ISO model and special routine in MLR. The identification of incidence angle dependence takes only a few seconds extra and is done at the same time and in the same programme as the other collector parameters are identified.**

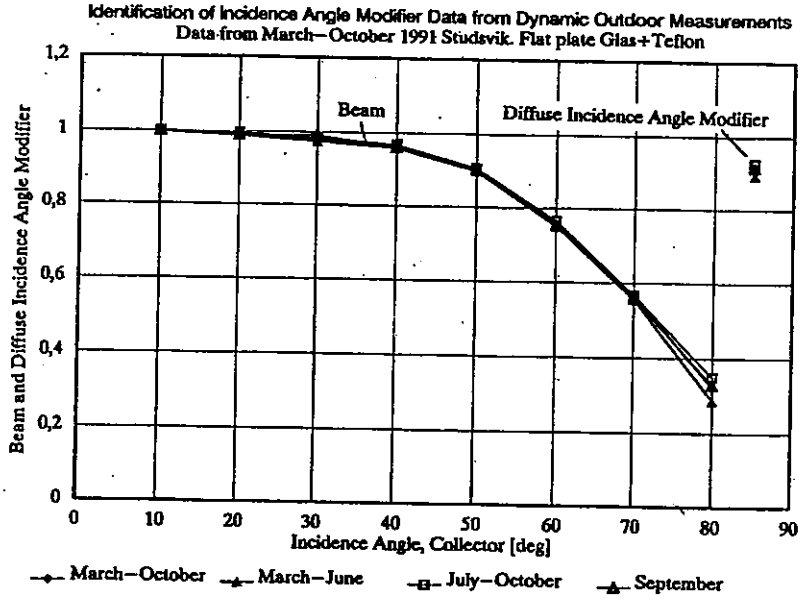

Figure 7.4: **Repeatability in incidence angle dependence of the zero loss efficiency and the zero loss efficiency for diffuse radiation.**

An other important question for the acceptance of dynamic testing standardised product evaluation, is also how stable the results are when mal test at different periods in time at the same laboratory (repeatability) a different test laboratories (reproducibility).

The reproducibility of dynamic collector testing with a round robin test of the collectors at different laboratories still needs to be done, but the repeatabilit been verified at several laboratories already.

The repeatability of the test results has been investigated, at ITW in Stuttga repeating the evaluation of the collector parameters for different test sequence comparing the results to see how stable the parameters are. The results are s in *Table 2.*

One can see here also that the collector parameters vary slightly but the var range is very small and similar for both stationary and dynamic testing. Thi very promising result as the stationary test data are selected very care according to the DIN 4757 part 4 standard, to get well controlled oper conditions and small parameter uncertainties.

The test data used for *Table 2* comes from a reference collector for v measurements have been done during 5 months. Five sets of six selected days mainly clear weather have been chosen to allow both stationary and dyr evaluation for the same set of days.

Table2: ***Comparison of repeatability of collector parameters derived with stationary (DIN) and dynamic (DCT) testing but for different test periods. Test data an results from five months of measurements at ITW in Stuttgart, Germany.***

Test period number	Test method	Zero loss eff. for the collector	First order Heat loss coefficient	Second Order Heat loss coefficient	Total Heat loss coefficient at DT=50C	Incidence angle coefficient r	Th ca tai : col
		[-]	[W/(m2*K)]	[W/(m2*K2)]	[-]	[-]	kJ/(:
Z1	DCT	0.771	3.945	0.009	4.4	0.3323	1
	DIN	0.764	3.567	0.014	4.27		
Z2	DCT	0.759	3.316	0.017	4.17	0.3452	9
	DIN	0.747	2.863	0.023	4.013		
Z3	DCT	0.768	4.022	0.01	4.52	0.3018	9.
	DIN	0.763	3.73	0.013	4.38		
Z4	DCT	0.75	2.953	0.02	3.95	0.3189	7.
	DIN	0.756	3.147	0.019	4.1		
Z5	DCT	0.76	3.22	0.018	4.12	0.3173	9.
	DIN	0.753	3.66	0.012	4.26		

collector will be more than 60°C at high irradiation conditions. Of course also changes in the heat transfer rate inside the absorber fluid channels will have an influence at low flow conditions but this has similar influences for both models.

For simulation purposes the MFC model has an advantage over the ISO model that it gives the outlet temperature of the collector without iterations. In the case of the ISO model, one or two iterations are needed to calculate a sufficiently accurate value of Tm in the ISO equation. This disadvantage for the ISO model is not a major problem as also other component models, as storages, need iterations in a system simulation.

6.1.4 The DF Dyncoll collector model

Dyncoll is a multinode collector model that is distributed together with the DF programme package. The absorber is divided into a number of nodes along the flow path, similar to the MFC model, but in this case no analytical solution is used. The focus is also here to take into account the temperature distribution along the absorber flow path. The optical part of the collector equation is the same as the ISO collector model except that the incidence angle dependence is described with the Ambrosetti equation instead of the ASHRAE b0 function. The parameter identification is done with Dyncoll as an external model. A more detailed description can be found in the DF manual delivered together with the programme.

6.2 Finite difference Collector model for detailed simulation

Some limited work has also been done with a finite difference collector model to investigate the wind, sky temperature and thermal capacitance effects during a test with rapid changes in inlet temperature and solar radiation. It was found that the back insulation of the collector gives a small additional very long time constant that none of the present collector models take into account. By avoiding or having symmetrical step changes, up and down, in inlet temperature in the test sequence this small effect is taken care of. The effect could also be seen experimentally in the ISFH indoor test described in *Chapter 7*.

Figure 6.2 shows an example of the results from one of the runs with the programme for a collector with high density back insulation. Step changes have been applied in solar radiation, inlet temperature, wind speed and effective sky temperature. It can be seen that the step changes in inlet temperature show that there is a very long time constant connected to the back insulation. This has a significant influence on the collector output for up to one hour after the temperature step. This second order capacitance effect is not taken into account in any of the collector models presented above. This is a research field where further collector modelling might shorten the test duration even more.

Figure 6.2: **Results from simulations with a finite difference model. Step changes have been applied in solar radiation, inlet temperature, wind speed and effective sky temperature.**

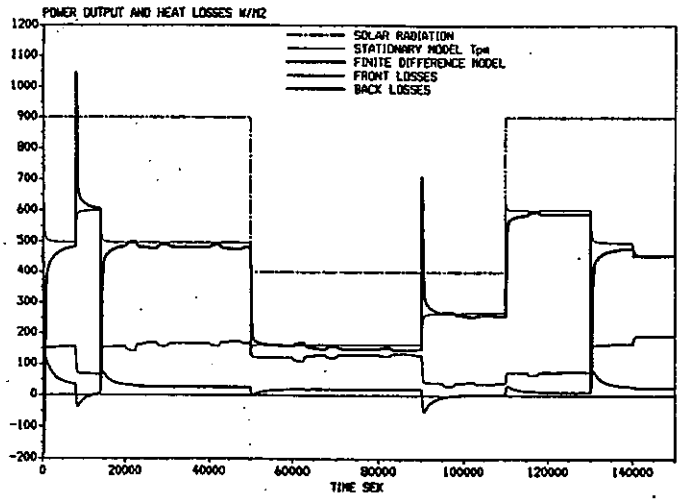

Another more advanced attempt to investigate short-term effects in collector modelling and testing with a reference model is described in Per Isakson's PhD Thesis [Isakson 1995]. A detailed reference model called FFC, based on Fast Fourier Transforms, was developed and compared to the MFC model. Similar problems were recognised, when modelling the collector output during fast changes in the input variables, also for the MFC model.

7 *RESULTS FROM INDOOR AND OUTDOOR TESTING*

For routine testing purposes it has turned out that the difference is very small between the different models and methods. The collector parameters that are common for the stationary ISO collector model also come out the same if a test is extended so that also stationary test points can be derived from the test period.

Therefore the MLR method, with a modification of the ISO(Tm) collector model used in the present stationary test standard, is sufficient for a wide range of collectors and is presently used by the Swedish National Testing and Research Institute for routine collector testing. Basically the collector equation is the same as in the present ISO standard with $T_m = (T_{out}+T_{in})\cdot 0.5$ as the reference temperature, but correction terms are added for thermal capacitance, wind speed, thermal sky radiation etc. The separate test for incidence angle modifiers and thermal capacitance can now be integrated into a single dynamic test.

collector will be more than 60°C at high irradiation conditions. Of course also changes in the heat transfer rate inside the absorber fluid channels will have an influence at low flow conditions but this has similar influences for both models.

For simulation purposes the MFC model has an advantage over the ISO model that it gives the outlet temperature of the collector without iterations. In the case of the ISO model, one or two iterations are needed to calculate a sufficiently accurate value of Tm in the ISO equation. This disadvantage for the ISO model is not a major problem as also other component models, as storages, need iterations in a system simulation.

6.1.4 The DF Dyncoll collector model

Dyncoll is a multinode collector model that is distributed together with the DF programme package. The absorber is divided into a number of nodes along the flow path, similar to the MFC model, but in this case no analytical solution is used. The focus is also here to take into account the temperature distribution along the absorber flow path. The optical part of the collector equation is the same as the ISO collector model except that the incidence angle dependence is described with the Ambrosetti equation instead of the ASHRAE b0 function. The parameter identification is done with Dyncoll as an external model. A more detailed description can be found in the DF manual delivered together with the programme.

6.2 Finite difference Collector model for detailed simulation

Some limited work has also been done with a finite difference collector model to investigate the wind, sky temperature and thermal capacitance effects during a test with rapid changes in inlet temperature and solar radiation. It was found that the back insulation of the collector gives a small additional very long time constant that none of the present collector models take into account. By avoiding or having symmetrical step changes, up and down, in inlet temperature in the test sequence this small effect is taken care of. The effect could also be seen experimentally in the ISFH indoor test described in *Chapter 7*.

Figure 6.2 shows an example of the results from one of the runs with the programme for a collector with high density back insulation. Step changes have been applied in solar radiation, inlet temperature, wind speed and effective sky temperature. It can be seen that the step changes in inlet temperature show that there is a very long time constant connected to the back insulation. This has a significant influence on the collector output for up to one hour after the temperature step. This second order capacitance effect is not taken into account in any of the collector models presented above. This is a research field where further collector modelling might shorten the test duration even more.

Figure 6.2: **Results from simulations with a finite difference model. Step changes have**

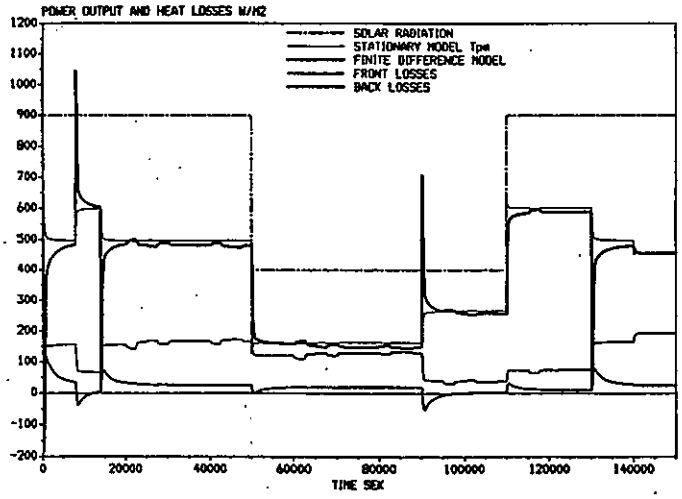

been applied in solar radiation, inlet temperature, wind speed and effective sky temperature.

Another more advanced attempt to investigate short-term effects in collector modelling and testing with a reference model is described in Per Isakson's PhD Thesis [Isakson 1995]. A detailed reference model called FFC, based on Fast Fourier Transforms, was developed and compared to the MFC model. Similar problems were recognised, when modelling the collector output during fast changes in the input variables, also for the MFC model.

7 *RESULTS FROM INDOOR AND OUTDOOR TESTING*

For routine testing purposes it has turned out that the difference is very small between the different models and methods. The collector parameters that are common for the stationary ISO collector model also come out the same if a test is extended so that also stationary test points can be derived from the test period.

Therefore the MLR method, with a modification of the ISO(Tm) collector model used in the present stationary test standard, is sufficient for a wide range of collectors and is presently used by the Swedish National Testing and Research Institute for routine collector testing. Basically the collector equation is the same as in the present ISO standard with $T_m = (T_{out}+T_{in})\cdot 0.5$ as the reference temperature, but correction terms are added for thermal capacitance, wind speed, thermal sky radiation etc. The separate test for incidence angle modifiers and thermal capacitance can now be integrated into a single dynamic test.

7.1 Experimental results

7.1.1 Outdoor test data

These outdoor test data comes from the long-term testing of solar collectors at the Vattenfall Älvkarleby laboratory in Sweden and certification testing of solar collectors at ITW in Stuttgart, Germany.

Figures 7.1a and *7.2a* show the result for the more advanced MFC matched flow collector model using parameters identified by the DF programme for the same period. The parameter fit takes about 30 minutes for 5 searches for local minima to determine the global minima in the difference in outlet temperature between model and measurements.

Figures 7.1b and *7.2b* show the extended ISO collector model, with correction terms for incidence angle effects and thermal capacitance. This model is evaluated with MLR. The parameter set is determined within a few seconds for a data set of about 5000 time steps using a standard programme such as Lotus, Excel or Minitab.

Figures 7.1 and *7.2* show that the difference in model fit of the outlet temperature is very small, for both models and methods, in spite of almost step changes in both flow rate and inlet temperature for one of the days. The other day shows the high temperature behaviour of the models. The flow rate is down to 30 % of standard test flows, close to what is normally called low flow. The collector is a large area 12 m^2 flat plate collector. It is designed for low flow with serpentine connection of the Sunstrip absorbers. The collector is the same as in the 4000 m^2 Lyckebo plant.

Figures 7.3 and *7.4* show the result of the extended MLR method to identify the zero loss efficiency variation angle by angle. *Figure 7.4* shows that the repeatability is very good even if the data was taken from a field test. Note also that the diffuse incidence angle modifier is very stable.

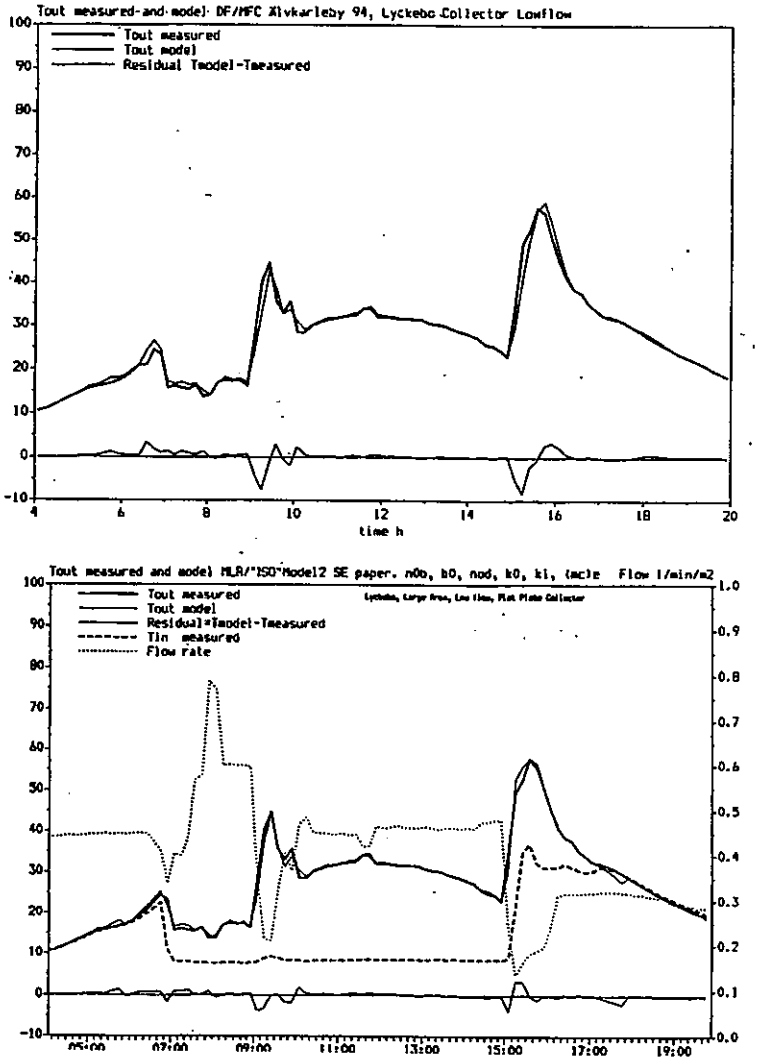

Figure 7.1 a-b: **The upper diagram is the MFC model with parameters identified with DF. The lower diagram is the "ISO" Tm based model with corrections and parameters identified with MLR.**

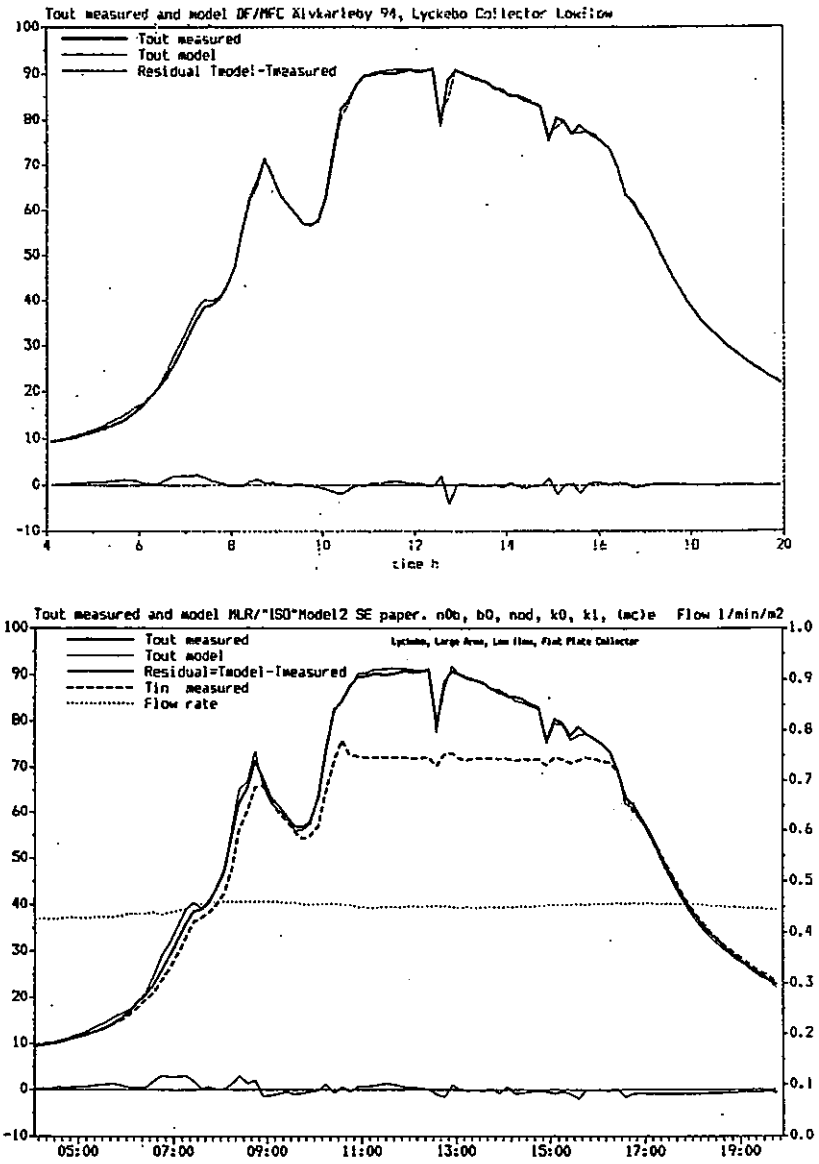

Figure 7.2a-b: The upper diagram is the MFC model with parameters identified with DF. The lower diagram is the "ISO" Tm based model with corrections and parameters identified with MLR.

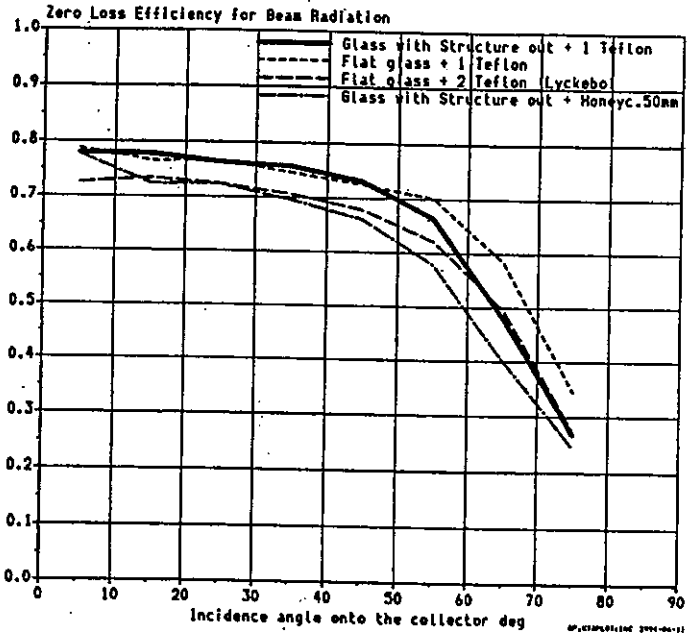

Figure 7.3: **Incidence angle curves for a number of different collectors identified with the extended ISO model and special routine in MLR. The identification of incidence angle dependence takes only a few seconds extra and is done at the same time and in the same programme as the other collector parameters are identified.**

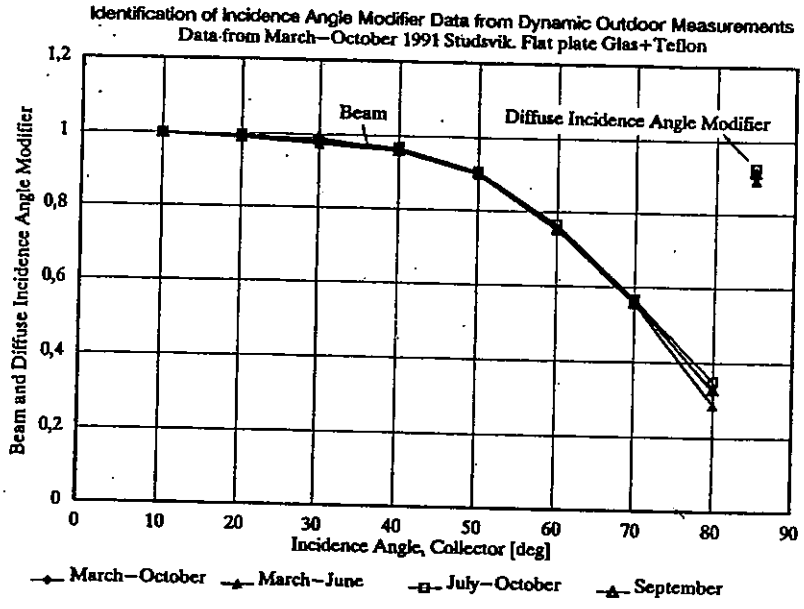

Figure 7.4: **Repeatability in incidence angle dependence of the zero loss efficiency and the zero loss efficiency for diffuse radiation.**

One of the most important questions for the adaptation of dynamic testing for routine testing is if dynamic testing gives the same results as the present stationary standards.

Table 1 shows a comparison between collector parameters derived both from stationary and dynamic outdoor testing. The test data and results come from ITW in Stuttgart. The measurement specifications and test sequence from IEA Task 14 described in chapter 2 and 3 were used for the dynamic testing.

All day dynamic test data from six days were used. In the dynamic method (DCT) data from the whole day were used, whereas only selected data at stable weather and temperature conditions near noon, according to the DIN 4757 part 4 requirements, were used for the stationary evaluation (DIN).

It can be seen that the results are almost independent of the test method even if small differences can be seen especially in the heat loss parameters. The two columns for effective collector efficiency at a certain operating condition indicates that the difference in long-term performance prediction can be expected to be much smaller than the variation in individual parameter values.

The collectors K0, K1 and K4 are flat plate collectors and K10 and K15 are evacuated tubular collectors of different designs. No significant variation of the results due to the collector design can be seen.

Table1: ***Comparison of collector parameters derived with stationary and dynamic outdoor testing for a number of different collectors. Test data and results come from ITW in Stuttgart, Germany.***

Collector type	Test method DIN = Stationary. DCT = Dynamic.	Zero loss eff. for the collector.	First order Heat loss coefficient.	Second Order Heat loss coefficient	Collector Efficiency at DT/G=0.01	Collector Efficiency at DT/G=0.05
		[-]	[W/(m2*K)]	[W/(m2*K2)]	[-]	[-]
K0	DCT	0.759	3.316	0.017	0.559	0.291
	DIN	0.747	2.863	0.023	0.558	0.277
K1	DCT	0.789	3.996	0.014	0.561	0.277
	DIN	0.788	4.377	0.011	0.547	0.262
K4	DCT	0.793	3.666	0.012	0.586	0.330
	DIN	0.791	3.735	0.011	0.582	0.330
K10	DCT	0.563	0.453	0.008	0.524	0.454
	DIN	0.557	0.542	0.006	0.518	0.455
K15	DCT	0.736	0.900	0.008	0.675	0.582
	DIN	0.748	1.299	0.005	0.673	0.578

An other important question for the acceptance of dynamic testing, for standardised product evaluation, is also how stable the results are when making a test at different periods in time at the same laboratory (repeatability) and at different test laboratories (reproducibility).

The reproducibility of dynamic collector testing with a round robin test of the same collectors at different laboratories still needs to be done, but the repeatability has been verified at several laboratories already.

The repeatability of the test results has been investigated, at ITW in Stuttgart, by repeating the evaluation of the collector parameters for different test sequences and comparing the results to see how stable the parameters are. The results are shown in *Table 2.*

One can see here also that the collector parameters vary slightly but the variation range is very small and similar for both stationary and dynamic testing. This is a very promising result as the stationary test data are selected very carefully, according to the DIN 4757 part 4 standard, to get well controlled operating conditions and small parameter uncertainties.

The test data used for *Table 2* comes from a reference collector for which measurements have been done during 5 months. Five sets of six selected days with mainly clear weather have been chosen to allow both stationary and dynamic evaluation for the same set of days.

Table2: ***Comparison of repeatability of collector parameters derived with stationary (DIN) and dynamic (DCT) testing but for different test periods. Test data and results from five months of measurements at ITW in Stuttgart, Germany.***

Test period number	Test method	Zero loss eff. for the collector	First order Heat loss coefficient	Second Order Heat loss coefficient	Total Heat loss coefficient at DT=50C	Incidence angle coefficient r	Thermal capaci-tance of the collector
		[-]	[W/(m2*K)]	[W/(m2*K2)]	[-]	[-]	kJ/(m2*K)
Z1	DCT	0.771	3.945	0.009	4.4	0.3323	10.57
	DIN	0.764	3.567	0.014	4.27		
Z2	DCT	0.759	3.316	0.017	4.17	0.3452	9.73
	DIN	0.747	2.863	0.023	4.013		
Z3	DCT	0.768	4.022	0.01	4.52	0.3018	9.525
	DIN	0.763	3.73	0.013	4.38		
Z4	DCT	0.75	2.953	0.02	3.95	0.3189	7.644
	DIN	0.756	3.147	0.019	4.1		
Z5	DCT	0.76	3.22	0.018	4.12	0.3173	9.056
	DIN	0.753	3.66	0.012	4.26		

7.1.2 *Indoor Solar Simulator data*

At the ISFH Solar Simulator two flat plate collectors have been tested according to the IEA test sequence with steps up and down in temperature and at different wind speeds. This solar simulator has also the possibility to control the "sky" temperature. The difference here is also almost insignificant between the two dynamic methods. Both can model the measured outlet temperature very well. The only visible difference is due to the long time constant of the collector insulation after changes in inlet temperature which induces large changes in the insulation temperature profile.

Table 3 and *4* give the stationary and dynamically derived parameters for the proposed test sequence with rising temperature, decreasing temperature and full test sequence. The zero loss efficiency is very stable within ± 0.3 %. The heat loss coefficient varies systematically in the same way for both static and dynamic testing within ± 0.15 W/(m^2·K) at 50°C overtemperature for example. When using all data the dynamic method also agrees very well with the stationary data. It can also be noted that the thermal capacitance is almost independent of rising or decreasing temperature steps.

Table3: ***Extended ISO model parameters derived with MLR for a selective flat plate collector with solar glass, teflon foil and Sunstrip absorber. Test data from ISFH in Germany.***

Test type	Selection of data	F'no	F'UL0	F'UL1	F'Uw	(mC)e
Stationary	All stationary data	0.780	2.93	0.012	0.13	-
Dynamic	All data	0.778	2.90	0.014	0.08	6720
Stationary	Heating up, all stat.	0.778	3.15	0.009	0.12	-
Dynamic	Heating up	0.777	3.15	0.011	0.07	6850
Stationary	Cooling down, all stat.	0.782	2.72	0.015	0.13	-
Dynamic	Cooling down	0.780	2.65	0.017	0.09	6600

Table 4: ***Extended ISO model parameters derived with MLR for a nonselective flat plate collector with green glass, Black painted copper absorber with serpentine flow. Test data from ISFH in Germany.***

Test type	Selection of data	F'no	F'UL0	F'UL1	F'Uw	(mC)e
Stationary	All stationary data	0.771	4.76	0.025	0.43	-
Dynamic	All data	0.771	4.98	0.026	0.30	5530
Stationary	Heating up, all stat.	0.775	5.03	0.022	0.43	-
Dynamic	Heating up	0.773	5.39	0.020	0.29	5670
Stationary	Cooling down, all stat.	0.769	4.50	0.028	0.45	-
Dynamic	Cooling down	0.769	4.56	0.031	0.32	5390

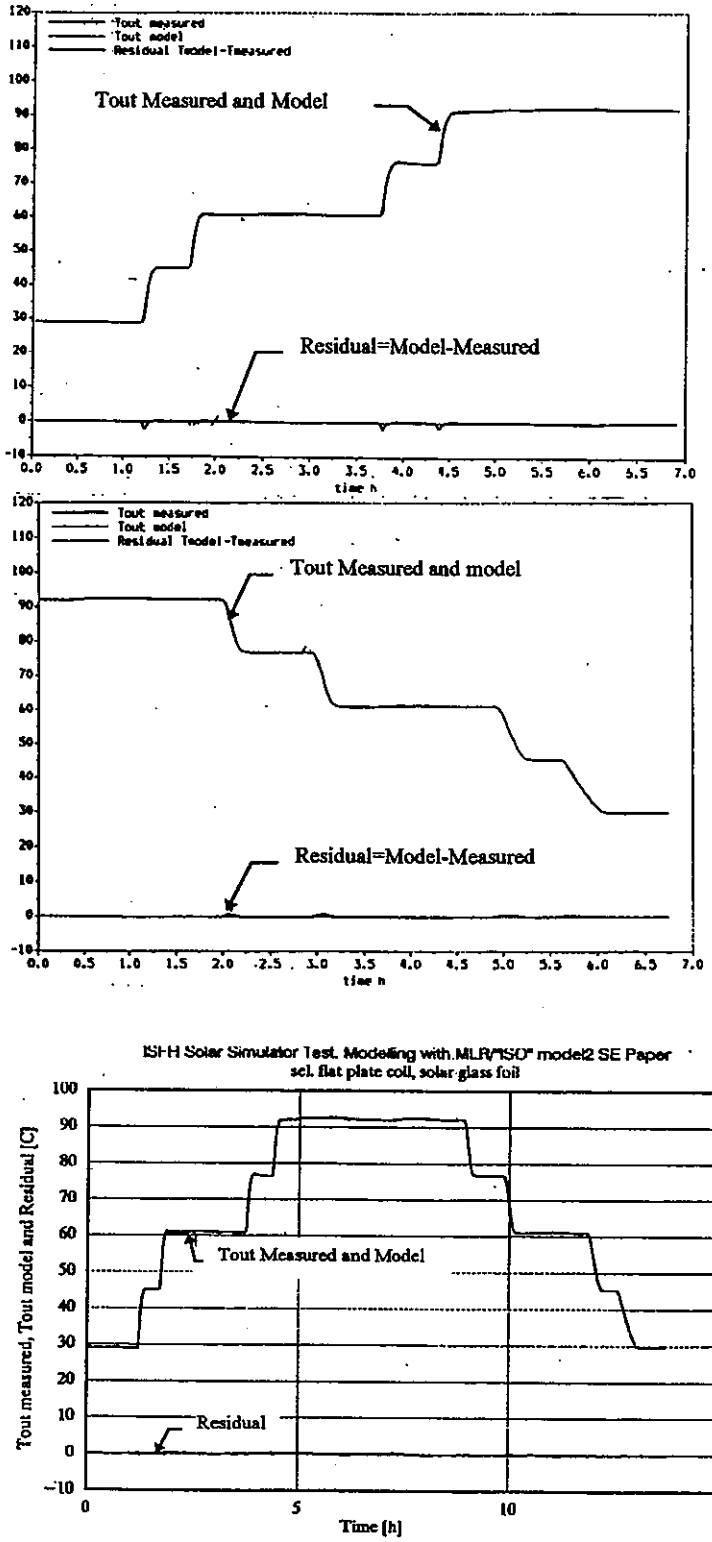

Figure 7.5 a-b: Shows a comparison between the measured and modelled outlet temperature during the test with the same methods and models as in figure 1 and 2. Test data from ISFH in Hameln.

7.2 Long term prediction

Two different checks are presented here. One based on results from indoor collector testing at ISFH and the other based on repeated outdoor testing at ITW.

First an example is given of the repeatability in long term prediction using the parameters derived in the non-stationary solar simulator test above, as input to an updated version of the MINSUN programme developed within the IEA Task VII that can use all model parameters in the extended ISO model. (This programme is presently used by the Swedish National Testing and Research Institute in Sweden to extrapolate collector test results to annual performance figures for collector certificates).

The annual performance prediction using parameters from either rising or decreasing inlet temperature was within 2 % from the result when using parameters identified with data from the whole test sequence (equal number of steps up and down). This indicates that the dynamic correction is very good and that reliable long-term performance results can be derived with the extended test method even under extremely biased dynamic conditions with step changes in inlet temperature. An other check of the accuracy in long-term prediction based on outdoor collector test data has been made at ITW in Stuttgart. . *Table 5* shows some results.

*Table 5: **Check of the accuracy in long-term prediction based on short term testing for one period and extrapolation to an other period. Test data and results come from ITW in Stuttgart, Germany.***

Collector Parameters from test period number Zx:	**asured Collector output for period Zy and Calculated(extrapolated) Collector Output for period number Zy using parameters from an other period Zx but climate and operating conditions from period Zy: [W] The difference is given relative to the measured performance [%]**				
	Z1	**Z2**	**Z3**	**Z4**	**Z5**
	Measured performance [W]				
	797	**811**	**890**	**949**	**941**
	Calculated (Extrapolated) Performance [W] and difference [%]				
Z1	799 ± 1.2 0.25 %	817 ± 1.4 0.74 %	882 ± 1.3 0.9 %	956 ± 1.4 0.74 %	934 ± 1.5 0.75 %
Z2	783 ± 0.95 1.76 %	812 ± 0.91 0.12 %	874 ± 0.84 1.8 %	939 ± 1 1.05 %	924 ± 0.96 1.8 %
Z3	803 ± 2.5 0.75 %	818 ± 2.1 0.86 %	884 ± 1.7 0.67 %	952 ± 1.8 0.32 %	929 ± 1.4 1.3 %
Z4	802 ± 1.5 0.63 %	837 ± 1.8 1.97 %	894 ± 1.5 0.45 %	953 ± 1.2 0.42 %	940 ± 1.3 0.10 %
Z5	802 ± 1.6 0.63 %	833 ± 1.8 2.77 %	893 ± 1.5 0.34 %	954 ± 1.1 0.53 %	938 ± 1.2 0.30 %

Collector parameters derived with dynamic testing from one test period has been used to calculate the collector output for several completely different test period to see how accurate the results are when extrapolating the test results to long term performance results. It can be seen that the difference in collector performance is less that 3%.

7.3 Demo diskette

Pierre Bremer, Sede SA in Switzerland made a Multiple Regression Programme in Pascal that demonstrates the MLR evaluation method. The input data is the same as for the Paper in Solar Energy [Perers 1993], and the results are compared. The demo diskette can be copied to a separate directory and started with the command "bengt". Copies of the demodiskette can be ordered from the authors.

The DF programme package also contains a demo option to demonstrate the iterative identification method.

8 STATUS OF STANDARDISATION

A proposal to ISO about dynamic collector testing has been given by the Swedish National Testing and Research Institute, SP. The proposal has been accepted as a work item within ISO. The next step will be a proposal for a test procedure that will be written by the same institution in close co-operation with the IEA Task 14 experts.

The same procedure has now started also within the European standardisation organisation CEN. A proposal has been sent to CEN and a validation of the test method as written has been started. The test sequence will be backwards compatible so that also stationary test data can be derived if the test duration is extended enough so that also stationary test data will be available.

Both proposals are put up as an extension to the present ISO 9806-1 standard and not a separate new standard. This will speed up the process due to the fact that the test equipment and procedure are similar in many respects. The proposals will be backwards compatible as the ISO collector model is still used but with correction terms for dynamic and incidence angle effects. For example standard efficiency diagrams can be produced if the extra correction parameters are fixed to representative values for stationary clear sky conditions.

9 ACKNOWLEDGEMENTS

Funding from National Research Organisations is gratefully acknowledged. Important contributions to this IEA work has come from Kingston University in Canada, Rappersville and SEDE SA in Switzerland, München University, ITW in

Stuttgart, ISFH in Emmerthal, TNO in the Netherlands, DTI in Denmark, SP in Sweden, The Royal Institute of Technology in Sweden and the Vattenfall Älvkarleby Laboratory in Sweden.

10 REFERENCES

This references list contains both official documents but also a list of internal reports within IEA Task 14.

10.1 Publications related to IEA 14 Group 1. Collector Testing

Internal IEA Task 14 Publications.

- *Data Requirement Specification for IEA SH&C Task 14 Sub Task DCST Collector Testing Group 1.* B Perers et. al. , VUAB, Sweden.
- *Dynamic Fitting of Matched Flow Collector Model to outdoor Test Data,* P.Isakson, KTH, Sweden, Ueli Frei, and Nigel Findlater, ITR, Switzerland, July, 1992.
- *Matched Flow Collector Model. Progress Report,* P.Isakson, KTH, Sweden, Jan 1993.
- *Influence of Variations in Wind Speed and Long Wave Sky Radiation on the Performance of Solar Collectors.* B. Perers VUAB Sweden.
- *Relations between Dynamic Fit Parameters and ISO Collector second order Linear Regression Equation.* P. Isakson. P. Bremer. N. Findlater.
- *MFC 1.0β Matched Flow Collector Model for Simulation and Testing.* Users Manual. P. Isakson. KTH Sweden. August 1993.
- *MFC_DF 1.1β An External Model to DF.* Based on the Matched Flow Collector Model. Users Manual. P. Isakson. KTH Sweden. March 1994
- *Review of Non Stationary Collector Test Data.* Evaluation Procedures. Th. Pauschinger, Th. Held. ITW Stuttgart. Germany. (1993)
- *Procedure for Testing Solar Collectors under Non Stationary Conditions.* Th. Pauschinger, ITW Germany. B. Perers, VUAB Sweden
- *Progress Report June 1994.* Dynamic Solar Collector Testing in Sweden. B. Perers, VUAB, Sweden. 940612

- *Comparison of Flat Plate Collector Performance Parameters Obtained with the Standard ISO Test Procedure and Dynamic Collector Testing.* Th. Pauschinger. ITW Germany.

- *Fitting the MFC Model to Data generated with the FFC Model.* P. Isakson. KTH Sweden.

- *A Flat Plate Collector Model in the Frequency Domain.* P Isakson. KTH Sweden.

- *Dynamic Test of Two Collectors.* M. Bosanac, J.E. Nielsen. DTI Denmark.

- *Comparison of Collector Parameters from an In Stationary and a Steady State Collector Test.* G. Rockdorf, Th. Barkmann. ISFH Germany

- *Dynamic Collector Testing, Group 1. Final Report from IEA Task 14. First Draft.* B. Perers, Th. Pauschinger M. Bosanac, G. Rockdorf, Pierre Bremer et. al. February (1995).

Official Publications related to the work in IEA 14 Group 1. Collector Testing

- Draper, Smith, H.: *"Applied Regression Analysis"*. John Wiley & Sons. New York. (1981).

- Duffie, A., Beckman, W.A.: *"Solar Engineering of Thermal Processes"*, John Wiley and Sons Inc. New York 1991 (1991).

- Gemmel, L., Chandrashekar, M., Vanoli, K.H.: *"Detailed Modelling of Evacuated Collector Systems"*, IEA SH&C Task VI (1986).

- Guigas, R., Kübler, N., Fisch: Untersuchung von Hocheffizienten Flachkollektoren mit Hilfe einer Instationären Testmetode. (*"Evaluation of High Performance Flat Plate Collectors with a Dynamic Test Method"*). Proc Erstes Symposium Thermishe Solarenergie, 1991, Kloster Banz, pp. 290-295 (1991).

- Guisan, A., Mermoud, B., Lachal, ,O. Rudaz: *"Characterisation of Evacuated Collectors, Arrays and Collection Subsystems"*. IEA SH&C Task VI (1986) .

- Hottel, H.C and Woertz, B.B.: *"The Performance of Flat Plate Solar Heat Collectors"*. Transactions of the American Society of Mechanical Engineers no 64(1942) pp 91-104.

- ISO 9806-1.2 *"Thermal Performance Tests for Solar Collectors -Part 1: Glazed Liquid Heating Collectors"*.

- Isakson, P.: Solar Collector Model for Testing and Simulation. PhD Thesis, Royal Institute of Thechnology, Stockholm (1995). ISSN 0284-141X.

- Josefsson, L., Dahlgren: *"Personal communication"*. Swedish Meteorological and Hydrological Institute, Norrköping, Sweden (1992).

- Klein, A: *"The Effects of Thermal Capacitance upon the Performance of Flat Plate Solar Collectors"*, Msc. Thesis, University of Wisconsin (1973).

- Klein, A. et. al.: *"TRNSYS Manual. A Transient System Simulation Program"*. Solar Energy Laboratory. Univ. of Wisconsin. Madison, USA, (1990)

- Pauschinger, T. et al: *VELS II. Report on Dynamic System Testing*. ITW, Stuttgart, Germany (1996)

- Perers, B: *"Optical Modelling of Solar Collectors and Booster Reflectors under Non Stationary Conditions. Application for Collector Testing, System Simulation and Evaluation"*. Doctoral Thesis, Uppsala University, ISBN 91-554-3496-7.(1995)

- Perers, B.: *"Dynamic Method for Solar Collector Array Testing and Evaluation with Standard Database and Simulation Programmes"*. Journal of the Int. Solar Energy Society Vol. 50, No. 6, pp. 517-526, (1993).

- Perers, B.: Linjärparaboliska solfångare för svenskt klimat. Mätning utvärdering och kostnadsanalys. (*"Parabolic Through Collectors for the Swedish Climate. Measurements, Evaluation and Cost Analysis"*). Studsvik AB Sweden. STUDSVIK/ED-90/12. (1990)

- Perers, B., Karlsson, H., Walletun: *"Simulation and Evaluation Methods for Solar Energy Systems"*. Swedish Council for Building Research, D20:1990. (1990).

- Perers, B., Holst, P: *"The Södertörn Solar District Heating Test Plant. Results 1982-1985"*, Studsvik AB, Sweden. (STUDSVIK-87/1) (1987).

- Perers, B: *"Performance Testing of Unglazed Collectors, Wind and Long Wave Radiation Influence"*, Report for IEA Task III, Studsvik Energy, Sweden (1987).

- Perers, B., Roseen, R: *"The Experience from the Central Solar Heating Demonstration Plant at Studsvik"*, ISES Solar World Congress Perth, 426-432 (1983).
- Proctor: *"A Generalised Method for Testing all Classes of Solar Collectors"*. Part I,II,III , Int. J. Solar Energy, Vol.32. No.3. (1984).
- Perers, B: *"Influence of Variations in Wind Speed and Long Wave Radiation on the Performance of Solar Collectors"*. Paper Presented to IEA SH&C Task 14. Vattenfall Utveckling AB. (1994).
- Roseen, R., Perers, B.: *"A Solar Heating Plant in Studsvik. Design and first Year operational Performance"*. Swedish Council for Building Research. D21:1980. (1980).
- Ryan, B.L., Joiner, T.A., Ryan Jr: *"Minitab Handbook"*. Second Edition. Duxbury Press. Boston, ISBN 0-87150-470-7 (1985).
- Walletun, B., Perers, B.: Vindens inflytande på oglasade solfångare respektive solfångare med konvektionshinder,(*"Wind influence for unglazed collectors and collectors with convection suppressing glazing"),* Studsvik Energy, Sweden, (STUDSVIK/ED-65/15) (1986).
- WATSUN. *"Users Manual and Program Documentation"*. Watsun Simulation Laboratory, University of Waterloo. Waterloo, Canada, (1990).
- Weisberg, S.: *"Applied Linear Regression"*. John Wiley & Sons. New York. (1985).

Appendix 1. Drawing of Collector test loop for dynamic testing with series connection.

The figure below shows a solar collector test loop at the Älvkarleby laboratory for series connection of several collectors but still having almost equal inlet temperatures. This gives a much higher accuracy when comparing solar collectors with small design changes for development purposes.

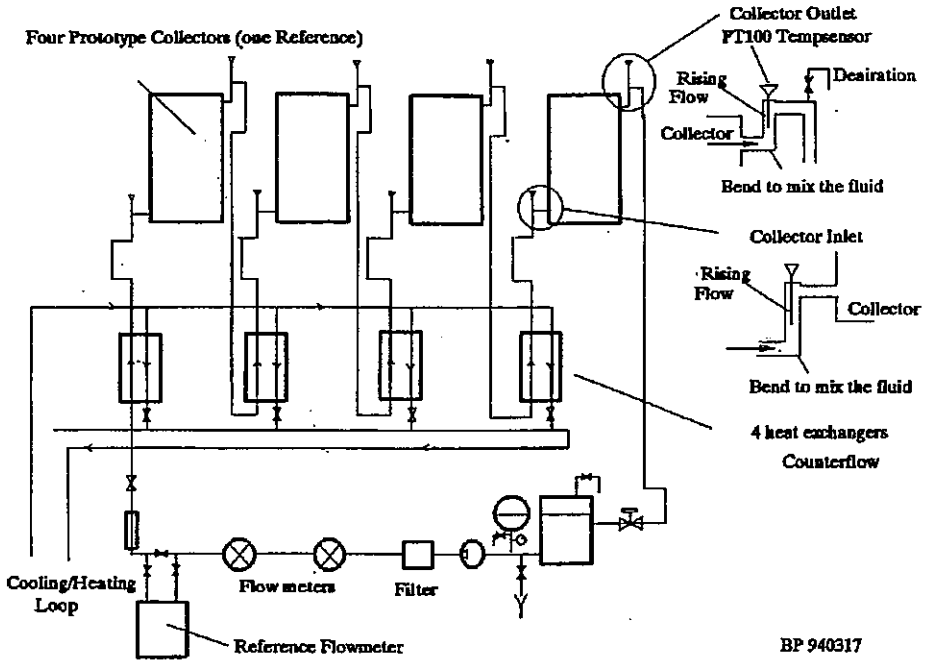
Four Prototype Collectors (one Reference)
Collector Outlet
PT100 Tempsensor
Rising Flow
Deairation
Collector
Bend to mix the fluid
Collector Inlet
Rising Flow
Collector
Bend to mix the fluid
4 heat exchangers
Counterflow
Cooling/Heating Loop
Flow meters
Filter
Reference Flowmeter
BP 940317

ANNEX B: TECHNICAL PAPERS ON COMPONENT TESTING AND SYSTEM SIMULATION OF SMALL SOLAR HEATING SYSTEMS

A MODEL FOR COMPONENT TESTING OF HOT WATER STORAGE TANKS

Achim Brunotte
Sektion Physik
Ludwig-Maximilians-Universität München
Amalienstr. 54, D 80799 München

June 7, 1995

1 Nomenclature

symbol	units	meaning
A	m^2	cross section area
C	J/K	heat capacity
$\dot{C}$	W/K	capacitance rate
f	1	fraction
$f(h)$	-	function of height
h	m/m	relative height
H	m	absolute height
P	W	power
R	K/W	reciproc heat transfer coefficient
S	-	stratification parameter
T	℃	temperature
U	W/K	heat transfer coefficient
V	W/K	heat loss coefficient
κ	W/K/m	heat conductivity
λ	W/K	heat conductivity coefficient

subscripts and superscripts:

symbol	meaning
A	ambient
Aux	auxiliary
bot	bottom of heat exchanger
cw	cold water
C	charging
D	discharging

HX	heat exchanger
mes	measurement
mix	mixing range
mod	model
N	no flow
S	store
top	top of heat exchanger
u	user
ww	warm water
Z	circulation

Contents

2 Abstract

A component test procedure for Domestic Hot Water (DHW) systems has been developed within the German research project VELS 2. Applications have been presented and discussed in the IEA Task 14, Subtask Dynamic Component and System Testing (DCST).

In this article, a one - dimensional parametrized model for the component hot water store is introduced. The model is capable of describing the following processes:

- convection during the charging of the solar heated part,
- convection during the charging of the auxiliary part,
- plug - flow through the store during discharging,
- heat losses to the ambient of the store,
- degradation of the stratification of temperature during discharging,
- degradation of the stratification caused by internal heat conduction,
- plug - flow through- and convection within the upper part of the store during circulation and
- degradation of the stratification during circulation.

The model is implemented as a component of the simulation program TRNSYS.
Two stores are tested, each means of two different experimental strategies, the Detail Test and the Integrated Test. In the Detail Test, few parameter values are identified from single test sequences. In the Integrated Test, a complete set of fit parameters is identified from one sequence. The Detail Test gives additional, more detailed and more reliable information. All identifications of parameters (fits) are performed by means of the Dynamic Fitting (DF) method, which has been developed within the German research project VELS 1 and the IEA Task 14, Subgroup Dynamic Fitting. The parameters values which can be identified in both tests differ typically by one to three percent.
The work contributed by the Task 14 members of the University of Munich has been funded by the Federal Minister for Research and Technology, Germany, grant number 032 87 68 C.

3 Introduction

In the last few years, more and more domestic hot water (DHW) systems have been installed. In 1991, solar collectors with altogether 200,000 m^2 aperture area have been sold in Germany [1]. It is pointed out that the user is not only interested in the ecological aspects of these systems, but also in the economical calculation. This requires a practical procedure for testing the performance and predicting the yearly gain under some reference conditions. In the following sections, one component of DHW – systems will be investigated: the hot water store.
A typical german DHW – system contains a hot water store of 300 ℓ to 500 ℓ volume. The solar part of the cylindrical tank is heated by an immersed heat exchanger. Its thermal insulation consists of PU – foam and is capable of keeping the heat inside the store for some days. In the upper part, a second heat exchanger or an electrical heating device is

intended to guarantee hot water at all times. All stores tested by the Stiftung Warentest fit this description ([2]).
This article presents a calculation model for hot water stores and provides an example test according to the component test procedure developed within the German research project VELS 2 ([3]) and the IEA Task 14, Subtask Dynamic Component and System Testing (DCST).

4 The store during operation

Many scientific articles have proven that the temperature distribution inside a store is - in general - not constant (e.g. [4, 5, 6]). The useable heat is not evenly distributed, but to be observed mainly in the upper part of the store. Due to the temperature - dependent density of water, the temperature distribution is largely one - dimensional in the vertical. For that reason, a one - dimensional model will be sufficient. Many such models have been developed. Veltkamp reported 1988 about the "state of the art" ([7]). He concluded: Mixing phenomena, like plumes rising from heat exchangers or by supply jets, are only weakly implemented in the models found in the open literature. In other words, none of them could join all important processes in one model. These processes are

- convection during charging of the solar heated part,
- convection during charging of auxiliary part,
- heat losses to the ambient of the store,
- degradation of the stratification of temperature during discharging,
- degradation of the stratification caused by internal heat conduction and in some cases
- degradation of the temperature during external recirculation.

5 Notation

Quantity and quality of energy inside the store can be evaluated by looking at the vertical *temperature profile* $T(h)$.
The user expects hot water at a particular minimum temperature (e.g. 45 °C). If the upper *auxiliary part* contains water of this temperature or higher, and the lower part contains cold water, there is a distinct *temperature stratification.* If the whole content of the auxiliary part can be withdrawn from the store without any mixing of cold and warm water or heat conduction, then the entire energy is usable. However, in real stores the stratification *degrades*, so that only a certain amount of the stored energy can be used immediately. The remaining energy has to be upgraded by supplying extra heat.

On a test rig the energy flows entering or leaving a store can be determined. In the discharging circuit for example, the cold water temperature T_{cw}, the warm water temperature T_{ww} and the volume flow $\dot{V}_u$ are measured. Instead of $\dot{V}_u$, the more pratical quantity

$$\dot{C}_u = \rho \cdot c_p \cdot \dot{V}_u \tag{1}$$

is used: the heat *capacitance rate*. With this the heat capacity of the streaming fluid per time interval is meant. Then, the discharging power P_u can be calculated easily:

$$P_u = \dot{C}_u \cdot (T_{ww} - T_{cw}) \tag{2}$$

Because the density ρ and heat capacity c_p are temperature - dependent, $\dot{C}_u$ is related to T_{cw} and T_{ww}. This means that density and heat capacity are to be averaged over the temperature interval $[T_{cw}, T_{ww}]$. This can be done on the test rig immediately during data acquisition with the program SDHWTest ([8]).
The measured data is evaluated similarly to the procedure of the Dynamic System Testing Group (DSTG) of IEA Task 14 ([9]). In contrast to that procedure, only the *components* of a system and not the whole domestic hot water system are tested. The best parameter values are determined again by the computer program DF. This is done by comparing the model with the measurement ([10]). This procedure is named *component test procedure.* In this report, two quantities will be used in order to evaluate the differences between model and measurement. Both are capacitance rate weighted quantities averadged over the time interval of measurement: the *mean temperature difference* $\overline{\Delta T}$ and the *mean quadratic temperature difference* σT [1].

$$\overline{\Delta T} = \frac{\int |T_{ww}^{mod}(t) - T_{ww}^{mes}(t)| \cdot \dot{C}_u(t)\, dt}{\int \dot{C}_u\, dt} \tag{3}$$

$$\sigma T = \sqrt{\frac{\int (T_{ww}^{mod}(t) - T_{ww}^{mes}(t))^2 \cdot \dot{C}_u(t)\, dt}{\int \dot{C}_u\, dt}} \tag{4}$$

6 One-dimensional store model

6.1 Basis model

The system – model (collector and heat exchanger) of the DSTG – group developed by Spirkl is the basis for further development ([9]): Its mathematical formulation consists of a group of differential equations (Equation 5). The main asumptions are:

1. The store is horizontally isothermal, i.e. the temperature depends only on the relative height h, $0 \leq h \leq 1$, and the time t.
2. By local convection $\partial T/\partial h \geq 0$ is guaranteed.
3. The heat loss coefficient V is evenly distributed over the height ($\partial V/\partial h = 0$).

[1] The programm DF uses a different approach with time filter.

4. The heat capcity C_S of the store is evenly distributed over the height (ρ and c_p do not depend on temperature).

For the explanation of symbols refer to Section 1.

$$\begin{aligned} C_S \frac{\partial T(t,h)}{\partial t} &= \delta_\epsilon(h) \cdot \dot{C}_C \cdot (T_{C,out} - T_{C,in}) \\ &+ \delta_\epsilon(h - (1 - f_{aux})) \cdot P_{aux} \\ &- V \cdot (T(t,h) - T_{SA}) \\ &+ \dot{C}_u \cdot \left(-\frac{\partial T(t,h)}{\partial h} + \delta_\epsilon(h)(T_{cw} - T(t,h)) \right) \\ &+ \frac{\partial}{\partial h} \left(b \cdot exp\left(-\frac{a}{\epsilon} \cdot \frac{\partial T}{\partial h} \right) \cdot \frac{\partial T}{\partial h} \right) \end{aligned} \tag{5}$$

with:

$T_{C,out}$	collector outlet temperature
$T_{C,in}$	collector inlet temperature
a, b	arbitrary positive constants

The terms on the right hand side of equation represent:

1. collector power [2],
2. auxiliary power,
3. heat losses to the store ambient,
4. plug flow and
5. convection.

$\delta_\epsilon(x)$ is defined as:

$$\delta_\epsilon(x) := \begin{cases} \frac{e^{-x/\epsilon}}{\epsilon} & x > 0 \\ 0 & \text{else} \end{cases} \tag{6}$$

With the passage to the limit $\epsilon \to 0$ in Equation 5 heat exchanger, auxiliary heating and cold water inlet will be punctually modelled. The convection term in Equation 5 has the function to dissolve temperature inversions ($\partial T/\partial h < 0$) immedeately by an infinite heat conduction coefficient.

$$\lim_{\epsilon \to 0} \left(b \exp\left(-\frac{a}{\epsilon} \frac{\partial T}{\partial h} \right) \right) = \begin{cases} \infty & \frac{\partial T}{\partial h} < 0 \\ 0 & \text{else} \end{cases} \tag{7}$$

The modelled store temperature $T_S(h,t)$ results with $\epsilon \to 0$. In Table 1 the parameters of the model are listed.

[2] In the original system model the collector power is calculated by the irradiance and the collector heat losses.

Table 1: Parameters of the basis model.

Parameter	units	meaning
C_S	MJ/K	heat capacity of the store including heat exchanger
V	W/K	heat loss coefficient
f_{aux}	-	fraction of auxiliary part of C_S
D_L	-	mixing parameter for cold water mixing during discharging

The mixing parameter D_L ($D_L \sim \dot{C}_u$, $\dot{C}_u$: discharging capacitance rate) describes in the original model the mixing of warm water and inflowing cold water by heat diffusion. The according term has been left out in Equation 5, since a different approach will be prosecuted.

6.2 Cold water mixing

In order to model the mixing of warm water with inflowing cold water, the cold water can be evenly distributed over the range $0 \leq h \leq h_{mix}$ in the store [11]. The capacitance rate of discharging $\dot{C}_u(h) = \dot{C}_u^{max} \cdot W(h)$ is a linear rising function in this interval (Figure 1):

$$W(h) := \begin{cases} h/h_{mix} & : h \leq h_{mix} \\ 1 & : h_{mix} < h \leq 1 \end{cases} \tag{8}$$

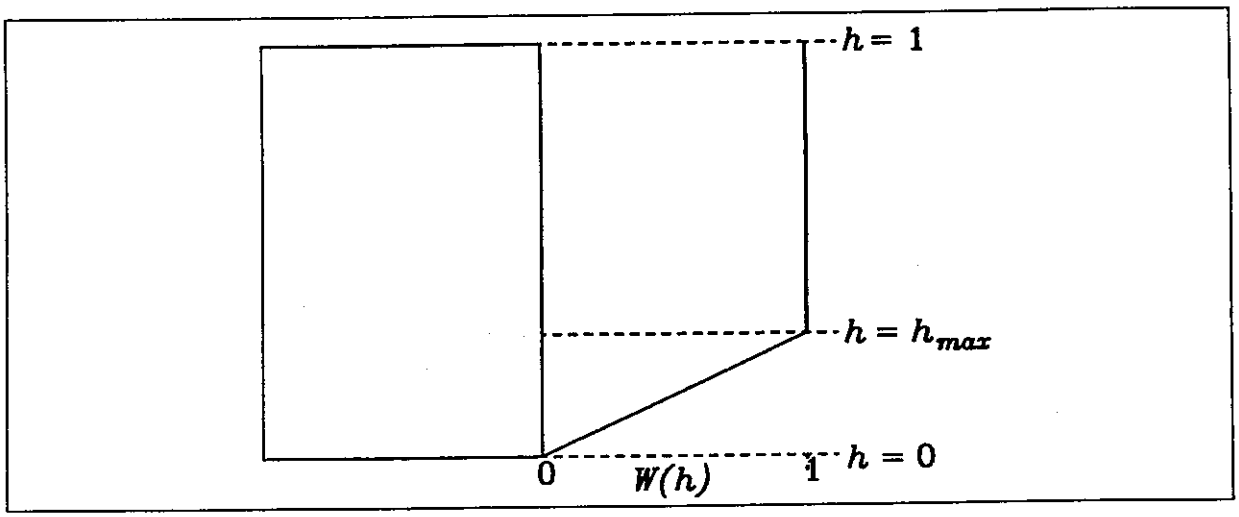

Figure 1: Even distribution of inflowing cold water. The function $W(h)$ rises linearly up to h_{mix} (h_{max} in the figure).

Then, the flow through the store will be described by the differential equation

$$C_S \frac{\partial T(t,h)}{\partial t} = \underbrace{-\dot{C}_u^{max} \cdot \frac{\partial T(t,h)}{\partial h}}_{\text{plug-flow}} \underbrace{- \frac{\partial \dot{C}_u(h)}{\partial h} \cdot (T(t,h) - T_{cw})}_{\text{flowingin}}. \tag{9}$$

6.3 Vertical heat conduction inside the store

The internal heat conduction has been neglected in the basis model. Asuming a heat conduction coefficient λ that depends on the height the differential equation is:

$$C_S \frac{\partial T(t,h)}{\partial t} = \frac{\partial}{\partial h}\left(\lambda(h) \cdot \frac{\partial T(t,h)}{\partial h}\right) \tag{10}$$

In general λ is a function of temperature and therefore a function of height. Because of the almost constant λ of water it would be sufficient to set $\lambda = constant$. But other processes can be modelled by misusing the heat conduction and restricting it to certain time intervals. For example:

- Cold water mixing according to the method of the Dynamic System Testing Group, IEA Task 14.
- Heat transport by convection into the so called dead volume below a heat exchanger.

6.4 Flow through the upper part of a store only (external recirculation)

Model equation:

$$\begin{aligned} C_S \frac{\partial T(t,h)}{\partial t} &= \dot{C}_Z \cdot \left(-\frac{\partial T}{\partial h} \cdot \Theta(h - h_Z) + \delta_\epsilon(h - h_Z) \cdot (T_Z - T)\right) \\ &+ \frac{\partial}{\partial h}\left(b \cdot exp\left(-\frac{a}{\epsilon} \cdot \frac{\partial T}{\partial h}\right) \cdot \frac{\partial T}{\partial h}\right) \\ &+ \frac{\partial}{\partial h}\left(\lambda_Z(\dot{C}_Z, h) \cdot \frac{\partial T(t,h)}{\partial h}\right) \end{aligned} \tag{11}$$

The terms on the right hand side represent:

1. Plug flow through upper part of a store,
2. convection and
3. heat transport from the upper part to the lower part.

The heat capacity C_S and the relative height h_Z of the inlet are parameters of the model.

6.5 Charging with immersed heat exchangers

In the *explicit* form, immersed heat exchangers are modelled similarly like stores. The asumptions are:

1. Plug flow in vertical direction.

2. One - dimensional temperature distribution.
3. $\partial T/\partial h \geq 0$, guaranteed by local convection.
4. The heat transfer coefficient heat exchanger / store is evenly distributed over the height.
5. The heat capacity C_{HX} is evenly distributed over the height.
6. The heat conduction inside the heat exchanger is neglectable small.

In the alternative *implicite* form an additional term in the store equation describes the distribution of charging power into the store.

6.6 Complete model equation

The complete model equation consists of two coupled sets of differential equations:

$$\begin{aligned} C_S \cdot \frac{\partial T(t,h)}{\partial t} &= \delta_\epsilon(h - h_{bot})) \cdot P_C \\ &+ U_C \cdot (T_{HX} - T) \cdot \Theta(h - h_{bot}) \cdot \Theta(h_{top} - h) \\ &+ \delta_\epsilon(h - (1 - f_{aux})) \cdot P_{aux} \\ &- V \cdot (T - T_{SA}) \\ &- \left(\dot{C}_u^{max} \cdot \frac{\partial T}{\partial h} \cdot \Theta(h - h_{mix}) + \frac{\partial \dot{C}_u(h)}{\partial h} \cdot (T - T_{cw}) \cdot \Theta(h_{mix} - h) \right) \\ &+ \frac{\partial}{\partial h} \left(b \cdot exp\left(-\frac{a}{\epsilon} \cdot \frac{\partial T}{\partial h} \right) \cdot \frac{\partial T}{\partial h} \right) \\ &+ \frac{\partial}{\partial h} \left(\lambda(h) \cdot \frac{\partial T}{\partial h} \right) \\ &+ \dot{C}_Z \cdot \left(-\frac{\partial T}{\partial h} \cdot \Theta(h - h_Z) + \delta_\epsilon(h - h_Z) \cdot (T_Z - T) \right) \end{aligned} \tag{12}$$

The terms on the right hand side of Equation 12 represent:

1. Charging power,
2. or alternative: heat transfer from heat exchanger to store,
3. auxiliary power,
4. heat losses to the store ambient,
5. flow through the store during discharging,
6. convection,
7. vertical heat conduction inside the store and

8. flow through the upper part of the store.

$$C_{HX}\frac{\partial T_{HX}(t,h_{HX})}{\partial t} = U_C\cdot(T-T_{HX}) - \dot{C}_C\cdot\left(-\frac{\partial T_{HX}}{\partial h}+\delta_\epsilon(h_{HX}-H_{HX})(T_{C,top}-T_{HX})\right) + \frac{\partial}{\partial h_{HX}}\left(b\cdot exp\left(-\frac{a}{\epsilon}\cdot\frac{\partial T_{HX}}{\partial h_{HX}}\right)\cdot\frac{\partial T_{HX}}{\partial h_{HX}}\right) \quad (13)$$

The terms on the right hand side of Equation 13 represent:

1. heat transfer from store to heat exchanger,
2. flow through the heat exchanger and
3. convection.

Table 2: Parameters of the store model with circulation mode and heat exchanger.

Parameter	Einheiten	Bedeutung
C_S	MJ/K	heat cacacity of the store
h_{bot}	-	bottom height of the heat exchanger
h_{top}	-	top height of the heat exchanger
U_C	W/K	heat transfer coefficient heat exchanger / store
f_{aux}	-	fraction of the auxiliary part of C_S
V	W/K	heat loss coefficient
h_{mix}	-	maximum height of cold water mixing range
λ	mW/K	(function) vertical heat conduction coefficient
h_Z	-	height of circulation return
C_{HX}	MJ/K	heat cacacity of the heat exchanger

With the passage to the limit $\epsilon \to 0$ the desired punctuality will result and $(\partial T/\partial h < 0)$ will be guaranteed. Table 2 contains a list of the model parameters.

7 Component test of two stores

Test data of two 300 ℓ stores are evaluated. Both stores have been placed on a test rig, one at the University of Munich (store SV) and one at the Institut für Thermodynamik und Wärmetechnik at the University of Stuttgart (store SI). SV contains one immersed heat exchanger and one electrical heating device in the auxiliary part. SI contains two immersed heat exchangers. The test aims to identify a set of model parameters - one for each store. With this set it is possible to simulate the stores behaviour under different operation conditions, e.g. with Test Reference Year (TRY) data. Two different test strategies are used.

1. Detail Test: Only singular parameters result from a single test sequence. A greater precision can be expected. The strategy is based on a proposal of the Institut für Thermodynamik und Wärmetechnik at the University of Stuttgart.

2. Integrated Test: A complete parameter set is identified from one sequence. The operation conditions are close to the conditions in real systems.

Table 3: Parameters to be identified.

parameter	units	meaning
C_S	MJ/K	heat capacity of the store including heat exchanger
V	W/K	heat loss coefficient
V_{aux}	W/K	heat loss coefficient if only the auxiliary part is heated
C_{aux}	MJ/K	heat capacity of the auxiliary part
λ_S	W/K	vertical heat conduction coefficient
U_C	W/K	heat transfer coefficient heat exchanger / store during charging
U_N	W/K	heat transfer coefficient heat, if the flow through the heat exchanger is zero
h_{mix}	m/m	maximum height of cold water mixing range

The values of the parameters listed in Table 3 are determined by adapting (fit) the model to the test data. Other parameter values like those of C_{HX} and the top height of the heat exchanger h_{top} are determined by weighting respective measuring. For store SI, there are second parameters U_C and U_N in the parameter set. The values of all U_C - parameters are identified in a separate fit. This means that in the first fit the implicit form of heat exchanger modelling is used. In the following, second fit, the explicit form is used (see Section 6.5). The reason for this procedure is the large error margin in U_C and the correlated errors in the other parameters.

7.1 Store SI

Test sequences, Detail Test:

Bb : Charging of the auxiliary part with constant power, 24 h rest time (Stillstand), discharging. Parameters to be identified: C_{aux}, λ_S, V_{aux} and U_C^2.

C1 : Charging of the solar part with constant power, discharging with capacitance rate $\dot{C}_u = 370\,\mathrm{W/K}$. Parameters to be identified: C_S, h_{mix}, and U_C^1.

C2 : Charging with constant power, discharging with capacitance rate $\dot{C}_u = 695\,\mathrm{W/K}$. Parameters to be identified: C_S, h_{mix}, and U_C^1.

B : Charging to stationary state of store, 24 h rest time, discharging. Parameter to be identified: V.

Test sequence, Integrated Test:

D : Sequence with two parts; first part: charging of the solar part with constant power, drawing-out half of the warm water, charging again, 16 h rest time, complete discharging; second part: as first part, but charging of the auxiliary part. Parameters to be identified: C_S, V, C_{aux}, λ_S, h_{mix}, and U_C^1, U_C^2.

Table 4: Identified parameter values, store SI, Detail Test and Integrated Test.

sequence	C_S [MJ/K]	V [W/K]	V_{aux} [W/K]	C_{aux} [MJ/K]	λ_S [mW/K]	h_{mix} [-]	U_C^1 [W/K]	U_C^2 [W/K]
Bb	-	-	2.09	0.592	286	-	-	300
	-	-	±0.05	±0.004	±9	-	-	±20
C1	1.165	-	-	-	-	0.077	345	-
	±0.002	-	-	-	-	±0.004	±9	-
C2	1.175	-	-	-	-	0.103	397	-
	±0.002	-	-	-	-	±0.003	±15	-
B	-	2.12	-	-	-	-	-	-
	-	±0.06	-	-	-	-	-	-
D	1.162	2.21	-	0.599	308	0.005	367	421
	±0.003	±0.07	-	±0.004	±15	±0.022	±7	±29

Results (Table 4) The three C_S – values differ by 1 %. The heat capacity 1.17 MJ/K corresponds to a water volume of 279 ℓ. This is, as frequently discovered in tests, 21 ℓ less than the volume indicated by the manufacturer. The heat loss coefficient does not depend on the operation conditions and its value is 2.1±0.1 W/K. The auxiliary fraction is 51 %. If the identified heat conduction coefficient $\lambda_S \approx 290\,\mathrm{mW/K}$ is compared to calculated values, it is found that the water conducts only one quarter of the transported heat. From the heat conductivity of water in the temperature range between 0 and 100 °C $\kappa_{H_2O} = 0.6 \pm 0.07\,\mathrm{W/m/K}$ ([12]) the heat conduction coefficient of the water results:

$$\begin{aligned} \lambda_{H_2O} &= \kappa_{H_2O} \cdot \frac{A_S}{H_S} \\ &\approx 0,6\,\mathrm{W/m/K} \cdot 0,13\,\mathrm{m} = 0,078\,\mathrm{W/K}. \end{aligned}$$

A_S and H_S are the cross section area and the absolute height of the store. The remaining three quarters are related to the heat conduction of the wall, made of steel. The mixing parameter h_{mix} depends on the discharging – capacitance rate $\dot{C}_u$. Its value can not be identified from sequence **D** because of two reasons: 1) the small $\dot{C}_u \approx 250\,\mathrm{W/K}$, 2) the

effect of the first mixing period during discharging is erased due to convection in the second charging period. The values of U_C are spread by 10 % around their mean value, because the charging power differs in the various test sequences.

Comparison of Detail Test and Integrated Test The parameter set identified from the Detail Test – sequences is used to simulate the store under the conditions (with the data) of the Integrated Test. In order to evaluate the differences between simulation and measurement $\overline{\Delta T}$ (definition in Section 5) is calculated. The $\overline{\Delta T}$ of the best possible set of parameters, the set identified from the Integrated Test, serves as a reference. In the first part of sequence **D** there are only very small differences (Table 5). Only in the second part the simulation is 0.27 K worse than the reference. In both parts the simulation is close to the measurement ($\overline{\Delta T} = 0.5\,\mathrm{K}$).

Table 5: Store SI: mean temperature difference of simulation (Detail Test) and reference (Integrated Test) in [K], measurement data of sequence **D**.

	Detail Test	Integrated Test
1. Teil	0.52	0.49
2. Teil	0.43	0.16

7.2 Store SV

Test sequences, Detail Test:

Bb : Charging of the auxiliary parts, 12 h rest time, discharging. Parameters to be identified: C_{aux}, λ_S, V_{aux}.

C1 : Charging with constant power, discharging with capacitance rate $\dot{C}_u = 390\,\mathrm{W/K}$. Parameters to be identified: C_S, U_N, and U_C.

C2 : Charging with constant power, discharging with capacitance rate $\dot{C}_u = 695\,\mathrm{W/K}$. Parameters to be identified: C_S, U_N, and U_C.

E : Charging with constant power, 20 h rest time, discharging. Parameter to be identified: V.

Test sequence, Integrated Test:

S4 : Three days test sequence, charging of the solar part only, discharging with variation of $\dot{C}_u$. Parameters to be identified: C_S, V, λ_S, U_N.

Table 6: Identified parameter values, store SV, Detail Test and Integrated Test.

Sequenz	C_S [MJ/K]	$\dot{V}$ [W/K]	V_{aux} [W/K]	C_{aux} [MJ/K]	λ_S [mW/K]	U_N [W/K]	U_C [W/K]
Bb	-	-	6.58	0.433	123	-	-
	-	-	±0.27	±0.004	±12	-	-
C1	1.293	-	-	-	-	221	543
	±0.006	-	-	-	-	±43	±50
C2	1.305	-	-	-	-	299	524
	±0.003	-	-	-	-	±34	±45
E	-	6.58	-	-	-	-	-
	-	±0.91	-	-	-	-	-
S4	1.267	5.65	-	-	147	243	-
	±0.007	±0.12	-	-	±20	±36	-

Results (Table 6) The two C_S – values from the Detail Test differ by 1 %, but the value from the Integrated Test is smaller by 3 %. The difference can be explained by the dead volume below the immersed heat exchanger. In the Detail Test sequences the whole water volume and the full information is withdrawn in each discharging period. In the Integrated Test the full information is only withdrawn once. The resulting under – estimation is typical for the component test procedure. $C_S = 1.3\,\mathrm{MJ/K}$ corresponds to a water volume of 310 ℓ. The heat coefficient from the Integrated Test is smaller, but the values can not be compared, because the thermal insulation has been modified several times. The heat loss conduction coefficient can be identified from both tests. The greater value $\lambda_S \approx 147\,\mathrm{mW/K}$ is partly the effect of processes other than heat conduction. Due to the thinner walls and the different wall material (stainless steel) there is less conduction than in store SI. A positive result of the dead volume is that cold water mixing can be neglected. But the volume of the immersed heat exchanger is rather large (13 ℓ). During discharging the temperature profile degrades significantly. The value of the heat transfer coefficient during discharging (no flow through heat exchanger) $U_N = 260 \pm 40\,\mathrm{W/K}$. The values of U_C are greater ($\approx 530\,\mathrm{W/K}$), since U_C is related to the temperature difference between the fluid inside the HX and the water in the store a long way from the heat exchanger walls. Only during the charging process a strong convection takes place and supports the heat transport into the store.

Comparison of Detail Test and Integrated Test $\overline{\Delta T} = 1.28\,\mathrm{K}$ of the simulation is only slightly greater than the best possible $\overline{\Delta T}$ for sequence **S4**. The comparatively high $\overline{\Delta T}$ values can be attributed to many short draw-offs in sequence **S4**. Because of the time constant of the temperature sensors the measured warm water temperature will always be underestimated at the beginning of a draw-off.

Table 7: Store SV: mean temperature difference of simulation (Detail Test) and reference (Integrated Test) in [K], measurement data of sequence **S4.**

Detail Test	Integrated Test
1.28	1.13

References

[1] J. Leuchtner, Oliver Reitebuch, Rainer Schüle und Martin Ufheil. *Thermische Solaranlagen Marktübersicht 1992.* Öko-Institut e.V., Institut für angewandte Ökologie, Freiburg, 1992.

[2] Stiftung Warentest. *Test spezial, Energie und Umwelt.* Öko-Institut e.V., Institut für angewandte Ökologie, Stuttgart, 1995.

[3] Editor: W. Schölkopf. Verbundforschung zur Ermittlung der Leistungsfähigkeit von Solaranlagen, Teil 2 (VELS 2). Technischer Bericht, Sektion Physik der Ludwig-Maximilians Universität München, Amalienstr. 54, D-80799 München, Herbst 1991 – Dezember 1994. BMFT-Projekt Nr. 0328768C.

[4] J.S. Turner. *Buoyancy effects in fluids.* Cambridge University Press, 1973.

[5] L.S. Fischer, C.W.J. van Koppen, and B.D. Mennink. The Thermodynamics and Some Practical Aspects of Thermally Layered Heat Storage in Water. Report WPS 3.75.11.R247, Eindhoven University of Technology, Eindhoven, The Netherlands, 1975.

[6] L.S. Fischer und C.W.J. van Koppen und J.Th.T. van Wolde. *Theorie und Praxis der thermisch geschichteten Wasserspeicher*, S. 33–37. VDI-Verlag, Düsseldorf, 1977.

[7] B. Veltkamp. Energy Conservation through Energy Storage, short term water heat storage systems. State of the art report, LEVEL, bureau for energy technology, The Netherlands, 1988.

[8] J. Muschaweck and W.Spirkl. Test Procedure for Solar Domestic Hot Water Systems, Technical Report and Program Manual, Version 0.23. Amalienstr. 54, D-80799 München, September 1992.

[9] H. Visser and A.C. de Geus. Dynamic Testing of Solar Domestic Hot Water Systems. Technical Report, Final report of the IEA Dynamic System Testing Group, TNO Building and Construction Research, Delft, The Netherlands, 1992.

[10] W. Spirkl. Dynamic SDHW System Testing, Program Manual, Version 2.4 α. InSitu Scientific Software, Klein & Partners, Baaderstr. 80, D 80469 München, April 1994.

[11] D. Küster-mann. *Ein Rechenmodell für Brauchwarmwasserspeicher unter Berücksichtigung einer externen Rezirkulation.* Diplomarbeit, Ludwig-Maximilians-Universität, München, 1994.

[12] C. Gerthsen und H.O. Kneser und H. Vogel. *Physik.* Springer–Verlag, Berlin, 14 Auflage, 1982.

[13] S.A. Klein, W.A. Beckman, and P.I. Cooper. TRNSYS: A Transient System Simulation Program, Version 13.1. Solar Energy Laboratory, Madison, Wisconsin, USA, 1990.

[14] W. Spirkl and J. Muschaweck. General Model for Testing Solar Domestic Hot Water Systems. *Solar Energy Materials and Solar Cells*, **28**:93–102, 1992.

A Plug flow store model, user manual

A.1 Short description

The model has been implemented as component TYPE 69 of the simulation program TRNSYS, version 13.1 ([13]). It is a so called *segment model.* The concept is similar to TYPE 38 `:Algebraic Tank (Plug-Flow)`, a standard component of TRNSYS. An important advantage of this implementation compared to so called *node models* is the variable segment size that saves computing time. Another advantage is the absence of numerical dispersion during the discharging. The segments are moved with the flow through the store. Numerical dispersion of node models with fixed nodes of given number N decreases $\sim 1/\sqrt{N}$. ([14]). Compared with TYPE 38, TYPE 69 has the following additional features:

- Up to 2 immersed heat exchangers.
- Connection to an external circulation line.
- Local mixing of inflowing cold and warm water inside the store.
- An improved algorithm for appropriate segment sizing during heat conduction (segments are divided properly).

A.2 Call of the model in the TRNSYS – command file (dek)

The component can be called as TYPE 69.

PARAMETER

number	name	units	meaning
1	*Mode*	-	*Mode* < 0: The model expects the Time as first INPUT quantity *Mode* > 0: The model gets the internal time (TRNSYS – standard)

			$\|Mode\| = 1$: no circulation $\|Mode\| = 4$: circulation, basis model $\|Mode\| = 2$: the water returned from the circulation line will be equally distributed over the range $[h_Z - \Delta h_Z, h_Z + \Delta h_Z]$ $\|Mode\| = 5$: the heat conduction coefficient will be increased by λ_Z during circulation $\|Mode\| = 6$: $\lambda_Z = f(h)$, Gaußverteilung
2	M_C	-	$M_C = 0, 1, 2$, number of charging loops
3	C_S	MJ/K	$C_S > 0.1$ MJ/K, heat capacity of the store without HX
4	V	W/K	heat loss coefficient of the store
5	λ_S	mW/K	vertical heat conduction coefficient
6	h_{mix}	m/m	$h_{mix} \geq 0$, inflowing cold water will be equally distributed over the range $[0, h_{mix}]$
alternative:			
6	λ_D	mW/K	$\lambda_D < 0$, during discharging: $\lambda = \lambda_S - \lambda_D$
optional:			
7	C^1_{HX}	MJ/K	$\|C^1_{HX}\| > 0.001$ MJ/K heat capacity of the heat exchanger (HX), dummy if $R^1 = 0$ $C^1_{HX} > 0$: implicit modelling $C^1_{HX} < 0$: explicit modelling
8	R^1_C	K/kW	reciproc heat transfer coefficient $1/U^1_C$ during charging $R^1_C > 0.1$ K/kW: immersed HX $R^1_C = 0$: direct charging flow through store
9	S^1	-	implicit, direct: $S^1 \geq 0$, stratification parameter
alternative:			
9	R^1_N	K/kW	explicit: $1/U^1_C$ if not charging
10	h^1_{bot}	m/m	height of bottom of HX, respective outlet of charging loop
11	h^1_{top}	m/m	height of top of HX, respective inlet of charging loop
optional:			
12	C^2_{HX}	MJ/K	see first HX
13	R^2_C	K/kW	see first HX
14	S^2	-	see first HX
alternative:			
14	R^2_N	K/kW	see first HX
15	h^2_{bot}	m/m	see first HX
16	h^2_{top}	m/m	see first HX

$M_C \cdot 5+7$	f_{aux}	m/m	fraction of electrical heated part of C_S $f_{aux}=0$: no electrical heating
$\|Mode\|>1$:			
$M_C \cdot 5+8$	h_Z	m/m	height of circulation return
$\|Mode\|=2$:			
$M_C \cdot 5+9$	Δh_Z	m/m	half of the mixing range during circulation
$\|Mode\|=5$:			
$M_C \cdot 5+9$	λ_Z	mW/K	additional heat conduction coefficient during circulation
$\|Mode\|=6$:			
$M_C \cdot 5+9$	λ_Z^{max}	mW/K	maximum additional heat conduction coefficient during circulation
$\|Mode\|=6$:			
$M_C \cdot 5+10$	σ	-	determines distribution width of function $f(h)$, $\lambda_Z(h)=\lambda_Z^{max} \cdot f(h)$, $f(h)=e^{-1/2 \cdot \left(\frac{h-h_Z}{\sigma}\right)^2}$

If $Mode<0$, then the model expects the Time as first INPUT variable and $i=1$. Else $i=0$.

INPUTS

number	name	units	meaning
$Mode<0$:			
1	t	h	Time
$i+1$	$T_{C,top}^1$	℃	temperature of the fluid at top connection of charging loop
$i+2$	$T_{C,bot}^1$	℃	temperature of the fluid at bottom connection of charging loop
$i+3$	$\dot{C}_C^1$	kJ/h/K	capacitance rate of first charging loop $\dot{C}_C>0$: flow from top to bottom $\dot{C}_C<0$: flow from bottom to top
$M_C=2$:			
$i+4$	$T_{C,top}^2$	℃	temperature of the fluid at top connection of charging loop
$i+5$	$T_{C,bot}^2$	℃	temperature of the fluid at bottom connection of charging loop
$i+6$	$\dot{C}_C^2$	kJ/h/K	capacitance rate of first charging loop $\dot{C}_C>0$: flow from top to bottom $\dot{C}_C<0$: flow from bottom to top
$i:=i+3$			
$i+4$	T_{cw}	℃	cold water temperature

$i+5$	$\dot{C}_u$	kJ/h/K	capacitance rate of discharging
$i+6$	T_{SA}	℃	temperature of store ambient
$f_{aux} > 0$:			
$i+7$	P_{aux}	kJ/h	power of the electrical heating
$i := i+1$			
$\|Mode\| > 1$:			
$i+7$	T_Z	℃	temperature of the recirculated water
$i+8$	$\dot{C}_Z$	kJ/h/K	capacitance rate of circulation

When calculating the capacitance rates the temperature dependent density and heat capacity of the fluids should be taken into account. This topic is discussed e.g. in [8]. The first and second OUTPUT can be used by the component test procedure. The first value of the INPUT variable $T^1_{C,top}(t_{start})$ that is transferred to the model determines which quantities will be returned by the model.

OUTPUTS

number	name	units	meaning
$Mode < 0$:			
1	P_{mod}	kJ/h	modelled power $T^1_{C,top}(t_{start}) = 1$: charging power of the first charging loop $T^1_{C,top}(t_{start}) = 2$: charging power of the second charging loop else: net power minus electrical power Heizung: $P_{net} = P_u + P_Z - P_{aux}$
2	$\dot{C}mod$	kJ/h/K	capacitance rate $T^1_{C,top}(t_{start}) = 1$: of first charging loop $T^1_{C,top}(t_{start}) = 2$: of second charging loop else: capacitance rate $\dot{C}_u + \dot{C}_Z$
3	P_{net}	kJ/h	power $P_{net} = P_u + P_Z - P_{aux}$
4	T_{ww}	℃	warm water temperature
5	P^1_C	kJ/h	charging power of first loop
6	$T_{C,out}$	℃	outlet temperature, first charging loop
7	P_u	kJ/h	power delivered to user (except circulation)
8	P_{aux}	kJ/h	power of electrical heating
9	P_Z	kJ/h	power of circulation $P_Z = \dot{C}_Z \cdot (T_{ww} - T_Z)$
10	P_{loss}	kJ/h	heat loss power to the ambient

Thermal Testing of Stores for Solar Domestic Hot Water Systems

H. Drück, E. Hahne

Institut für Thermodynamik und Wärmetechnik (ITW)
University of Stuttgart
Pfaffenwaldring 6, D-70550 Stuttgart
Phone: ++49-(0)711-685-3536, Fax: ++49-(0)711-685-3503

Abstract

In order to compare the thermal performance of different stores and to assess the thermal behaviour of stores in solar domestic hot water (SDHW) systems, the thermal parameters of these stores must be known. Therefore test procedures for SDHW stores have been developed at the ITW. This article describes the developed test procedures and the determination of the thermal store parameters used in the ITW test report.
The Multiport Store Model for TRNSYS, developed at ITW to describe the thermal behaviour of different types of hot water stores is introduced. Finally some results of performed store tests are discussed with respect to reproducibility and accuracy of the test results.

1. Introduction

The technical requirements on conventional hot water stores and domestic hot water systems are standardised in DIN 4753 and others. In addition to these requirements concerning closeness, corrosion protection and drinking water hygiene, stores for SDHW systems have to fulfil some other specifications, especially with regard to thermal aspects. The knowledge of these attributes or corresponding thermal parameters respectively, is very important for the comparison of different stores and the choice of a suitable store.

The store test method presented in this article enables the determination of the thermal capacity and the heat loss capacity rate of the store and an identification of the temperature, mass flow and power dependency of the heat transfer capacity rate of the immersed heat exchangers as well as the qualification of the thermal stratification inside the store. Due to the large number of determined physical parameters the thermal behaviour of the store can be described in detail by using a suitable numerical store model, such as the Multiport Store Model, which is available as TRNSYS Type 74.
As a further important advantage for the presented test method measurements inside the store are not required. Hence no interventions in the store are necessary and its behaviour of thermal stratification will not be affected by any immersed measuring equipment.

The thermal parameters being necessary for the description of the thermal behaviour of a SDHW store are shown in figure 1. In order to determine these parameters the store is connected to the testing stand located in an air-conditioned laboratory with a constant ambient temperature of 20 °C. The testing stand consists of a charge and a discharge loop, which allows for the thermal charging and discharging of the store according to well defined test sequences.
During operation the volume flow rates, all inlet and outlet temperatures of the store and the ambient temperature is measured approximately every 8 seconds, and the mean values of three measurements are recorded.

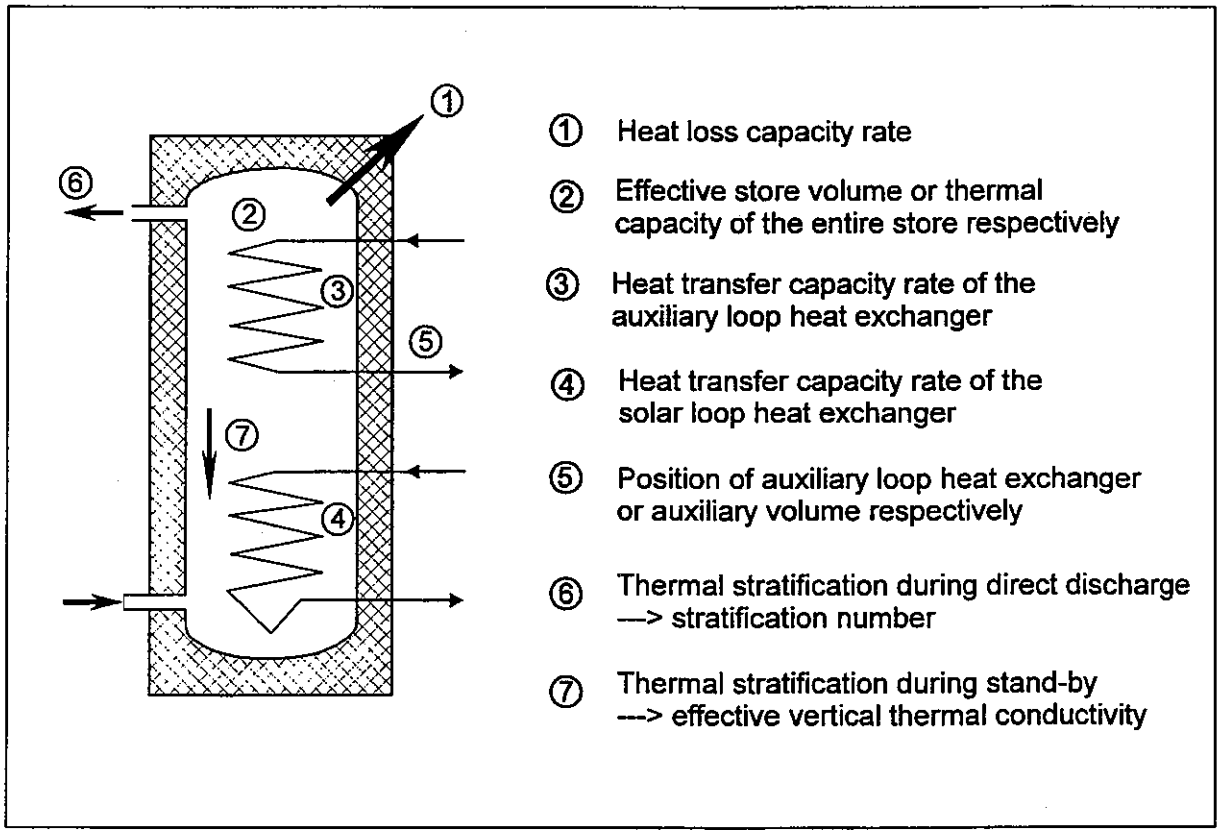

Figure 1: Thermal parameters of a SDHW store

2. Determination of the thermal store parameters

The thermal store parameters (as shown in figure 1) are determined on the basis of the temperatures and volume flow rates recorded during the operation of the store at the testing stand. In order to determine the capacity of the entire store and the overall heat loss capacity rate a simple combined power and energy balance is sufficient. All further thermal store parameters are determined by means of parameter identification.

In order to identify the parameters of the store, the measured input values of the store are used as inputs for a suitable mathematical store model. The output values calculated by the model depend on the inputs as well as on the thermal store parameters used for the calculation, i.e. the volume and the heat loss capacity rate. In order to determine the parameters of the store they are varied according to the Levenberg-Marquardt algorithm until the difference between the measured and calculated output values has reached its global minimum. We use the parameter identification program DF /1/ and the Multiport Store Model /2/ for the program TRNSYS /3/ combined with the communication tool TRANSMIT /4/.

The following pages give a description of the determination of the different store parameters as well as of the test sequences used.

2.1 Heat loss capacity rate

The heat loss capacity rate indicates the heat loss from store to ambient per Kelvin temperature difference between mean store temperature and ambient temperature. This method of determining the heat loss capacity rate, as well as the method for the determination of the capacity of the entire store as described in chapter 2.2, are based on the work of the European Solar Storage Testing Group (SSTG) /5/ during the eighties.

In order to determine the heat loss capacity rate the store is charged via the solar loop heat exchanger, starting from ambient condition with a constant volume flow rate and a constant inlet temperature of approximately 60 °C. After a certain time a steady state is reached, at which the power transferred to the store does not change any more. In this condition the heat loss rate from store to ambient is equal to the input power to the store.
In this steady state condition the heat loss capacity rate is calculated as the ratio of the input power to the temperature difference between mean store temperature and ambient temperature. Since there are no measurements inside the store, the mean store temperature has to be calculated from the measured in- and outlet temperatures of the heat exchanger and the transferred power in the steady state. The necessary equations can be found in /5/.

2.2 Thermal capacity of the entire store

The data recorded during the steady state test sequence described in chapter 2.1 can also be used for the determination of the thermal capacity of the entire store (C_s), if the store is discharged to ambient condition after the steady state.

The heat capacity of the entire store determined from a charge test ($C_{s,c}$), results from the energy transferred into the store minus the heat losses during the charge period, divided by the temperature increase of the store.

The heat capacity of the entire store determined from a discharge test ($C_{s,d}$), results from the energy transferred out of the store plus the heat losses occurring during the discharge period, divided by the temperature decrease of the store.

Theoretically it can be assumed that $C_{s,c}$ and $C_{s,d}$ are equal. In reality there is a difference between both capacities due to measurement errors. Hence this test sequence enables also a check of the measurement technique and the evaluation method. If the difference between $C_{s,c}$ and $C_{s,d}$ exceeds ±3 %, the test cannot be considered as valid.

The thermal capacity of the entire store (C_s) is calculated as the mean value of $C_{s,c}$ and $C_{s,d}$ determined from a valid test sequence.

2.3 Heat transfer capacity rate of the heat exchangers

To heat up drinking water inside the store, often immersed smooth or finned tube heat exchangers are used. The dependence of heat transfer capacity rate $(UA)_{hx}$ on the mass flow rate through the heat exchanger, the temperature difference between heat exchanger and store as well as on the temperature level can be expressed by the empirical equation (1):

$$(UA)_{hx} = C_{hx} \cdot \dot{m}_{hx}^{b_{hx,1}} \cdot \left[\left|\vartheta_{hx,in} - \vartheta_s\right|\right]^{b_{hx,2}} \cdot \left[\frac{\vartheta_{hx,in} + \vartheta_s}{2}\right]^{b_{hx,3}} \quad (1)$$

with
- $(UA)_{hx}$: heat transfer capacity rate between heat exchanger and store [W/K]
- C_{hx}: constant [-]
- $\dot{m}_{hx}$: mass flow rate through the heat exchanger [kg/h]
- $\vartheta_{hx,in}$: inlet temperature of the heat exchanger [°C]
- ϑ_s: local store temperature [°C]
- $b_{hx,1}$: exponent describing the dependence on the mass flow rate [-]
- $b_{hx,2}$: exponent describing the dependence on the temperature difference [-]
- $b_{hx,3}$: exponent describing the dependence on the temperature level [-]

Note: If several heat exchangers are used in one store, the index x represents the number of the heat exchanger.

The temperature level inside the store and the heat exchanger is taken into account by the last term of equation (1). This term can be substituted by the mean local temperature ϑ_m, which is calculated as the mean value of the heat exchanger inlet temperature and the local store temperature. If the mass flow rate through the heat exchanger is constant, the temperature difference term in equation (1) corresponds to the transferred heat flow $\dot{Q}_{hx}$.
Figure 2(a) shows the qualitative dependence of $(UA)_{hx}$ on the temperature and heat flow for a typical smooth tube heat exchanger operating with a mass flow rate of $\dot{m}_{hx}$ = 360 kg/h. For a heat flow of 3 kW figure 2(b) shows $(UA)_{hx}$ versus the mass flow rate and the mean local temperature.

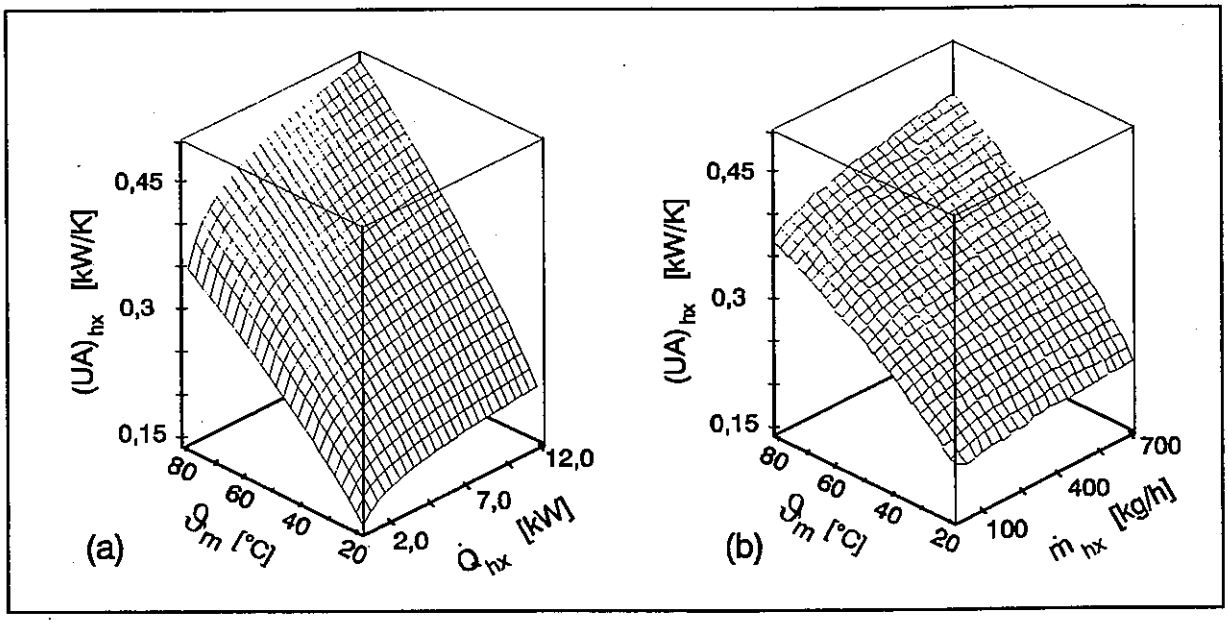

Figure 2: Heat transfer capacity rate of an immersed smooth tube heat exchanger

The dependence on the mass flow rate is small. Since, regarding forced circulated systems where the mass flow rate is almost constant, the dependence of $(UA)_{hx}$ on the mass flow rate has not to be determined in general.

In figure 2(a), the heat flow is varied in a range of 1.0 to 12 kW. If the store is integrated in a solar heating system, the available heat flow of the collector is limited by its data (i.e. collector area, η_0) and the maximum solar radiation. This upper limit is approximately 5 kW for a reasonable solar domestic hot water system for a family of four persons. The transferred heat flow has also a lower value, due to the necessary temperature difference between collector outlet and store, which is necessary to switch the circulation pump on and off.

On the basis of these considerations for a standardised store test it is sufficient to determine the heat transfer capacity rate as a function of the mean local temperature using a typical flow rate and a mean heat flow. For this, the store tank is charged via the appropriate heat exchanger with a constant heat flow and a constant mass flow rate. After reaching a heat exchanger outlet temperature of 60 °C the store is discharged to ambient conditions.
From the temperatures and flow rates recorded during this test sequence, the heat transfer capacity rate $(UA)_{hx}$ is determined as a function of the mean local temperature by parameter identification.
The test sequences for the determination of $(UA)_{hx}$ shall be carried out for the solar loop heat exchanger and for the auxiliary loop heat exchanger. From the test carried out with the solar loop heat exchanger, the effective thermal capacity of the entire store, in addition to $(UA)_{hx}$, can be determined. Based on the test for the determination of $(UA)_{hx}$ of the auxiliary loop heat exchanger, also the position of the lower connection of the auxiliary heat exchanger can be identified. This position is very important, since the store volume above is the part heated by auxiliary energy (auxiliary part).

2.4 Effective vertical thermal conductivity

The degradation of thermal stratification inside the store during stand-by is described by the effective vertical thermal conductivity (λ_{eff}). In order to determine λ_{eff} the auxiliary part of the store is charged twice by the auxiliary heat exchanger. The first time the discharge is performed immediately after charging, the second time a stand-by of 24 hours is included. Figure 3 shows the two different draw-off profiles.

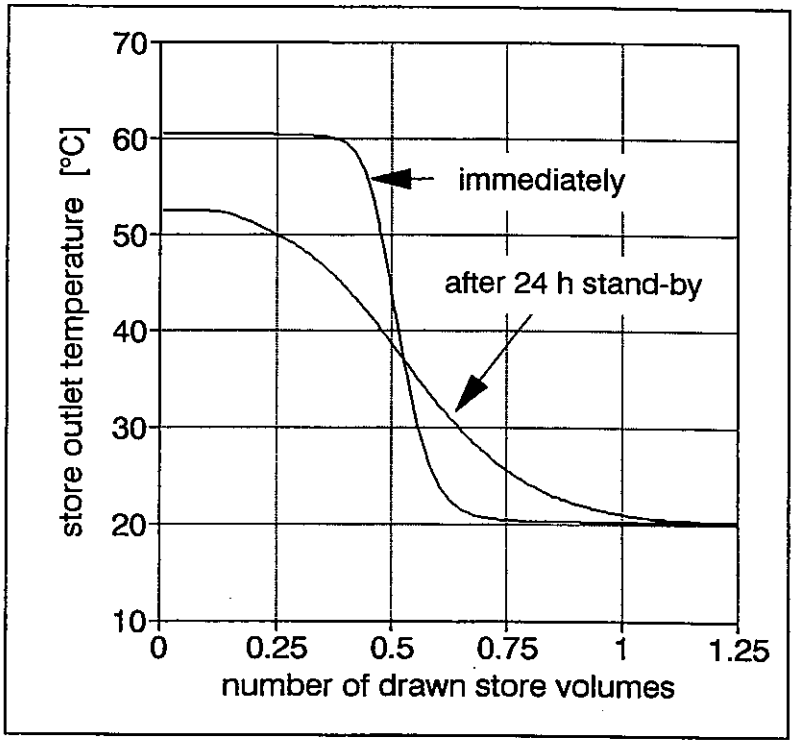

Figure 3: Draw-off profiles of auxiliary part

The draw-off profile obtained after 24 h stand-by starts at a lower temperature and the curve is less inclined. The lower temperature at the start of discharge is caused by two effects:

First, the store has lost energy during the 24 h stand-by to the environment. Therefore the amount of stored energy after stand-by is lower than the energy stored immediately after charging. **Second**, a heat transport from the hot auxiliary part to the cold solar part of the store has occurred during the 24 h stand-by.

This transport takes place by heat conduction in the wall of the steel tank, the water and other inner components of the store (e. g. heat exchangers), as well as by convection flows in the water. Both effects are combined in the effective vertical thermal conductivity.

The degradation of stratification caused by the heat transport during stand-by has two negative aspects:

1. The energy transferred from the auxiliary part of the store to the solar part has to be compensated by the auxiliary heater in order to guarantee the operating temperature in the auxiliary part.
2. The energy transferred to the solar part increases its temperature and causes higher temperatures in the collector loop.

The effective vertical thermal conductivity should be as low as possible. It can of course not be lower than the conductivity of the water in the store.

For good stores without immersed components the effective vertical thermal conductivity is close to the thermal conductivity of water (0.6 W/(mK)). For stores with immersed heat exchangers an effective vertical thermal conductivity between 1,0 and 1,5 W/(mK) can be reached.

2.5 Stratification number

The stratification number is an index for the conservation of the temperature profile during direct discharge. Draw-off profiles for different stratification numbers are shown in figure 4. For stratification numbers > 1 the store outlet temperature is constant at first, but then decreasing relatively fast. Ideally a step would occur. The steeper the curve the better the thermal stratification of the store during the discharge, and the more water can be drawn with a constant (high) temperature. The reason for the round edges of the profiles is the mixing between the hot water in the store and the cold water flowing into the store at the bottom. In order to reduce mixing the cold water should be calmed and fatigued by a baffle plate while entering the store.

High stratification numbers indicate a good conservation of the temperature stratification during discharge. The stratification number refers to the number of nodes, if the measured draw-off profile is simulated with a store model based on a finite-difference method.

The stratification number is determined by parameter identification.

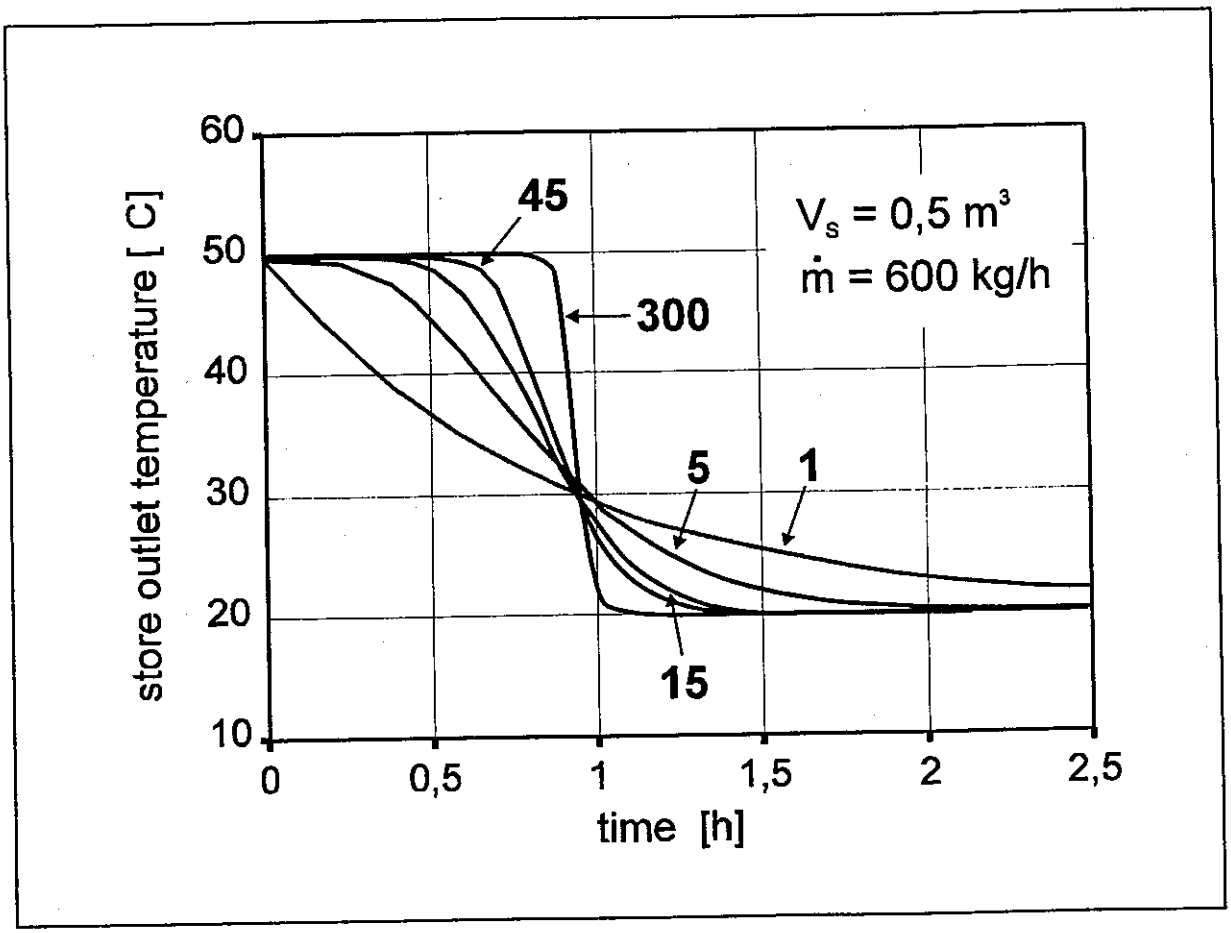

Figure 4: Draw-off profiles for different stratification numbers

3. Multiport store model

The Multiport Store Model is implemented in the TRNSYS Type 74 for the dynamic simulation of the thermal behaviour of hot water stores. The Multiport store model provides 16 connections (ports) for transferring energy into or out of the store. The store can be directly charged and discharged with a maximum of five inlets and outlets which are correspondingly connected (double ports).
For indirect charging and discharging a maximum of three immersed heat exchangers can be used. The heat transfer capacity rate between these heat exchangers and the store can be specified individually for each heat exchanger as a function of the mass flow through the heat exchanger, the transferred heat flow and the mean local temperature.
Both, the heat exchangers and the double ports, can be used to charge the store optionally in a stratified way. The flow directions through all components can be chosen individually, up- or downwards.
An internal electrical auxiliary heater is provided. It is controlled by an internal thermostat. The heater is switched on if the temperature of the thermostat is equal to, or smaller than a selected temperature T_{set}. It is switched off if the temperature of the thermostat is equal to, or greater than $T_{set} + \Delta T_{db}$, where ΔT_{db} is the deadband temperature of the thermostat.

A common application for TRNSYS is the prediction of the annual performance of a solar heating system. Developing store models for TRNSYS results in a compromise between detailed modelling of physical phenomena and acceptable computation time. The goal of the Multiport Store Model is to describe the influence of the different physical effects on the thermal behaviour of a store, without modelling this effect in detail.

The following assumptions were used:
The store tank and the heat exchangers are assumed to be isothermal in horizontal direction. The temperatures inside the store tank and in the heat exchangers are calculated as a function of the store height (z) and time. Hence, regarding the store tank or the heat exchangers, the model can be considered as one-dimensional.
Inversion inside the store tank, which means $\partial\vartheta/\partial z < 0$, is removed by mixing resulting in a mean temperature.

The Multiport Store Model is based on a finite difference method. The fluid inside the store tank and in the heat exchangers is assumed to consist of a discrete number (N) of completely mixed volume segments (nodes). All temperatures are calculated by solving a set of N x 3 coupled partial differential equations using iterative and direct solving algorithms. Furthermore a method is implemented to handle the errors which occur in the calculated transferred energies due to the analytical mixing procedure used.

4. Reproducibility of the test method

Up to now the described test method was applied to 12 different stores for solar heating systems. One important aspect of a test method is the reproducibility of the test results. Hence, to confirm the reproducibility, repeated tests were carried out on two stores. The test results of the repeated tests are presented and discussed.

Besides the reproducibility of the parameters itself their impact on the performance of the whole system is considered. Therefore long term performance predictions were carried out by using different stores or store parameters respectively in the same 'reference' solar heating system, which is described below.

Parameters of the reference solar domestic hot water system:

- Collector:	$A_C = 5\ m^2$ $\eta_0 = 0{,}8$; $k_1 = 3.5\ W/(K\ m^2)$; $k_2 = 0{,}002\ W/(K^2\ m^2)$
- Collector loop:	Pipe length between collector and store 2 x 15 m
- Daily load:	3 draw offs at: 7am 80 liter; 12am 40 liter; 7pm 80 liter Hot water temperature 45 °C: Cold water temperature 10 °C (annual energy consumption: 2940 kWh)
- Auxiliary heating: (Only for store A)	Thermal, via an immersed heat exchanger (constant inlet temperature of 70 °C until a temperature of 60°C is reached at the auxiliary heater sensor).

4.1 Store A

The design of store A is similar to the one shown in figure 1. The store is an upright steel tank with a nominal volume of 300 liters and two immersed smooth tube heat exchangers. For insulation 60 mm polyurethane foam is used.

The following test sequences, indicated by letters at the beginning, were performed:

- Test sequence A in order to determine the heat loss capacity rate as described in chapter 2.1.
- Test sequence C in order to determine the heat transfer capacity rate of the solar loop heat exchanger and thermal capacity of the entire store as described in chapter 2.3
- Test sequence S in order to determine the stratification number as described in chapter 2.5
- Test sequence NA in order to determine the heat transfer capacity rate and position of the auxiliary loop heat exchanger
- Test sequence NB in order to determine the effective vertical thermal conductivity as described in chapter 2.4

The available test sequences are compiled to three complete tests, as listed in table 1.

Test 1	Test 2	Test 3
A_0621	A_0624	A_0617
S_0809	S_0809	S_0809
C_0627	C_0125	C_0622
NA_0627	NA_0118	NA_0125
NB_0629	NB_0123	NB_0120

Table 1: Tests and test sequences

The test sequences A were evaluated by using the STEP /5/ program, which is based on analytical energy and power balances.
In order to determine the stratification number the test sequence S is evaluated separately.
Based on the test sequences (C, NA, NB) all other store parameters are determined during a single parameter identification procedure.

Test results and reproducibility

As mentioned above, information about the thermal behaviour of the store as a part of the solar heating system is important. Therefore simulations of the reference system have been carried out by using the store parameters determined from three tests. The result of these simulations is indicated by the solar fraction f_{sol}.
The store parameters determined from the different tests, as well as the solar fraction are listed in table 2.

	Test 1	**Test 2**	**Test 3**
heat loss capacity rate $(UA)_{s,a}$ [W/K]	2.06	2.05	2.05
effective storage volume V_s [liter]	271	266	272
stratification number [-]	120	120	120
effective thermal conductivity λ_{eff} [W/(mK)]	1.61	1.76	1.97
$(UA)_{h1}$ solar loop heat exchanger (for ϑ_m=50 °C) [W/K]	467	457	449
$(UA)_{h2}$ aux. loop heat exchanger (for ϑ_m=50 °C) [W/K]	335	333	357
relative position of aux. heat exchanger outlet z_{aux} [-]	0.50	0.52	0.53
solar fraction of store in reference system f_{sol} [%]	46.68	46.66	47.14

Table 2: Test results of store A

The reproducibility of the heat loss capacity rate is very high, since almost the same value for $(UA)_{s,a}$ is determined from all three tests.
The scatter of the effective store volume is also low. The maximum difference of approximately 2% between Test 2 and Test 3 is within the measuring accuracy.

Since only one S-test sequence was available, the same stratification number was determined for all three tests.

The scatter in the effective vertical thermal conductivity is approximately 10 % (based on the mean value). This is due to correlation between λ_{eff} and z_{aux}. Hence a higher value of λ_{eff} causes a higher value of z_{aux}. The scatter of approximately 10 % seems to be high, but its impact on the performance of the store is relatively low, since λ_{eff} is a second order store parameter.

The temperature dependent heat transfer capacity rate of the immersed heat exchangers is described by the empirical equation (2), which results from equation (1) if $b_{hx,2}$ and $b_{hx,3}$ are set to zero:

$$(UA)_{hx} = C_{hx} \cdot \vartheta_m^{\,b_{hx,3}} \qquad (2)$$

with $(UA)_{hx}$: heat transfer capacity rate between heat exchanger and store [W/K]
C_{hx}: constant [-]
ϑ_m: mean local temperature [°C]
$b_{hx,3}$: exponent describing the dependence on the temperature level [-]
Note: If several heat exchangers are used in one store, the index x represents the number of the heat exchanger.

The constant C_{hx} and the exponent $b_{hx,3}$ describing the dependence of $(UA)_{hx}$ on the mean local temperature are highly correlated. Based on the three sets of parameters determined for the solar loop heat exchanger three curves for $(UA)_{h1}$, calculated with equation (2), are shown in figure 5. The scatter in the three curves for $(UA)_{h1}$ is approximately ± 5 % (based on the mean value).

For the auxiliary loop heat exchanger $(UA)_{h2}$ also scatters within ±7 %.

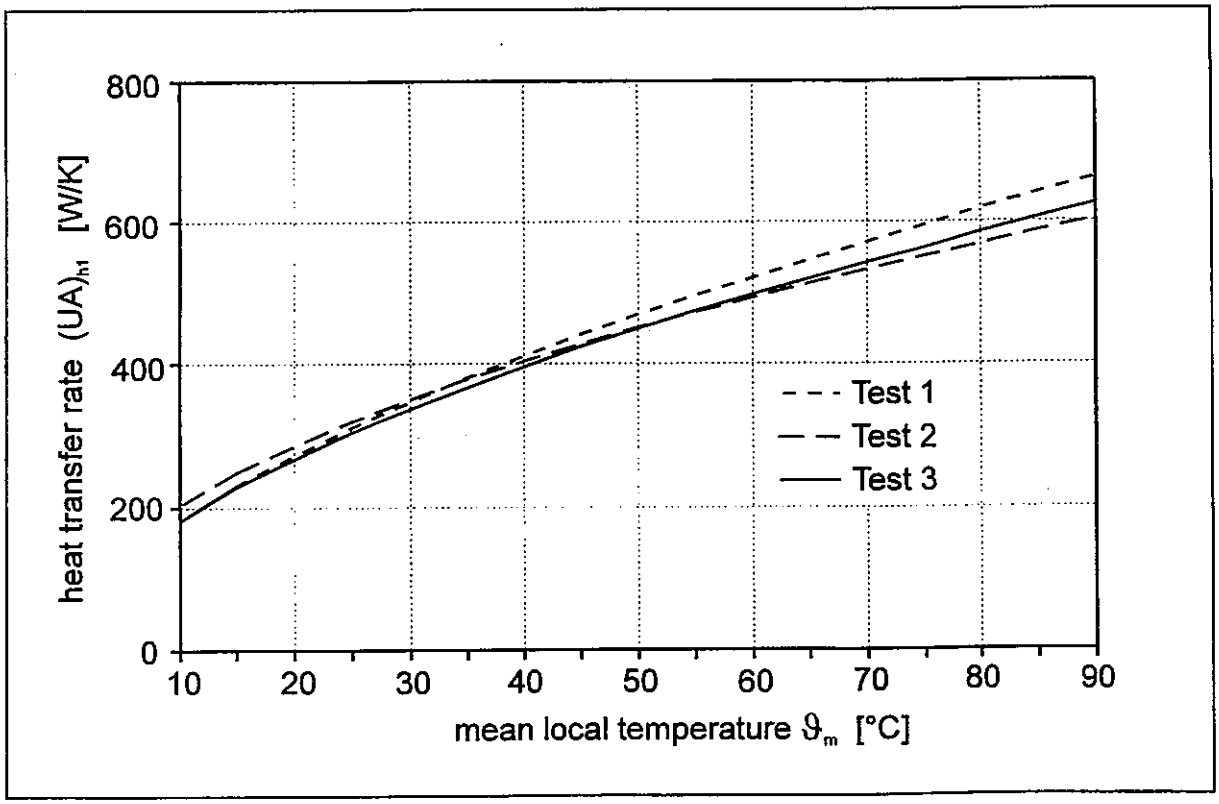

Figure 5: Heat transfer capacity rate of the solar loop heat exchanger determined from three tests

The relative position (z_{aux}) of the outlet (lower connection) of the auxiliary loop heat exchanger is an important parameter, since it indicates the auxiliary volume of the store. The difference, based on the mean value, of z_{aux} is less than ± 2 % absolute, which is within the measuring accuracy.

The maximum difference in the predicted solar fraction f_{sol} is with less than 0.5 % (absolute) quite small.

Verification of test results

The results of the tests described previously are verified by 're-simulating' a 'dynamic test sequence'. This sequence covers a wide range of operating conditions. These data were not used for identifying the store parameters. The verification test sequences are separately performed for each heat exchanger. Each dynamic test sequence consists of the following phases:

charge - discharge of half volume - recharge - stand-by - complete discharge

Figure 6 shows the measured in- and outlet temperatures as well as the temperature difference between the measured and calculated outlet temperatures. The in- and outlet temperatures of the solar loop heat exchanger are plotted for the charge phase (C), and those of the tank for the discharge phase (D). The relative difference between the measured and calculated energy, transferred into the store is 1.51 %, and that of the energy transferred out of the store is -0.12 %.

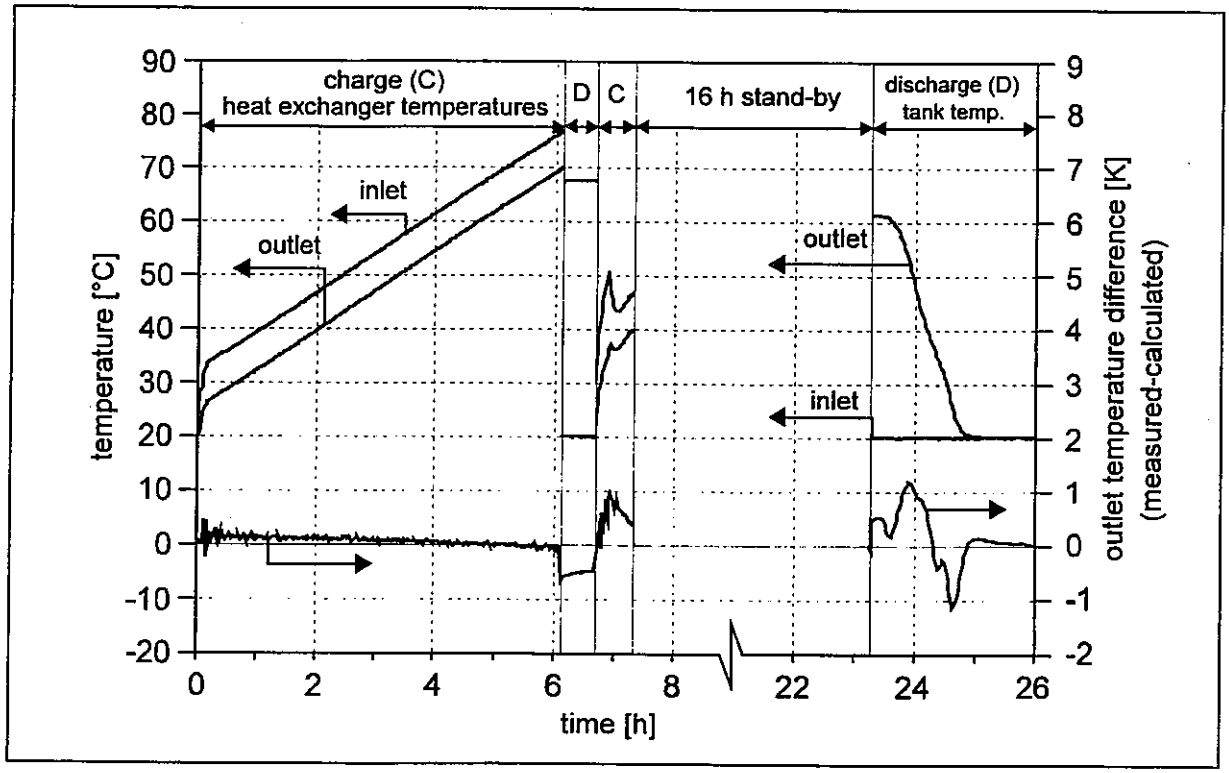

Figure 6: Temperatures and temperature difference between measurement and calculation

4.2 Store B

Store B is a horizontal steel tank with a nominal volume of 250 liter. The store is insulated with 35 mm polyurethane foam. The internal heat exchanger consists of a tube with closed end walls and a fluid content of 32 liters. The store was tested at the Renewable Energy Research Centre at Amman, Jordan. Figure 7 shows the schematic design of store B.

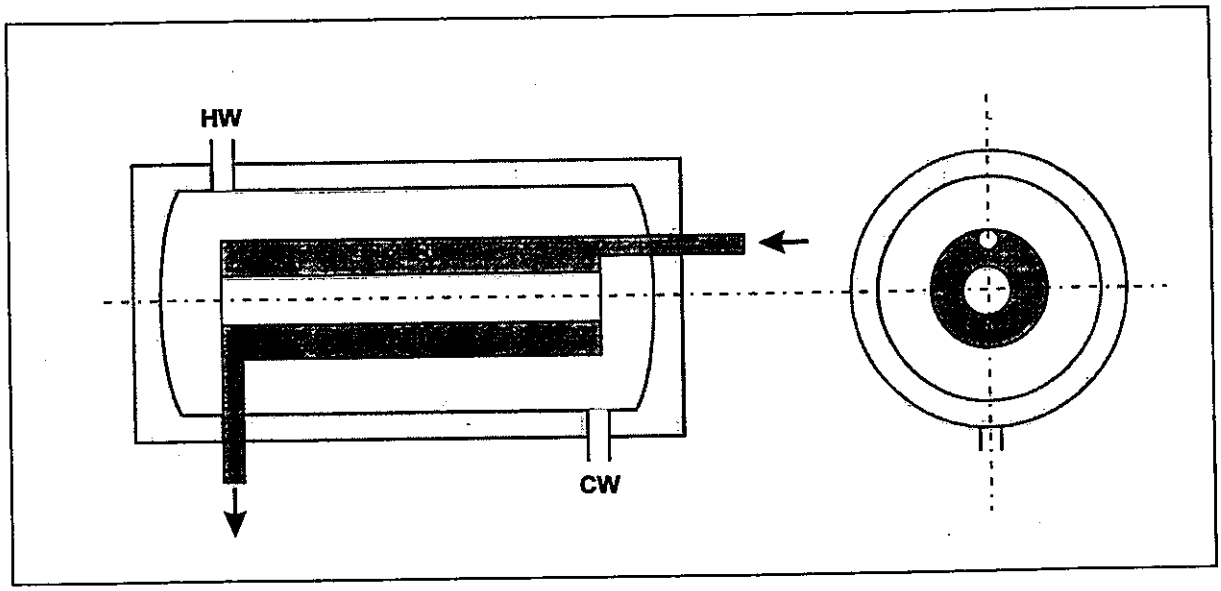

Figure 7: Schematic design of store B

The following test sequences were carried out in order to determine the thermal parameters of the store:

- Test sequence A in order to determine the heat loss capacity rate as described in chapter 2.1.
- Test sequence C in order to determine the heat transfer capacity rate of the heat exchanger and the thermal capacity of the entire store as well as the thermal stratification during direct discharge.

Since the store does not have an auxiliary heated part which is on high temperature most of the time, the effective vertical thermal conductivity does not have to be determined. Hence a default value of 1.7 W/(mK) is used.

The available test sequences are compiled to three complete tests, as listed in table 3.

Test 1	Test 2	Test 3
AX_0611 CX_0606	AX_0611 CX_0613	AX_0611 CX_0614

Table 3: Tests and test sequences

The test sequence A is evaluated by using the STEP /5/ program. The test sequences C were evaluated by means of parameter identification. Note that only one test sequence A was available.

Test results and reproducibility

The determined parameters as well as the predicted solar fraction are listed in table 4. For the long term prediction the solar domestic hot water system was considered as a preheat system, since only one heat exchanger is inside the store.

	Test 1	Test 2	Test 3
heat loss capacity rate $(UA)_{s.a}$ [W/K]	2.63	2.63	2.63
effective storage volume V_s [liter]	247.6	243.2	242.7
stratification number [-]	70	59	65
$(UA)_{hl}$ solar loop heat exchanger (for ϑ_m=50 °C) [W/K]	296	266	286
solar fraction of store in reference system f_{sol} [%]	60.55	60.21	60.35

Table 4: Test results of store B

For all three tests the heat loss capacity rate was determined to the same value, since only one A-test sequence was available, which was evaluated separately.

The scatter of the determined effective storage volume is within the measuring accuracy. The stratification number differs by approximately 17 %. This seems to be very high, but as shown in figure 4, the influence of different stratification numbers decreases for high stratification numbers. Hence the scattering of the values for the stratification numbers can be accepted.

The maximum difference in the heat transfer capacity rate $(UA)_{hl}$ as a function of the mean local temperature (ϑ_m) is approximately 10 % between Test 2 and Test 3 at ϑ_m = 90 °C (see figure 8).

The last row of table 4 shows the predicted solar fraction if store B is used in the reference system. The maximum deviation is approximately 0.4 % (absolute) between test 1 and test 2.
Figure 8 shows that the largest heat transfer capacity rate $(UA)_{hl}$ results from Test 1 and the smallest from Test 2. Since the influence of $(UA)_{hl}$ on the predicted solar fraction is decreasing for large values of $(UA)_{hl}$, also the reproduction of errors in $(UA)_{hl}$ on f_{sol} depends on the quantity of $(UA)_{hl}$.
On the other hand, deviation of small $(UA)_{hl}$ values affect the thermal behaviour of the store stronger than the deviation of high $(UA)_{hl}$ values. Consequently small $(UA)_{hl}$ values can be determined with a higher accuracy by means of parameter identification.

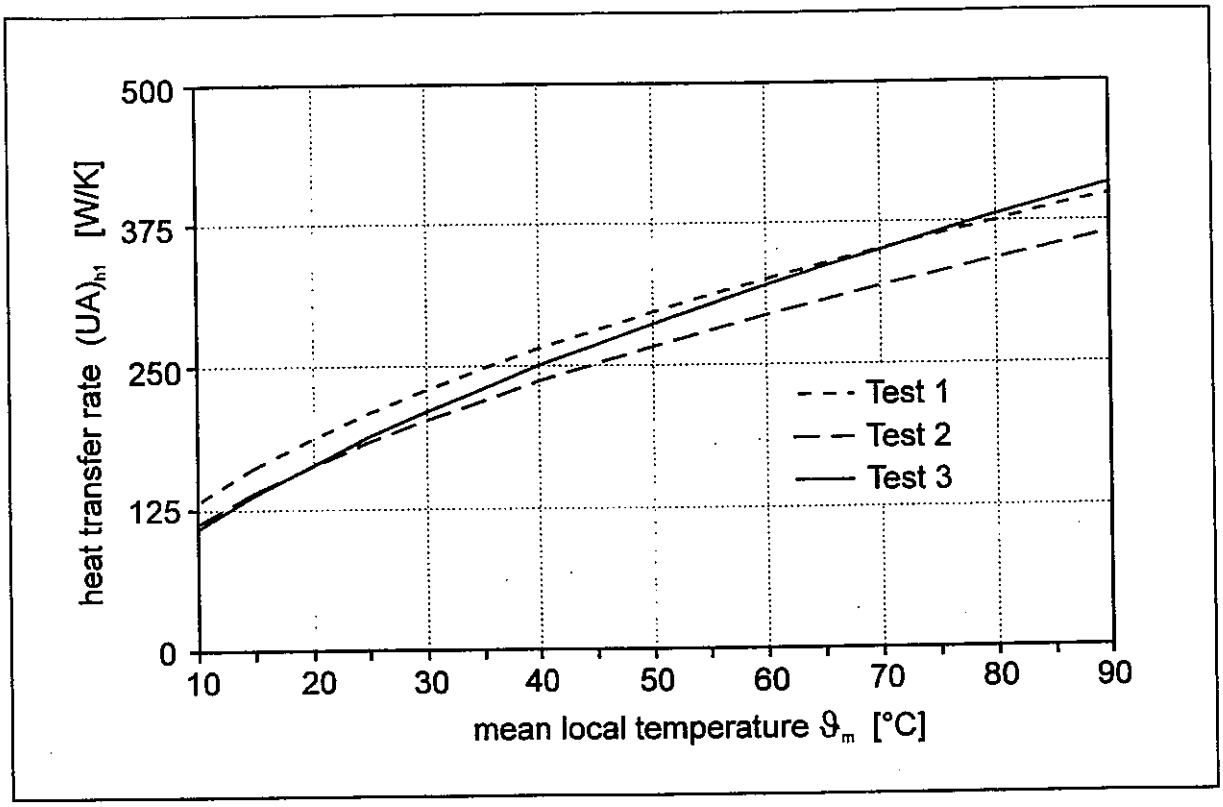

Figure 8: Heat transfer capacity rate of the heat exchanger determined from three tests

5. Conclusions and future outlook

With the described procedure for the thermal test of hot water stores all relevant thermal store parameters can be determined. Hence, using an adequate store model, the thermal behaviour of a store can be described in detail.
Up to now 12 stores with partly strong varying design have been tested with success according to this procedure. Detailed information about the thermal behaviour of the store was gained, which was provided to the manufactures to improve their design.

As a further application of the determination of thermal store parameters by means of parameter identification, the store parameters can be determined from the measuring data gained during a test of the whole solar heating system. For that purpose the flow rate and the inlet and outlet temperature of all fluids entering or leaving the store have to be measured. If the system is tested, e. g. according to ISO 9459, Part 5 /6/, additional measurements of the volume flow rate as well as of the inlet and outlet temperature of the heat exchanger in the collector loop are necessary. The data gained during the test of the whole solar heating system provide enough information for the determination of the most important store parameters.

A comparison of the store parameters and the predicted f_{sol} determined one time on the store testing stand (Test 1) and the other time on the base of system test data (*in sys*) is shown in table 5.

	Test 1	***in sys***
heat loss capacity rate $(UA)_{s,a}$ [W/K]	2.06	1.93
effective storage volume V_s [liter]	271	257
stratification number [-]	120	120 (fix)
effective thermal conductivity λ_{eff} [W/(mK)]	1.61	1.99
$(UA)_{h1}$ solar loop heat exchanger (for ϑ_m=50 °C) [W/K]	466	299
$(UA)_{h2}$ auxiliary loop heat exchanger (for ϑ_m=50 °C) [W/K]	335	381
relative position of aux. heat exchanger outlet z_{aux} [-]	0.50	0.48
solar fraction of store in reference system f_{sol} [%]	46.68	45.70

Table 5: Comparison of store parameters determined by a test on a testing stand (test 1) and within a test of the whole system (*in sys*)

With the exception of $(UA)_{h1}$ the agreement between the results of the two test methods is acceptable. The different values of $(UA)_{h1}$ are due to the different fluid used. For the tests carried out on the store testing stand (Test 1) water was used. The system test (*in sys*), however was performed with antifreeze. The larger viscosity of the antifreeze results in a lower $(UA)_{h1}$ value. The two predicted performance indicators f_{sol} show a good agreement.

The *in sys* test method is very powerful, since if the system is tested according to ISO 9459, Part 5 no complete store test has to be performed. Up to now three comparisons between store tests on a store testing stand and *in sys* test have been carried out with good agreement. But further investigations are still necessary.

Both developed test procedures deliver all relevant parameters for the thermal behaviour of a hot water store. The test procedures are therefore proposed as a testing standard for hot water stores /7/. Due to the large number of determined parameters the influence of constructive elements of the store on the operation of a solar heating system can be quantified in detail.

6. References

/1/ W. Spirkl:
Dynamic System Testing Program Manual, Version 2.4α, InSitu Scientific Software, Klein & Partners, Baadstr. 80, 80469 München, März 1994

/2/ H. Drück, Th. Pauschinger:
Type 74 - Multiport Store Model for TRNSYS, Version 1.8, Institut für Thermodynamik und Wärmetechnik, Universität Stuttgart, 1994

/3/ S. A. Klein et al.:
TRNSYS, A Transient Simulation Program Version 13.1, Solar Energy Laboratory, University of Wisconsin-Madison, Wisconsin 53706 USA, April 1992

/4/ Th. Pauschinger, Th. Held:
Parameter Identification with TRNSYS and DF, Version 0.3, User Manual, ITW, Universität Stuttgart, Dezember 1992

/5/ Commission of the European Communities, Test Procedures for Short Term Thermal Stores, edited by H. Visser and H.A.L. van Dijk, Kluwer Academic Publishers Dordrecht/Boston/London, 1991, ISBN 0-7923-1131-0

/6/ W. Spirkl et al.:
ISO/CD 9459, Part 5, Solar Heating - Domestic Water Heating Systems, System Performance Characterisation by Means of Whole System Testing and Computer Simulation (Draft), February 1994

/7/ H. Drück, Th. Pauschinger:
ISO 9459, Part 4A, Solar Heating - Domestic Water Heating Systems, Performance Characterisation of hot water storages of solar heating systems (First draft for discussion), August 1995

Acknowledgement

This work was financed by the German Ministry of Research and Technology under grant Nr.0328768E and Stiftung Energieforschung Baden-Württemberg under grant Nr.A00001990. The authors gratefully acknowledges this. Furthermore, the authors appreciate for the measuring data of store B from Mr. B. Sc. Mech. Eng. Ammar Al-Taher from The Royal Scientific Society, Renewable Energy Research Centre in Amman, Jordan.

CTSS - A Component Oriented Performance Test Method for Solar Heating Systems

Th. Pauschinger

Institut für Thermodynamik und Wärmetechnik (ITW)
Universität Stuttgart
Prof. Dr.-Ing. E. Hahne
Pfaffenwaldring 6, D-70550 Stuttgart
Phone: (0)711/685-3536, Fax: (0)711/685-3503

1 Introduction

Several performance test methods for solar heating systems have been established as international standards or drafts as ISO 9459 (ISO 9459, Part 1 /1/, Part 2 /2/, Part 3 /3/ and Part 5 /4/).

Within the so called *Rating Test* according to ISO 9459, Part 1, a performance indicator is determined based on indoor measurements of the system performance. The test result cannot be extrapolated to other climates and does not indicate the yearly energy delivered by the system.

The test methods according to ISO 9459, Part 2, Part 3 and Part 5 are based on two steps:

1. A **short term test** under outdoor conditions is carried out with the **whole system**, to determine parameters for either a physical model or a correlation model for the solar heating system.
2. A **performance prediction** is carried out for reference conditions (e.g. weather data, hot water load) using the same model and the determined parameters.

Alternatively to these whole system test methods a method by means of **component testing and whole system simulation** is proposed. In stead of the test of the whole system the system components, namely the collector, the store and the controller are tested. The performance prediction is then carried out by a computer simulation of the whole system, using a modular computer program such as TRNSYS /5/. In the following this method is called CTSS method, standing for *Component Testing - System Simulation*. Fig. 1 shows the structure of the CTSS method.

The development of the CTSS method is motivated by several advantages over the whole system tests:

- The CTSS method is flexible with respect to exchanging and combining of the system components. A large part of the solar heating systems on the market are not offered in fix sizes. This means components can be alternatively chosen from an assortment of a company and be combined in different sizes. The components can also be assembled in different system configurations e.g. to a system for domestic hot water preparation only or a system for combined domestic hot water preparation and space heating. For these type of systems, the so called custom built systems, the CTSS method allows for more flexibility and cheaper testing.

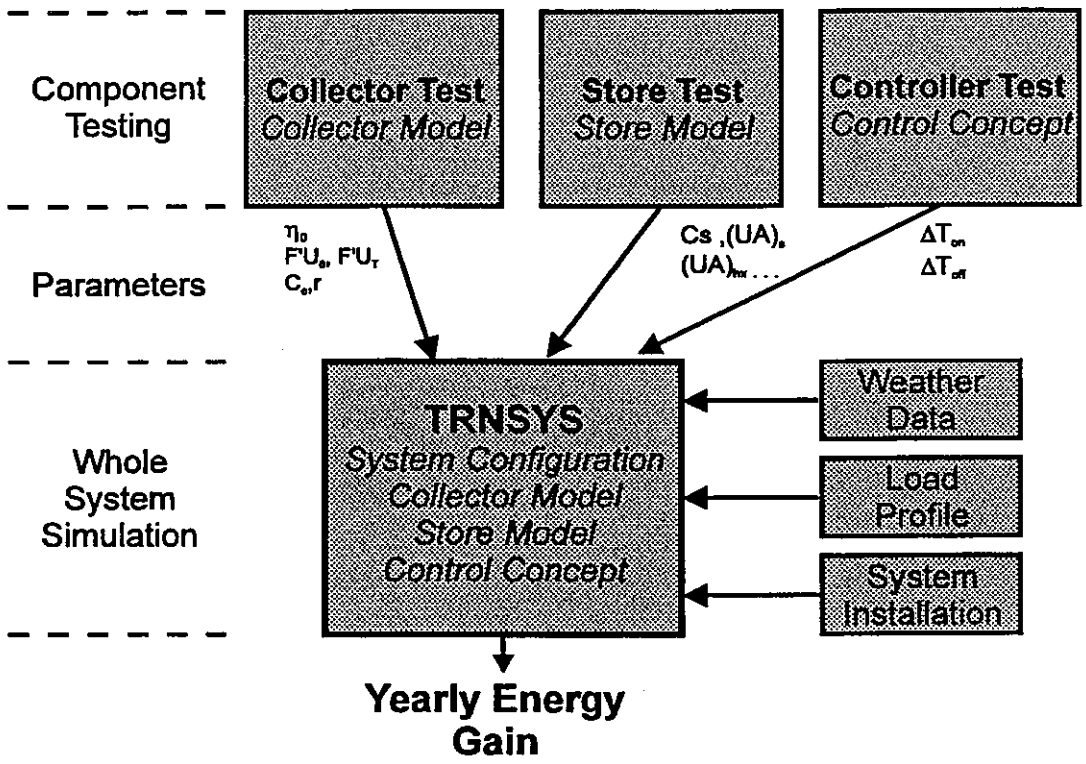

Figure 1: Procedure for testing solar heating systems with the CTSS method

- The CTSS method is based on component tests, thus the installation of the whole system becomes superfluous.
- The CTSS method is currently the only test method that makes testing of systems for combined hot water preparation and space heating possible.
- The CTSS method yields more insight in the component's behaviour.

2 Test method

The four steps of the CTSS method are:

Step 1: The components collector, store and controller are tested with a suitable test method.

Step 2: The function of the whole system is checked by inspecting all components and parts as well as the system documentation.

Step 3: The whole system is modelled using a simulation program for the relevant system configuration and the obtained component parameters. The yearly energy gain is predicted for reference conditions.

Step 4: If for the relevant system configuration no validated system simulation model is available, then the model used for step 3 shall be validated by a test of the whole system, a so-called validation test.

In the following these steps are described in detail.

2.1 Component testing

2.1.1 Collector test

For collector testing the standardised steady-state collector test methods or Dynamic Collector Testing are used. It is important, that all parameters are obtained, which are necessary for dynamic simulation of the collector. These are:

- The standard steady-state parameters: zero heat loss efficiency η_0, collector heat loss coefficients a_1 and a_2 as well as the effective collector heat capacity C_c;
- an incidence angle modifier for the full description of the angular dependence of the transmission absorptance product (for direct and diffuse irradiance);
- for unglazed collectors: the wind speed dependence of the efficiency;
- optional: parameters that describe the dependence of the efficiency on the collector mass-flow rate or the collector tilt respectively.

2.1.2 Store test

The test method described in /6/ delivers all necessary parameters for dynamic simulation of the store.

2.1.3 Controller test

It is the goal of the controller test to obtain all data, which are necessary for modelling the behaviour of the collector loop controller and the controller of the auxiliary heater (if present). For more complex system configurations further controller features are possible.

The most simple case is a temperature difference controller for the solar loop and a thermostat controller for the auxiliary heater. Here the method described by Katic /7/ can be applied. The controller switch point temperatures and temperature differences are experimentally determined.

For more complex controllers (like for matched flow systems) an exact test procedure cannot be specified, because the controller concept can vary widely (e.g. PID controllers or adaptive controllers). In general the control concept as specified by the manufacturer in the technical documentation shall be checked by measurement. This can be done either by using thermostatic bathes or by simulating the sensors with resistance boxes. For the whole system simulation the control concept shall be implemented in the simulation program using the obtained control parameters.

2.2 Functioning test of the whole system

One of the major disadvantages of the CTSS method is the fact, that typical system errors such as a not working check valve or a misplaced controller sensor are not recognised, because only the components are tested by measurement, however not the whole system. Nevertheless, an installation of the whole system shall be avoided, because by this the CTSS method would loose its flexibility and testing cost would rise significantly. On the other hand these system failures lead very often to problems in practice. Therefore a functioning test of the whole system must be considered as important part of the CTSS test procedure.

The functioning test is carried out by a **visual inspection** of all components and parts as well as a check of the technical documentation. Some of the aspects to be checked as they were adopted for a draft CEN standard /8/ are listed below:

- Balanced flow in the collector array
- Location and installation of all temperature sensors
- Thermosiphonic backflow in the collector loop
- Insulation

A complete functioning test is described in /9/.

2.3 Simulation of the whole system

The long term performance prediction, i.e. the determination of the yearly energy gain for reference conditions, is carried out by computer simulation of the whole system. Practice shows that due to the large number of parameters to be entered in a simulation program and due to the different calculation models the results from simulations can scatter significantly. Therefore the CTSS method takes following precautions:

- The model of the system simulation program shall be experimentally validated (see 2.4)
- For the simulation of the whole system the parameters obtained from testing the collector, the store and the controller shall be used. Further the component models as they were used for the component tests shall be implemented in the program for the whole system simulation. This particularly holds, when parameter identification methods were used for the component tests, as described in /10/ and /6/ for testing the collector and store.
- All data and parameters referring to the installation between the components (e.g. pipe length and insulation) shall be provided as reference values.

In the following the necessary specifications with regard to this aspects are summarised. Available specifications from already existing guidelines were adopted.

2.3.1 General

The simulation program shall enable to model the hydraulic connections of the components and the control concept. No simplifications are allowed for modelling the system configuration, e.g. two stores connected in series may not be modelled as one store.

The dynamic effects of the components (e.g. the heat capacity of a collector or the PID behaviour of a controller) shall be taken into account. Short time constants in the range of several minutes and fast transients, e.g. during draw-offs, require short simulation time steps that are also in the range of several minutes. In any case the simulation time step shall be chosen according to the rules of simulation theory.

2.3.2 Simulation of the collector

Suitable models and their implementation in the simulation program TRNSYS are described in /10/. The parameters obtained from collector testing shall be used.

2.3.3 Simulation of the store

The store test method as described in /6/ already comprises a store model as integral part, which is used for parameter identification. The same model and the parameters obtained from store testing shall be used.

2.3.4 Simulation of the controller

The control concept shall be modelled and implemented in the simulation program. This holds for simple temperature difference and thermostat controllers as well as for more complex controller concepts. The parameters obtained from controller testing shall be used.

2.3.5 Specifications for modelling the whole system

Apart from the models and parameters for the components, the modelling of all further system parts (e.g. piping and insulation) has significant influence on the results of the system simulation. Specifications for installations are available from standards for whole system tests like /4/. In order to ensure comparable results from whole system tests and the CTSS method, this specifications must be adopted as far as possible. In table 1 the specifications for modelling the whole system installation are listed.

Collector orientation	south, collector tilt equals latitude
Collector loop piping	total length 2 x 15 m; inner pipe diameter DN 16; insulation thickness 25 mm, $\lambda = 0.04$ W/(m K) piping location half indoors and half outdoors
Cold water mixer	if the store outlet temperature exceeds the maximum desired temperature, cold mains water is mixed to the hot water flow
External auxiliary heater	operation with constant supply temperature connecting piping without heat losses set temperature = desired temperature + 2 K supply temperature = set temperature + 10 K
External heat exchanger	acc. to technical documentation

Table 1: Specifications for modelling the whole system

2.3.6 Reference conditions for systems for domestic hot water preparation only

Also for the reference conditions for the long term performance prediction a maximum compatibility must be ensured for the whole system test methods and the CTSS method. For systems for domestic hot water preparation the specifications from /4/ were adopted (see table 2).

Location	for Germany: Hannover, Würzburg, Stötten for Europe: Stockholm (SW), Brussels (B)/Würzburg(D), Davos(CH), Athens(GR) international: Edmonton (CAN), Würzburg (D), Alice Springs (AUS)
Hot water load	50, 70, 100, 150, 200, 300, 500, 700, 1000, 1500 l/d with three draw-offs (7^{00}: 40 %; 12^{00}: 20 %; 19^{00}: 40 %) cold water temperature 10 °C; desired hot water temperature 45 °C

Table 2: Reference conditions for systems for domestic hot water preparation only

2.3.7 Reference conditions for systems for combined domestic hot water preparation and space heating

So far the CTSS method is the first method dealing with systems for combined domestic hot water preparation and space heating. Guidelines with suitable reference space heating loads are not yet available.

For this purpose a method of Schulz /11/ is recommended, which generates reference heat loads by dynamic simulation of reference buildings taking into account passive solar gains and the building heat capacity. The simulation is performed separately from the simulation of the solar heating system in order to produce a reference space heating load file which can be used in a similar way as e.g. the meteorological data in test reference years.

2.3.8 Reference conditions for the CEN standards

Reference conditions for the CEN standards are currently under elaboration. This list of reference conditions is more detailed as given in the tables above. Four climatic zones are defined for Europe. Drafts of the CEN reference conditions are included in /8/.

2.4 Validation test

The variety of system types which are marketed requires more than one system simulation model for the performance predictions. Further it is not possible to chose only one simulation program from the large number of available programs. Thus the CTSS method does specify neither the system simulation model nor the simulation program to be used. Instead the validation of the system simulation model is included as an integral part of the test method. This means that the system simulation model must be checked with a so called *'validation test'*, using data gained from measurements on a whole system.

A validation of the simulation **for each system test** would lead the CTSS method ad absurdum, because it is just the installation of the whole system that shall be avoided. Thus it is only required that the system simulation model is validated **once for each system configuration**. The validated system simulation model can then be used for each further test of a system with the same system configuration. This specification requires a definition of the system configuration (see /12/):

> System configuration: characteristics of a solar heating system including its hydraulic and control concept. Systems differing by any other parameter or only by the collector interconnection within the collector array are considered to have the same configuration.

This means, that for the case that only different components are used but the system configuration remains the same, no validation must be carried out. Only the components must be tested, the performance prediction can be carried out by using the already validated simulation program. This also holds if the size of the components changes (e.g. store volume or collector field size).

For the case that e.g. two stores are used instead of one or the control concept is modified, the system configuration is changed and, if a validated simulation program is not available, a validation test has to be carried out.

A procedure for the validation of the system simulation model is proposed in /8/. The procedure is rather similar to a test of the whole system according to the DST method /4/. According to specific test sequences measurements are made on the whole system. For the validation of the system simulation model a comparison of the measured and simulated system output is carried out using the same input data from the measurements.

3 Experimental results

So far experience has been mainly gained on two types of solar heating systems:

1. Forced-circulation systems for hot water preparation. The heat is transferred from the collector loop to an upright standing hot water store via an immersed heat exchanger. Auxiliary heat is provided by an immersed electrical heating element.
2. Like 1, however the auxiliary heat is transferred from an external heater to the upper part of the store via a second immersed heat exchanger.

For the first system configuration one system was tested in detail in the laboratory during 1993. The measurements were carried out according to the recent version of the DST method /13/ at that time. Additional sensors were mounted to determine also the component parameters according to the Dynamic Collector Test and the store test method. The yearly energy gain was then predicted with the CTSS method. A comparison of the results from evaluation with the DST method yields an agreement of better than 0.02 for the solar fraction. The results are presented more in detail in /14/.

During 1994 eleven systems of configuration 2 were tested. These are:

- seven conventional systems with flat-plate collector
- two conventional systems with ETC
- one system with flat-plate collector and a store with stratifier
- one matched-flow system with concentrating ETC and external heat exchanger in the charge loop

For these systems a separate test of the collector, the store and the controller has been carried out. The yearly energy gain was predicted using a validated system simulation model.

In addition each system was installed as a whole and tested according the DST method, so that a direct comparison is possible.

Figure 2 shows the test results for these eleven systems according the DST and the CTSS method.

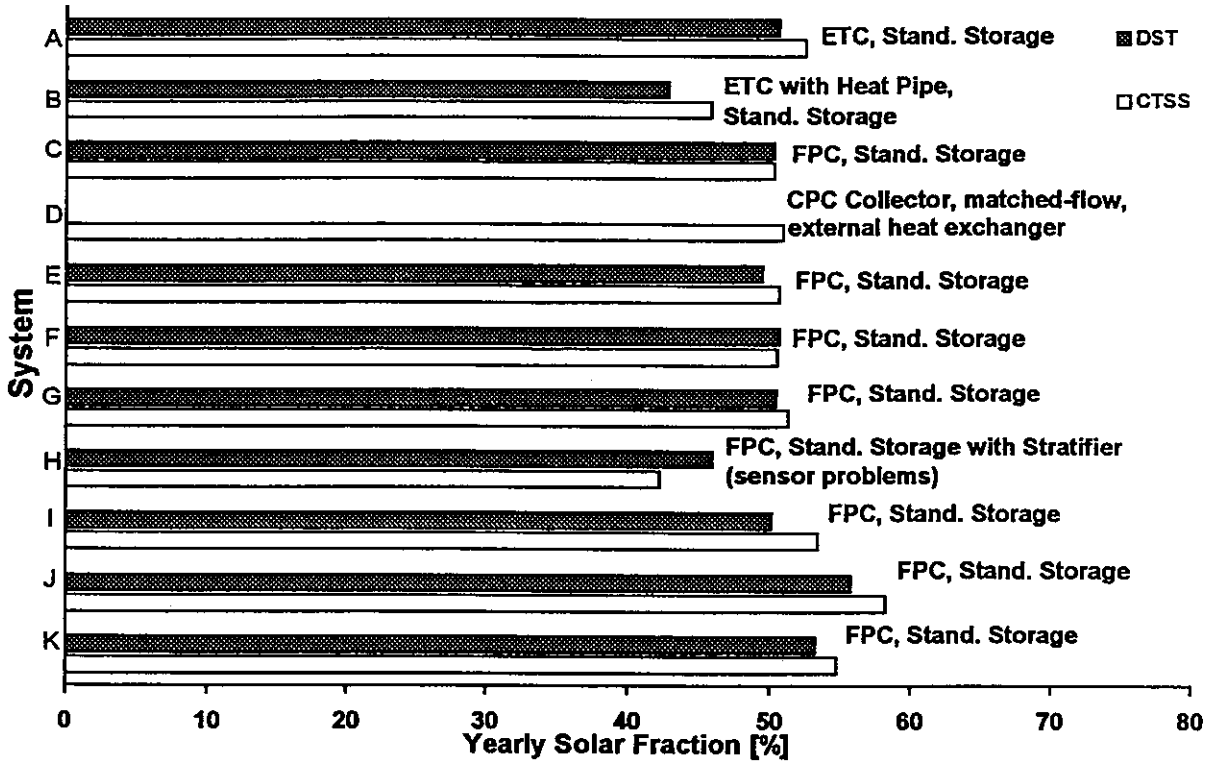

Figure 2: Comparison of the test results for eleven solar heating systems according to the DST and the CTSS method

In general the test results show a very good agreement. Apart from two exceptions the deviation remains below 0.03 for the solar fraction.

The CTSS method consistently produces higher results. An analysis of the results leads to the supposition, that this effect origins from the different heat transfer fluids used: The DST tests were carried out with a mixture of water and glycol, whereas the component tests were carried out with pure water. The heat transfer fluid has a significant impact on the inner heat transfer coefficient of the solar loop heat exchanger. For smooth tube heat exchangers with large tube diameters this effect has a stronger impact as for finned tube heat exchangers. The largest deviation occurred for systems with smooth tube heat exchanger (A, B, G, J and K). However, also the fact that the CTSS method assumes a 'perfect' installation between the components can contribute to this effect.

For system H the energy gain was overestimated. The reason for this was a wrong positioned controller sensor of the auxiliary heater. This leads to the effect that the auxiliary heated part of the system is heated to much higher temperatures as set at the thermostat. The DST method identifies only the fraction of the store which is auxiliary heated. It does not identify a deviation between the real and the adjusted temperature reached in the auxiliary heated part. Thus this malfunction was not recognised by the DST method.

The data of system D (matched-flow system with concentrating ETC and external heat exchanger) could not be evaluated with the DST method.

4 Assessment of the method

A large part of the solar heating systems for hot water preparation or combined hot water preparation and space heating is offered as components that are combined to the whole system. For these systems a component oriented test method, as the CTSS method, has several advantages over the whole system test methods.

The first experimental investigations show, that the CTSS method delivers accurate and reliable results and that it enables a detailed analysis in cases problems occur. The component tests and the detailed modelling of the solar heating system allows to pass also additional valuable information to the manufacturer of the system. In two cases the solar heating system could be improved in cooperation with the manufacturers.

By now the CTSS method is implemented as draft standard by the committees of ISO and CEN. For a wide acceptance of the CTSS method further international validation especially an extension of the scope beyond the currently treated systems is necessary. These activities are planned for the years 1996 and 1997.

5 References

/1/ ISO 9459-1: Solar heating - Domestic Water heating systems - Part 1: Performance rating procedure using indoor test methods, Reference Nr. ISO 9459-1:1993(E), ISO, Geneve, 1993

/2/ ISO/DIS 9459-2: Solar heating - Domestic Water heating systems - Part 2: Performance test for solar only systems, ISO, Geneve, 1993

/3/ ISO/DIS 9459-3: Solar heating - Domestic Water heating systems - Part 3: Performance test for solar plus supplementary systems, ISO, Geneve, 1993

/4/ Spirkl et al.: ISO/CD 9459, Part 5, Solar Energy System Performance Characterization by Means of Whole System Testing and Computer Simulation (Draft), November 1994

/5/ S.A. Klein et. al.: TRNSYS, A Transient Simulation Program Version 14.1, University of Wisconsin, 1994

/6/ H. Drück: Thermal Testing of Stores for Solar Domestic Hot Water Systems, Universität Stuttgart, Institut für Thermodynamik und Wärmetechnik, Stuttgart, 1995

/7/ I. Katic: Domestic Hot Water and Space Heating Solar Systems, Testing of Controls; Danish Technological Institute, November 1992

/8/ CEN TC 312, WG 3: EN TC 312, Part 6; Thermal Systems and Components; Custom Built Systems, Test Methods for Small Systems, Institut für Thermodynamik und Wärmetechnik der Universität Stuttgart, Oktober 1995

/9/ IEA Inspection Procedure for Solar Domestic Hot Water Heating Systems, Paul Scherrer Institute, Villigen, Switzerland, April 1990

/10/ B. Perers et al.: Dynamic Collector Testing, Final report from the IEA Task XIV Dynamic Component and System Testing Group (to be published)

/11/ M.E. Schulz, R. Kübler, E. Hahne: Investigation of Central Solar Heating Plants with Various Heat Distribution Systems, Proc. ISES Solar World Congress, Budapest 1993, Vol. 4, S 185-190

/12/ CEN TC 312, WG 3: EN TC 312, Part 5; Thermal Systems and Components; Custom Built Systems, General Requirements, Institut für Thermodynamik und Wärmetechnik der Universität Stuttgart, Oktober 1995

/13/ Spirkl et al.: ISO/CD 9459, Part 5, Solar Energy System Performance Characterization by Means of Whole System Testing and Computer Simulation (Draft), 1991

/14/ E. Hahne, Th. Pauschinger, N. Fisch: Test Method for Solar Domestic Hot Water Systems by Means of Component Tests and Whole System Simulation, Proc. of the ISES Solar World Congress Budapest, 1993

ANNEX C: TECHNICAL PAPERS ON IN SITU TESTING OF LARGE SOLAR HEATING SYSTEMS

IN-SITU COLLECTOR ARRAY TEST

Miroslav Bosanac, Jan Erik Nielsen
Solar Energy Laboratory, Danish Technological Institute, P.O. Box 141, DK-2630 Taastrup, Denmark

Abstract - In the scope of the EU-ALTENER project 'Guaranteed Yield of Solar Water Heaters' we deal with a procedure for in-situ check of collector array performance i.e. the array energy yield in particular. A procedure for dynamic, in-situ check of collector array performance has been used. Dynamic testing deals with a determination of collector performance under non-stationary test conditions. Main advantage of dynamic testing to the steady-state methods are basically that there is no limitations regarding stability of operation conditions. Using TRNSYS-simulations the working conditions most probable for the collector array has been found. On that basis the range of parameters to be scanned during short term test has been determined and the criteria for termination of test has been established. We consider it as a crucial question how close operation conditions during the test covers possible operation conditions which might appear in normal operation. In that sense, the accuracy and repeatability of identified parameters are addressed in this article.

1. INTRODUCTION

Dynamic testing deals with the determination of collector performance under non-stationary test conditions. Main advantages of dynamic testing regarding the steady-state methods are briefly: operating and meteorological conditions (fluid inlet temperature, flow-rate irradiance and wind velocity) may vary during a test thus enabling in-situ test (see for example (Bosanac *et al.* 1993).

In this work we discuss a possibility to perform a short-term test attaining at the same time acceptable accuracy and repeatability of test results. A short-term test is important for several reasons i.e.: (1) reducing of measurements costs and (2) - for many climatic regions - seldom occurrence of longer periods of time with high irradiance over a considerable part of the year.

In order to investigate the possibility to minimise test duration, series of in-situ tests have been carried out in the summer and in the autumn 1994. These tests were performed outdoors on a Danish system having the collector array of 60 m² delivering hot water for an institution for elderly people.

The measurements were carried out under normal working conditions i.e. various weather conditions and various collector inlet temperatures.

2. COLLECTOR MODEL

The modified multi-node collector model (Bosanac *et al.* 1993) and (Muschaweck & Spirkl 1993)

has been used for this analysis. The model has the following features:

1.A linear dependence of the collector efficiency factor on collector flow rate is assumed.

2.A linear dependence of the heat loss coefficient on the surrounding air speed as well as on the temperature difference between collector and ambience is assumed.

3.Incident angle modifiers for beam (as a function of incident angle) and diffuse irradiance are introduced.

We recall here briefly the main features of the model. Each node of a flat-plate collector is characterised by:

$$C_n \, dT_n/dt = A_n \, k_m \, F'[(\tau\alpha)_0 \, G_{eq} - U_L(T_n - T_a)] - q_{u,n} \quad (1)$$

where: G_{eq} is the equivalent normal irradiance taking into account irradiance components multiplied by respective incident angle modifiers : $G_{eq} = K_{\tau\alpha,beam} \, G_{beam} + K_{\tau\alpha,diff} \, G_{diff} + K_{\tau\alpha,alb} \, G_{alb}$; U_L is the overall heat loss coefficient : $U_L = U_0 + U_v \, v + U_T \, (T_n - T_a)$; q_{un} is the rate of energy gain by the collector node: $q_{u,n} = m c_p (T_n - T_{n-1})$; Coefficient characterising flow-rate dependence: $k_m = 1 - a_0 m_t$; C_n is the heat capacity of each node - the total capacity is NC_n, N being the number of nodes; A_n is the area of each node, total area is NA_n; T is the node temperature; T_a is the ambient temperature; F' is the collector efficiency factor; $(\tau\alpha)$ is transmittance-absorptance-product at normal incidence. An incidence angle modifier for beam irradiance is defined by the modified Ambrosetti (Ambrosetti 1983) equation: $K_{\tau\alpha,beam}(\theta) = 1 - \tan^{1/r}(\theta/2)$. The incident angle modifier for diffuse irradiance assuming isotropic distribution is used as derived in (Bosanac *et al.* 1993). The incident angle modifiers for diffuse irradiance and for albedo we assume to be equal. They are both derived in (Bosanac *et al.* 1993) as a function of parameter r.

Hence, the following parameters fully characterise the presented model:

- The optical efficiency of collector array, $F'(\tau\alpha)$.
- The overall heat loss coefficient if $T_n = T_a$ and v=0, U_o.
- The coefficient characterising wind dependence of overall heat loss, U_v.
- The coefficient characterising temperature dependence of overall heat loss, U_T.
- The total thermal capacity of collector array, C.
- The incident angle modifier coefficient r.

The test result relies strongly on the dynamic variability of the operation conditions. Here we represent operation conditions by four of the influencing variables. These influencing variables are:

1.Difference between collector fluid temperature and ambient air temperature.

2.Reduced temperature.

3.Surrounding air speed.

4.The incident angle of direct irradiance on the collector plane.

A condition for accurate identification of collector parameters is the sufficient variations of the influencing variables. By these variations the collector is driven in various states which are assumed most representative for its operation under real conditions. As soon as the recommended variations of each of influencing variables are reached, the test is accomplished. It is assumed that enough data for accurate identification of the collector parameters are then collected.

Accuracy of the prediction depends how close operation conditions during the test cover the most probable operation conditions during the long-term operation. In order to define the operation conditions most probable for collector array, simulation by TRNSYS program has been carried out. Operation conditions are represented by three influencing variables:

1.Difference between collector fluid temperature and ambient air temperature.

2.Reduced temperature : $(T_m-T_a)/G$.

3.Surrounding air speed.

On the basis of these simulations, the range of variables to be scanned during short term test has been determined, and the criteria for termination of the test have been established. The in-situ test is conducted by the dynamic test method which are able to determine collector performance under non-stationary test conditions. The parameters obtained from the test have a physical meaning. Therefore, the application of the test results is not restricted to performance prediction, but it allows diagnostics of system malfunctions as well. The reliability and repeatability of the identified parameters by various test sequences is checked out in this work.

3. MEASUREMENTS

During long-term - six months - monitoring, normal operating conditions for the solar water heater system have been applied. The relevant measurement data are collected with one minute time resolution, i.e. collector array inlet and outlet fluid temperature, array fluid flow rate and meteorological parameters: global and diffuse irradiance, ambient temperature and wind velocity. The long-term measurement is used to identify the 'reference' collector parameters.

4. TEST RESULTS

During the six month measurement period, several short-term (five days) tests were selected for identification of collector parameters. The collector parameters were identified by the dynamic fitting algorithm (Spirkl 1992). The repeatability of the identified collector parameters for the array (collector with selective absorber) for short-term (5 days) tests is satisfactory as it is shown in the Figures 1. and 2. At the same Figures the reference values are shown with the abbreviations: S - steady state, laboratory values and, D - identified parameters using complete measurement period (six months).

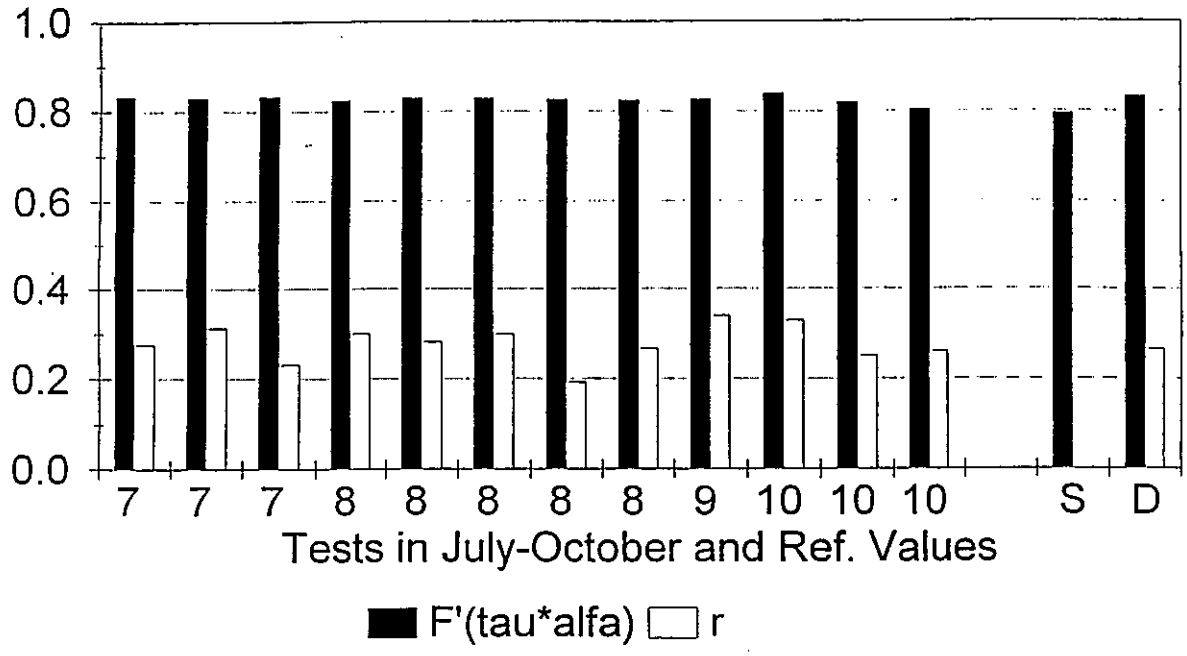

Fig. 1. Optical properties $F'(\tau\alpha)_0$ and r estimated from independent 5-day periods in the months 7 to 10 of 1994 - compared with laboratory steady-state values (S) and long-term values (D).

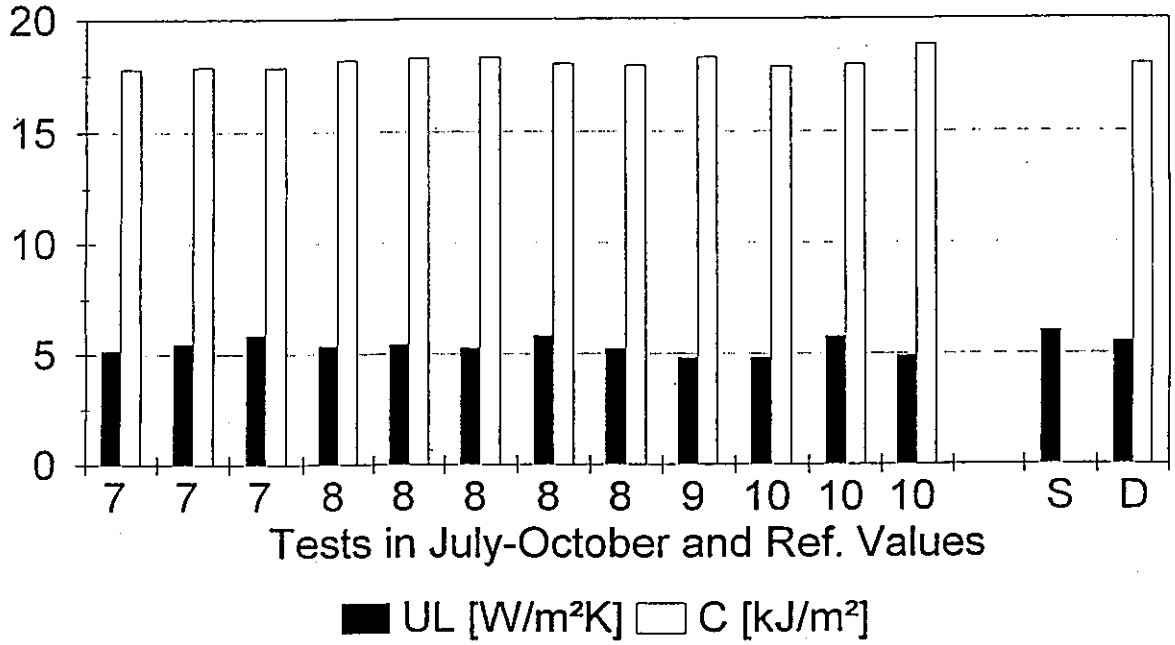

Fig. 2. Heat loss U_L and heat capacity C estimated from independent 5-day periods in the months 7 to 10 of 1994 - compared with laboratory steady-state values (S) and long-term values (D).

The results of the analysis have shown that a temperature dependence of heat loss coefficient can hardly be identified. The correlation coefficient between U_0 and U_L was very high - in principle it exceeds 0.80. That's why we referred to 'effective' heat loss coefficient representing overall heat loss coefficient without temperature and wind dependence. This 'effective' heat loss

coefficient is repeatable within 10% and optical efficiency within 2%. The seasonal effect on collector parameters is not noticeable. However, we were not able to determine accurately the temperature dependence of the heat loss coefficient.

Comparison of dynamic test results with those obtained indoors under steady-state conditions shows good agreement for the collector in question.

On the basis of statistical analysis of input data, we suggest the variations of influencing variables which are considered sufficient. These variations are specified in Table 1 as minimum variations of influencing variables requested during a test. If they are not covered during few first days of measurement the test is to be continued.

Table 1. Recommended range of variations of the influencing variables to be scanned during an outdoor test.

Influencing Parameter	Recommended Range of Variations
Tm - Ta	10 - 70 K
Reduced Temperature	0.02 - 0.2 Km^2W^{-1}
Wind Velocity	1 - 5 ms^{-1}
Incident Angle	10 - 70 deg

The reliability of identified parameters of collector array is checked by cross prediction of the energy yield.

In particular, the yield of process heat by using the identified collector parameters is compared with measured values for the days proceeding and following the short-term test. This analysis has shown that an accuracy better of 5 % in prediction of daily energy yields for collector power exceeding 10 kW is obtained.

5. CONCLUSION

It has been proved that dynamic collector test might be performed in few days under normal operating conditions and assuming favourable weather conditions (i.e. some sunshine).

A statistical analysis of the operation conditions during short-term tests is used to propose the necessary variations of the influencing variables to be covered during the test as shown in Table 1. This might be used as an indicator whether sufficient data for an accurate identification of the important collector parameters are collected.

The repeatability of identified parameters is satisfactory during six month monitoring period.

Acknowledgement: This work is funded by the EU-ALTENER Programme and the Danish Energy Agency.

NOMENCLATURE

A - *total collector (aperture) area of array,*
C - *collector array total thermal capacity,*
c_p - *specific heat coefficient of fluid in collector loop,*
F' - *collector array efficiency factor,*
G - *incident total radiation on a flat surface per unit area,*
G_{beam} G_{diff} G_{alb} - *incident beam, diffuse and albedo radiation,*
K_{beam} K_{diff} K_{alb} - *incidence angle modifiers, beam, diffuse and albedo radiation,*
m_c - *collector fluid mass flow rate,*
r - *parameter for incident angle modifier,*
N - *number of nodes,*
$q_{u,n}$ - *rate of energy gain by collector node,*
T_a - *ambient air temperature in vicinity of collector array,*
T_m - *collector mean fluid temperature,*
T_n - *collector node temperature,*
U_L - *overall heat loss coefficient,*
U_o - *overall heat loss coefficient when $T=T_a$, and $v=0$,*
U_v - *coefficient characterising wind dependence of heat loss coefficient,*
U_T - *coefficient characterising temperature dependence of heat loss coefficient,*
v - *wind velocity,*
dt - *time step,*
dT - *increment in node temperature over the time step,*
$(\tau\alpha)_0$ - *product of cover(s) transmittance and absorber absorptance for normal incident angle,*
θ - *incident angle of radiation*

REFERENCES

1. Bosanac M, Souproun A, Nielsen J E, Sizmann R (1993) In-Situ Test of Solar Collector Array. Procedings of ISES World Congress, Budapest, Hungary, Pergamon Press, New York, Vol. 5 pp 335-340.
2. Muschaweck J, Spirkl W (1993) Dynamic Solar Collector Testing. J. Of Solar Energy Materials & Solar Cells, 30: 95-105.
3. Bosanac M, Brunotte A, Spirkl W, Sizmann R (1994) Use of Parameters Identification for Flat Plate Collector Testing under Non Stationary Conditions. J. Renewable Energy Sources, 4: 217-222.
4. Ambrossetti J P (1983) Das neue Bruttowärme-ertragsmodel für Sonnenkollektoren. Technical Report, EIR Würenlingen, ISBN-3-85677-012-7.
5. Spirkl W (1992) Dynamic SDHW System Testing, Program Manual, Sektion Physik der Ludwig-Maximilians Universität München.

Development of *in situ* test procedures for solar domestic hot water systems

J.Spehr, W.Schölkopf

Bayerisches Zentrum füpr Angewandte Energieforschung e.V.
ZAE Bayern
Department 4: Thermal Conversion of Solar Energy
Domagkstrasse 11, 80807 München Germany
Phone: +49-89-356250-11; Fax: +49-89-356250-23
e-mail: justus.spehr@physik.uni-muenchen.de

1 Introduction

Since its foundation in 1992, ZAE has been engaged in the *in situ* measurement of systems, in particular of solar domestic hot water preparation. Measurement programmes are supported by the Bundesministerium für Bildung und Forschung (BMBF) and the Bayerisches Staatsministerium für Wirtschaft, Verkehr und Technologie (BayStMWVT) [1]. In the frame of the ALTENER-Program of the European Union methodical principles were developed for testing Guaranteed Solar Results (GSR) [2].
Until now, nine systems were measured *in situ* and recommendations for *in situ* measurements were tested experimentally. In parallel, these systems were also simulated during the corresponding measurement programs. Additionally the systems were simulated by detailed programs (TRNSYS) and the calculated results were compared with experimental results.

2 *In situ* Measurements

At ZAE Bayern, *in situ* dynamic testing has been applied to 9 solar domestic hot water (sdhw) systems during the past three years. The area of the collectors ranges from 3 m^2 to 64 m^2 and the storage volumes from 0.27 m^3 to 3.6 m^3. Meteorological data and data from all relevant energy flows (e.g. collector loop, warm water load, storage loop) were recorded with high time resolution for a period of three years, according to the ISO TC 180 9459/5 standard. However, diffuse irradiance is not measured, as all systems are situated at a large distance from ZAE Bayern.

2.1 Description of Systems

Table 1 presents the technical data of a typical small German sdhw system for a single family house and of a preheating system of a multi-family house with 32 apartments. Figure 1 represents schematically the small system configuration, together with the sensors and their location. Figure 2 represents the equipment of the large sdhw system. The total system can be divided into a solar and a conventional part. The solar part consists of 54 collectors with a total absorber surface of 64 m^2, which are arranged in 3 parallel connected collector fields of 15, 18 and 21 collectors respectively.

	Small system	**large system**
collector type	flat plate collector	flat plate collector
absorber area	7.1 m^2	64 m^2
storage volume	500 *l*	2×1500 *l*
stand-by volume	150 *l* integrated	600 *l* separate
tilt of roof	30°	45°
orientation of roof	0°	25° east
number of users	4	66
circulation	hand controlled	time controlled
auxiliary heating	oil/wood	gas burner 2×124 kW
data logger with data transmission to the ZAE	15 measurement channels	32 measurement channels

Table 1: Data of the *in situ* measured sdhw systems

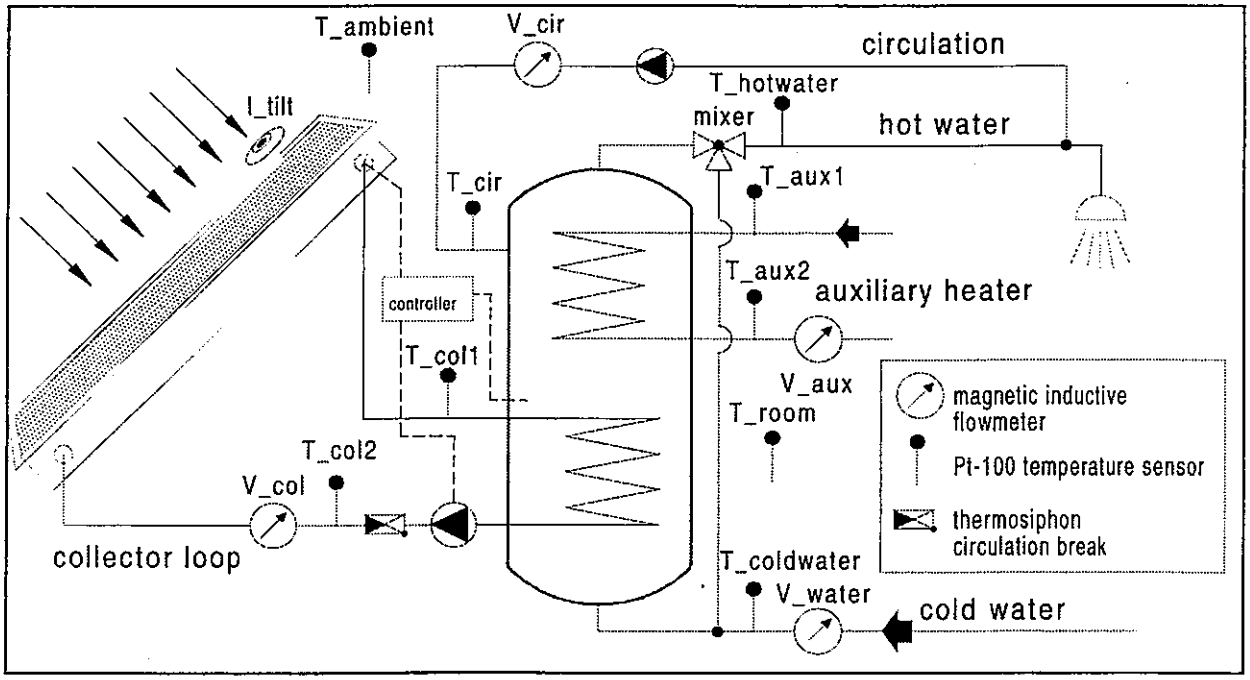

Figure 1: Diagram of the small system with position of temperature sensors and flow meters

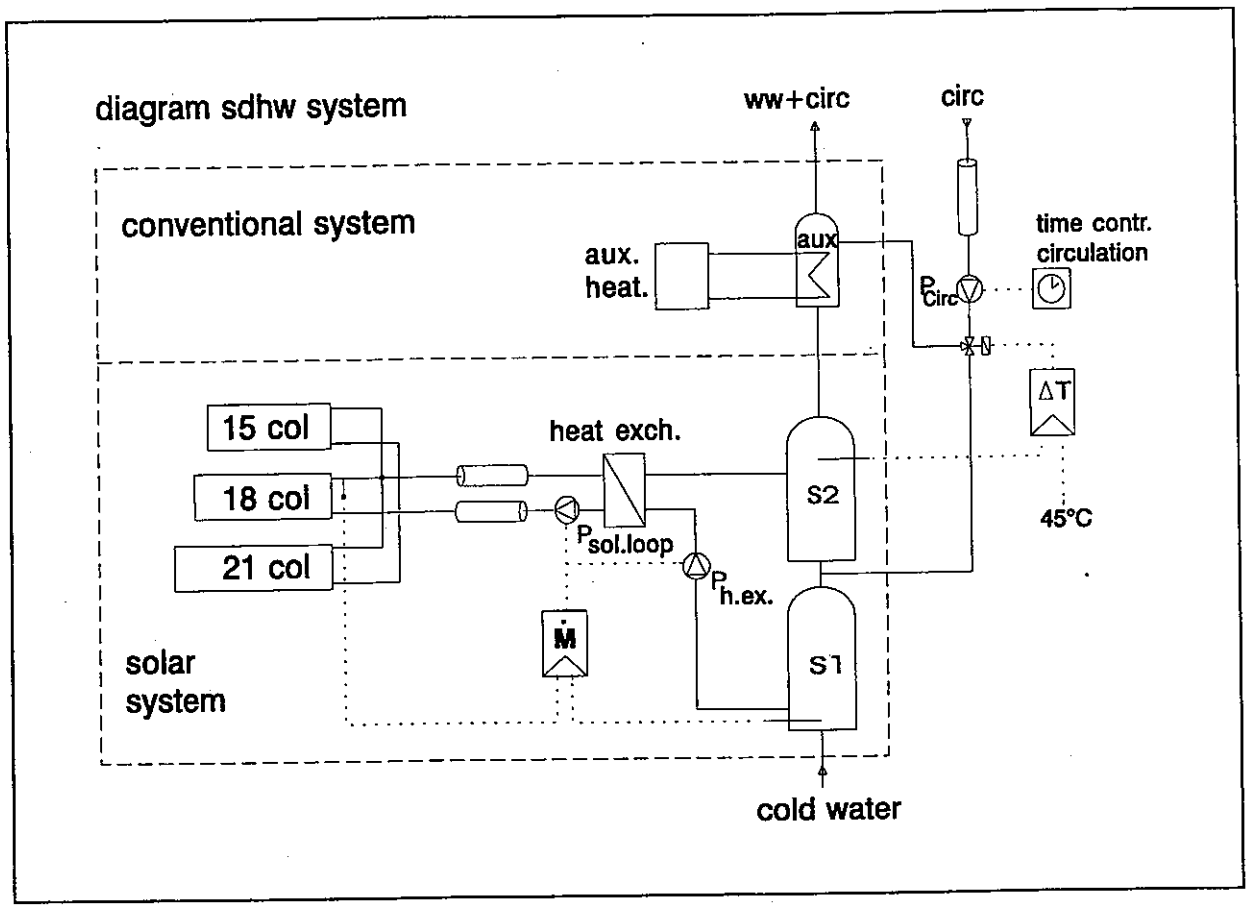

Figure 2: Diagram of the large sdhw system. Solar system: 3 collector fields with 15, 18 and 21 collectors, $P_{sol.loop}$: collector loop pump, $P_{h.ex.}$: pump in storage loop, heat exch.: external heat exchanger, S_1,S_2: solar warm water storage. Conventional system: aux.heat.: auxiliary heating, aux: warm water storage, ww: warm water, circ.: circulation, P_{circ}: circulation pump.

2.2 Test of the Collector Model

The measurement and simulation results of the collector loop of a small sdhw system are presented. The collector parameters were determined by *in situ* data with Dynamic Fit [3] and the collector model DynColl [3]. All temperature measurements were performed in the collector loops near by the heat exchangers which are located in the basement and the collector model had to be extended for the pipes from collector to storage. The following parameters were taken into account for our model:

- ε_{col}: optical efficiency coefficient of collector,
- U_0: linear heat loss coefficient of collector,
- U_v: wind dependent heat loss coefficient of collector,
- U_t: temperature dependent heat loss coefficient of collector,
- C_C: heat capacity coefficient of collector,
- U_P: heat losses of pipes between collector and heat exchanger,
- C_P: heat capacity of pipes between collector and heat exchanger.

The parameters U_v and U_t were determined from data over an entire year. U_P and C_P were determined from geometrical considerations. These four parameters were set constant for the following fits. The data basis for the determination of ε_{col}, U_0 and C_C was of 1 month for each case during the time period July/93 - October/95. In the four winter month (November until February) a reliable determination of parameters is not possible (snow on collector or pyranometer). The predictions for the collector loop were simulated using the same collector model as was used for the parameter determination. From figure 3 it can be assured that the deviations between prediction and measurement are smaller than ±3 %. Hence, the applied collector model represents the solar loop very well.

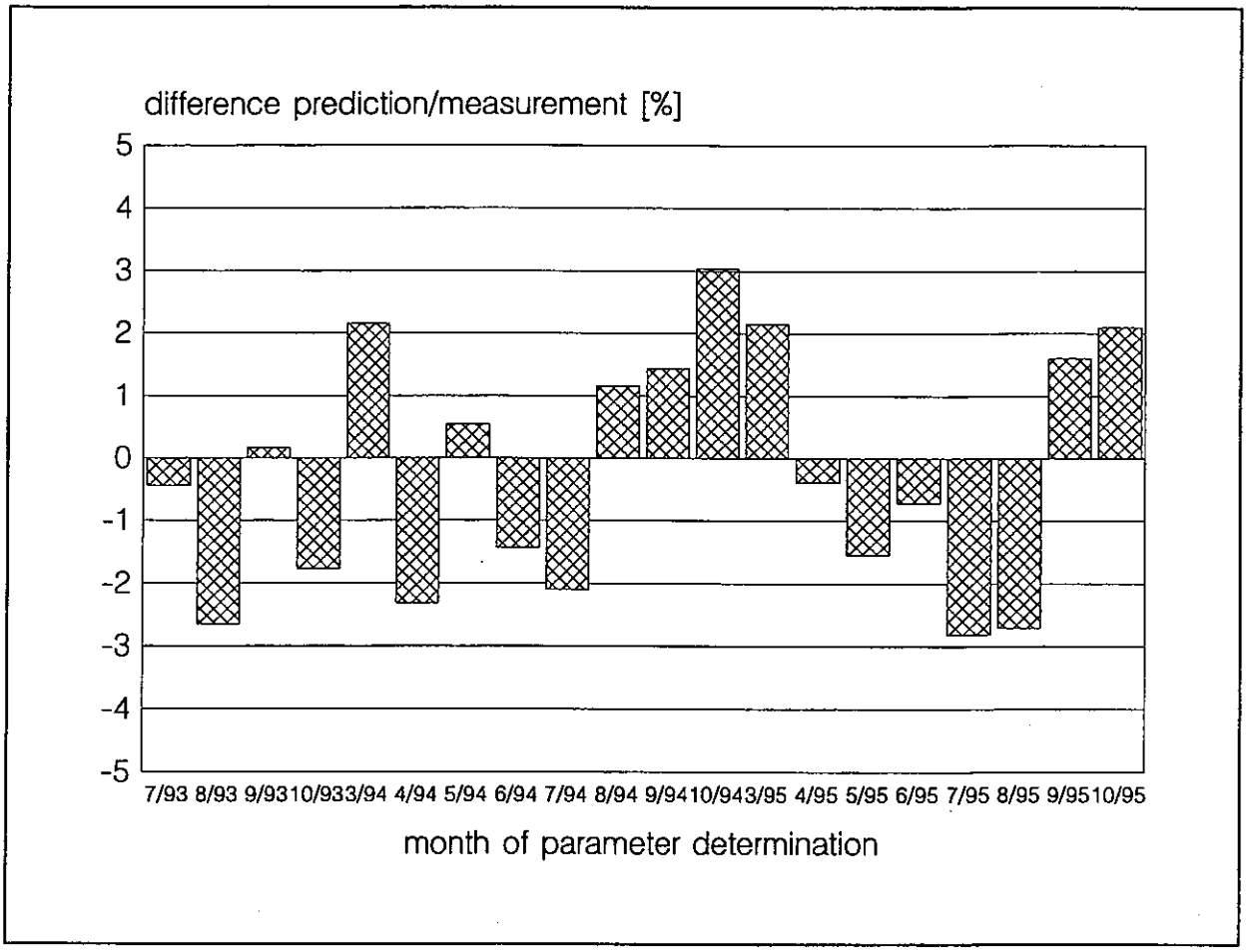

Figure 3: Prediction of the collector loop for 1 year. Data for the determination of a parameter set is always 1 month (the x-axis contains 20 parameter sets). The prediction is always for the entire year 1994.

3 Dynamic System Simulation

In parallel to the experimental evaluation the sdhw systems were simulated by the dynamic simulation program TRNSYS [4].
Yearly simulations were performed under different input conditions (see also table 2):

1. **Simulation type 1:** (real collector loop controller, real auxiliary heating)
   In this simulation the auxiliary heating energy was obtained from measured data. Especially this procedure is necessary for the small system as the user regulates manually the auxiliary heating. During the summer he disconnects the auxiliary heating for long periods of time and switches between wood and oil heating.
   The TRNSYS controller for the solar loop was adapted to the real controller of the system. Only in this manner it is possible to reproduce the system behaviour by simulations. Cold water temperature, hot water load profile and meteorology were introduce as time dependent input data.

2. **Simulation type 2:** (TRNSYS auxiliary heating control, real control of solar system)
   In this simulation (and in all following simulation types) the auxiliary heating was controlled by TRNSYS control unit, that means, the auxiliary heating is entirely simulated. All other inputs are as in simulation type 1.

3. **Simulation type 3:** (ideal TRNSYS controller in collector loop)
   The ideal TRNSYS-controller for the collector loop is used. This ideal control mode transposes the projected control algorithm without errors. Out of the set of measurement data the cold water temperature, the hot water load profile and meteorological data are introduce as time dependent input.

4. **Simulation type 4:** (standard load profile)
   The ideal TRNSYS-controller for the solar loop and a standard load profile is used (50 *l* hot water/person and day at three intervals: morning, noon and night). Time dependent meteorological inputs are supplied from measured data.

5. **Simulation type 5:** (Test Reference Year (TRY))
   Use of ideal TRNSYS-controller for the solar loop, standard load profile and TRY [5].

Determination of TRNSYS parameters

It is necessary to supply each component of the simulation programme with a parameter set. These values were determined for the small system by Dynamic Fit [3] from measured data and appropriate models (collector and collector pipes: DynColl [3], storage and heat exchanger: multiport storage-model for TRNSYS, Type 74 [6]).
Parameters for the large system were supplied from the Solarenergie Prüf- und Forschungsstelle, Internationales Technikum Rapperswil/Switzerland. The specific heat capacity of the collector was obtained from material data. The parameters of all other components were identified from geometrical considerations or from measured data.

3.1 Small System

The small system is first simulated over a year according to simulation type 1. TRNSYS parameters and system behaviour are checked by comparing measurement data and simulation type 1.

Comparison simulation-measurement

Figure 4 shows the simulated and measured collector output over one day. The simulated curve is based on simulation type 1. With this parameter set a very good correspondence of the dynamical behaviour of the collector field and of the entire system is obtained. Measured and simulated daily yields differ by 1.3 %. From table 2 it can be assured that measurement results and results from simulation type 1 are in very good agreement. That means, the identified TRNSYS parameters and the simulation model correctly reproduce our system and represent a secure, reliable basis for the simulation of systems behaviour under different conditions.

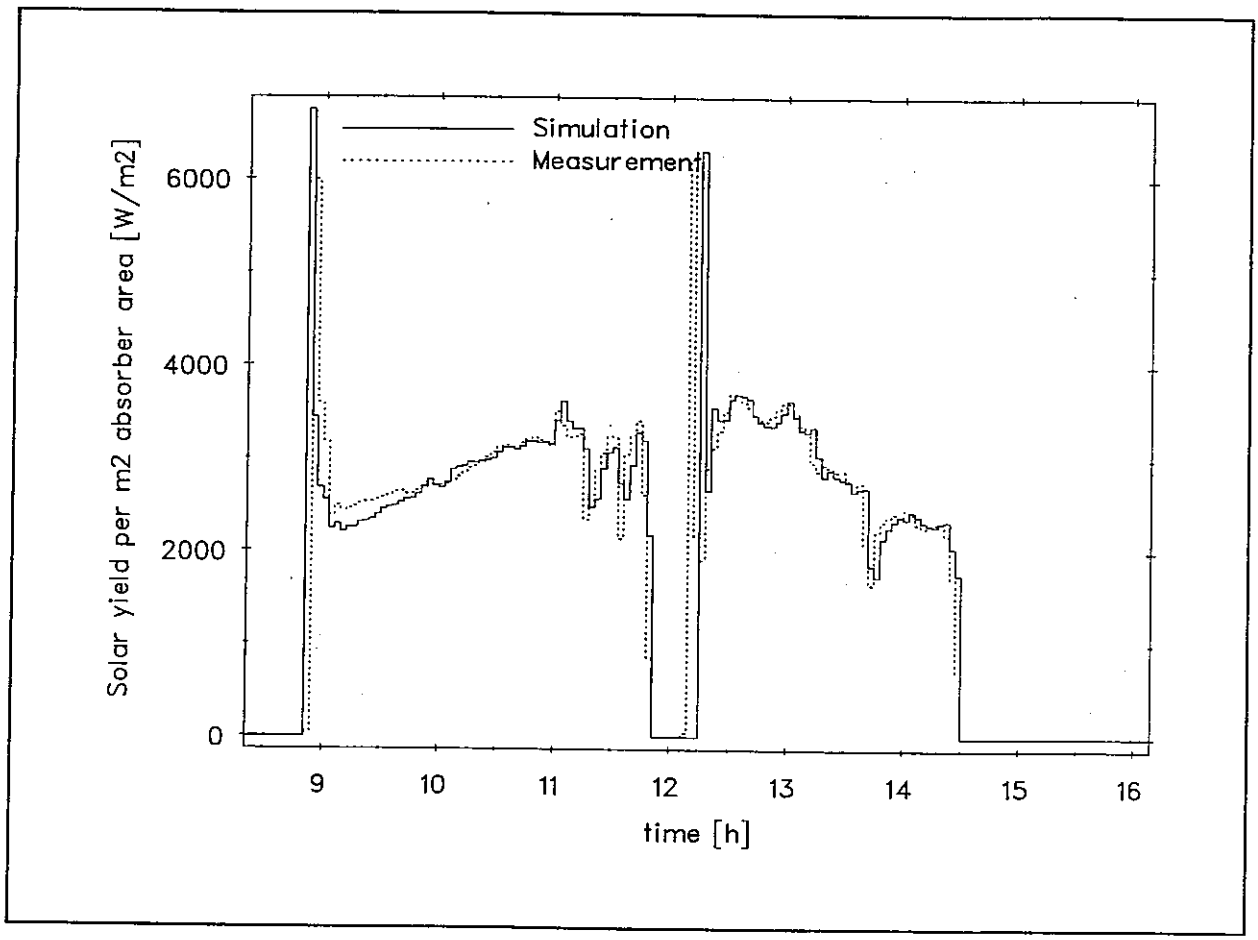

Figure 4: Simulation type 1 of the whole sdhw system. Shown are the simulated and measured collector yields for one day. For simulation type 1 of the whole system only the auxiliary heating, warm water load and weather data have been retained from measured data.

In order to simulate the system under different conditions, the auxiliary heating must be simulated in a next step. The results from this simulation type 2 are given in table 2. The solar fraction is lower. The reason is, that the auxiliary heating in simulation type 2 is in stand-by throughout the year. Under real operation conditions the user of the system disconnects the auxiliary heating over long periods of time accepting lower hot water temperatures.

In order to determine the quality of the controller in the collector loop and its influence to the achievable solar yield, results from the simulation type 2 are compared with results of simulation type 3 over a year (table 2). A disagreement between results of simulation type 2 and type 3 indicates a malfunction of the control unit. Simulation results show that under unchanged input data and ideal TRNSYS-controller (simulation type 3) a 10 % higher collector yield is obtained as compared with real controller (simulation type 2).

Simulated yearly yield under standard conditions

Since the simulation describes correctly the system behaviour, the yearly yield for the standard load profile and/or Test Reference Year (TRY) can be calculated. The measured hot water load is only 60 % of the standard hot water load which was assumed for the design of the sdhw system. The simulation type 3 with measured load profile and simulation type 4 with standard load profile point out the effects of different load profiles on the solar yield. From figure 2 it can be observed that the specific collector yield q_{col} and the collector efficiency η_{col} is about 30 % higher for simulation type 4 than for simulation type 3. Correspondingly, the solar fraction α_{sol} is about 10 % smaller.

According to TRY the total irradiation in collector plane is 10 % larger than the measured one. Therefore, the specific collector yield q_{col} and the solar fraction α_{sol} for the simulation type 5 alike is about 10 % larger than for the simulation type 4 with measured weather data. The collector efficiency η_{col} remains practically constant.

	Weather	load	controller solar system	auxiliary heating	α_{sol}	q_{col} [kWh/m²a]	η_{col}
meas. 1 year	real	real	real	real	0.61	259	0.23
sim type 1	real	real	real (TRNSYS)	real	0.62	262	0.23
sim type 2	real	real	real (TRNSYS)	TRNSYS	0.55	252	0.22
sim type 3	real	real	ideal (TRNSYS)	TRNSYS	0.59	280	0.25
sim type 4	real	standard	ideal (TRNSYS)	TRNSYS	0.52	372	0.33
sim type 5	TRY	standard	ideal (TRNSYS)	TRNSYS	0.56	405	0.32

Table 2: Comparison of coefficients of efficiency of the small sdhw system between measurement and different types of simulation for one year.

3.2 Large System

Comparison simulation - measurement

The real system behaviour was simulated with simulation type 2. Table 3 shows that the simulation type 2 agrees very well with the measurement. Comparing simulation type 2 and type 3, a first inspection shows that the system controller of the collector loop was defective. This defect leads to a reduction in solar yield of almost 30 %. The improvement potential was predicted with simulation type 3. Using a repaired controller in a second short term test the predicted improvement was verified.

	weather	load	controller solar system	α_{sol}	q_{col} [kWh/m²a]	η_{col}
short term test	real	real	real	0.251	23.8	0.258
sim type 2	real	real	real (TRNSYS)	0.254	24.0	0.254
sim type 3	real	real	ideal (TRNSYS)	0.357	33.7	0.378

Table 3: Comparison of coefficients of efficiency of the large sdhw system between measurement (real defective controller in collector loop), simulation type 2 (real controller in collector loop) and simulation type 3 (ideal TRNSYS controller) for a three weeks period.

Simulated yearly yield under standard conditions

Incidentally, the yearly total solar irradiance of the TRY (1219 kWh/m²a) agrees with the measured yearly total solar irradiance on the collector plane (1201 kWh/m²a). An analysis of weather data on a monthly, respectively daily basis shows, however, that the distribution of irradiance in TRY strongly differs from the measured distribution.

	Weather	load	controller solar system	α_{sol}	q_{col} [kWh/m²a]	q_{sys} [kWh/m²a]	η_{col}
meas. 1 year	real	real	real	0.39	510	395	0.33
sim type 5	TRY	standard	ideal (TRNSYS)	0.34	507	491	0.38

Table 4: Comparison of coefficients of efficiency of the large sdhw system between measurement and simulation type 5 (standard load and TRY) for 1 year.

Table 4 lists the characteristic values obtained from simulation type 5 against the measured ones (from 12 months measurement time). The simulated solar fraction α_{sol} is clearly lower than in the real case. In spite of that, the simulated system yield q_{sys} and collector efficiency η_{col} are about 15 %- 25 % larger than the measured ones. The following differences between simulation with standard conditions and measurements are responsible for this discrepancy:

1. In TRY there is a different temporal distribution and a different correlation between diffus irradiance, direct irradiance and ambient air temperature as in the measured meteorological data.

2. The expected hot water load (3.5 m³/d) is clearly larger than the measured load (2.4 m³/d)

For the simulated specific collector yield q_{col} similar values are obtained as for the measured results. This agreement was not expected as the input data as well as the results for α_{sol} and η_{col} were different. The agreement is caused by the very different distribution of seasonal irradiance and the low level of used load in summertime for the measured case.

4 Conclusions

In order to proof solar guaranteed results, measurement results should not be compared with simulation results by standardised input data. The parameters of the entire system or individual components should be identified from measured dynamical data and the simulated yield is to be determined from real data of the hot water load profile, circulation and meteorology as input data for the simulation.

5 Outlook

For future quality assurance of sdhw systems Guaranteed Solar Results should be determined and verified through integrated procedures (design and measurement). The following points are to be worked out in additional projects:

Design and simulation

1. System types for which GSR can be calculated and proofed should be listed in a system catalogue which should cover 80 % - 90 % of all systems.

2. A standardised system catalogue should be developed which makes use of already existing simulation programmes (TRNSYS, T-SOL, etc.) and which can be used as an efficient tool for the design of solar systems.

3. Development of models for single and multi storage systems with direct circulation feeding is suggested.

The engineer would thus receive a powerful and extensive tool for the design and estimation of sdhw systems. Results could be used for determination of GSR.

Short term tests

1. On the basis of existing components a prototype measurement unit is to be developed and tested.

2. Existing sensors (temperature, flow meters) should become further developed and tested as appropriate clamp-on sensors.

3. On the basis of existing software a simplified user surface should be developed and tested. With this software it could be possible to judge whether the data from a running measurement contain sufficient information for an extensive analysis of the solar system.

4. Development of appropriate evaluation methods and simple to operate evaluation software is required.

Engineer's offices would obtain a powerful tool for the testing of GSR.

Literature

[1] B. Pummer, J. Fenzl, J. Spehr, W. Schölkopf; Abschlußbericht Feldtest Solaranlagen, ZREU Wieshuberstr. 3, 93059 Regensburg, FRG; ZAE Bayern, Domagkstr. 11, 80807 München, FRG, 1996.

[2] J. Spehr, W. Schölkopf; Guaranteed Yields of Solar Hot Water Systems under Reference Conditions - Guaranteed Solar Results (GSR), Europeen Comission, ALTENER Programme Directorate General for Energy DG XVII, 1996.

[3] Klein & Partners; Dynamic System Testing Program Manual, Version 2.6β, Scientific Software for Solar Testing, Mozartstr. 13, 80366 München, FRG, 1996.

[4] S.A. Klein, W.A. Beckman, P.I. Cooper; TRNSYS: A Transient System Simulation Program , Version 14.1, Solar Energy Laboratory, Madison Wisconsin, 1995.

[5] K. Blümel, E. Hollan, M. Kähler, R. Peter; Entwicklung von Testreferenzjahren (TRY) für Klimaregionen der Bundesrepublick Deutschland, BMFT-Forschungsbericht, T 86-051, Freie Universität Berlin, 1986.

[6] T. Pauschinger, H. Drück; Storage Model for TRNSYS - Type 74, Institut für Thermodynamik und Wärmetechnik, University of Stuttgart, FRG, 1994.

DEVELOPMENT OF THE ISFH I/O-PROCEDURE AND TEST IN THE PROJECT 'SOLAR DISTRICT HEATING GÖTTINGEN'

K. Vanoli, R. Tepe and H. Felten

1. Objective and goal of the development

" Increase the credibility in the technology of (large scale) solar thermal systems by improvement of the concept "Guaranty and Verification of solar output "

Goal:

Develop a measurement device for simplified in-situ monitoring with integrated control functions for

IN-SITU VERIFICATION OF THE PREDICTED COLLECTOR ARRAY YIELD

Today's Solar Guaranty Procedures are generally limited to an annual check of the heatmeter reading installed in the collector system and the comparison with the "Solar-guaranty-value", which may be corrected to possible differences between the actually available irradiation and the long term average irradiation.

There are two shortcomings of these procedures:

- the annual verification period is too long, because failures of the solar system, which are hidden to the user by the action of the conventional back-up system, are detected too late; this limits the readiness of an installer / manufacturer to guarantee the operation of the system.

- the use of regionally measured irradiation as basis for the irradiation available in a specific system is feasible only for annual periods and does not account for possible micro-climatical changes and for effects of collector orientation.

The ISFH-I/O-Controller procedure will overcome these problems by introducing daily verification intervalls and by in-situ measuring the actual irradiation in the plane of each collector array using low-cost PV-irradiation sensors.

This document describes briefly the ISFH-I/O-Procedure and reports on experiences of applying this concept to three collector-arrays in the IEA-Task 14 Project Solar District Heating Göttingen.

2. Methodology

This chapter describes the mathematical background used for performance characterization in the ISFH-I/O-Procedure as well as the associated measurement hardware.

Introduction

The general concept of the ISFH-I/O-Procedure is rather simple: it can be described as an intelligent "Solar-Energy-Heat-Meter" which first is capable of measuring the actual daily collector output and the daily incident irradiation, and second is able to calculate the expected daily collector output on the basis of daily Input/Output-Regressions, taking into account the measured daily irradiation and the actual operating temperature of the collector.

2.1 Characterization of predicted performance

Input/Output-Regression curves have been investigated in the past 15 years, mainly by former members of IEA Task VI [1 - 4], in order to characterize and analyse the useful thermal output of collector arrays. Furthermore, this I/O-Regression has been applied as basic mathematical approach in several simulation programs conceived for system design calculations. As an example, Figure 1 shows the Input/Output-Diagram of the Corning Collector operating in the Solarhaus Freiburg in 1980.

The general form of I/O-Regression may be written in the form of the multi-linear regression equation:

$$q112 = a_0 + a_1 * h100 + a_2*DT*DL \qquad \text{Eq. 2.1}$$

with the following quantities (daily values):

q112	daily collector output kWh/(m²d)
h100	daily **total incident global irradiation** onto the collector plane kWh/(m²d)
DT	daily average of the temperature difference between collector fluid and ambient air
DL	day length or collector pump operating time, resp.

Optionally, with high capacity collectors, a capacity term, + (a_3*TT), can be added to the regression formula in order to consider the effect of capacity related heat losses, TT beeing the daily temperature increase "sunrise ambient to evening

collector temperature at stop of operation".

A second, optional form of the I/O-Regression relates the daily collector output to the restricted daily irradiation **during collector operation** h101:

$$q112 = a_0 + a_1 * h101 + a_2*DT*DL \qquad \text{Eq. 2.2}$$

with the following quantities (daily values):

q112	daily collector output kWh/(m²d)
h101	daily **Collector - ON global irradiation** onto the collector plane kWh/(m²d)
DT	daily average of the temperature difference between collector fluid and ambient air
DL	day length or collector pump operating time, resp.

Figure 2 gives a definition of the two irradiation quantities mentioned. Experimental results show that especially in systems with high operating temperatures - like in the Solar District Heating Project Göttingen - , the difference of the two irradiation values have to be taken into account.

Once these regression coefficients are determined, Equation 2.1 will sufficiently characterize the collector array output, taking into account the specific conditions of system operation as for example actual irradiation and ambient temperature, collector operating temperature, collector orientation and load conditions.

Two alternative procedures to determine the regression coefficients will be described in chapter 2.2.

2.2 Description of the ISFH-I/O-Procedure

Rationale of the development:

The ISFH-I/O-Procedure has been conceived for two major tasks of **LOW-COST IN-SITU MONITORING:**

- **OPERATION-CHECK**
- **VERIFICATION OF THE PREDICTED COLLECTOR YIELD.**

Therefore, the ISFH-I/O-Controller, a sort of intelligent "Solar-Energy-Heat-Meter" has been developped in cooperation with two companies [5,6]. This device will be

installed in the collector loop of a solar system as indicated in Figure 3. The operational modes of this device will be explained in chapter 2.3.

The first task, low-cost in-situ operation check, as it is current practice in all conventional energy technologies, is not at all a trivial problem in solar systems. Experience has shown, that it is nearly impossible to make a diagnostic check of a solar system in a short time just by taking the readings of some instantaneous sensors like thermometers and flowmeters; and if ever, it requires stable irradiation and operational conditions, and a lot of practical experience.

This is why the Input/Output-Regression Eq. 2.1 has been implemented into the ISFH-I/O-Controller. Using actual daily measurements of incident irradiation, av. collector temperature, ambient temperature and operating time, a rather accurate estimation of the daily collector yield can be calculated.

An example for this task is shown in Figure 4: a flow-meter failure on the 20.5.94 - a collector pump failure would have the same effect on collector output - can easily be detected by comparison with the predicted value of the I/O-regression.

Determination of the I/O-Regression Coefficients:

In order to utilize the Input/Output Methodology described in chapter 2.1 for collector output prediction, the regression coefficients of Eq. 2.1 have to be determined. The ISFH-I/O-Procedure proposes two alternative paths of coefficient determination.

Path I: Design-Phase-Coefficients:

During the design phase of a solar system - especially for medium and larger systems, simulation programs are used for designing and sizing the system. As most detailed simulation programs (e.g. TRNSYS, ISFH, G^3) are calculating the independent variables in Eq. 2.1 and Eq. 2.2 as well as the collector output, it is a straightforward approach to use these data for determination of the I/O-regression coefficients by multi-linear regression. An example for this path I is presented in Figure 5a: in a first step, TRNSYS-Simulation data were used for coefficient determination; in a second step, these coefficients were taken to re-calculate the collector output based on Eq. 2.1 and the independent variables of the TRNSYS run. The standard deviation of simulated minus regression output is smaller than 0.1 kWh/(m^2day). Moreover, broader ranges of operating conditions (e.g. set-temperatures) than in the designed system can be selected during design simulations. Thus, the determination of the coefficients can be much more precise than with experimental conditions.

Path II: Commissioning-Phase-Coefficients

Experience in the cooperation with practitioners of the sanitary and heating equipment installers shows, that many of them still do not use simulation tools during the design process of solar systems. Some of them even do not trust calculations and rather rely on experience and measurements.

Therefore, the end of the commissioning phase of the solar system, the ISFH-I/O-Controller could be used during an in-situ "commissioning-measurement" period (Operation Mode 0 in Chap. 2.3) to establish the measured data-base for subsequent determination of the **Commissioning-Phase-Coefficients**.

An example of this kind of experimental coefficient determination is presented in Figure 5b, showing measured and regression output data for a typical small size solar DHW-System. The standard deviation of measured minus regression output is smaller than 0.1 kWh/(m²day), corresponding to a relative error of 3 %.

2.3 The Hardware of the ISFH - I/O - Controller

The integration of this device into a collector loop is shown in Figure 3. Its general function consists essentially of four operation modes:

MODE 0 data acquisition and storage mode for daily values of the collector output as well as for all independent variables in Eq. 2.1 resp. Eq. 2.2. At the end of the "commissioning-measurement" period, these data are processed by multi-linear regression to determine the regression-coefficients.

MODE I or "collector-heat-meter-mode", used for continuous on-line measurement of the collector array output and integrating the daily collector output for each day.

MODE II data acquisition procedure for daily values of the climate and the operating conditions of the collector (irradiation and ambient air temperature, average collector fluid temperature during operation, daily operating time) in order to determine the independent variables of the regression formula.

MODE III in-situ execution of the regression formula to determine the daily expected collector output, thus considering both the design characteristics and the real in-situ meteo- and operation conditions.

MODE IV performance verification by comparing the actually measured (mode I) and the expected collector output (mode II). In order to smooth the expected daily scatter of these values, "scrolling integration" periods over the last several days may be calculated and displayed.

3. Test of the I/O Regression in the Collector arrays of the project: Solar District Heating Göttingen

3.1 Implementation of the I/O-Regression for In-Situ Operation-Check of the collector arrays in Göttingen

As the staff of the co-generation power plant of the District Heating System Göttingen needed continuous information on the operational status of the solar systems, the ISFH-I/O-Controller software has been implemented into the data acquisition system used for the scientifical evaluation of the project. There are good operational experiences since mid-october 1994. Every day, there are now actually measured and predicted I/O-regression data of the collector output ready for mutual comparison with the measured output. But due to the low irradiation values in october, there are no results available yet.

3.2 Analysis of collector output prediction by long-term regression

Long-term regression coefficients have been determined using measured data of the Göttingen collector arrays of the period 1993/94. A comparison of the collector output determined both by measurement and regression is presented in Figure 6 (East-Array, 455 m^2), Figure 7 (West-Array 162 m^2) and Figure 8 (South-Array 166 m^2). In each of these Figures, the diagram on top of the page shows the regression based on total daily irradiation, the diagram on the bottom of the page presents the regression based on collector-ON irradiation.

The data period for the South and West array is from 4.93 - 10.94; for the East array, a reduced period is presented from 5.94 to 10.94, partly because of flow-meter failures, partly because of changes in the collector pump control strategy.

Statistical information is compiled in Table 1. The following conclusions can be drawn from the mutual comparison of these diagrams.

Like in all I/O-Diagrams of many other projects, the collector output increases linearly with daily irradiation; however, the regression based on the total daily irradiation shows a larger scatter (r^2-values 0.90 ... 0.93) than the regression based

on collector-ON irradiation (r^2-values 0.974 ... 0.9885). The standard deviation of the daily difference of measured minus regression output is in the order of 0.18 ... 0.21 kWh/(m^2day) for the H100 regression, and in the range of 0.06 ... 0.12 kWh/(m^2day) for the H101 regression. Thus, the prediction accuracy can be more than doubled by executing additionally the collector-ON irradiation.

In this context it has to be pointed out, that the H101 collector-ON regression can not replace the H100 regression, because H101 depends on the behaviour of solar system components which have to be checked. For example, if the collector pump fails, the I/O controller software will not integrate the irradiation during collector operation; thus with H101 = 0, no output would be predicted for those days.

The reason for the strong influence of the H101 on the correlation is the high operating temperature (65 ... 78 °C) of the collector array. This operating condition requires high irradiation levels for collector operation, causing a great difference between total and collector-ON irradiation. Moreover, the number of hours with irradiation levels just below threshold irradiation increases strongly with collector temperature. This explains the larger scatter of the H100 regression diagrams.

		East	West	South
n [day]	H100	159	210	256
	H101	159	218	254
R^2	H100	0.930504	0.902202	0.913652
	H101	0.973537	0.988493	0.985026
sigma	H100	0.204136	0.183112	0.215976
	H101	0.125966	0.063638	0.089371

Table 1: Collector Output Verification by I/O-Regression (H100,H101)
Statistical Data for East, West and South Collector Arrays of the Solar District Heating System Göttingen

n[day]: number of days per period
R^2: correlation-coefficient
sigma: standard deviation of residua [kWh/(m^2day)]
(H100): regression based on total daily irradiation
(H101): regression based on daily collector-ON irradiation

A detailed analysis of Table 1- Data is presented in Figures 6a, 6b ... 8a,8b.

3.3 Analysis of collector output prediction by short-term regression

Short-term regression coefficients have been determined using measured monthly sets of daily data of the Göttingen collector arrays of the period 1993/94.

Figure 9a presents the regression coefficient determination (Eq. 2.2 col-ON irrad. H101) using the data set of 8.93 as a "commissioning-measurement" period. The comparison of the measured and regression collector output gives a r^2-value of 0.996 and a standard dev. of residua of 0.04 kWh/(m^2d), corresponding to 3.5 % of the av. daily collector output (length of the data period of 24 days).

Figure 9b presents the verification of collector output in 7.94 by using this set of regression coefficients. The prediction error is - 4.2 % of the monthly average collector yield, the average daily residual is -0.08 $\pm$ 0.09 kWh/(m^2day). This result proves clearly that the concept of I/O-Regression based on collector-ON irradiation is well suited for in-situ collector yield verification.

(With Regression of Eq. 2.1 total daily irrad. H100, the prediction accuracy decreases to: r^2-value of 0.927 and a standard dev. of residua of 0.16 kWh/(m^2d), corresponding to 14 % of the av. daily collector output.)

Both of these sets of regression coefficients (Eq. 2.1 and Eq. 2.2) have then been used to predict the collector output for the whole data period 4.93 to 10.94. Detailed daily data are presented for the col-On regression (Eq. 2.2) in Figure 9b and Figure 10. Figure 11 and Figure 12 will show the prediction accuracy month by month for both types of regression.

Figure 10 shows the south array collector output verification by the (H101)-Regression set obtained by monthly data of 8.93. The prediction error over the whole data period 4.93 - 10.94 is - 4.6 % of the total collector output with a standard dev. of 8.2 %. Further investigations (presented in chapter 3.4) have been carried out in order to analyse the impact of reference-month selection on prediction accuracy.

A month by month comparison of measured and predicted collector output is displayed in Figure 11 for the total irrad. regression and in Figure 12 for the col-ON irrad. regression. As the period of august 93 has been selected as "Commissioning-measurement" period to determine the regression coefficients, both figures show identical collector output values for measurement and regression in that month.

For the H100 regression in Figure 11, the prediction error in the different months is much larger (5 .. 35 %) than in the H101 regression type (+4 .. -11 %) (Figure 12), the reason being the much larger scatter observed in the H100 regression diagrams (Figures 6a - 8a).

3.4 Dependency of reference-month selection on monthly verification accuracy.

This chapter gives a summary of a preliminary investigation on the feasibility of the second path of regression coefficient determination as proposed in chapter 2.2 (Commissioning-Phase-Coefficients). The question is: is there enough variation of the independent variables of Eq. 2.1 or Eq. 2.2 in e.g. monthly periods ?

In order to carry out this investigation, the same kind of regression analysis (based on Col-On Irrad.) as explained in chapter 3.3 (Figures 9a, Figure 10 and Figure 12) has been undertaken for the East, West and South arrays while selecting different months as "Commissioning-Measurement" periods for the I/O Regression.

The results presented in Table 2 (South), Table 3 (West) and Table 4 (East) collector array give the verification accuracy as percent values of the monthly difference between measured and predicted collector output as well as the corresponding vaules for the whole period. Different columns display the values for the selected reference month.

The results can be summarized as follows:

During the months of resonable energy production (discarding the fall and winter month, when the collector output is less than 5 % of the annual yield), the monthly errors are all below 11 %, typical errors are between $\pm$ 5 %. The results over whole periods are in the order of magnitude of $\pm$ 5 %.

(Note: percent values in winter and fall months are rather high because of the very small monthly collector output during this time , but they are of no importance for the long term accuracy)

It can be concluded, than within an error band of $\pm$ 11 % of monthly collector output, the selection of a reference month between april and august is certainly possible.

However, more detailed analysis is necessary in order to specify clearly the general rules for the data structure (i.e. required distribution, range of variation etc.) of the reference period which can be declared as "Commissioning-Measurement".

4. General Conclusions

The investigations presented show, that the general goal, stated as two major tasks of **LOW-COST IN-SITU MONITORING:**

- **OPERATION-CHECK**
- **VERIFICATION OF THE PREDICTED COLLECTOR YIELD.**

can be achieved by the I/O-Regression Procedure proposed.

The experience of applying the ISFH I/O-Regression Procedure to the Göttingen Solar District Heating Project has clearly demonstrated, that the first of the two tasks

- **OPERATION-CHECK**

can be well accomplished by the total daily incident irradiation regression. This has been proved by the Figures 4 and Figures 6a - 8a.

In order to fulfill the requirements of the second task:

- **VERIFICATION OF THE PREDICTED COLLECTOR YIELD,**

the results discussed indicate, that the I/O-Regression based on daily collector-ON irradiation data is more suited for a quantitative verification of the collector yield.

The need of using this supplementary regression type is increasing with the operating temperature of the solar system, the threshold irradiation value and thus the difference between total and collector-On irradiation. Former experience has shown, that I/O-Regression in standard DHW-systems does not show such large differences as observed in the high temperature systems of Göttingen.

5. Future Activities

investigate verification accuracy for other months

analysis of regression coefficients for different operation periods (effects of daylength, shading etc.)

produce regression coefficients based on ISFH- and TRNSYS-simulation runs typical for the design phase performance prediction for solar systems, using steady state collector efficiency parameters. A new version of the ISFH-Simulation and design programm will produce these regression coefficients in a standard way.

produce regression coefficients based on ISFH- and TRNSYS-simulation runs typical for characteristic ranges of operating conditions of collector systems.

investigate the effect of different ranges of operating temperatures both on the regression coefficients as well as on the verification accuracy.

analyse the differences between the two types of regression proposed (Eq. 2.1 and Eq. 2.2) with respect to the topics stated above.

6. Summary

The first part of the report contribution describes the development of the ISFH - Input/Output Procedure. The key feature of this procedure is the use of a low-cost measurement device designed for in-situ monitoring and control of the solar collector system, which performs a permanent

- **IN-SITU COLLECTOR OPERATION CHECK AND**
- **VERIFICATION OF THE PREDICTED COLLECTOR ARRAY YIELD**

by means of integrated control functions. The verification of the predicted collector yield is performed by a day to day comparison of the actual measured and the expected collector output based on a daily Input/Output Regression analysis. The report presents two different possibilities to obtain the required regression coeffients:

- path I: Design-Phase regression coefficients
- path II: Commissioning-Phase regression coefficients.

Examples for the determination of regression coefficients based on daily TRNSYS calculations and of experimental data for a solar DHW system are presented. The typical verification accuracy on monthly data is better than 0.1 kWH/(m^2day)

The second part of the report gives results of the application of this verification procedure in the Project **Solar District Heating Göttingen.**

The conclusions of this test can be summarized as follows:

- The linear correlation of Input/Output diagramms has been shown for the differently oriented collector arrays (162... 455m^2); however,

- due to the rather high collector operating temperature, the scatter of the daily collector output values is much larger than in systems for solar DHW heating.

- Regressions based on the total daily irradiation can be utilized for a daily check of collector operation.

- Detailed regression analysis has shown, that regressions based on the daily collector-on-irradiation reduce the scatter of daily collector output values by a factor of 3 as compared to the total daily irradiation regression; standard deviations of measured - predicted daily collector yield are in the order of 0.06 to 0.12 kWh/(m^2*day).
  This result proves, that the daily I/O-regression is capable to verify the actual collector yield against values obtained by the two reference procedures explained above.

- Furthermore, a preliminary study of the influence of reference month selection on monthly performance verification shows, that a verification accuracy of 5-10 % can be achieved on a monthly basis.

7. References

[1] Schreitmüller K.R.: "The Development of Mathematically Highly Condensed Computer Simulation Models", Task VI Report, International Energy Agency, ISFH, Hameln, December 1992

[2] Guisan O.; Lachal B.; Mermoud A. Rudaz O.: "G^3-Model: A Simple Model for the Evaluation of the Thermal Output of a Solar Collector System an a Daily Basis." Advances of Solar Energy, Vol. 1., 848. Pergamon Press, Oxford, 1988

[3] Perers B.; Zinko H.; Holst P.: "Analytical Model for the Daily Energy Input/Output Relationship for Solar Collector Systems. Swedish Council for Building Research, Document D11:1985

[4] Vanoli, K.: "Solarhaus Freiburg, Theoretische und Experimentelle Systemanalysen", Dissertation Univ. Stuttgart 1986, Sanfte Energie Verlag, Eldagsen, 1986

[5] Cornelius, C.: "y-logger", Product Information 1994, Dipl.Ing. C. Cornelius, Wittekindstr. 33a, D-30449 Hannover

[6] Solar Equipment: "Solarregler mit integriertem I/O-Controller", Product Information 1994, Niederstr. 30, D-41812 Erkelenz

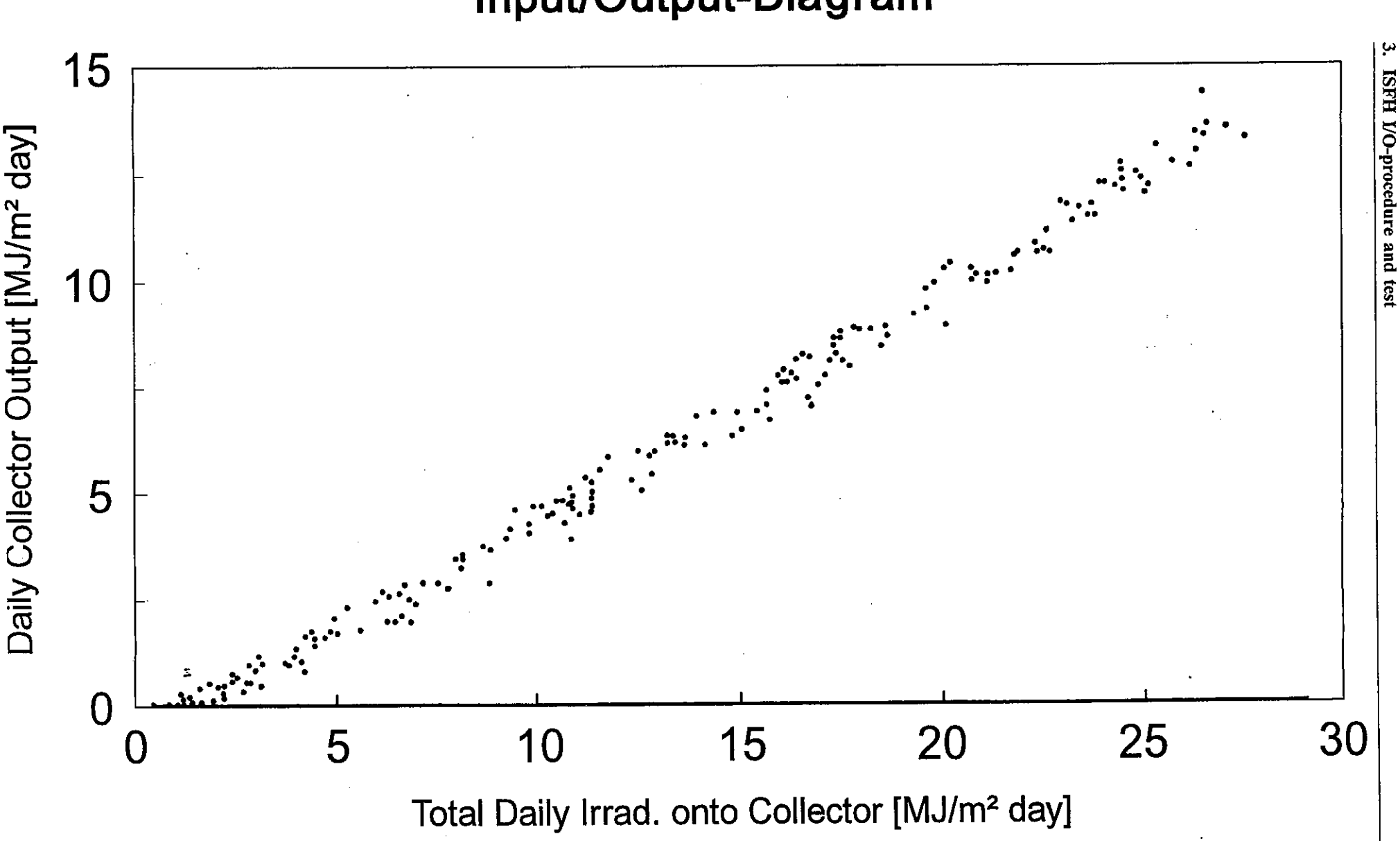

Figure 1: Corning Glass Collector operation in Solarhaus Freiburg 1980
\Duff et al, IEA Task VI 1986\

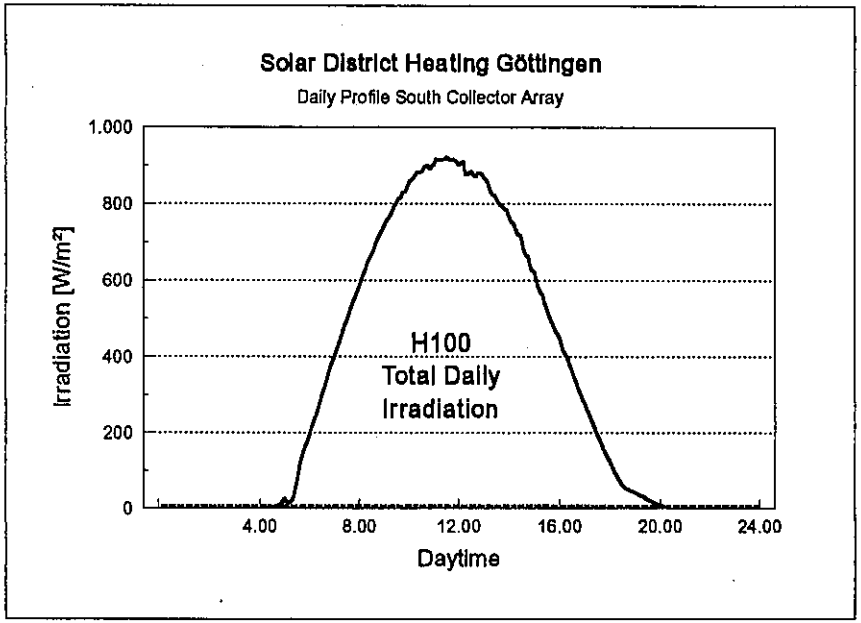

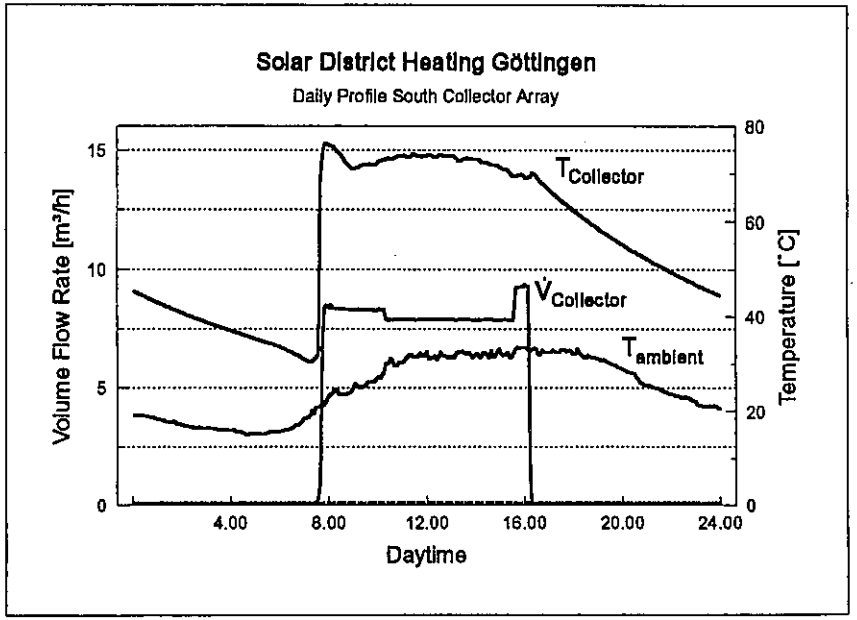

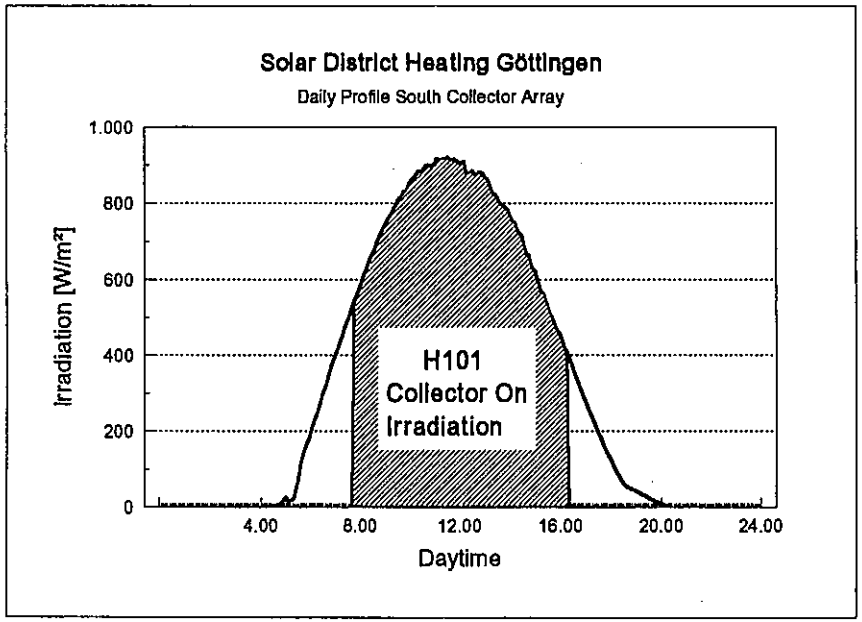

Figure 2: Definition of Total Daily Irradiation H100 and of Collector On Irradiation H101

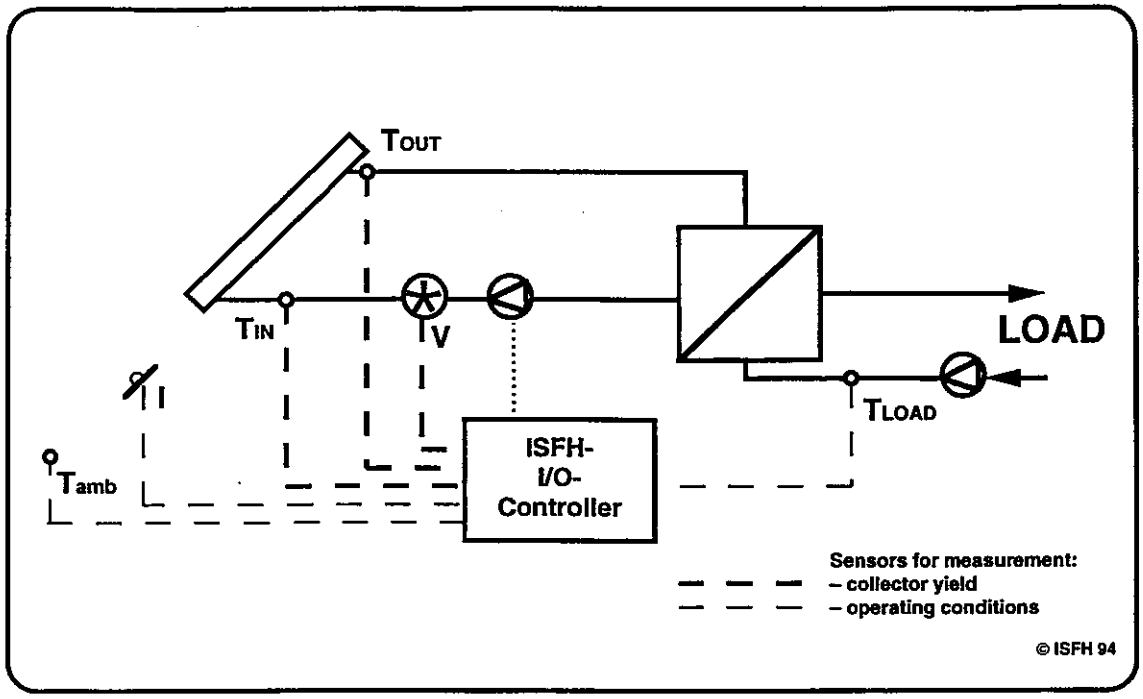

ISFH I/O-Controller

Figure 3: Typical Integration of the I/O-Controller into a Collector loop

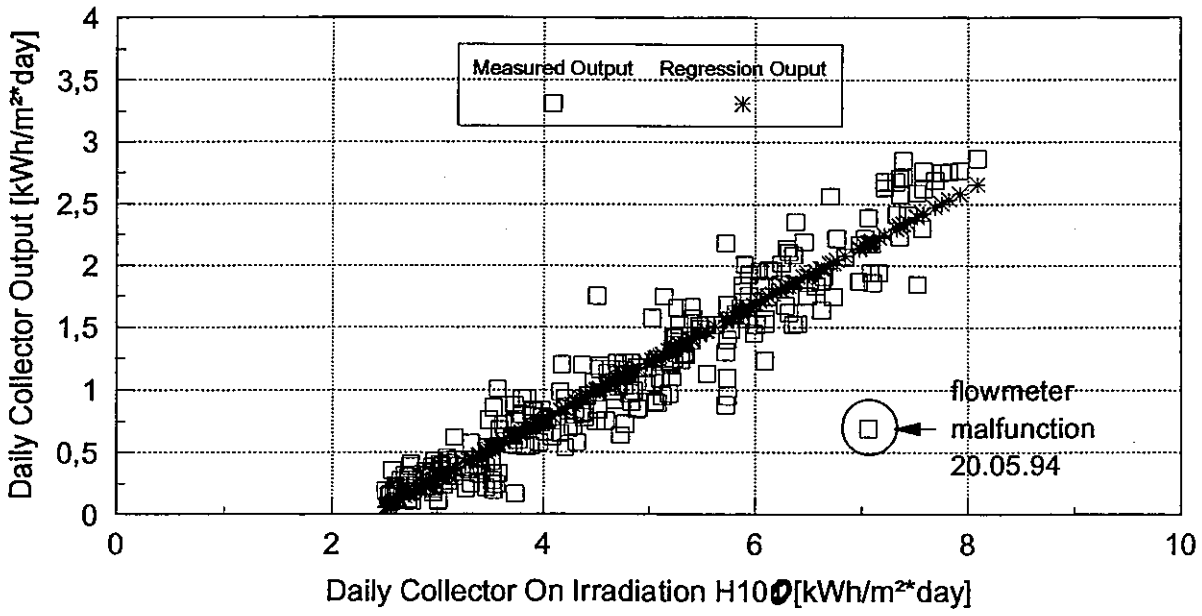

Figure 4: Typical Integration of the I/O-Controller into a Collector Loop

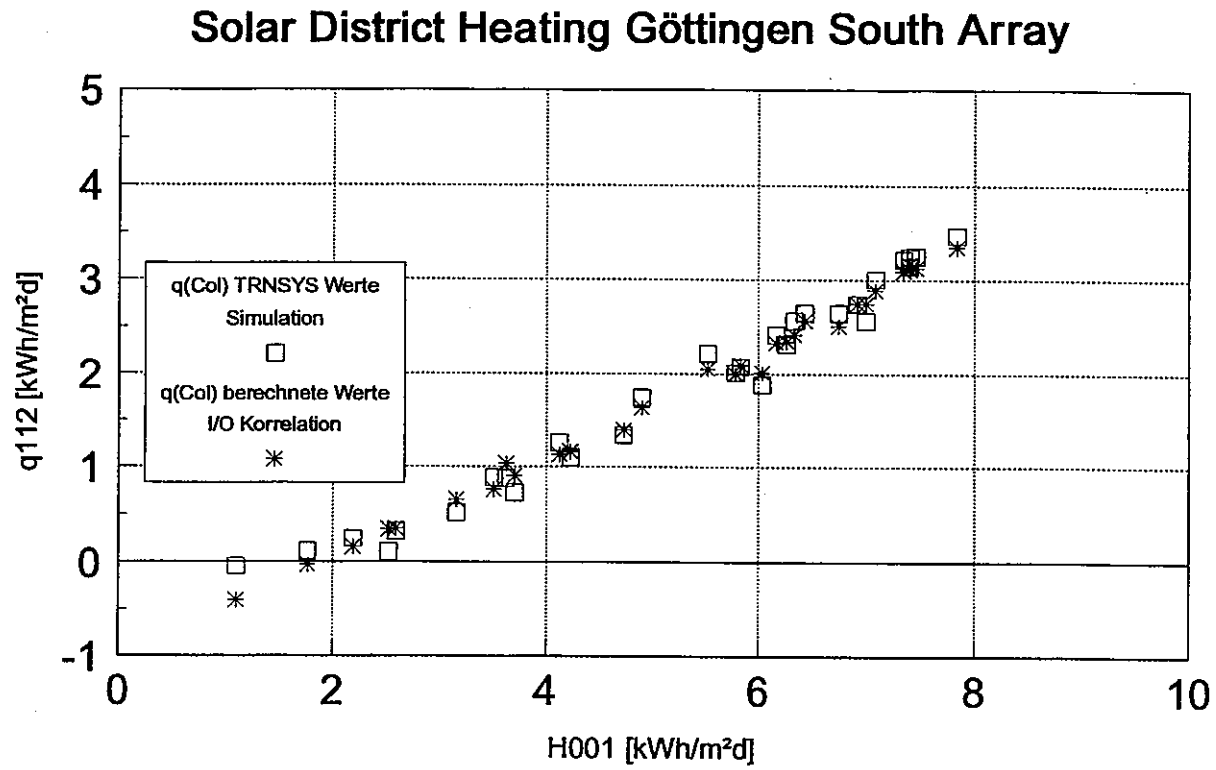

Figure 5a: Determination of the I/O-Correlation Coefficients using simulated Data during the design process (TRNSYS-Simulation Collector Type 1)

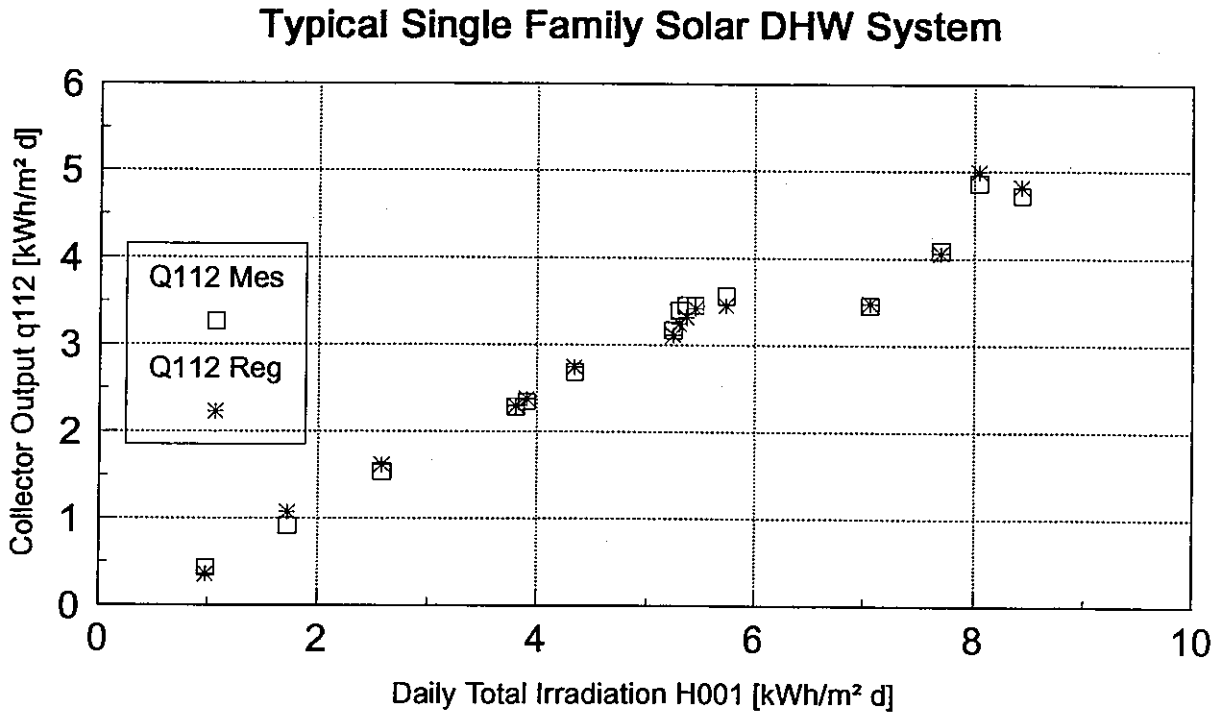

Figure 5b: Determination of the I/O-Correlation Coefficients using Data of an In-Situ Commissioning-Measurement Period

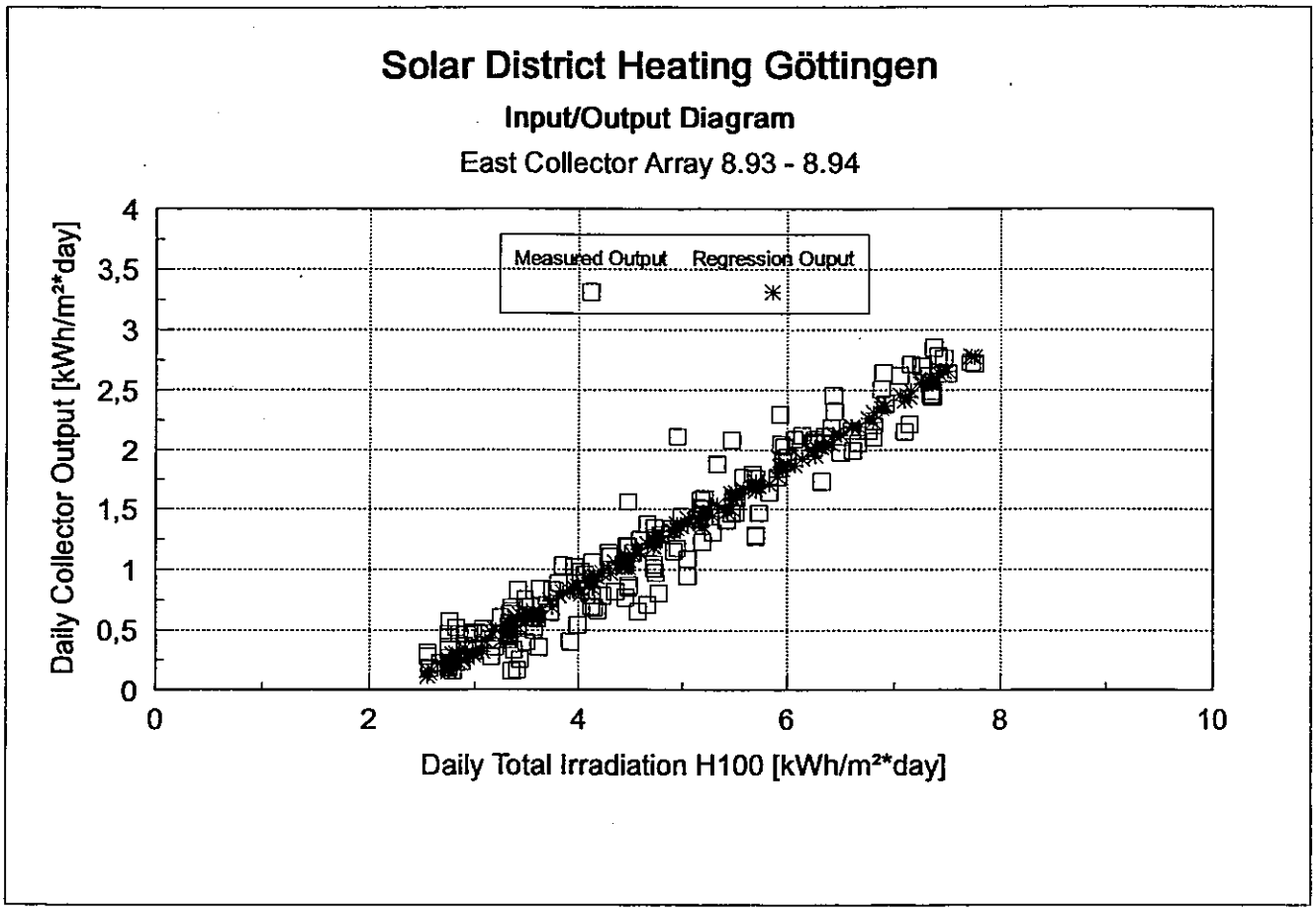

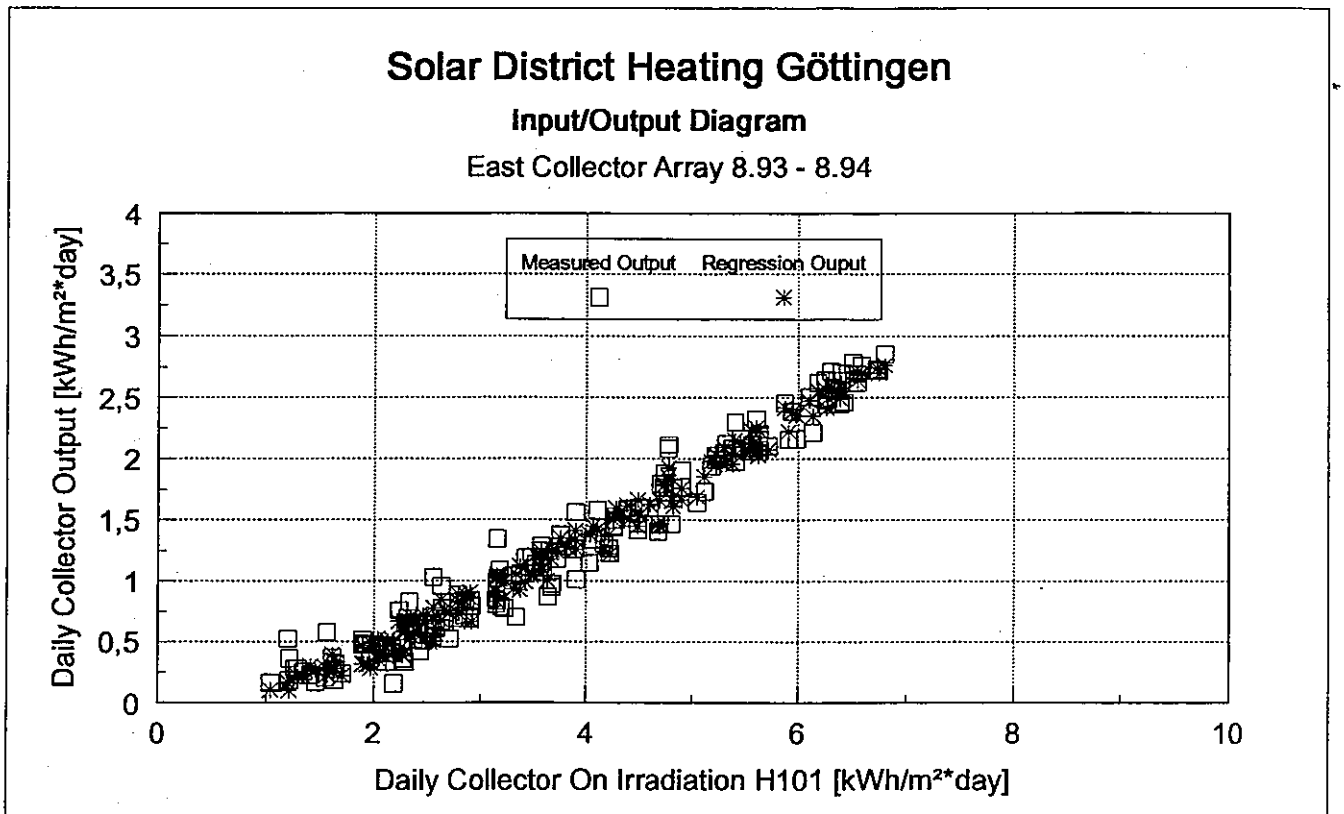

Figure 6: Input/Output-Diagram based on Total Irradiation (Top) and Collector On Irradiation (Bottom)

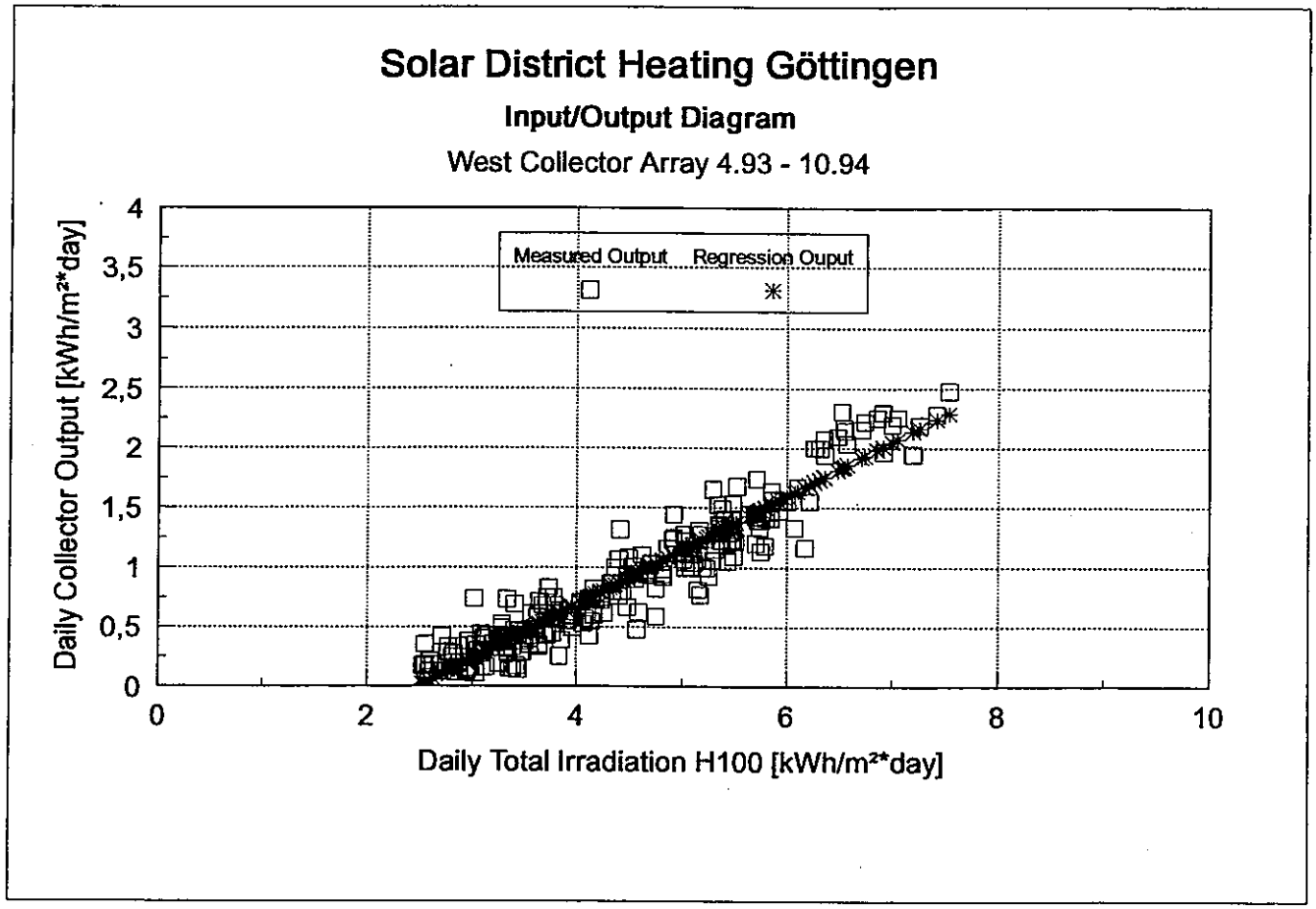

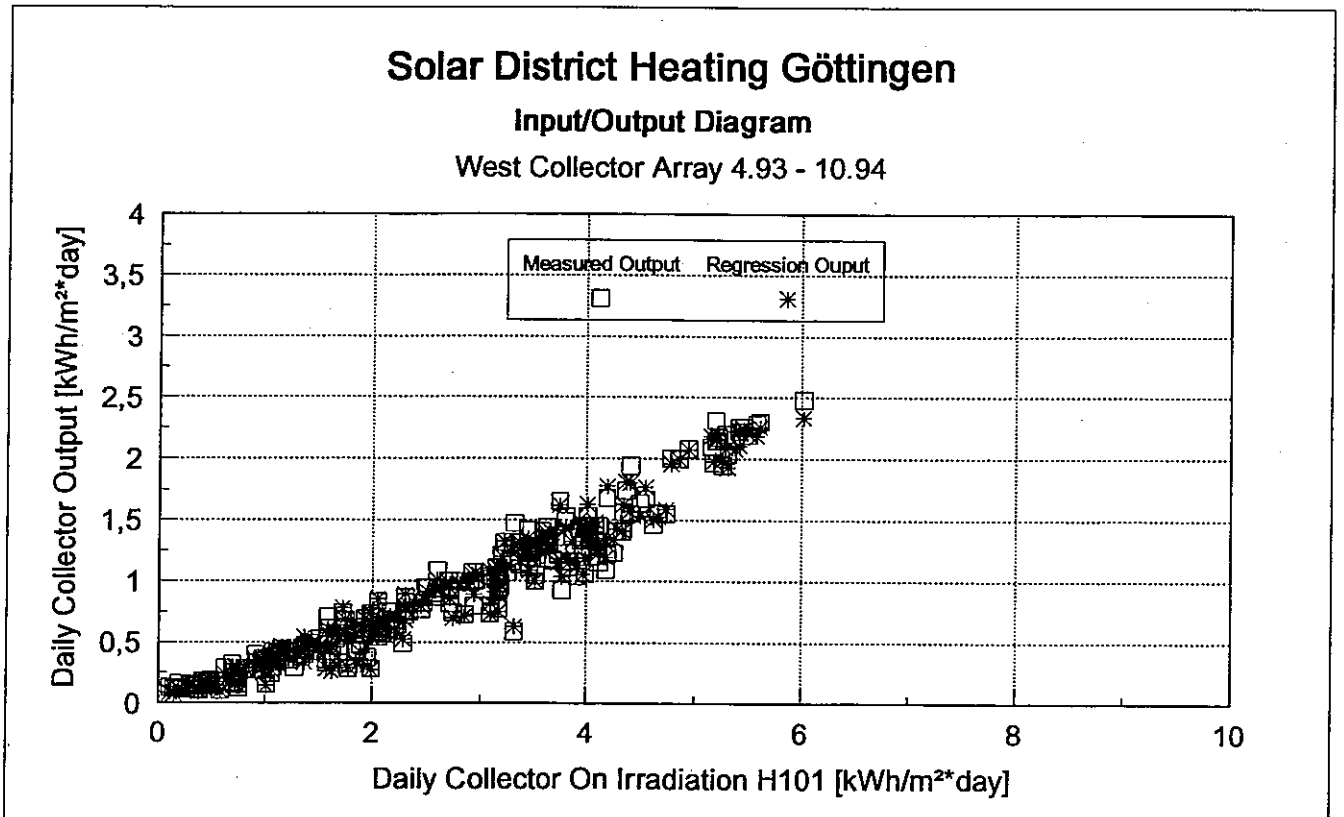

Figure 7: Input/Output-Diagram based on Total Irradiation (Top) and Collector On Irradiation (Bottom)

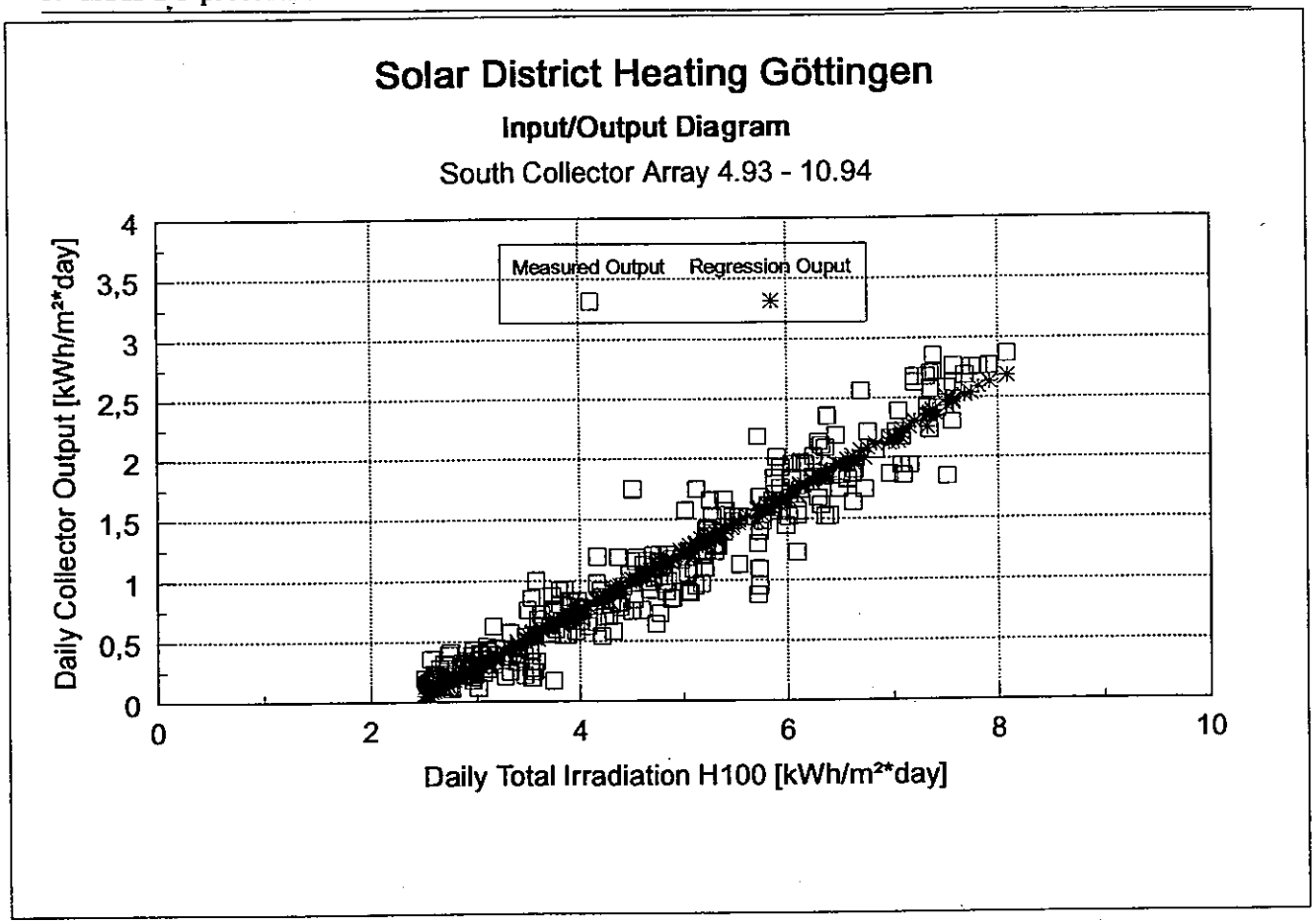

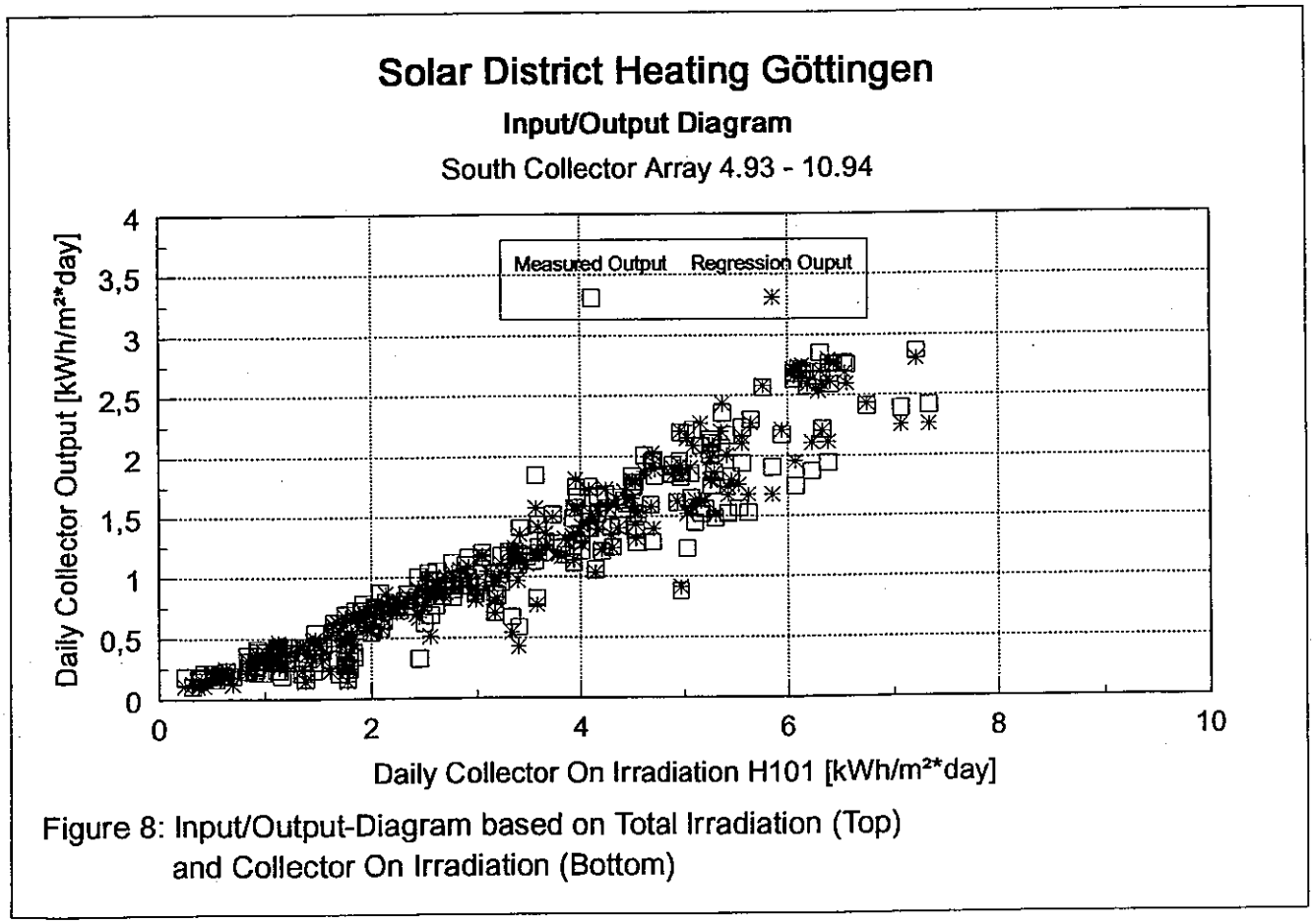

Figure 8: Input/Output-Diagram based on Total Irradiation (Top) and Collector On Irradiation (Bottom)

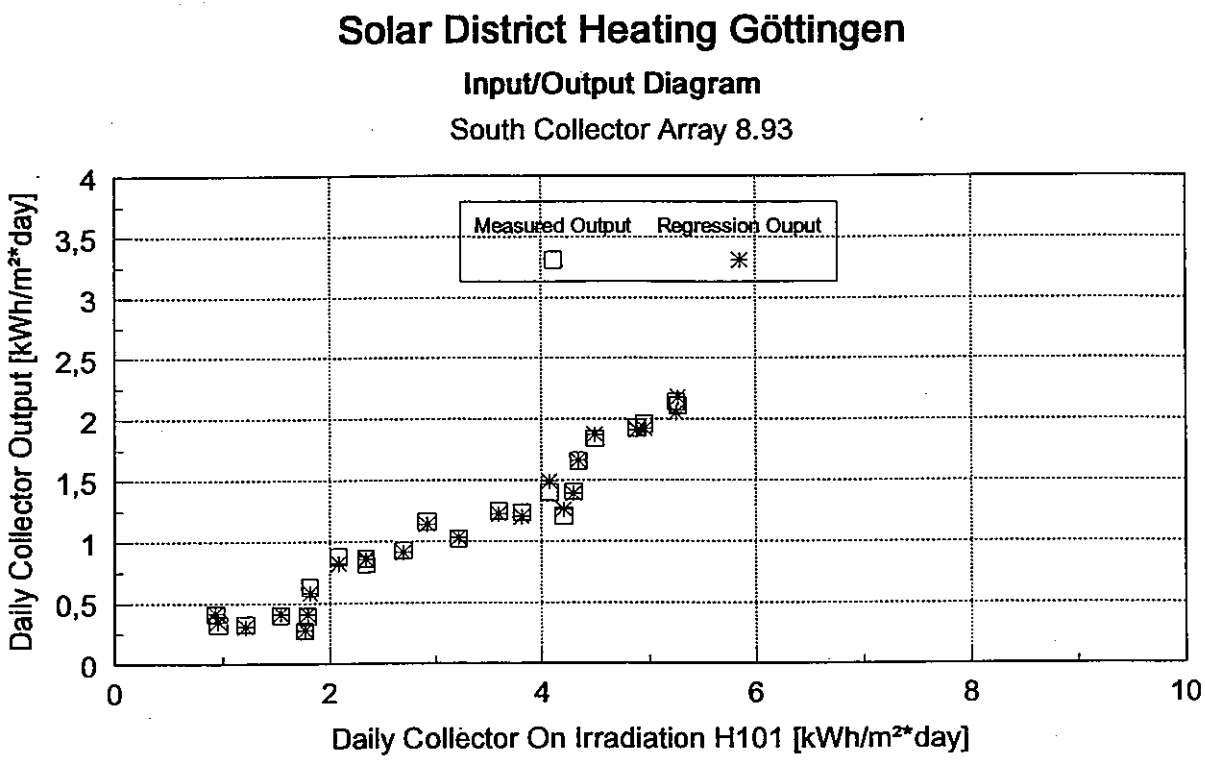

Figure 9a: South Array 08.93 Data used as Commissioning - Measurement

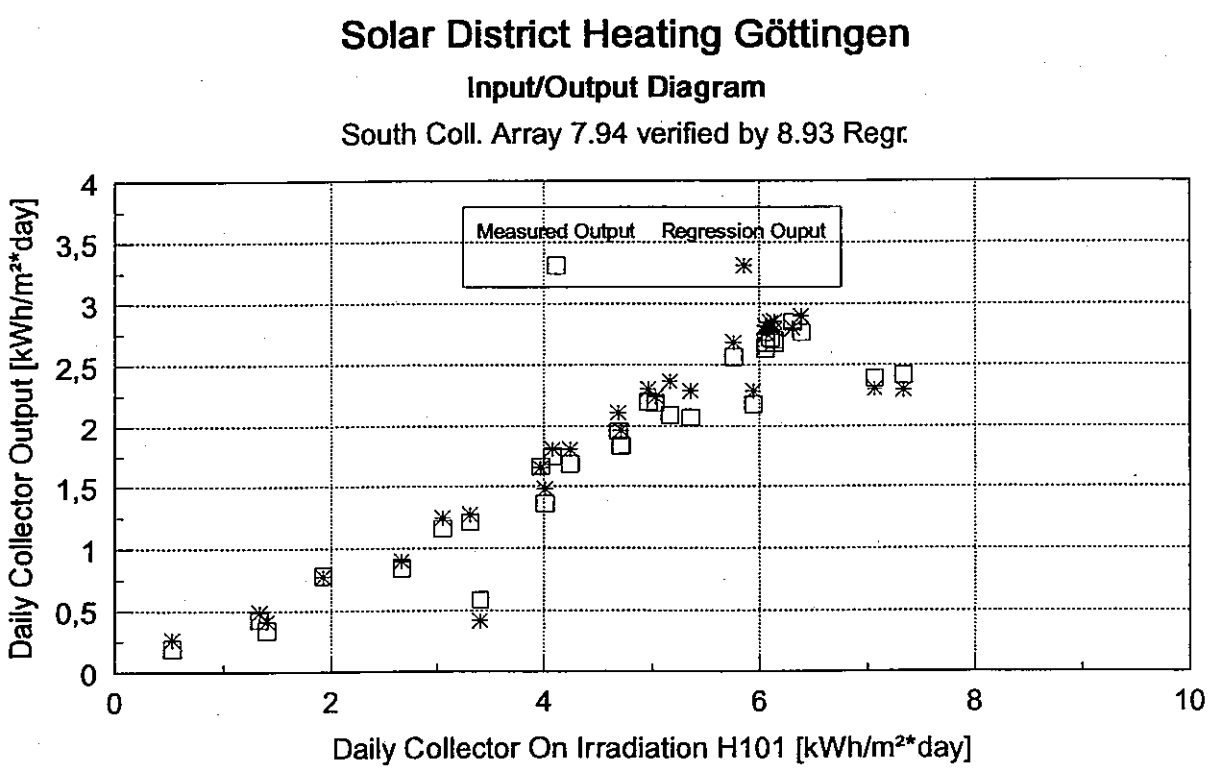

Figure 9b: South Array 7.94 Data compared wirth Commissioning Measurement 8.93
Prediction error - 4 %

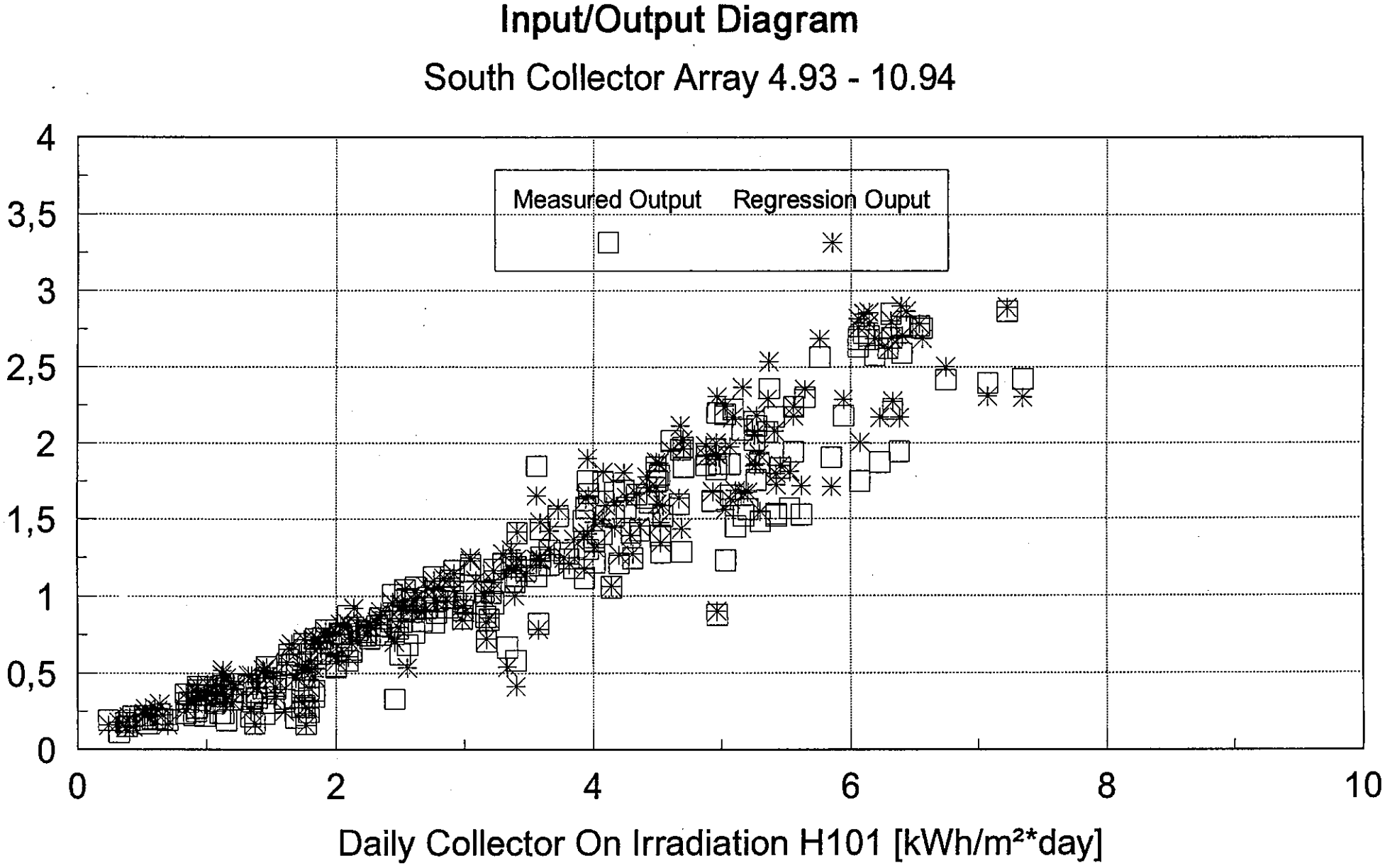

ure 10: South Array Data 04.93 - 10.94 with Commissioning Measurement 8.93
Prediction Error - 4.6 %, Standard Deviation 8 %

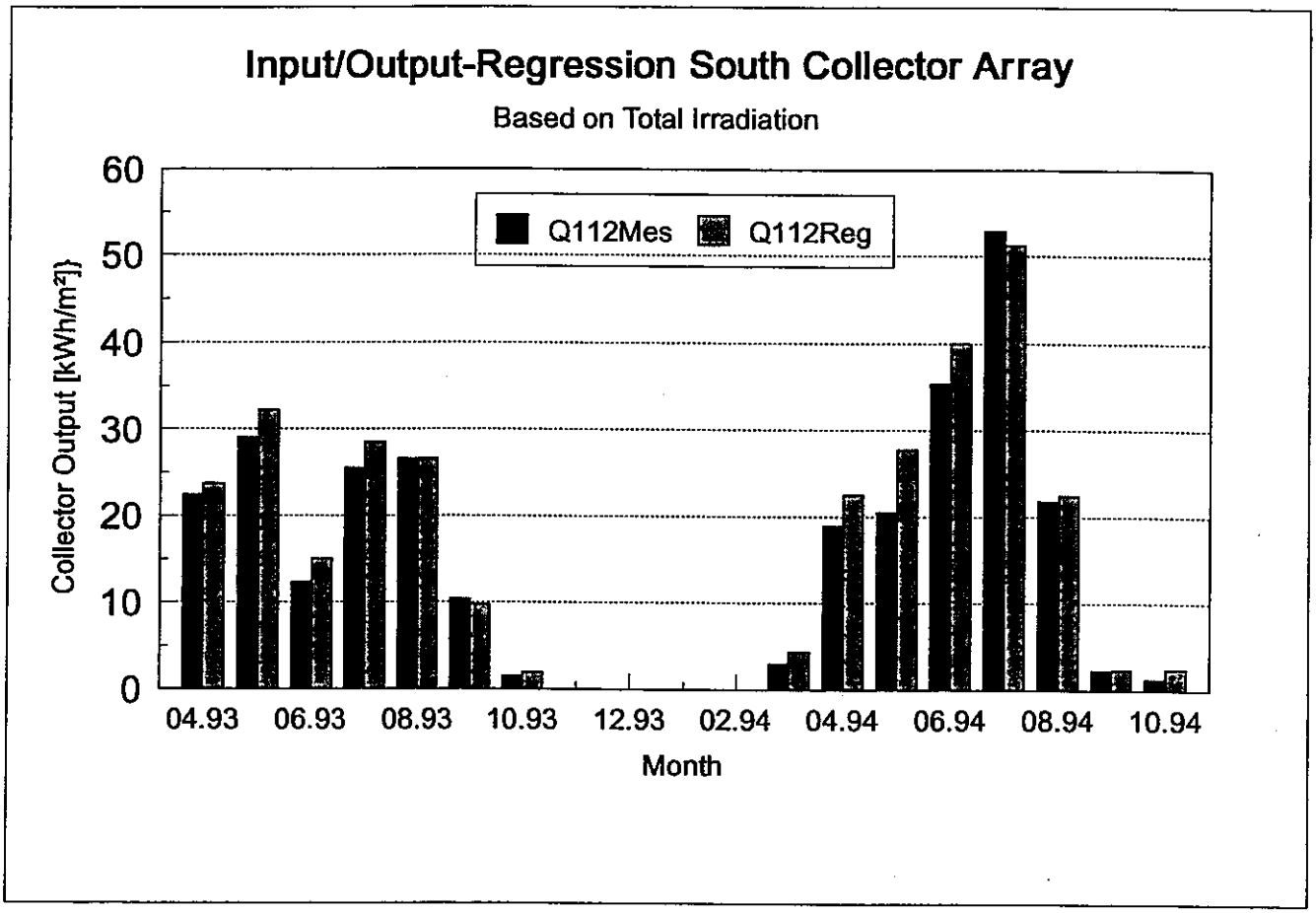

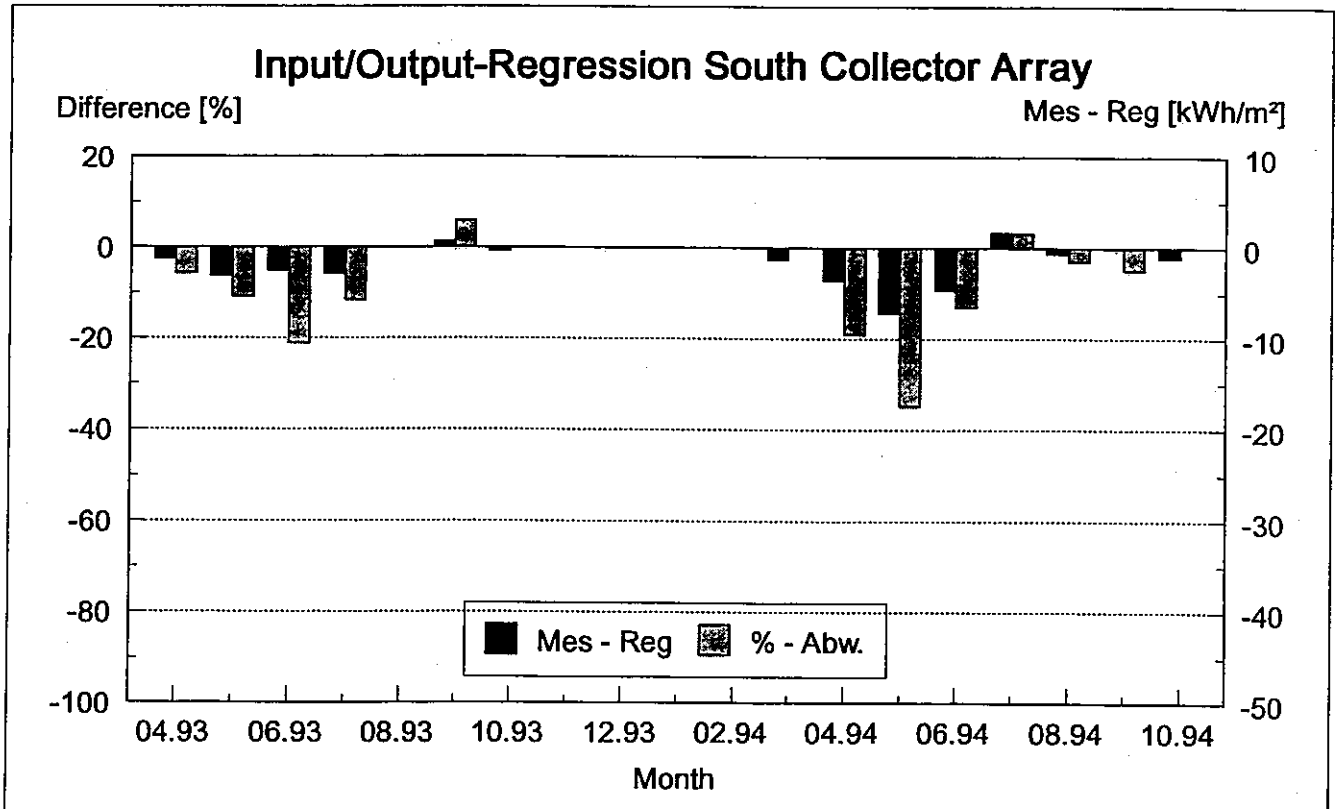

Figure11: Monthly Distribution of measured and predicted Output (Top) and Prediction Error (H100 Regression ≙ Total Irradiation)

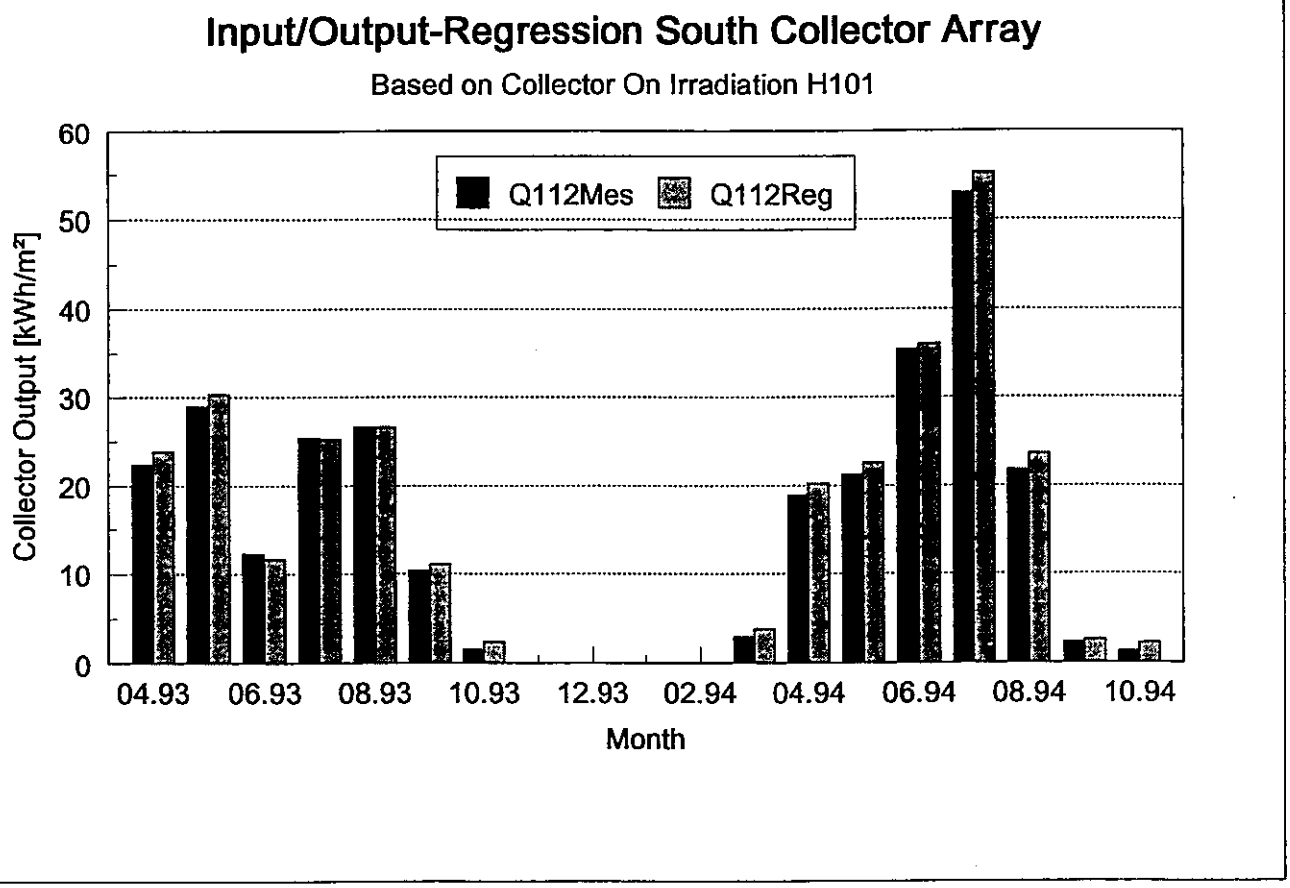

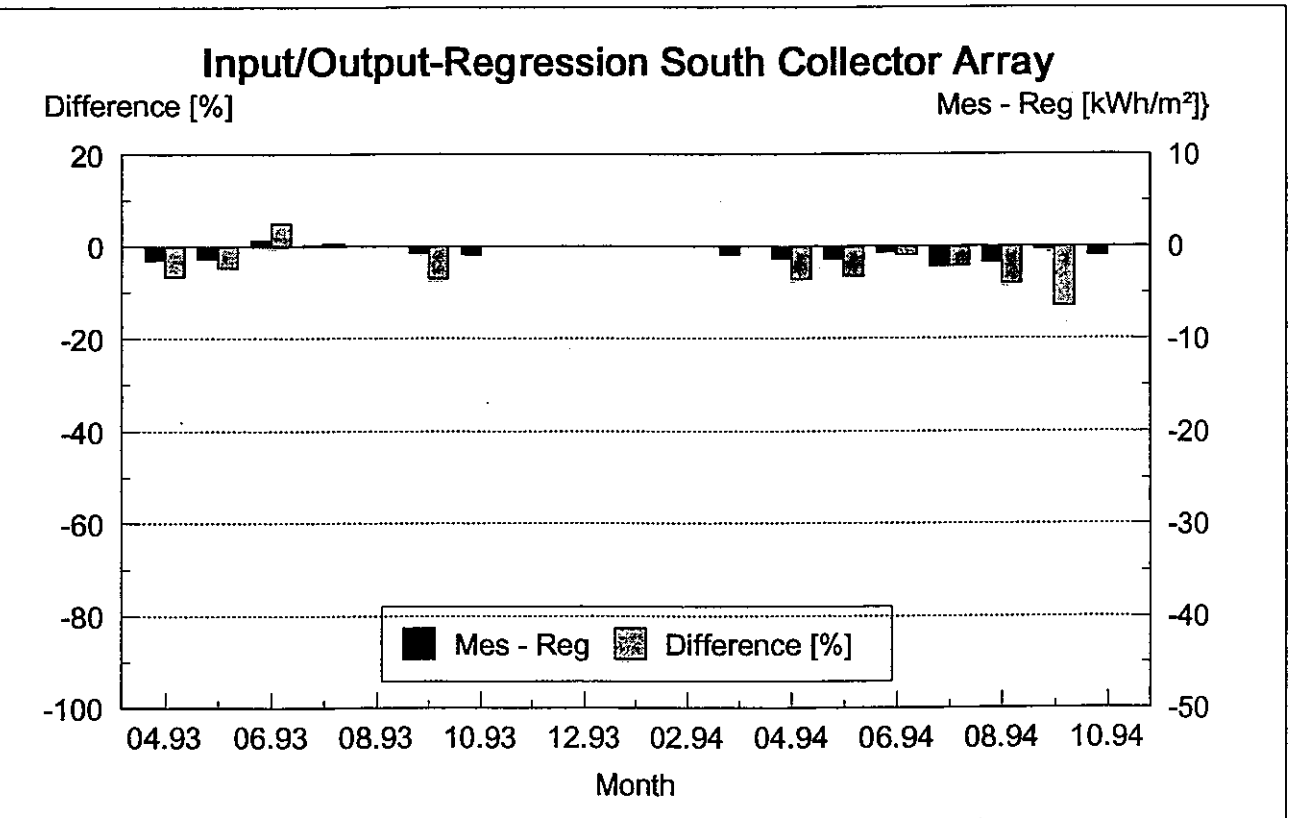

Figure 12: Monthly Distribution of measured and predicted Output (Top)
and Prediction Error (H101 Regression ≙ Collector On Irradiation)

Verification Accuracy Q112meas–Q112reg [%]				
Period of Measurement	Data–Month of I/O Regression "Commissioning Measurement"			
	April.93	Mai.93	Aug.93	Aug.94
4.93	0.0	–2.8	–6.6	–3.4
5.93	4.5	0.0	–4.6	–1.8
6.93	10.7	10.6	5.1	11.4
7.93	8.0	6.7	0.6	6.7
8.93	7.8	6.0	0.0	5.8
9.93	–2.0	–0.9	–7.0	0.8
10.93	–60.4	–49.0	–55.9	–40.2
3.94	–36.8	–26.2	–34.4	–18.3
4.94	–0.4	–0.7	–7.1	0.1
5.94	2.0	1.0	–6.4	1.3
6.94	9.0	5.6	–1.8	4.3
7.94	8.1	3.5	–4.2	1.4
8.94	2.1	0.2	–8.1	0.0
9.94	–5.4	–4.6	–13.1	–3.2
10.94	–77.0	–60.7	–71.7	–48.9
4.93..10.94	4.1	1.9	–4.6	1.4

Table 2: Verification of South Array
Dependence of Reference–Month selection on monthly verification accuracy

Verification Accuracy Q112meas–Q112reg [%]					
Period of Measurement	Data–Month of I/O Regression "Commissioning Measurement"				
	Apr.93	Mai.93	Aug.93	Aug.94	Apr.93–Aug.94
4.93	0.0	0.1	10.2	–0.5	1.3
5.93	3.9	–0.1	5.8	2.6	1.7
6.93	3.4	3.2	5.4	5.9	5.1
7.93	2.8	3.1	2.8	6.7	5.2
8.93	0.5	–1.7	–0.0	2.2	0.5
9.93	–17.7	–8.1	–11.4	–6.2	–5.8
3.94	–39.6	–19.8	–24.0	–20.8	–17.7
4.94	–13.5	–8.4	–9.0	–5.9	–6.2
5.94	–3.4	–6.0	–5.6	–1.3	–3.6
6.94	4.1	–2.0	–3.1	4.4	0.5
7.94	3.9	–4.0	–6.4	3.7	–1.1
8.94	–8.4	–4.8	–10.2	0.0	–2.2
9.94	–12.2	1.2	–6.9	3.4	3.5
4.93..9.94	0.2	–2.2	–1.6	2.2	0.0

Table 3: Verification of West Array
Dependence of Reference–Month selection on monthly verification accuracy

Verification Accuracy Q112meas–Q112reg [%]			
Period of Measurement	Data–Month of I/O Regression "Commissioning Measurement"		
	Mai.94	Aug.94	Mai.94–Aug.94
5.94	0.0	5.7	6.1
6.94	–11.1	–5.9	–5.7
7.94	–5.7	–1.9	–1.6
8.94	–6.1	0.0	–1.5
9.94	–1.6	5.2	3.9
10.94	–3.5	8.1	7.2
5.94..10.94	–6.0	–0.8	–0.9

Table 4: Verification of East Array
Dependence of Reference–Month selection on monthly verification accuracy

DYNAMIC IN SITU TESTING OF A LARGE SOLAR SYSTEM

C. Arkar, S. Medved, P. Novak
University of Ljubljana
Faculty of Mechanical Engineering
Askerceva 6
61000 Ljubljana
Slovenia

1. INTRODUCTION

Outdoor laboratory measurements have many advantages in comparison with in situ measurements. The testing time is short because the system operates so that wide range of system states is considered [1]. Another advantage is that sensors could be chosen, mounted and located according to recommendations.

But something is obvious. It is impossible to make laboratory measurements on large systems and the real system is almost never mounted so as it is by laboratory testing (pipe length, pipe insulation, flow rate).
So in some occasions only in situ measurements are possible and relevant for determination of real system parameters and prediction of system performance.

For evaluation of DF method for large in situ tested systems we chose a system with complex configuration. We took this system mainly because of measured collector loop gain which was used for comparison with LTPP.

2. DESCRIPTION OF THE INVESTIGATED SDHW SYSTEM

Chosen solar system is installed on a medical center in Litija. System has been designed for solar hot water heating. Solar system successfully operates for many years.
It has 32 flat plate solar collectors with 56.6 m^2 of aperture area or 1.77 m^2 each. They are tilted to an angle of 45° and oriented 10° towards east. They are mounted on a flat part of the roof.

Solar system has two well-insulated heat stores with volume of 1.5 m^3 each. One has external jacket heat exchanger and the other coil heat exchanger. They both have mounted electrical auxiliary heaters on the upper sixth of the store volume. The second store has also circulation loop driven by circulation pump.

Solar system configuration changes seasonally.

In the summer system has two stores. Collector loop water goes trough both heat exchangers in each heat store; first trough the second store. Both electrical heaters are in operation. They have different power and they are set on different temperature. Heat stores are mounted in series. By system modeling they are treated as one.

In the winter the system has a configuration of solar preheat systems. Only the first heat store is heated with solar energy and it is used to preheat the sanitary water. In collector loop is antifreeze mixture. Electrical heaters are not in operation. The second store is heated by oil burners.

Fig. 1 shows summer and winter system configuration.

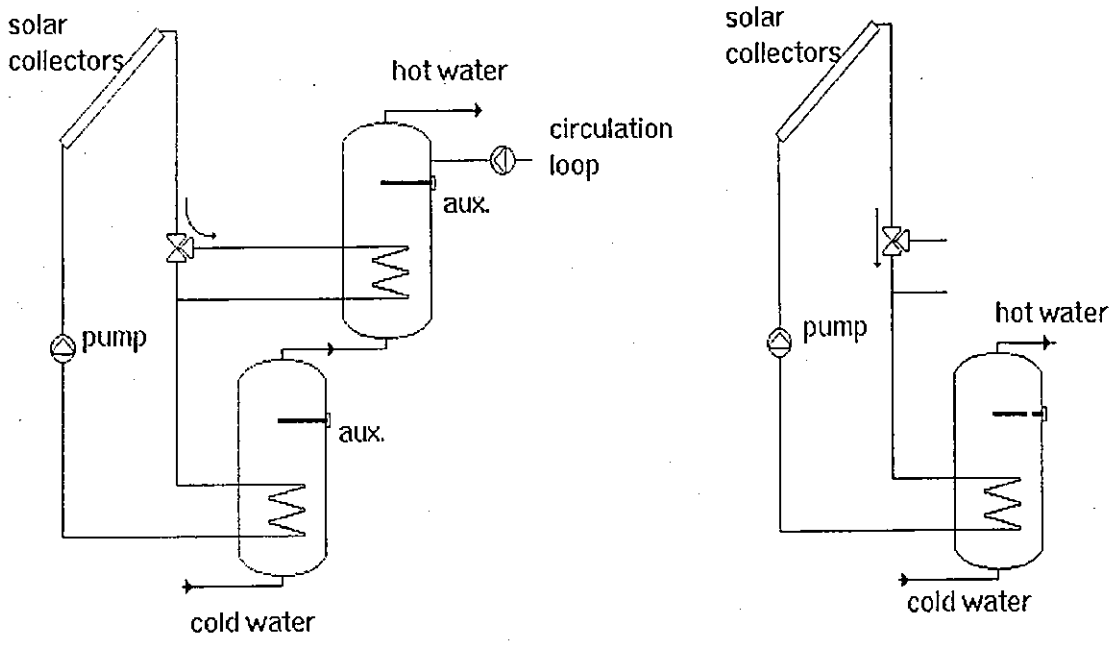

Figure 1: Summer and winter system configuration.

These two configurations have been of our major interest. Solar system usually operates in summer configuration from June to September and in winter configuration from November to April.

The third possible operating condition is used between these two periods. System has summer configuration. The second store is heated by oil burners to maintain desired set temperature and electrical heaters are out of operation. This period has been out of our interest because it is usually short (it last approx. one month), it is set manually and it would cause problems by auxiliary energy measurements. In long term performance prediction this period is treated as winter period.

2.1. Sensors and instruments mounting

Constant requirements for hot water in the building (medical center) did not allow us to close the hot water, empty the system and make necessary corrections in the system for mounting the sensors.

Therefore we used wire resistant Pt-100 sensors for cold and hot water temperature measurements and mount them on the pipe.

For flow measurements we used ultrasonic flow meter.

All the other sensors were chosen and mounted according to recommendations for mounting and location of the sensors.

Additional effort was required for determination of actual power of electric heaters because they have been in operation for many years.

3. MEASUREMENTS AND SIMULATION RESULTS

For each system configuration measurements were lasted approximately one month.

The measurement data were sampled every 5 seconds and recorded every 30 seconds when there was hot water consumption and every 10 minutes when there was no load.

Measurements had shown the daily hot water consumption to be almost uniform in working days and that it does not exceed 2 m^3 despite that system was designed for consumption of 4 m^3 per day. This small load causes long preconditioning phase.

The load profile is also very dynamic. It has a lot of short term withdrawals following one after another during all the day. This is evident from Fig. 2 where volume flow rate for a typical working day is shown.

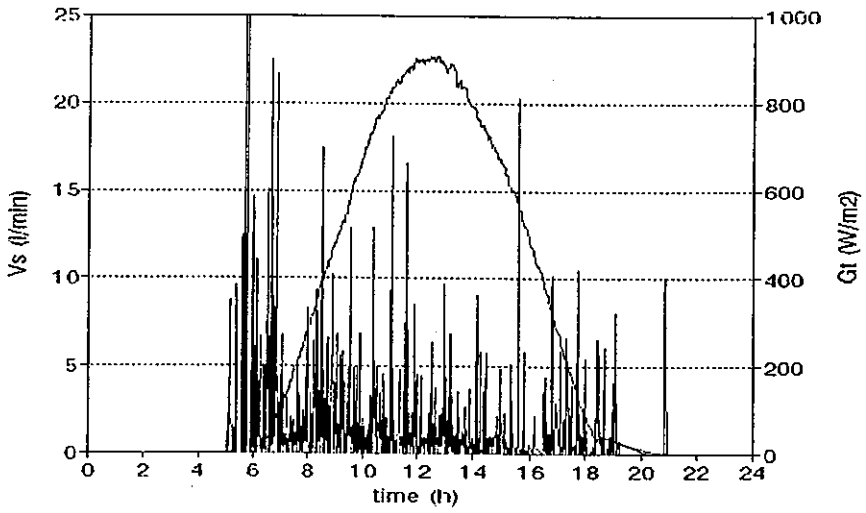

Figure 2: Typical load profile.

Precondition phase was so set to 120 and 60 hours for summer and winter system configuration respectively. This corresponds to 3 to 3.5 store volumes. This very long precondition phase and very often draw offs makes data files very large. Consequently this limits the number of measurement days which could be used for system evaluation. Namely computer software program could take only limited number of data [2].

3.1. Summer system configuration

System summer configuration is in comparison to the P model much more complicated. System has two stores, auxiliary heaters in two locations and circulation loop which all could not be modeled properly.
Table 1 shows the best fitted parameter values of summer system configuration.

Table 1: Expected and fitted parameter values for summer system configuration

	Ac*	uc*	Us	Cs	f_{AUX}	D_L
	m^2	W/m^2K	W/K	MJ/K	-	-
EXPECTED	34	8.3	25+240	12.6	.6	
FITTED	18.9	8.4	442	15.4	.47	5

From the Table 1 it is seen that is system poorly modeled. Fitted parameter values are far from expected ones. Too little experimental data and uniform operation conditions are the main reasons for poor modeling of system parameters. Collector loop and store heat losses are correlated.

Circulation loop heat losses (too low top store temperature) could be the reason for higher store parameters and lower effective collector area. These heat losses are not equally distributed over height of the store but they are concentrated to upper 100 l of heat store.

As we found later also cold water mixing between the stores was possible. This could higher the store capacity and store heat losses too.

3.2. Winter system configuration

Parameter values obtained from data of winter system configuration measurements are shown on Table 2.

Table 2: Expected and fitted parameter values for winter system configuration.

	Ac*	uc*	Us	Cs	D_L
	m^2	W/m^2K	W/K	MJ/K	-
EXPECTED	34	8.3	25	6.3	
FITTED	20.1	6.5	44.3	7.5	.04

Results of winter configuration simulation are better. This has to be expected since system has simple configuration.

From the Table 2 it is seen that we got lower value for effective collector area and store parameters which are higher than expected parameters.

The reason for small effective collector area could be the quality of solar absorbers. The optical efficiency of new solar collector was 75% but today, after 9 years of operation it is surely lower.

Inspection of the measured data shows that some small circulation exists between both heat stores during the nights. Mixing valve between stores enables circulation of water. This causes the temperature of water (approx. 5% of store volume) at the top of the store to increase during the night close to the temperature of the second store.

In addition the untight mixing valves most probably cause cold water mixing. We did not take this possibility into account during the measurements. This could be the reason for higher store heat capacity and higher store heat losses.

4. SYSTEM PERFORMANCE PREDICTION

On the basis of the system model we carried out long term performance prediction for summer and winter period.
We have used TRY for Ljubljana. We took that summer period last from May 15 to November 15, the remind of the year was winter period.
We have tried to define the load profile which is as close as possible to the real one.
The results of LTP prediction and system efficiency are presented on Table 3.

Table 3: Results of LTP prediction.

LTPP		Summer	Winter	
Average system gain	Pnet	825 ± 20	807 ± 10	(W)
Fractional system gain	f	.37 ± .4	.333 ± .3	(-)
Effective solar system area	As	4.46 ± .3	12.6 ± .2	(m^2)

LTPP with specified auxiliary sequencer for summer period gives us unuseful results. Also withought it the system gain seems to be too low (Table 3).

This is also evident from Fig. 3 where measured collector loop gain (calorimeter) and computed system gain (LTPP) are presented.

For direct comparison the calorimeter data should be reduced for store heat losses. These are in summer system configuration high because of circulation loop heat losses.

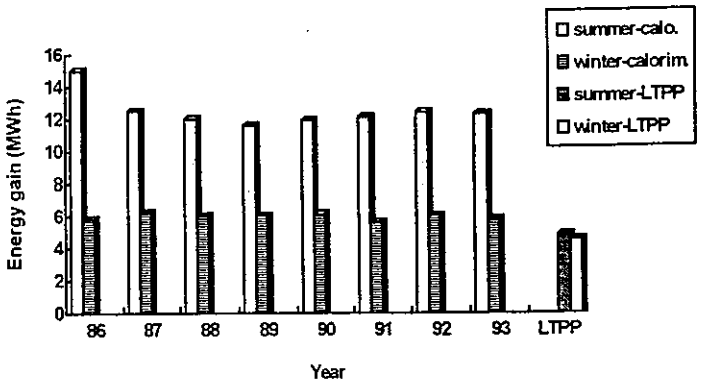

Figure 3: Calorimeter data and computed system gain.

5. CONCLUSIONS

Our measurement had shown that with relatively simple P model only simple systems could be modeled [3]. More complicated system as our summer system configuration could not be modeled satisfactory. Unequally distributed heat losses and more auxiliary heating locations cause improper system modeling.

The results of winter system modeling seem to give us good results despite small amount of measurement data. Comparison of LTPP results with calorimeter data proves this. Of course for better modeling more data would be required especially because of in situ measurements.

In our opinion for large or more complicated system combination of component (collector loop) and whole system testing should be considered. Separately determined collector parameters could shorten the measurements of the whole system. There would also most probably be no problems with correlation between system parameters. This combination of measurements would require more sensors and modified computer program.

REFERENCES

[1] Arkar C., Medved S., Novak P., 'Different SDHW system testing using dynamic method', Dynamic Testing of Solar Domestic Hot Water Systems, Final Report of the

IEA Dynamic System Testing Group, Part B, Delft, The Netherlands, 1992, p.209-216

[2] Spirkl W.,'Dynamic System Testing', Program Manual, Version 2.3β, Ludwig-Maximilians Universität München, Germany, 1994

[3] Arkar C., Medved S., Novak P., 'New proposal of ISO standard for SDHW system testing method-introduction and first experiences', Energy and the Environment, Opatija, Croatia, 1994, p. 291 - 297

Towards a performance test for large collector arrays

Per Isakson

Department of Building Services Engineering
Royal Institute of Technology
S - 100 44 STOCKHOLM, Sweden
Fax: +46 8 411 8422, E-mail poi@ce.kth.se

This contribution summaries my work on an in situ test procedure for large collector arrays connected to district heating plants. Isakson (1995) provide a detailed report on this work. The goal is a test, that is accurate, easily understood, and not to expensive to apply. The test is aimed at routine use in commissioning of new corrector arrays and performance monitoring of arrays in operation.

1. Introduction

An *in situ* test of the thermal performance of large collector arrays is required for commissioning tests of new plants and continuous monitoring of plants in operation. The large amounts of heat produced by large arrays justify to strive for an accurate test procedure. The purpose of the commissioning test is to determine whether or not the array is able to deliver the amount of heat claimed by the constructor. Performance monitoring of operating arrays is justified, since malfunctions may cause large losses of heat and measures to improve the performance are likely to pay-off. Moreover, large solar heating plants are owned and operated by professional organisations, which want to use performance data for decisions on guaranties, maintenance, etceteras.

What level of accuracy is needed and what level can be achieved at a reasonable cost? In Sweden a ten per cent difference in the yearly collector yield is significant when choosing between competing constructors of collector arrays for district heating plants. Thus, I think the goal should be a performance test that is able to safely distinguish between arrays the predicted performance of which differs ten per cent. I deem that a confidence interval of ± 20 [kWh/m^2.a] in combination with a confidence level of 90 per cent is justifiable. For example, if the result of the evaluation is 360 ± 20 [kWh/m^2.a] there is a five per cent risk that the 'true' value is larger than 380 and another five per cent that is smaller than 340. If an array is guaranteed to produce 380 [kWh/m^2.a] and we predict 360 ± 20 [kWh/m^2.a] based on the evaluation we would accept the array. However, the risk is 95 per cent that the array in reality would not produce 380 [kWh/m^2.a] for the given sequence of operating conditions.

Several sources will contribute to the inaccuracy of the performance evaluation, e.g. measurement and model errors. The inaccuracy in the load and the meteorological data sequences will contribute to the inaccuracy of the long term prediction. However, these sequences should be defined together with the specifications of the collector array performance. Hence, they will not contribute when evaluating the performance against that specification. To achieve a total confidence interval of ± 20 [kWh/m^2.a], the requirement on the test method need to be $\pm$ 10 [kWh/m^2.a], to allow for contributions from systematic measurement errors.

In large arrays a performance test based on measured data acquired during regular operation would offers advantages. Firstly, because of the size and the amount of heat involved, most special test sequences are expensive to carry out. Secondly, because of modelling errors I doubt that the accuracy of the resulting long term prediction would be improved by including special test sequences, which involve operating conditions not experience during regular operation. The model is an idealisation and modelling errors are inevitable. Thus, there is no true set of parameters, which would make the model mimic the real collector perfectly for all operating conditions. The modelling errors will contribute to the prediction errors and the larger the difference between the operating conditions of the testing sequence and those of the prediction the larger the prediction errors. I doubt that our current collector models well enough predict the performance over a wide range of operating conditions.

To my experience fitting a collector model to experimental data form regular operation will yield a set of parameters values, which in turn will yield good predictions of the heat collected by the same collector loop. However, there will be large correlation between the fitted parameter values and typically the values will not agree with the values we expect based on prior knowledge. Furthermore, the estimated values of single parameters will usually vary between fits to different sequences of measured data. In my opinion a set of fitted parameter values in which the single parameter values neither agree with expected values nor are reproducible is not acceptable because of two main reasons. Firstly, such a set raises difficult questions regarding the range of operating conditions for which a predictions is trustworthy. Secondly, such a set gained from the first month of operation of a new plant is difficult to judge and hence difficult to use.

1.1 Goal

The goal is an *in situ* performance test for central solar heating plants. I restrain my current goal to a test for collector arrays in district heating plants. It shall produce

- an accurate prediction of the yearly heat delivered (± 20 [kWh/m^2.a] at a confidence level of 90%). The load and weather data used in the prediction are given and do thus not contribute to the inaccuracy of this test.
- a mean to detect degradation in the thermal performance
- a result suitable to use in system simulations

The procedure should require no major inputs besides

- measured data from regular operation during no more than a month
- hourly data of a meteorological reference year
- hourly data of the return temperature of the district heating network

- technical data on the actual design of the collector loop

The objective of my current study is to outline and assess the feasibility of such an *in situ* test.

1.2 Outline of the study

To assess the feasibility of an *in situ* test for collector arrays I need long sequences of measured data. Such sequences are rare. However, there are year long sequences of reliable hourly data from experimental solar district heating plants in Sweden. Although not ideal, I find it reasonable use these sequences for an assessment of a test. The main reason is their length, which allows for cross-predictions between periods from different times of the year. I chose to use data from the central solar heating plant in Falkenberg.

My tentative test is an application of dynamic fitting (Spirkl, 19xx). Firstly, I fit the dynamic collector array model (MFCA) to a sequence of measured hourly data. I use only one free parameter. Secondly, I predict the long term performance using the fitted MFCA model. My current study comprises the following steps

- Parameterization of the MFCA model with one free parameter (π^*). The data available in the data sequences is not informative enough to simultaneously estimate many parameters. Thus, I avoid 1) the strong correlation between estimated parameter values and 2) unreasonable estimated parameter values.
- Estimations of the single free parameter (π^*) by fitting the parameterized MFCA model to each of 23 monthly sequences of hourly data
- Month to month cross-predictions using fitted MFCA models. I make 23 predictions of the collector output for each of the 23 months.

The outcome of these cross predictions is my criterion on whether this approach is workable.

2. Data from the Falkenberg project

An experimental Central Solar Heating Plant with Diurnal Storage (CSHPDS) is connected to the production unit in the district heating system of the small town, Falkenberg, Sweden. The solar heating plant has been in operation since January 1990. It was monitored during the three years 1990, 1991, and 1992. The yearly average of the solar heat delivered to the district heating network was 1.53 GWh (280 kWh/m^2), which makes up six per cent of the total heat delivered. During a few days in the summer the solar heating plant carries the total load. The monthly solar fraction exhibited its highest value 61 per cent in July 1991. P. Isakson and K. Schroeder (1996) report on the project in the Task 14 Large System Group.

2.1 The Solar Collector Loop

The solar collector loop consists of a 5500 m^2 collector array, a 720 m district heating pipe buried in the ground, a circulation pump, and a flat plate heat exchanger. The working fluid

used is a 50 per cent mixture of water and propylene glycol and the flow rate is equivalent to 0.0046 kg/m^2.s of water. The volumes of working fluid are 3.1 m^3, 4.2 m^3, and 14.1 m^3 in the collectors, the pipes in the array, and the pipes connecting the array and the heat exchanger, respectively. The hydraulic residence time of the entire loop is fifteen minutes.

The collector module (TeknoTerm AB, model HT) comprises one pane of low iron glass, one layer of Teflon film, and the selective SunStrip absorber.

The control of the flow in the collector loop is simple. The circulation in the collector loop starts when the temperature in a separate "reference collector" reaches a certain temperature, pre-set to 40°C. The circulation in the charging loop starts and heat is injected into the storage, when the fluid temperature at the inlet of the heat exchanger exceeds the temperature at the bottom of the tank by a small value, pre-set to 4°C.

2.2 Operation and maintenance

A number of problems have been encountered some of which are relevant to this study. The Teflon film exhibits malfunctions in many collector modules. In roughly two per cent of the collector modules the film has broken. TeknoTerm has repaired these convection barriers on site. In another, maybe ten per cent of the modules, the upper edge of the film is sagging although we cannot see any rip. From time to time the Teflon film adheres to the outer cover in a significant portion of the collectors. However, visually, the Teflon film convection barriers are in a better condition now after few years in operation than when they were new.

At two occasions we have detected low flow rates in a few collector rows. Subsequently, TeknoTerm has balanced the flows in the array. Moreover, grass and shrub grow between the collector rows and cause minor shading.

2.3 Monitoring Programme

The plant was monitored from January 1990 through November 1992. Values from 57 sensors were recorded every second minute and 87 derived quantities were stored every hour. Flow and temperatures are measured separately and the heat flow rates are calculated by the data acquisition computer. Figure 1 shows the sensors and Table 1 lists the recorded quantities used in this study.

The data acquisition system used exhibit a high availability. From the start in January 1990 to the end of November 1992 the system was down for only 30 days. Measured data for 10 days were lost in December 1991 and 8 days in September 1992. Data for very few days were lost in the summers.

The sensors were calibrated before and at least once during the monitoring period. The inaccuracy of the absolute temperatures is estimated to be less than ±0.1°C. The flow rates on both sides of the storage tank are measured with an inaccuracy of ± 0.5%. The inaccuracy of the heat flow rate from the solar collector field is less than ±1%. The inaccuracy of the solar irradiation is momentarily less than ± 3%. The accuracy of the orientation of the pyranometer is estimated to be better than ±1° in both the azimuth and slope. The total irradiance in the plane of the collector is sampled only every second minute. Under conditions with quickly fluctuating irradiance, which is common in the summer, the low sampling rate yields a substantial random

error in the hourly values. The pyranometer is situated half a kilometre off the collector array, which will contribute to the inaccuracy during times with passing clouds.

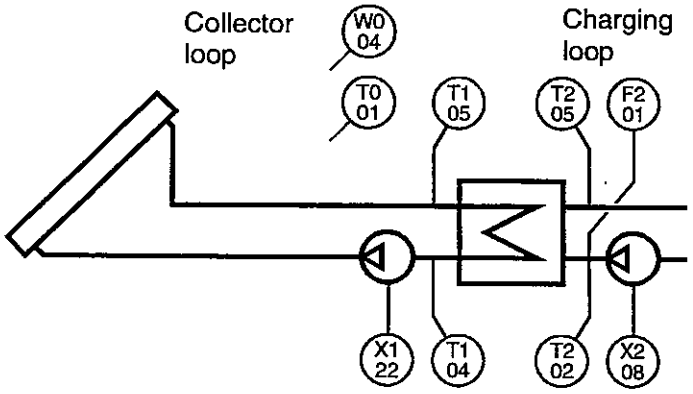

Figure 1 Sensors in the collector loop and the charging loop. All sencors are located at the DH plant 500 meter off the collector array.

The first letter in the sensor designation stands for F=Flow rate, T=Temperature, W=Solar irradiance, and X=Status.

Table 1 The recorded quantities used in this study.

Symbol	Unit	Description
Hour	h	Time of the year
H001	W/m^2	Solar irradiance in the plane of the collector..
H004	W/m^2	Solar irradiance in the plane of the collector while the storage is charged.
T001	°C	Ambient temperature.
K101	h	Operating time of pump in collector loop
K102	h	Operating time, preheating the collector loop
T101	°C	Supply temperature of collector loop while the storage is charged
T102	°C	Return temperature of collector loop while the storage is charged
T103	°C	Supply temperature of collector loop while preheating the collector loop
T104	°C	Return temperature of collector loop while preheating the collector loop
F200	m^3/s	Volume flow rate in the charging loop
K201	h	Operating time of pump in charging loop
Q200	kWh	Solar heat charged into the storage
Q201	kWh	Heat lost from storage to the collector loop

The measurement programme includes the total irradiance in the plane of the collector, but neither the beam nor the diffuse irradiance. I used the Erbs correlation and the HDKR model (Duffie and Beckmann, 1991) to estimate the diffuse irradiance on the basis of the total irradiance in the plane of the collector. Furthermore, the points in time of starts and stops of the collector loop are not recorded. I estimated the points in time of starts and stops on the basis of the running hour of the two circulation pumps (K101, and K201).

The collector rows shade one another. In this study I did only reduce the beam irradiance in proportion to the shaded area.

2.4 Characterisation of the experimental data

The Falkenberg project provided a three year long time sequence of reliable experimental data from a large solar heating plant in regular operation. However, at the time we did not plan for dynamic testing and from that point of view there are drawbacks. The time resolution of the data is one hour, whereas the hydraulic residence time of the loop is fifteen minutes. Neither the diffuse irradiance nor the points in time of starts and stops were measured. Moreover, the variation in the inlet temperature is small.

Figure 2 and Figure 3 provide an overview of the collector data of 1990. The correspondent diagrams of 1991, and 1992 are very similar.

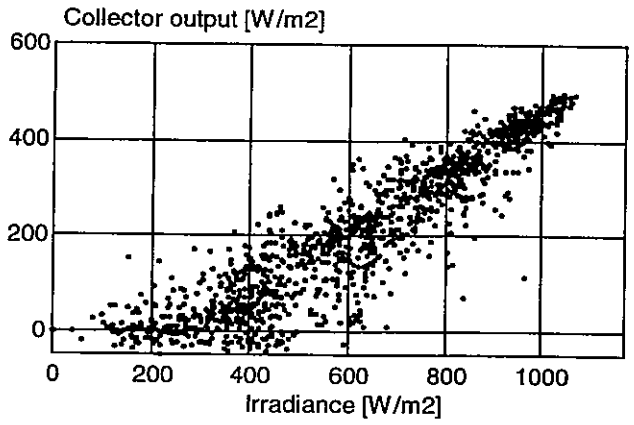

Figure 2 Simplified hourly Input/Output diagram. For almost all points the temperature difference between the collector fluid and ambient is in the range 40 - 60°C.

No corrections are applied and all hourly observations are included.

Period: April - October 1990

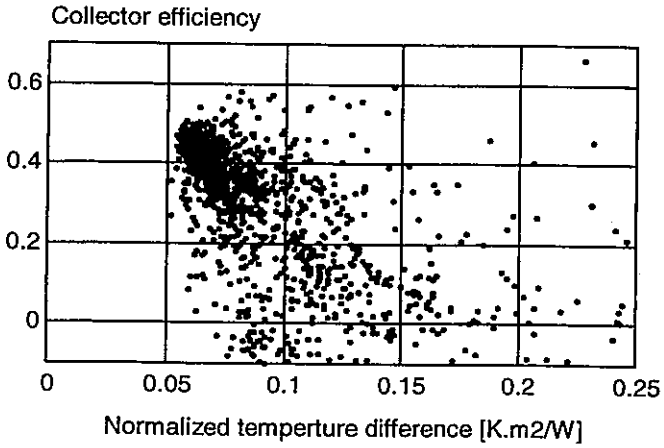

Figure 3 Simplified collector loop efficiency diagram.

No corrections are applied and all hourly observations are included.

Period: April - October 1990

There are significant correlations between various input signals. The total irradiance in the plane of the collector G_t and the temperature difference ΔT are together with the incident angle θ the most important input signals to the MFCA model. Thus, correlation among these is a potential problem to the parameter estimation. Figure 4 illustrates the correlation between G_t

and ΔT. It also shows the fairly narrow range of ΔT, which by large is due to the small variation of the return temperature of the district heating network.

The collector power P_c is positively correlated to the temperature difference ΔT and the inlet temperature T_{fi}, respectively (see Figure 5). The heat loss from the collector to ambient is driven by the temperature difference ΔT and thus the power output decrease with increasing ΔT. However, that is when the other driving signals are unchanged. In this case the situation is obviously more complicated, since there is a positive correlation between the power output and ΔT.

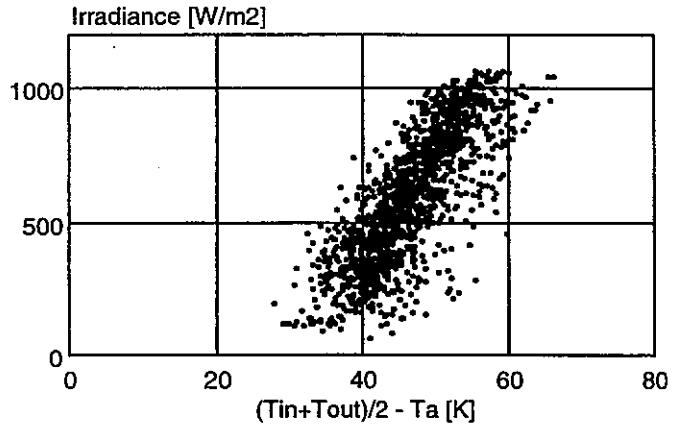

Figure 4 The correlation between the total irradiance in the plane of the collector G_t and the temperature difference between the collector fluid and ambient ΔT significant.

All hourly observations are included.

Period: Mars - October 1991.

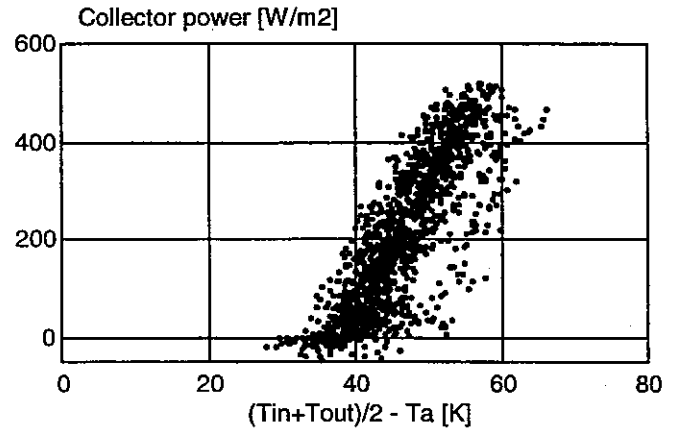

Figure 5 There is a marked correlation between the collector power P_c and the temperature difference between the collector fluid and ambient ΔT.

All hourly observations are included.

Period: Mars - October 1991

3. Collector array model

The MFCA model, which I use in this study, is a component subroutine compatible with the transient simulation program TRNSYS version 13.1 (Klein et.al. 1990). Moreover, it is implemented as an external model to the parameter estimation program DF. It is based on the physically derived partial differential equation

$$\begin{cases} \left(C_{eff} + V_f \rho c_p\right) \cdot \dfrac{\partial T}{\partial t} + \dot{m} \cdot c_p \cdot \dfrac{\partial T}{\partial x} = q(T) \\ q(T) = \eta_0 \cdot G - \left(a_1 + a_2 \cdot \left(T - T_a\right)\right) \cdot \left(T - T_a\right) \end{cases} \quad (1)$$

where $q(T)$ mimics a steady state collector model. The model accounts for

- An effective collector heat capacity C_{eff} lumped into the absorber pipe
- The mass flow rate $\dot{m}$, the fluid volume V_f, and thus the fluid residence time
- Various options to account for the incidence angle modifier.

The software implementation is based on an analytical solutions of this partial differential equation. The MFCA models used here model one rows of flat plate collectors in series with a supply and a return pipe. The pipe submodel is based on the partial differential equation (1), where $\eta_0 = 0$ and $a_2 = 0$.

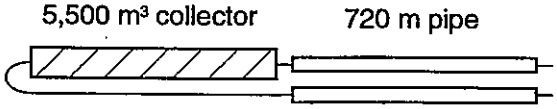

Figure 6 The MFCA model used in this study comprises a supply pipe, a colletor, and a return pipe in series. The heat capacity and the fluid residence time of each of these three components is accounted for in the model.

The MFCA heat loss model relates to the local temperature $T(x,t)$ rather than to the average temperature as in the models used in standard collector tests. This results in differences in the parameter values, which are negligible at high flow rates but significant at low collector flow rates.

The code of MFCA has due to the analytical solution a number of attractive characteristics. It runs efficiently with both long and short simulation time steps. The numerical effects are negligible. For constant boundary conditions it agrees exactly with the corresponding steady state solution.

3.1 Parameterization

Only a few parameters may simultaneously be estimated by fitting the MFCA model to the Falkenberg data. There is too little information in the data, since the district heating return temperature is within a narrow range.

How to find appropriate parameters to fit? Firstly, there are generally prior knowledge on the collector loop based on which one may choose a reasonable set of parameter values. Secondly, the *Analysis of variability and intercorrelation of data* of the DF output shows that for each monthly sequences there were two direction in the parameter space the importance of which dominated over all the others. Furthermore, these two directions were nearly the same for all monthly data sequences. One of the directions was dominated by heat capacity Ceff. The other was a linear combination of most of the other parameters. That is, in all fittings the estimated value of the heat capacity Ceff is almost uncorrelated to the others parameters values. Other important parameters are the zero loss efficiency n0, the heat loss coefficient a1, and the coefficient b0 of the incident angle modifier model. The latter are strongly correlated.

However, I see little reason why the heat capacity Ceff of the Falkenberg collector loop should vary and hence I will assign Ceff a constant value based on the preliminary fittings.

These findings encouraged me to try a one parameter model. Thus, the questions is whether it is possible to limit the number of fitting parameters to one without sacrificing on the accuracy in the predictions of the yearly energy yield? Let *MFCA*(**p**) denote a MFCA model. The set of parameters $\mathbf{p} = (p_1, p_2, .., p_{np})$ may be interpreted as a point in the parameter space $\mathbf{R}^{np}$, and *np* is the number of parameters.

Firstly, I choose to keep the value of the heat capacity Ceff constant since I see little reason why it should vary in the Falkenberg collector loop. Secondly, I assign a set of reasonable values $\mathbf{p}^1$ to the parameters. Thirdly, I introduce one free parameter π^*, which allows me to calibrate the model by fitting it to the measured data. Now, I may write

$$\mathbf{p} = \mathbf{p}^1 + \pi^* \cdot \mathbf{c} = \left(p_1^1 + \pi^* \cdot c_1,\ p_2^1 + \pi^* \cdot c_2, \ldots, p_{np}^1 + \pi^* \cdot c_{np}\right)$$

where **c** is a vector in the parameter space. I want **c** to point in the most important direction in the parameter space, i.e. the direction in which the objective function increase the fastest. Figure 7 illustrates the approach.

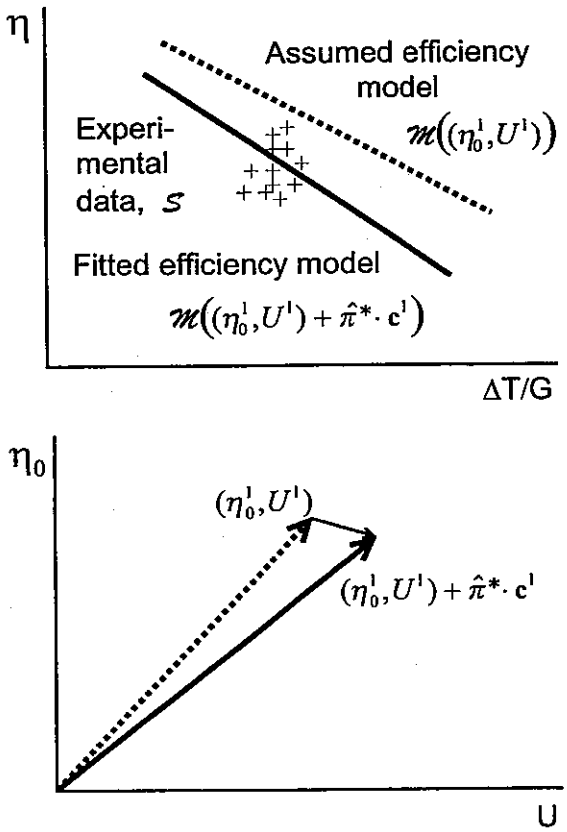

Figure 7 An illustration of the proposed approach based on a linear collector model. The upper diagram shows the collector efficiency diagram, the lower is the parameter space.

We want to fit the model $\mathcal{M}(\eta_0, U)$ $\eta = \eta_0 - U \cdot \Delta T / G_t$ *to a given data sequence* $\mathcal{S}$. *However, since the data* $\mathcal{S}$ *form a cloud, fitting of* $\mathcal{M}(\eta_0, U)$ *to* $\mathcal{S}$ *would give a poor result.*

Procedure:

- *Choose* (η_0^1, U^1) *and* (c_1^1, c_2^1) *based on prior knowledge and preliminary fittings*
- *Estimate* π^* *by fitting*

$$\mathcal{M}((\eta_0^1, U^1) + \pi^* \cdot (c_1^1, c_2^1))$$

to the data sequence $\mathcal{S}$

Result:

$\mathcal{M}((\eta_0^1, U^1) + \hat{\pi}^* \cdot (c_1^1, c_2^1))$ *as shown by the heavy line in the efficiency diagram*

In this study I try three MFCA models MFCA$(\mathbf{p}^i, \pi^* \cdot \mathbf{c})$, $(i = 1, 2, 3)$, which differ only with respect to the set of parameter values $\mathbf{p}^i$, i.e. the point in the parameter space choosen based on prior knowledge on the collector. I choose the vector **c** to take the same value in all three models.

$c_{18} = 0.5$, $c_{19} = -6.2$ W/K.m^2, and $c_i = 0$ when $i \neq 18$, and $i \neq 19$

In the MFCA model $p_{18} = \eta_0$, and $p_{19} = a_1$. Thus fitting MFCA$(\mathbf{p}^i, \pi^* \cdot \mathbf{c})$ is searching the minimum of the objective function along a line in the plane defined by the point $\mathbf{p}^i$ and the axes of n0 and a1. The length of **c** makes the derivative of the collector efficiency η with respect to π^* approximately equal to that with respect to the zero loss efficiency η_0

$$\frac{d\eta}{d\pi^*} \approx \frac{\partial \eta}{\partial \eta_0}$$

Thus, a 0.01 change in π^* causes approximately the same change in the efficiency as does a 0.01 change in η_0.

The first model is based on the results of the preliminary fittings of the MFCA model to the Falkenberg data. I derived the vector **c** from results of estimating the two free parameters n0 and a1. Since $\mathbf{p}^1$ is close to the global minimum I expect MFCA$(\mathbf{p}^1, \pi^* \cdot \mathbf{c})$ to fit to the Falkenberg data equally well as MFCA models with many free parameters.

However, the parameter set $\mathbf{p}^1$ include parameter values not reasonable from a physical point of view. The estimated values of the parameters of η_0 and a_1 are very low and the value of the parameter b0 is very high (0.595, 0.40, and 0.40, respectively). Thus, to assess the approach I need to try it with sets of parameter values that do not strongly depend on the Falkenberg data. Thus, I try to mimic the situation when the first month worth of data arrives. I make two MFCA models mainly based on parameter values not owing to the Falkenberg plant.

The **second model** MFCA$(\mathbf{p}^2 + \pi^* \cdot \mathbf{c})$ I base on estimated values of n0, a1, a2, and b0 found by Perérs (1993) in a dynamic test of an 11 m^2 collector module similar to that at Falkenberg. I deem these estimated values be close to those expected for the Falkenberg collector when it was taken into operation.

I define **a third model** MFCA$(\mathbf{p}^3 + \pi^* \cdot \mathbf{c})$ based mainly on the test results for a TeknoTerm HT collector module. This test does provide parameter values for three parameters, n0, a1, and a2. At the time of installing the collector array it could have been claimed that the set $\mathbf{p}^3$ of parameter values was the best set available.

Table 2. Three one parameter MFCA models.

	Model	Main source of information
$\mathcal{M}_1$	MFCA$(\mathbf{p}^1 + \pi^* \cdot \mathbf{c})$	Experimental data from Falkenberg
$\mathcal{M}_2$	MFCA$(\mathbf{p}^2 + \pi^* \cdot \mathbf{c})$	Prior knowledge on a similar collector
$\mathcal{M}_3$	MFCA$(\mathbf{p}^3 + \pi^* \cdot \mathbf{c})$	Official test result for the actual collector type

4. Fitting MFCA models to Falkenberg data

The fitting process is conceptually simple. I use the non-linear parameter identification programme DF 2.4β (Insitu, 1994) in combination with my programme MFCA_DF, which serves as an external model to DF. DF executes MFCA_DF in an iterative process passing new parameter values to MFCA_DF and comparing its output signal to the corresponding measured output signal. The process converges to the set of parameters that makes the modelled and measured output signals agree the best in a least square sense. Finally, DF makes a formal error analysis based on a linearisation of the model.

Fitting several variants of a model to many sequences of data and evaluating the result is a time-consuming and laborious task. Furthermore, the process is error-prone. Thus, I have developed some small tools, which allow me to run DF in large batch-jobs. The parameters, which I want to change between the batch-jobs, appears as arguments to the batch-file. The batch-files have comments and serves as documentation. Furthermore, I transferred the entire content of the DFS-file and the result of the *Analysis of variability and inter-correlation of data* in the DFR-file to an askSam™ database. Finally, I use small askSam-programs to make reports. In this way the effort is reasonable to run a new batch of fittings and present the result in a table.

4.1 Preliminary parameter estimation

To start, I fitted the MFCA model parameterized with 5, 4, 3, and 2 free parameters to data sequences with the length of one season, and one month, respectively. The free parameters were the effective collector heat capacity Ceff, the zero loss efficiency n0, the heat loss coefficients a1, and a2, and finally the parameter b0 in the incident angle modifier model. Then, I successively excluded the parameters Ceff, a2, and b0 from the fit. All these preliminary fits produced models the outputs of which agree well with the measured output. However, there is a complex pattern in the results, which is difficult to fully comprehend.

The estimated parameter values deviated from the values anticipated based on prior knowledge. The value of the collector heat capacity Ceff was low. The estimated values of n0 and a1 were both low. A small value of the radiation captured may be compensated for by small heat losses. Finally, the value of b0 was twice as large as expected, $b0 \approx 0.4$. Furthermore, the correlations were large between the estimated values of the parameters n0, a1, a2, and b0. The standard deviations of the the estimated values were large especially for the parameter a1. There is a remarkable stability in the results; the over-all pattern repeat itself for all seasons and all months.

The following diagrams illustrate some characteristics. (They are based on fitting different variants of the MFCA-model to Falkenberg data. However, all the fitted models are close to MFCA($\mathbf{p}^1$)). There is a notable difference between clear and cloudy days regarding the agreement between predicted and measured output power. Figure 8 and Figure 9 illustrate this for some consecutive days and a full year, respectively.

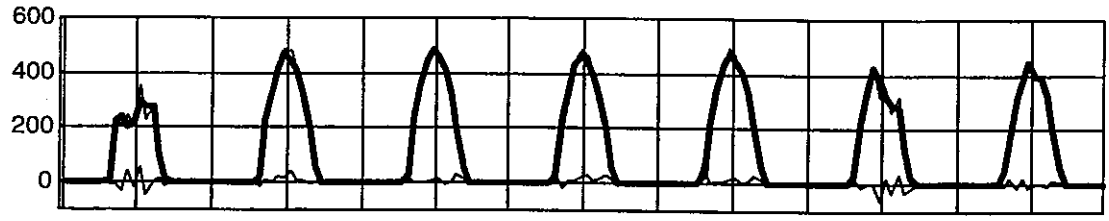

Figure 8 The diagram show the measured (heavy line) and the predicted (fine line) output power of the collector loop as well as the residuals (fine line) [W/m^2]. The diagram covers the periods 92-06-06--12.

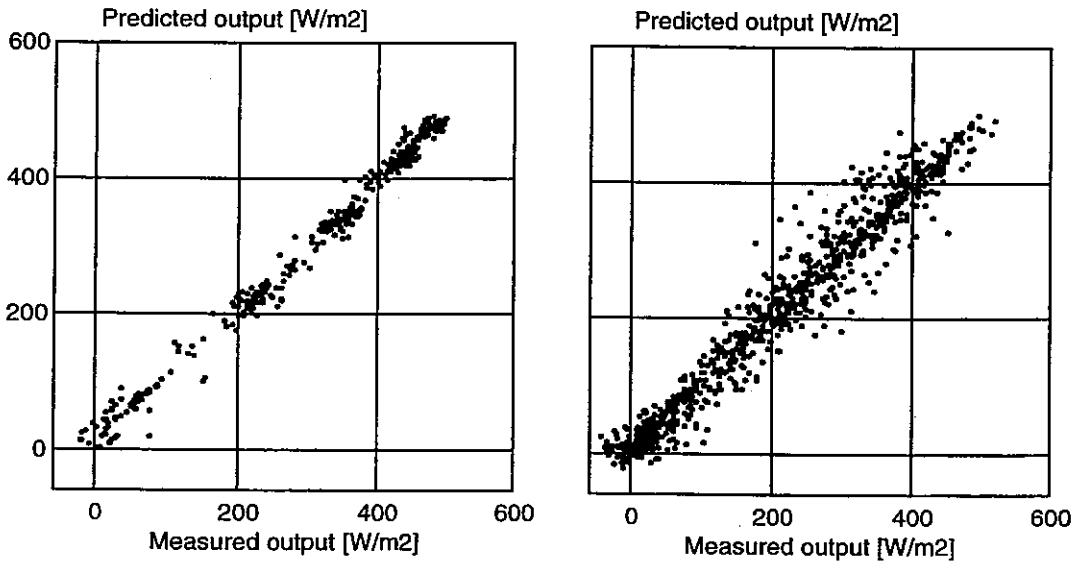

Figure 9 Predicted versus measured output power of the collector loop [W/m^2] during 1992-03--10. The left hand side diagram is based on clear days and the right hand side on the other days. Together the diagram include all hourly observations. I have made the selection of clear days by on-screen inspection of the smoothness of the irradiance curve.

Figure 10 shows results of a sequence of parameter estimations. I fitted the MFCA model with two free parameters (n0, and a1) to each of the 23 data sequences. The estimated values of both n0 and a1 are low, in some cases even very low compared to the values we anticipate; approx. n0=0.74, and a1=2.5. Roughly, the pairs form a line along which given the operation conditions in Falkenberg the yearly yield is constant.

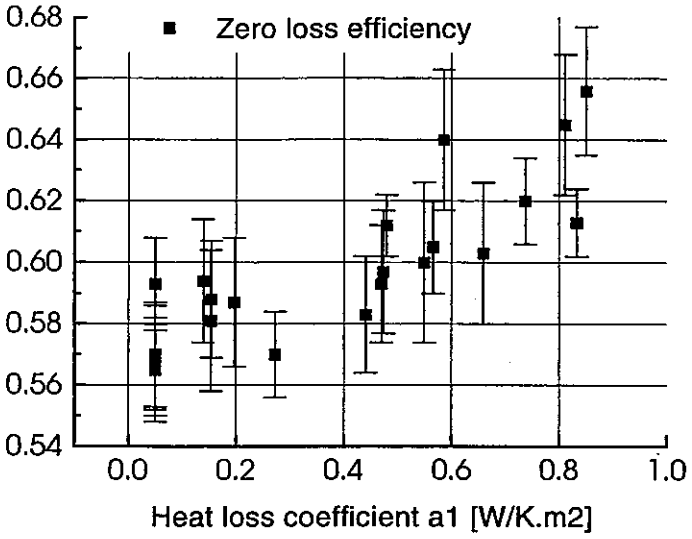

Figure 10 Estimated values of the zero efficiency n0 versus estimated values of the heat loss coefficient a1 [W/m^2.K]. Each point represents one fit and the error bars indicate one standard deviation of the n0-value. The corresponding error bars of a1 are approx. of the same length. (One point is outside the diagram: Oct '90 (0.70 ±0.05, 1.3 ±0.4))

A MFCA model with two free parameters (n0, a1) was fitted to 23 month-long sequences.

The performance of the collector loop may vary for a number of reasons. To search for trends in the residuals I prepared the diagrams of Figure 11, Figure 12, and Figure 13. They include all the residuals of clear days when the incident angle $\theta < 30°$ at the mid of the hour. In this way I selected residuals, which are less affected by random disturbances. Furthermore, this

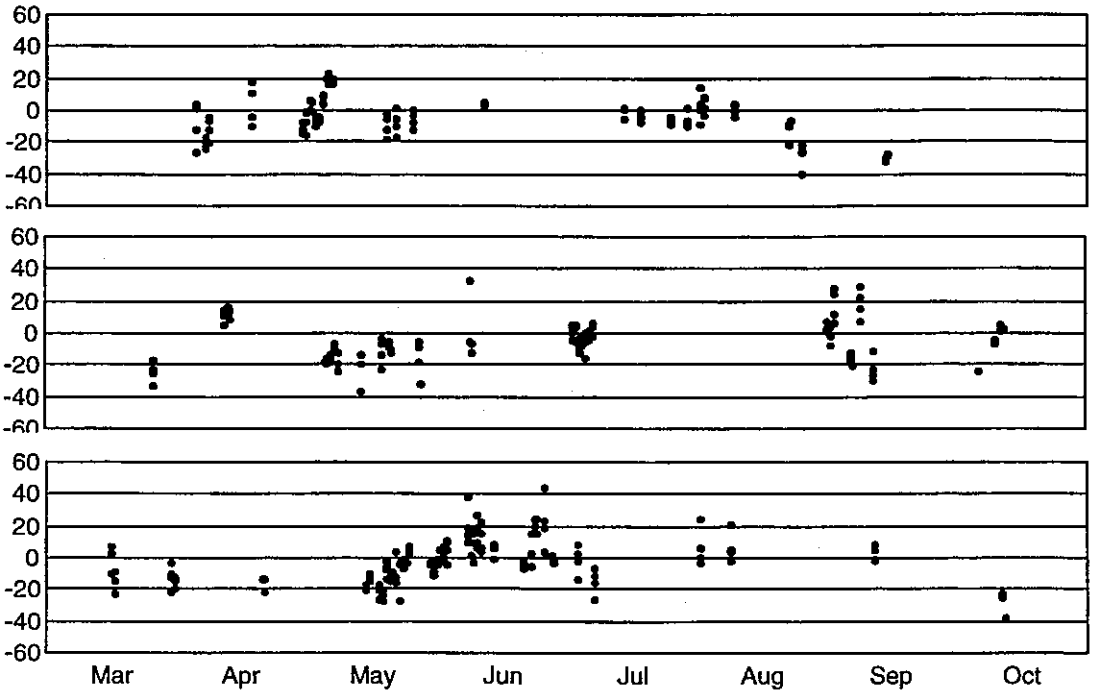

Figure 11 The residuals [W/m^2] around noon of clear days for the seasons '90, '91, and '92. The diagrams comprise residuals for all hours during clear days when the incident angle at the mid of the hour $\theta < 30°$. Consequently, the four observations from of the period 10:00 to 14:00 contribute to the diagram.

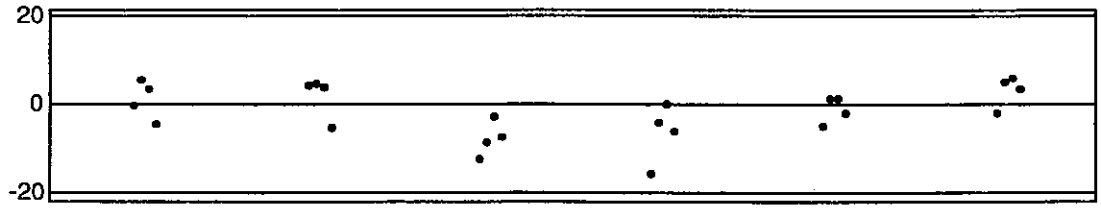

Figure 12 Blow-up of the period 91-07-03--08

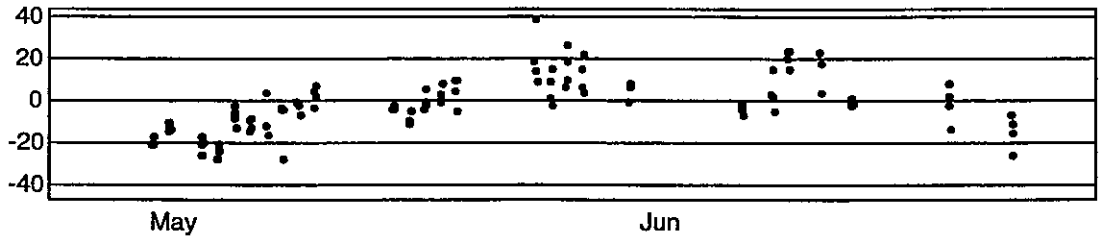

Figure 13 Blow-up of a period starting in the beginning of May and ending in the beginning of July 1992.

limits the influence of the shortcomings of the model to estimate the fraction diffuse radiation.

There appears to be trends on different time scales. The residuals often increase before noon and decrease after constituting a daily pattern. The opposite does not occur. Sometimes they just increase or decrease. The four residuals of the one day often span an interval as large as 20 W/m^2.

The period 91-07-03--08 (see Figure 12) exhibits a continues decrease and increase of the residuals within a week. The period 92-05--07 (Figure 13) demonstrates an increase followed by a decrease in the residuals over a couple of months. The first half of September 1991 exhibits a few days during which the residuals span the interval $\pm$ 30 [W/m^2]. However, there does not seem to exist an annual pattern.

4.2 Fitting MFCA models with one free parameter

Is it possible to use a one parameter model without sacrificing on the accuracy in the predictions of the yearly energy yield? I fitted each of the three one parameter models to each of the 23 monthly sequences of hourly data. The scatter plots in Figure 14 and Figure 15 shows the estimated values of the parameter π^* for the models $\mathcal{M}_1$, and $\mathcal{M}_2$, respectively. The values $\hat{\pi}^*$ estimated by fitting the models $\mathcal{M}_1$, $\mathcal{M}_2$, and $\mathcal{M}_3$ span the intervals (-0.015, 0.026), (-0.064, 0.013), and (-0.062, 0.045), respectively. The width of the interval is twice as large for the models $\mathcal{M}_2$, $\mathcal{M}_3$ compared to that of the model $\mathcal{M}_1$. The standard deviations of the estimated parameters are in the range (0.002, 0.005), (0.03, 0.06), and (0.003, 0.007), respectively. Thus they increase slightly for the series of models.

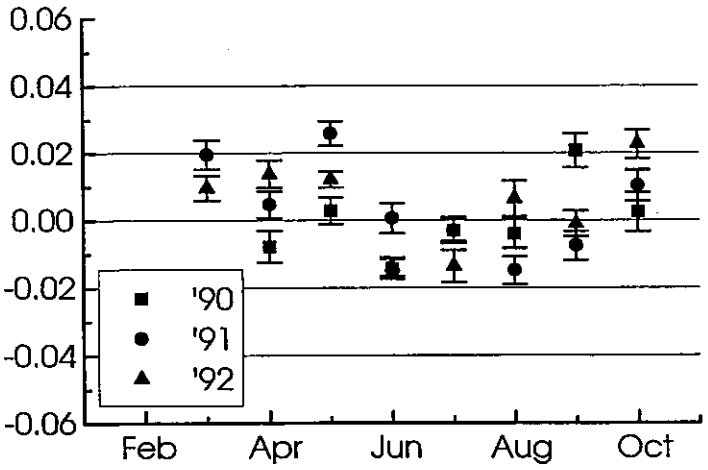

Figure 14 Values of the parameter π^* estimated by fitting $\mathcal{M}_1$ to the monthly data sequences. Each point represents one month. The error bars indicate one standard deviation. An increase of 0.01 in π^* yields an increase of approx. 2% in the predicted output.

There is a seasonal effect. The estimated values $\hat{\pi}^*$ of spring and autumn are larger than those of the rest of the year. The values of June and July tend to be the smallest. This means that the collector loop in Falkenberg in comparison to the MFCA models fitted to yearly data exhibits a peak in its performance in spring and autumn. The results suggest that this effect is linked to the large incident angles, which occur in summertime only. With $\mathcal{M}_1$ where b0=0.40 the effect is less pronounced than with $\mathcal{M}_2$ and $\mathcal{M}_3$ where b0=0.21.

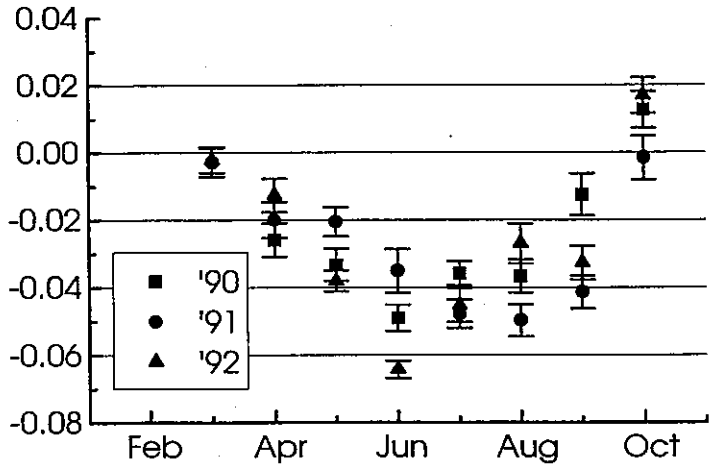

Figure 15 Values of the parameter π^* estimated by fitting $\mathcal{M}_2$ to the monthly data sequences. Each point represents one month. The error bars indicate one standard deviation.

5. Cross prediction

I estimated the parameter π^* for each of the 23 months yielding 23 estimated values $\hat{\pi}^*$. For each one of these values I predicted the energy collected for each of the 23 months, which yielded 23x23 predictions 23 of which are self-predictions. The predictions use the measured values of the inlet temperature and flow rate as driving signals. Figure 16 shows

$$\frac{predicted - measured}{measured}$$

for the month to month predictions and the month to the total of 23 months prediction. The cells of the table are hatched to indicate the goodness of the prediction. Along the diagonal the cells represent self-predictions, which should be good; they are mostly a fraction of a per cent. There is a symmetry around the diagonal, which arises because when the parameter value of month A provides a good prediction of the energy production of month B then the same often holds the other way round.

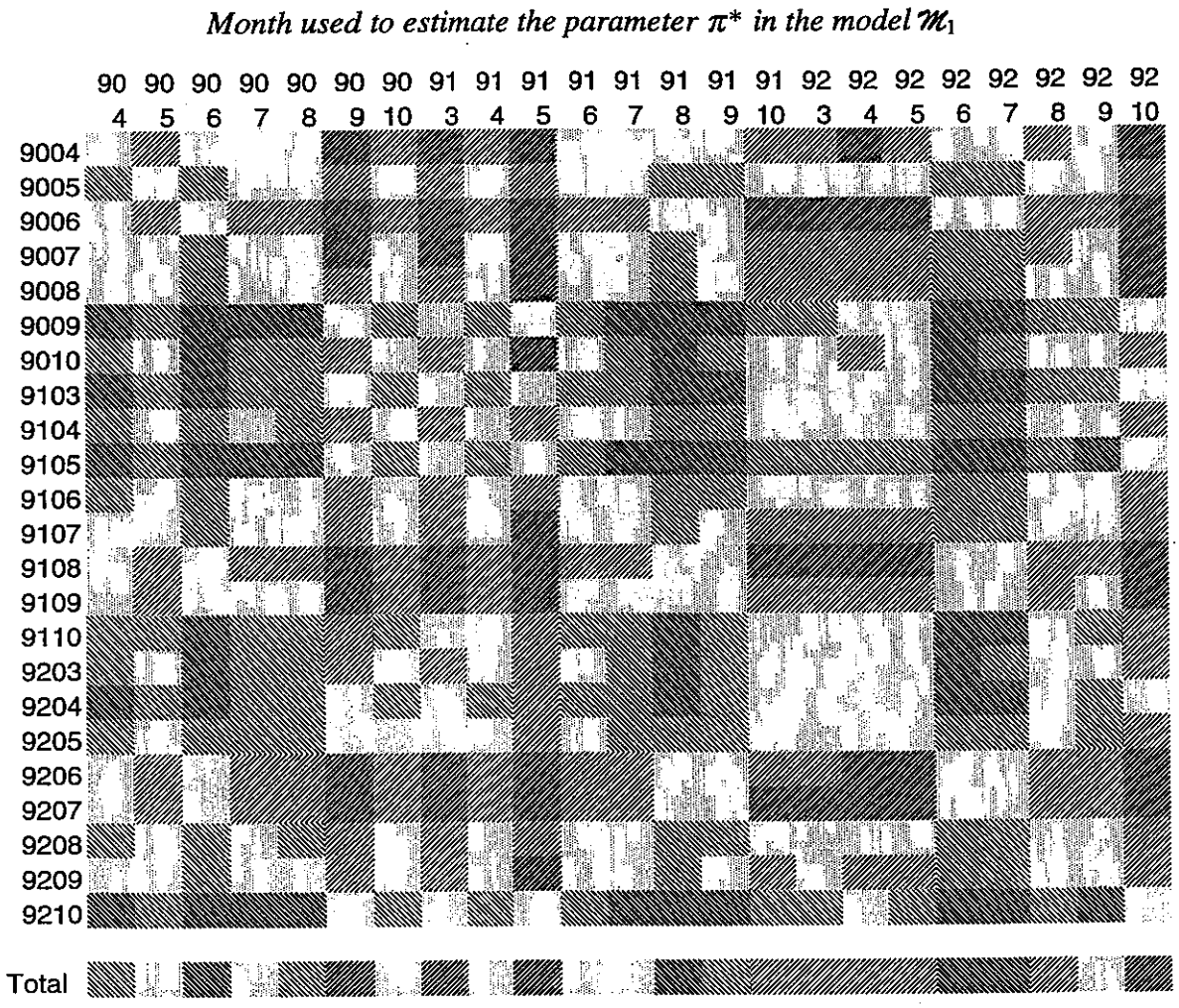

Figure 16 Cross-prediction using model $\mathcal{M}_1$. The diagram shows the relative difference of the collected energy (P-X)/X. (P=predicted, X= experimental.) The months of the columns were used to estimate $\hat{\pi}^*$, and the months of the rows were used in the prediction. The bottom row shows the predictions of the yield of the total period.

The bottom row of the figure shows how well the total heat production of the 23 months is predicted by models fitted to a single month of data. Table 3 summarises the goodness of the predictions. We see that with model $\mathcal{M}_1$ two thirds (i.e. 3+7+5 out of 23) of the predictions are within ±3% of the experimental value and that one third is within ±1%. However, with the models $\mathcal{M}_2$ and $\mathcal{M}_3$ the predictions are less accurate.

The month to month cross-predictions are in most cases within ±5% of the measured value and in many cases within ±2% as shown in the Figure 16. The predictions based on the model $\mathcal{M}_1$ are better than those based on the model $\mathcal{M}_2$ or $\mathcal{M}_3$.

Table 3. The frequency distribution of the goodness of the predictions of the yield during the 23 months; (P-X)/X.

Model	Intervals				
	-∞, -0.03	-0.03, -0.01	-0.01, 0.01	0.01, 0.03	.03, ∞
$\mathcal{M}_1$	4	3	7	5	4
$\mathcal{M}_2$	5	5	4	2	7
$\mathcal{M}_3$	6	5	3	2	7

Figure 17 presents summarise the the results of the month to month cross-prediction in a frequency distribution diagram. We see that all predictions based on the model $\mathcal{M}_1$ are within ±10% of the measured value, whereas almost all predictions based on the model $\mathcal{M}_2$ or $\mathcal{M}_3$ are within ±20%.

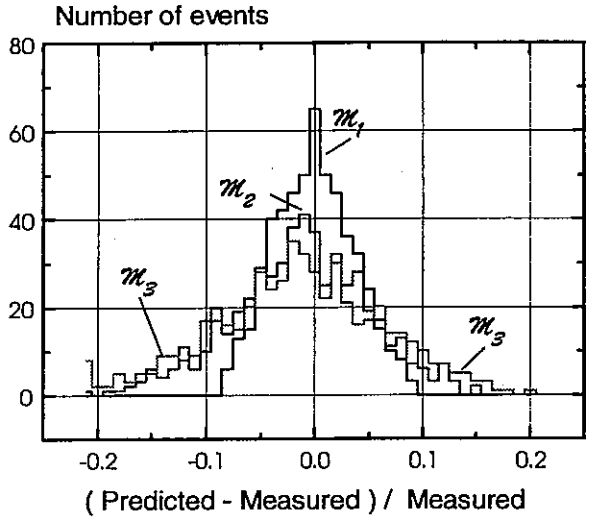

Figure 17. Frequency distribution of the relative difference between predicted and measured monthly collector output for the three MFCA models. Each distribution is based on 23x23 predictions 23 of with are self-predictions. The values of the self-predictions of the models $\mathcal{M}_2$ and $\mathcal{M}_3$ are nearly all negative.

6. Discussion

This feasibility study is not conclusive. The cross-predictions presented above do not meet the requirements, nor do they rule out the proposed test procedure. The main reason to this uncertainty is the 'seasonal effect', which dominates the results. Models fitted to summer data make poor predictions of the collector output during spring and autumn. Likewise models fitted to spring and autumn data do not predict the summer heat production well enough. There are many details that deserve to be discussed, but before doing so I will summarise my thoughts on the proposed test.

The basic approach appears to be sound. The test procedure combines the information of the measured data in the actual range of operation conditions with the general knowledge on collectors built into the model. The resulting set of parameter values is constrained to values, which are plausible from a physical point of view. The number of free parameters is not higher than justified by the richness of the data. The magnitude of the standard deviation of the fitted parameters is reasonable.

The accuracy required is probably within reach at a marginal extra cost. In 15 out of 23 cases the best model so far ($\mathcal{M}_1$) predicts the total collector output of the three seasons within $\pm 3\%$[1] of the measured value (see Table 3)[2]. The two other models accomplish this in 10, and 11 cases out of 23 cases, respectively. A large part of the discrepancies are due to the 'seasonal effect', i.e. a systematic effect. The discrepancies in the cross-predictions due to random errors are acceptable. Thus, the target ($\pm 3\%$ and reasonable parameter values) is not that far off and there are a number of measures that most probably would decrease the systematic errors and improve the accuracy of the cross-predictions. Possibly, data of October through March cannot be used for calibration of the collector model.

6.1 A performance test for commissioning

Modelling errors contribute to the prediction error and the larger the difference in operating conditions the larger the prediction error. Thus, the requirement specification must include the variations in the operating conditions. This is an aspect that needs to be further investigated.

6.2 Comparison with an other study

Perérs' (1993, 1995) made a study, which is comparable to this study in many respects. In both studies dynamic collector models are used to evaluate long sequences of hourly data from flat plate collectors of similar type. Both studies also focus on the assessment of a method, rather than on the thermal performance of the collector. However, Perérs designed his experiment with

---

[1] The measured data to which the model is fitted, and the measured data to which the predictions are compared are all acquired with the same instrumentation. Thus, this figure is not affected by bias errors in the instrumentation.

[2] However, the single parameter values of the model $\mathcal{M}_1$ are not reasonable from a physical point of view.

the purpose to evaluate his method and he performed it at an outdoor test site next to his laboratory. In addition to the quantities in my monitoring program he measured the diffuse and the long wave irradiance in the plane of the collector, and the wind velocity. Furthermore, his sensors were situated close to the collector. The collector inlet temperature spanned the wide range. The collector was operated continuously day and night, thus avoiding starts and stops.

Perérs' results differ substantially from mine. His estimated parameter values are indistinguishable from the values, which would be produced by a standard collector test. The formal standard deviations of his estimated parameter values are an order of magnitude smaller than mine. However, the accuracy of his cross-predictions is only slightly better. The discrepancy in his predictions for one season is larger than 1% in five out of eight cases, compare to my 16 cases out of 23 cases for three seasons. Moreover, Perérs' result indicates systematic under-predictions as do my month to month cross-predictions with the models $\mathcal{M}_2$ and $\mathcal{M}_3$.

6.3 Modelling errors

The MFCA model is an idealisation and there is no true set of parameters, which make the model mimic the real collector perfectly. One may improve the model, but one cannot avoid the modelling errors completely. Firstly, the MFCA-models used here do not account for certain driving forces such as the wind velocity, and the sky temperature. Secondly, certain thermal processes are accounted for by simplified models.

The magnitude of the modelling errors depends on the difference between the operating conditions of the calibration experiment and those of the prediction. With operating conditions close to those of the calibration experiment I expect the modelling errors to be small. On the other hand I expect the modelling errors to be larger with operating conditions, which differs significantly from those of the calibration experiment. If one test a collector in dark one may not expect the resulting efficiency model to perform well in sunshine. I believe the seasonal effect discussed in the previous section to be a result of a modelling error.

6.4 Measures to improved the accuracy

Conceptually, it is possible to achieve a very good accuracy. One only need to bring the model and measurement program to perfection. However, the interesting questions is whether one can reach a good enough accuracy at a reasonable cost.

6.4.1 Verification of the MFCA model

In virtually every fit the collector heat capacity Ceff obtained unreasonable low values. To verify the dynamic part of the MFCA model I fitted it to some data sequences generated by the FFC model provided with a pipe model. This numerical experiment parallels the experiment I did fitting the MFC model to data generated with the FFC model (section 3.2 in Isakson, 1995). The result did not indicate any problems with the MFCA software model.

6.4.2 Refinements of the measurement programme

Perérs´ (1993) and my own experiences indicate that the accuracy in the cross predictions may be improved by higher recording rate. The points in time of starts and stops would be better resolved. Furthermore, it would provide a better accuracy to the calculation of the fraction diffuse radiation.

Measuring the diffuse irradiance in the plane of the collector would most likely improve the accuracy of the cross predictions substantially. However, the cost for the sensor and its maintenance cannot be neglected.

6.4.3 Refinements of the experiment

The variability in the data sequences from Falkenberg is limited as a consequence of the small fluctuation in the return temperature of the district heating network. There are some possibilities to increase the variability of the inlet temperature of the collector loop. Firstly, one may circulate the working fluid during periods with low insolation and control the temperature level by manipulating the flow rate in the charging loop. Temperature as low as ambient are possible. Secondly, high temperatures are possible to achieve by increasing the temperature of the storage. However, unless the model is good enough these observations acquired during irregular operation will not improve the accuracy of the cross predictions.

6.4.4 Refined models for the fraction diffuse irradiance and the shading

Refined models to calculate the radiation that actually hits the collectors are likely to reduce the 'seasonal effect' (see Figure 14, and Figure 15). This effect is the main source to the inaccuracy of the cross-predictions. However, 'seasonal effect' is just a symptom of a complex of related effects, which I so far do not fully understand. Probably, it includes shortcomings in the model I use to estimate the fraction diffuse radiation, the incident angle modifier, the internal shading, and more. These items do all in one way or another depend on the solar position, the range of which differs between the seasons.

Succeeding the results presented in this report I have made some efforts to resolve the problem of the 'seasonal effect'. Firstly, I have redone part of the parameter estimations using the shading model of the Collector Array Shading component of TRNSYS (Klein et.al. 1990). This model accounts for both the shading of the direct and the diffuse radiation. However, it did not really improve the situation. Secondly, I have looked into the model I used for the fraction of diffuse irradiance in the plan of the collector. It obviously produces a fraction diffuse that is too high, especially so for clear days. Firstly, the fraction diffuse in my data is higher than that of Perérs' (1993, 1995), which is based on measured diffuse radiation. Secondly, I applied my model to data from the Nykvarn project (Hansson and Isakson, 1989), which provided measured diffuse radiation data. I inspected the residuals for a complete season. That supported my conclusion: the model I use over-estimating the fraction diffuse. Furthermore, during the last decade appropriate radiation databases have been compiled. Thus, I think it would be possible to develop a correlation model for the fraction diffuse that is accurate enough for the proposed test. Possibly, that model will take advantage of the solar zenith angle, and the time of the year, the type of day (clear/cloudy), but not involve the radiation on the horizontal plane.

6.5 Three seasons of data reveal systematic effects

Systematic features become more evident in long sequences of data. The data sequence from Falkenberg comprises three successive seasons. This unusually long sequence of data from regular operation highlights the systematic features of the result. Patterns repeat themselves, especially the 'seasonal effect'. The fitted parameter values are not reasonable from a physical point of view, but they are consistent. These values and their correlation matrix vary little between different months and even less between the same month of different years. Thanks to the length of the data sequence the systematic features are obvious. However, would I have based the study on a few months of data I might have taken the variations to be random the agreements to be coincidental.

7. Conclusions

This work aim at an *in situ* performance test for large collector arrays. The test should be accurate enough for commissioning, and at the same time the cost to apply it must be low enough not prohibit its use.

I have proposed a procedure and made a feasibility study. The result however is not conclusive and further assessment is required. However, I deem that an *in situ* test based on one month data acquired during regular operation is possible despite the lack of richness in the data.

7.1 Future perspectives

I see a number of possibilities to improve the proposed *in situ* test. Firstly, I need more accurate data on the fraction diffuse radiation, either by a new regression model or by measuring. Secondly, I need to calculate in detail the shading effects. Thirdly, I need to increase the time resolution of the data. Lastly, it is possible to refine the model with regard to the wind, and the sky temperature. Below, I present a tentative list of tasks, which need to addressed to complete the proposed test.

- Develop a dedicated model to calculate the fraction diffuse irradiance in the plane of the collector based on the total irradiance in the that plane.
- Validate the shading model and if needed refine it.
- Redo the fitting and the cross-predictions for other long sequences of data. Such data are available from projects similar to the CSHPDS at Falkenberg. e.g. the projects at Nykvarn, and Säter.
- Try the test on data from a new project, the measuring program of which is designed for the purpose.
- Analyse the cost of applying the proposed test in real situations. Calculate the marginal cost of additional sensors, and the cost of using special test sequences, etceteras.

Furthermore, it would be worth the effort to apply the same approach to the heat storage at Falkenberg. Then finally, it would be possible to make a system model based on the fitted component models.

References

Duffie, J.A. and Beckman, W.A., 1991. *Solar Engineering of Thermal Processes*. John Wiley & Sons, New York.

Hansson, G.,. Isakson, P., Solvärme i fjärrvärmnät för Nykvarn, (Solar Heating for District Heating in Nykvarn.) Swedish Council for Building Reserach, Stockholm, Report R26:1989. (In Swedish)

Klein, S. A. et.al., 1990, TRNSYS Users manual, Version 13, EES Report 38, University of Wisconsin, Engineering Experiment Station.

InSitu, 1994, *Dynamic System Testing Program Manual.* InSitu Scientific Software, Klein & Partners, Baadestr. 80, D-80469 München, Germany

Isakson, P., *Solar Collector Model for Testing and Simulation*, Bulletin 36, Building Services Engineering, Royal Institute of Technology, Stockholm, Sweden, ISSN 0284-141X.

Perérs, B., 1993, *Dynamic Method for Solar Collector Array Testing and Evaluation with Standard Database and Simulations Programs*, Solar Energy, **50**, 517-526, (1993)

Perérs, B., 1995, Private communication.

IN SITU DYNAMIC SYSTEM TEST APPLIED TO A LARGE SOLAR DOMESTIC HOT WATER SYSTEM

D. Cabrera and B. Lachal
University of Geneva, Switzerland

This paper presents the almost integral text of the Final Report from the University of Geneva on their activities in the DCST Subtask.

CONTENT

Annexes 1 - 3 have not been included. For these Annexes is referred to the University of Geneva Final Report:

In-situ dynamic system test applied to a large solar domestic hot water system. IEA Task 14 Advanced Solar Energy Systems Final Report. D. Cabrera and B. Lachal. CUEPE University of Geneva, 1231 Conches, December 1994.

A. DESCRIPTION OF THE SYSTEM

This chapter gives a brief overview of the system and the climatic conditions of Geneva.

A.1 DESCRIPTION OF THE DOMESTIC HOT WATER SYSTEM

The solar domestic hot water system is principally composed of:
- 200 m^2 of flat plate collectors (oriented 23° east and tilted 30° from the horizontal plane).
- An external heat exchanger with a nominal power of 10 kW/K.
- Four parallel solar storages (1 m^3 each).
- A regulation to control the pumps (temperature difference between collectors and bottom of the solar storage).

The above components are intended to preheat the domestic water. In addition (to heat the domestic water at the desired temperature), there are:
- Four auxiliary storages heated by an old district system.
- A mixing valve to limit the domestic hot water at 55°C.

A schema for the installation is shown in Figure A.1.

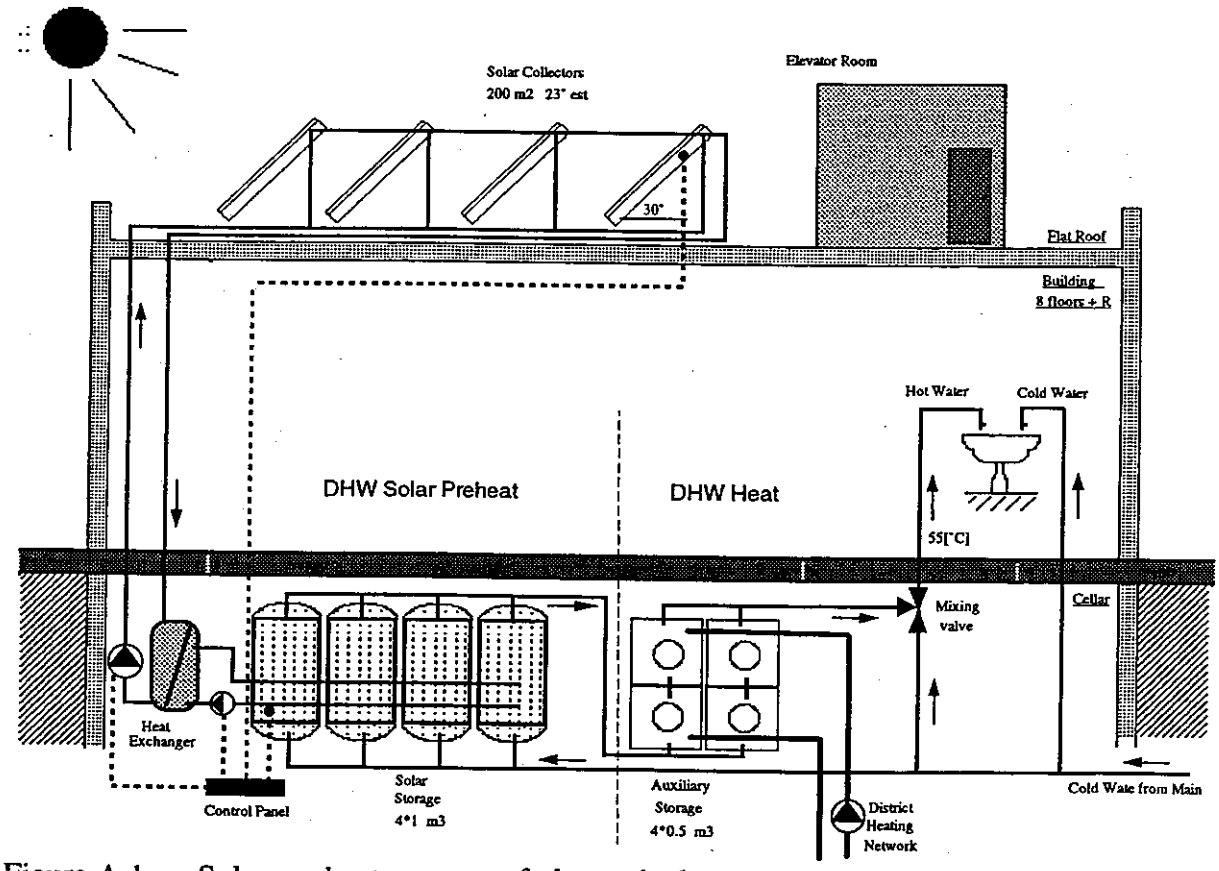

Figure A.1 : Solar preheat system of domestic hot water in a appartment house in the suburb of Geneva. This system is principally composed of 200 m² of collectors (azimuth 23° East, tilted 30°), an external heat exchanger, 4 solar storages (1 m3 each), 4 auxiliary storages, a regulation, and a mixing valve. The elevator rooms represent the obstacles that can shadow the collectors.

A.2 DESCRIPTION OF LOCATION AND SITE

The solar collectors have been installed on the flat roof of an appartment house. This building (126 flats) is in the suburb of Geneva, more precisely in the commune of Onex (8-14 Comte Geraud Street). The geographic location is given by:

Latitude:	46° 12' north.
Longitude:	6° 9' east (from Greenwich meridian).
Altitude:	430 m above sea level.
Orientation:	-23° from south to east.

The figure A.2 shows the trajectory of the sun in Geneva for some dates of the year (the reference time here is the local winter time, for the summer time, one hour must be added to the given time).

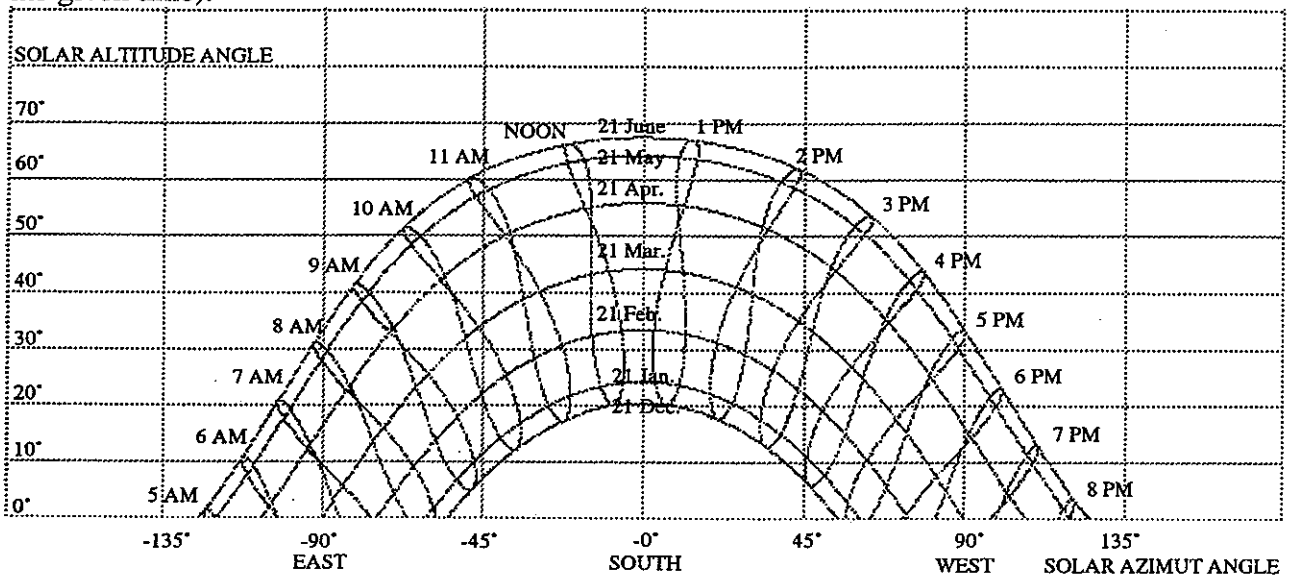

Figure A.2 : Solar position plot for Geneva (46° 12' north). The figure shows the trajectory of the sun for different dates of the year. The solar azimuth angle is represented in the horizontal axis and the solar altitude angle in the vertical axis.

A.3 DESCRIPTION OF CLIMATE

In Geneva, the climate is maritime with snow in winter, and fog during cold seasons. Rain falls can happen all year round. Outdoor temperature can vary between -15[°C] up to 36[°C], but monthly average values range usually from -2[°C] up to 22[°C]. The yearly average solar radiation (horizontal) in Geneva is a little higher than 12 [MJ/m^2.day], with relatively important variations between winter and summer. For example, we can expect a solar radiation of 6 [MJ/m^2.day] for a clear winter day, and 30 [MJ/m^2.day] for a clear summer day.

A.4 SOLAR PRE-HEAT SUBSYSTEMS

A.4.1 THE COLLECTORS

The collectors are mounted on the flat roof of the building and are oriented parallel to the edge of the roof (see figure A.3). The collector field takes up nearly all the useful surface of

the roof. The elevator rooms, very near to the collectors, partially shadow the latter in the morning and in the evening, specially during winter months. The collector field consists of 100 collector modules, each one having an area of 2 m^2. They are oriented 23° from south to east (same orientation as the building) and tilted 30° with respect to the horizontal plane. Due to this orientation, the captation of the solar radiation is a little bit penalised during summer from 6 PM (winter hour, i.e. 7 PM summer hour) as can be seen in figure A.4. In this figure, the incidence angle (between the sun and the normal to the collector plan) against the winter hour is shown. The collector field is composed of one solar loop, connected trough a heat exchanger to the solar storages.

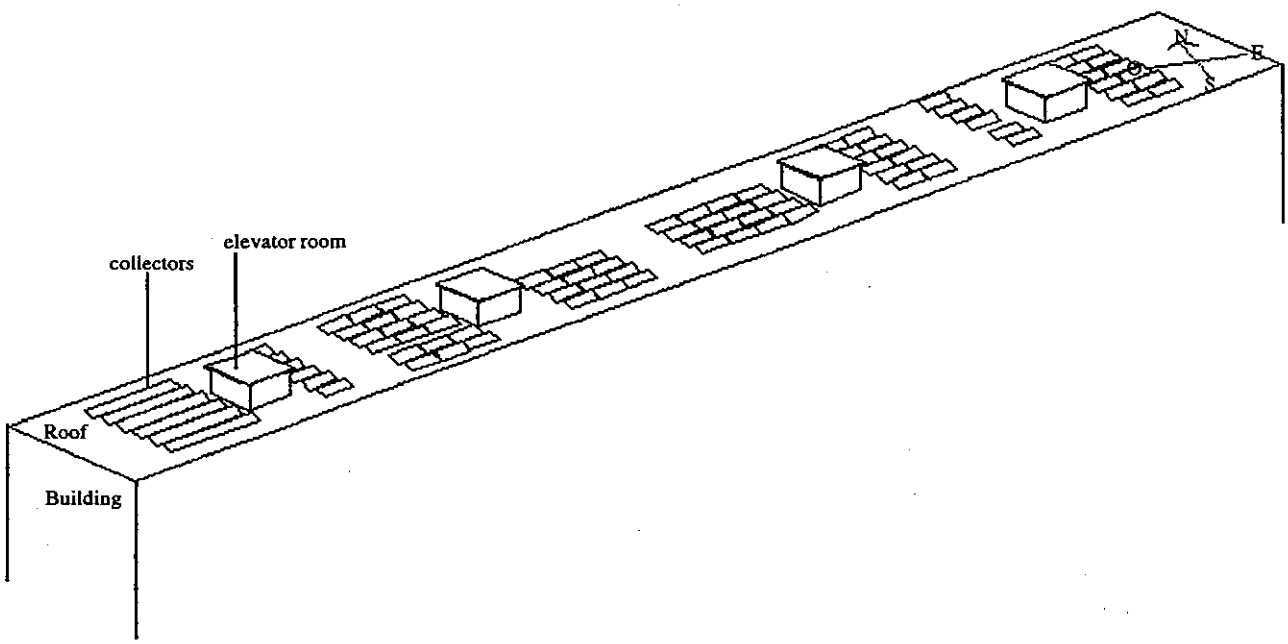

Figure A.3 : The field consists of 100 collector modules. They are oriented 23° from south to east and tilted 30° with respect to the horizontal plane. The pipes connecting the collectors are not represented here.

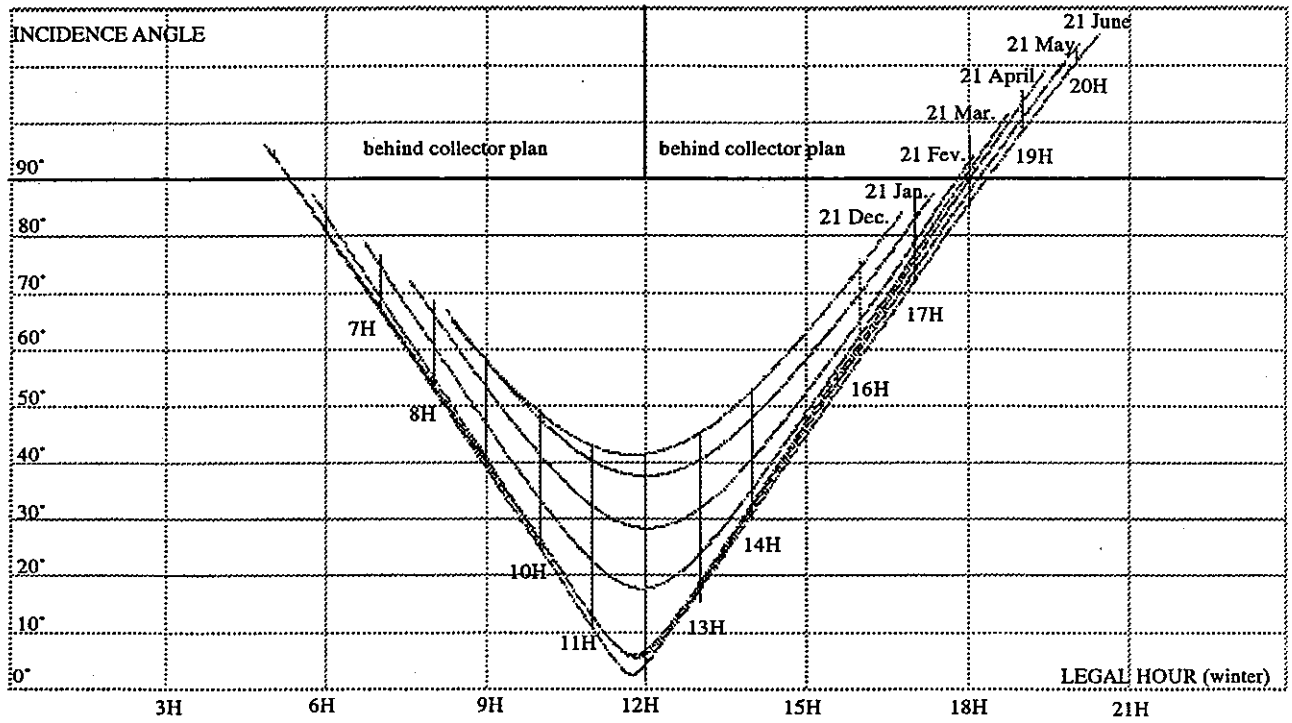

Figure A.4 : This figure shows the incidence angle of the sun (with respect to the normal to the collector plane) for the same dates of the year in figure A.2 . The horizontal axis represents the legal winter hour.

The collectors are connected in serial and parallel groups. A small flow meter "Taco" is placed in the entry of every serial collector group. A screw in these flow meters sets the flow of the fluid in the serial groups so that the same amount of heat is collected. The flow is near 50 [lit./m^2.h]. In addition, a check valve is installed in the loop to prevent reverse circulation. Also an expansion tank to accommodate fluid volume changes (Stucklin PNU 600 0.5 bars), and a safety valve (Stucklin SV M 3 bars) are installed on the roof.

The collectors are fabricated by Agena (Moudon-Switzerland). The collectors have single glass cover. They have an absorber fabricated by Energie Solaire S.A. (Sierre-Switzerland). This absorber is in stainless steel with selective black chromium coating applied by electroplating. Figure A.5 shows a cross section of these collectors.
The collector dimensions are:
- Gross Area : 2.43 [m] x 0.93 [m] = 2.26 [m^2].
- Absorber Area : 2.36 [m] x 0.85 [m] = 2.0 [m^2].

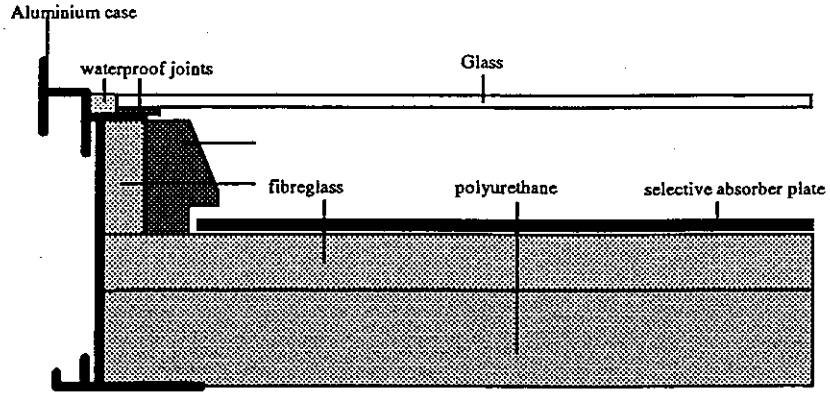

Figure A.5 : An "Agena" collector.

The heat transmission fluid inside the collector loop is composed of a mixture of water and antifreeze (monopropylen glycol, mixed at 40%). The circulation of the fluid is forced by a pump (Grundfos UPC 40-120).
The total fluid volume has been estimated to be approximately 1600 litres from the dimension of the pipes, where: 500 litres are in the collectors, 500 litres in the pipes joining the collectors (e.g. on the roof), and 600 litres in the two vertical pipes leading from the roof to the cellar. The time taken by an element of fluid to make the loop is 10 minutes.

A.4.2 THE CONTROL SYSTEM

The control system is based on the measurement of two temperatures (see figure A.6), the first, in the bottom of one of the storage units and the other on the absorber plate of the last collector of the loop . A differential thermostat turns the pumps on when the temperature of the collectors is 10 °C higher than the temperature of the water in the bottom of the tank. The pump in the collector loop is turned on, and the pump of the secondary loop 10 minutes later. When the difference of these two temperatures is zero, the two pumps are stopped.

The control system performs some measurements, but they are completely independent of the data acquisition system.

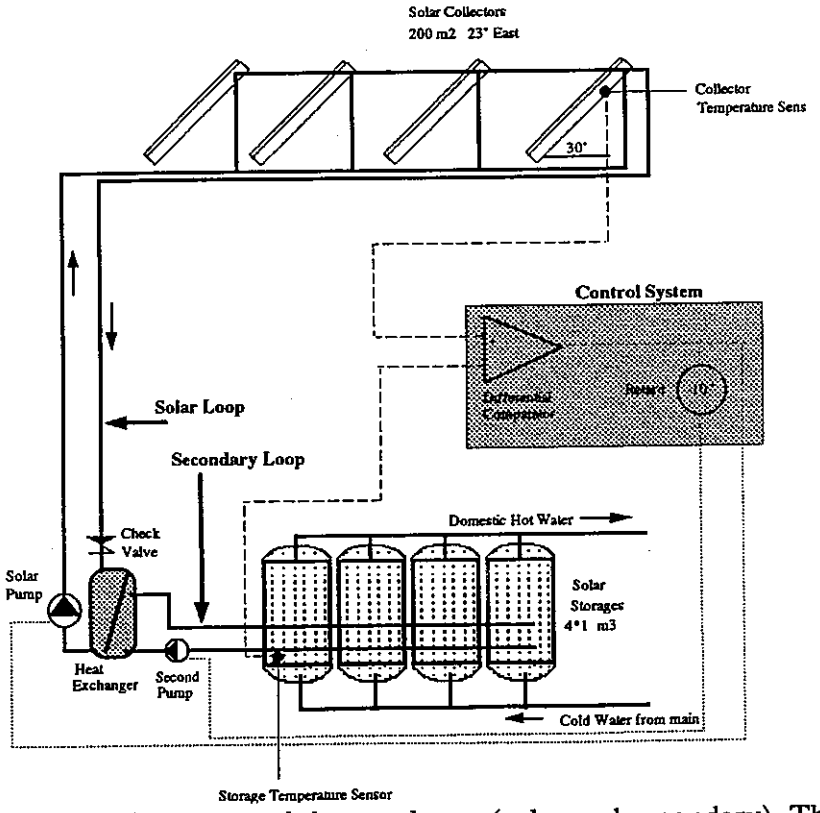

Figure A.6 : The control system and the two loops (solar and secondary). The two loops are separated by an external heat exchanger.

A.4.3 THE HEAT EXCHANGER

An external heat exchanger (Agena 650 N2 -34) of 10 [kW/K] is used to transfer the heat from the solar loop to the secondary loop. This is equivalent to 50 [W/K] per square meter. We notice that this heat exchanger is somewhat undersized given the characteristics of the collectors.

A.4.4 THE SOLAR STORAGES

Four solar storage tanks of one cubic meter each (Capito, Ausfürung D, 1000 l), are used to store the heat provided by the solar field. These four solar storages are placed in parallel to each other. There is no immersed heat exchanger in these storages. The secondary loop is connected to the storages and the hot water collected from the heat exchanger, enters directly (see Figure A.7). The solar storages are located in two contiguous rooms in the cellar of the building. The fluid in the secondary loop is forced by a pump (Grundfus 40-50 FB).

The storages tanks are in stainless steel, and the thermal insulation is composed of foam of closed cells, and 8 cm thick.

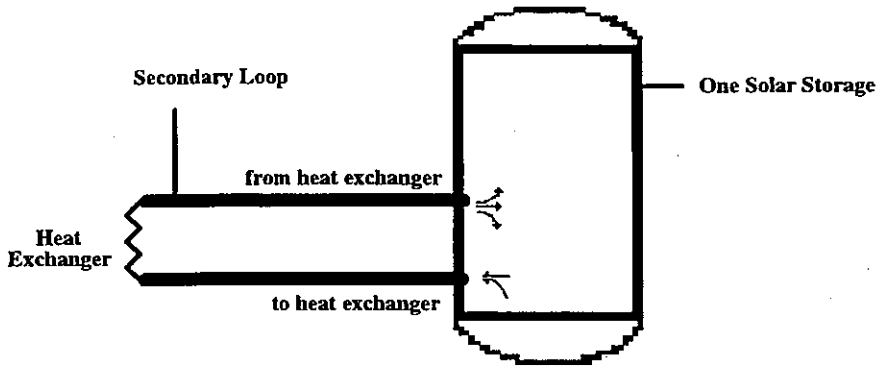

Figure A.7 : The solar storages. The secondary loop is connected to the storages and the hot water collected from the heat exchanger, enters directly. There are four solar storages placed parallel to each other, in this figure only one is represented.

A.5 THE AUXILIARY SUB-SYSTEM

The auxiliary heating sub-system is made of two storages of two cubic meters (Viessmann, Horicell_HG). This sub-system follows the solar tanks. The storages are heated by an old District Heating Network, which was the primary source of heating before the installation of the solar system. The auxiliary storages are placed together with two solar storages in a room located in the cellar of the building.

A.6 DESCRIPTION OF THE LOAD

The load was estimated for a consumption of 50 [lit/day] per person, for a total number of users of 400 (126 flats). The average for a year is correct, but large differences have been found between winter and summer.

A.7 GENERAL RESULTS OF THE SYSTEM

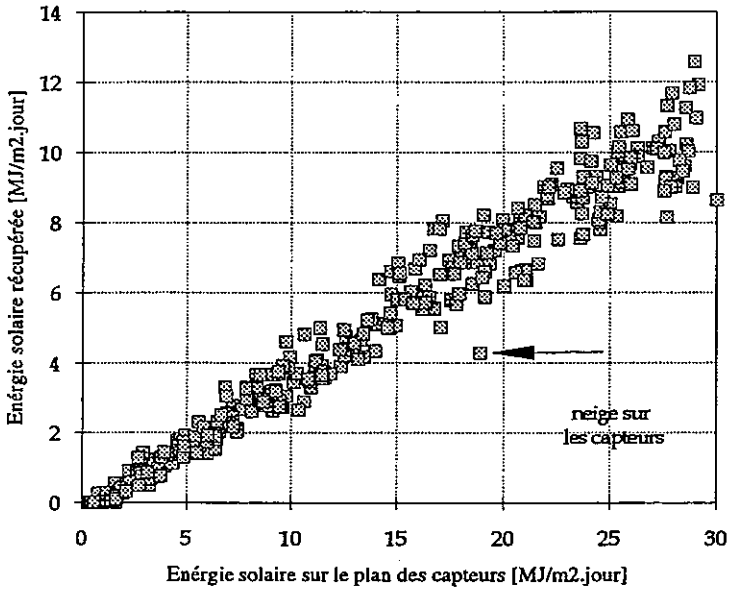

Figure A.8 : Daily Input-Output diagram for the Large Solar Domestic Hot Water System at Geneva. Data from September 1 1992 to 31 August 1993.

The Input-Output diagram is presented in figure A.8 and shows the well known linear relation. The energetic diagram is seen in figure A.9. The main features are [ref A1]:
- The mean efficiency of the field of collectors is 36%, equivalent to 96 [MWh/year]of solar production.
- The yearly solar storage tank heat loss energy is negative because of the overheated room temperature.
- The auxiliary storage tank heat losses are very high. This is due to problems of the old district heating (pipes always at high temperature).
- The balance-error between the two energy independent measurements are surprisingly very low and indicates a good quality of measurements.

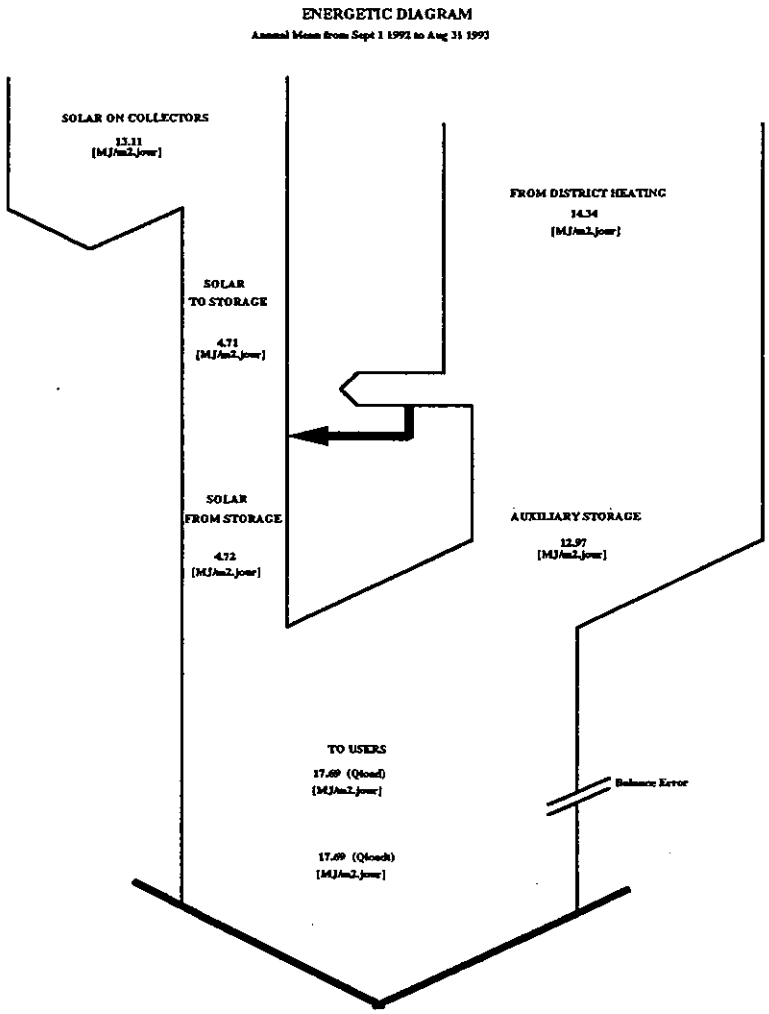

Figure A.9 : Energetic Diagram for the Large Solar Domestic Hot Water System at Geneva. Data from September 1 1992 to 31 August 1993.

REFERENCE

[A.1] C. Cabrera, B. Lachal, W. Weber « prechauffage solaire de l'eau chaude sanitaire d'un immeuble des années 60 », rapport CUEPE 1993.

B. DATA ACQUISITION SYSTEM

This chapter gives a brief overview of the data acquisition system and of the data quality tests.

B.1 DESCRIPTION OF THE SENSORS

Fig B.1 and table B.1 show the measurement system.

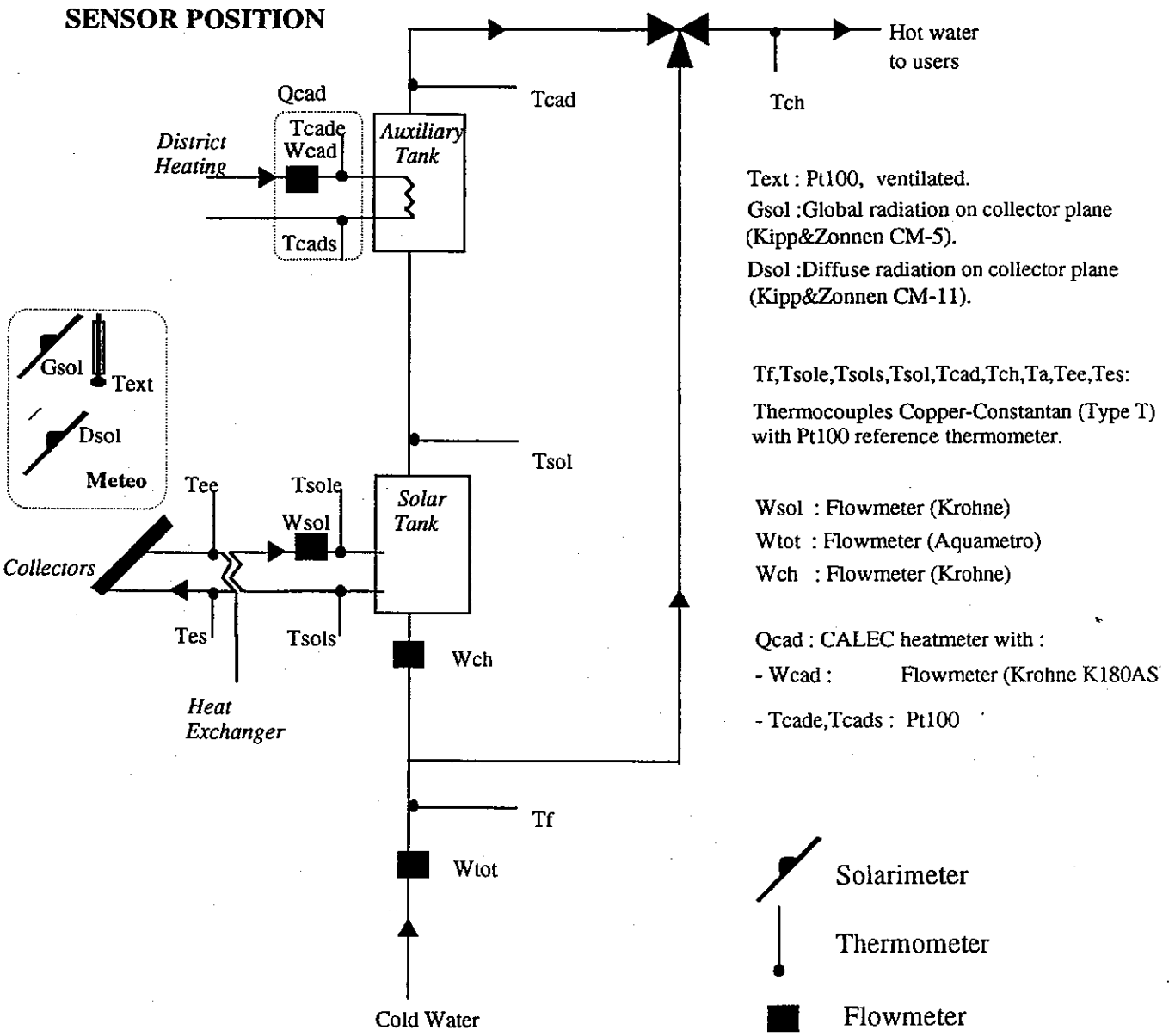

Figure B.1 : Sensor locations.

SONDES	DESIGNATION	PRECISION	TYPE	DESCRIPTION
Radiation	Gp	2%	pyranomètre Kipp&Zonnen CM-5	Global collector plan
Radiation	Dp	5%	pyranomètre Kipp&Zonnen CM-11	Diffus collector plan
Temperature	Text	0.03[°C]	résistance Pt100 (ventilated)	External Temperature
Temperature	Tref	0.03[°C]	Pt100 resistor	cold reference
Temperature	Tf	0.05[°C]	thermocouple type T with Tref(Pt100)	cold water
Temperature	TTsole	0.05[°C]	thermocouple type T with Tref(Pt100)	Input Heat Exchanger (sec. loop)
Temperature	Tch	0.05[°C]	thermocouple type T with Tref(Pt100)	Hot water to users
Temperature	Tsols	0.05[°C]	thermocouple type T with Tref(Pt100)	Output Heat Exchanger (sec. loop)
Temperature	Tcad	0.05[°C]	thermocouple type T with Tref(Pt100)	Output Auxiliary tanks
Temperature	Tsol	0.05[°C]	thermocouple type T with Tref(Pt100)	Output Solar tanks
Temperature	Ta	0.05[°C]	thermocouple type T with Tref(Pt100)	ambiente(storage room)
Temperature	Tee	1 [°C]	thermocouple type T with Tref(Pt100)	Input Heat Exchanger (prim. loop)
Temperature	Tes	1 [°C]	thermocouple type T with Tref(Pt100)	Output Heat Exchanger (prim. loop)
Flow	Wtot	3%	mechanical flowmeter Aquametro	Total hot water to users
Flow	Wsol	1%	electromagnetic flowmeter Krohne K180AS	Solar loop, after Heat-exchanger
Flow	Wch	1 à 3 %	electromagnetic flowmeter Krohne K180AS	Hot water through storage tanks
Heat	Qcad	3%	Heatmeter Aquametro	
Heat	Qsolin		computed from Tsole,Tsols and Wsol	
Heat	Qsoltot		computed from Tf,Tch and Wtot	
Heat	Qsol		computed from Tf, Tcad and Wch	

Tableau B.1 : Sensor description

A Campbell 21X Data Logger is used. All the sensors are read once every ten seconds, averaged as six minute values (and 1 minute values during 4 two-week periods)

Temperatures are measured with Copper-Constantan thermocouples. Great care is taken to obtain an isothermal cold reference temperature (special box) and to avoid electrical noise (see figure B.2). Individual small corrections are applied (0.1 to 0.3°C at 80°C).

The Krohne Electromagnetic flowmeters 180 are used. The mechanical counter for the water supply is also read and allows a check of the energy measurements (indicated by « balance error » in the energetic diagram, see figure A.9).

Three meteorological variables are measured : the global and diffuse solar radiation on collector plane (with respectively a CM5 and a CM11 Kipp&Zonnen pyranometer) and the ventilated external temperature on the roof (calibrated Pt100).

The sensors and the Data Acquisition system were installed in May 1992. Complete measurements have been available since July 3 of the same year untill august 31 1993.

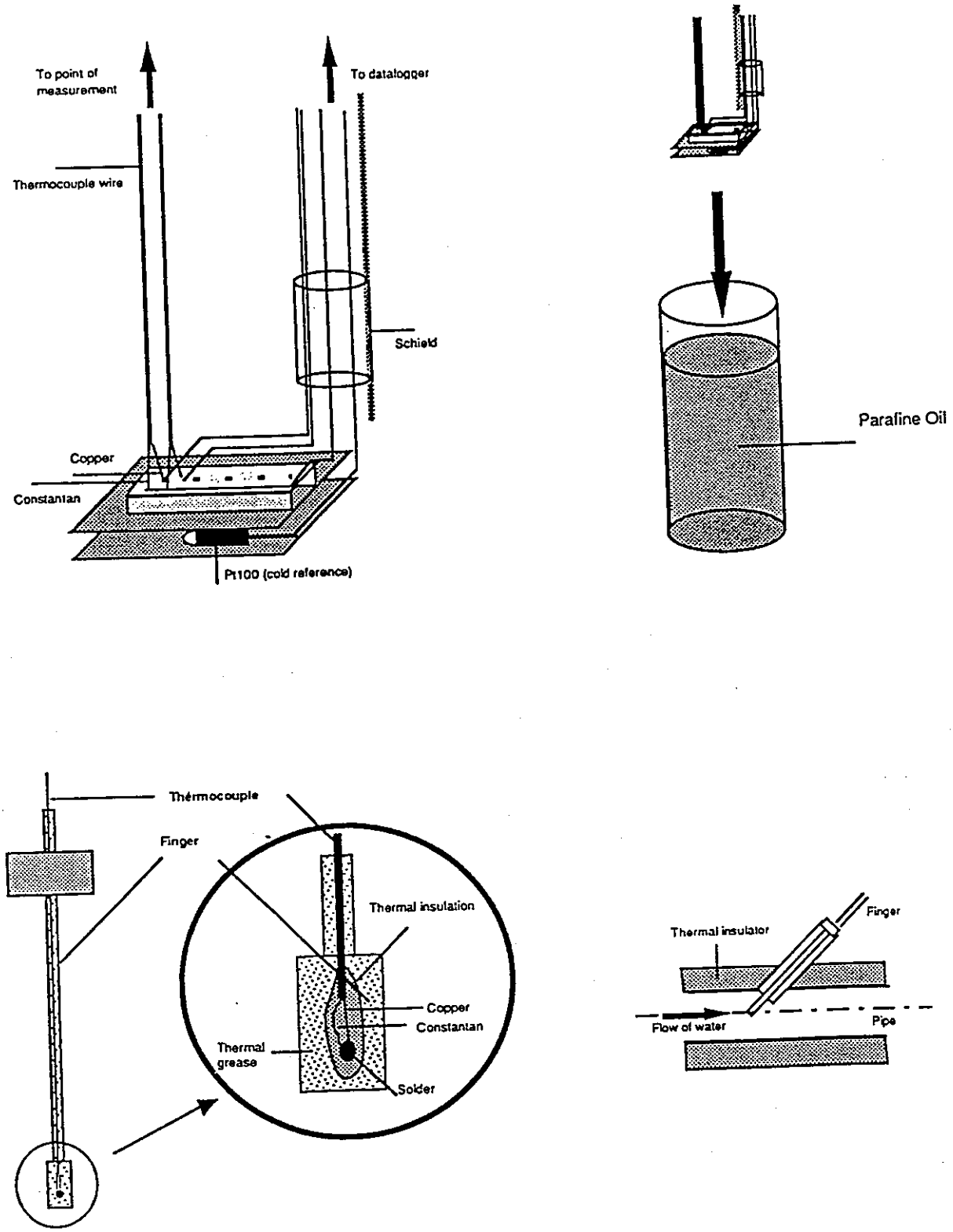

Figure B. 2 Temperature sensors.

Figure B3 to B7 examples of measurements.

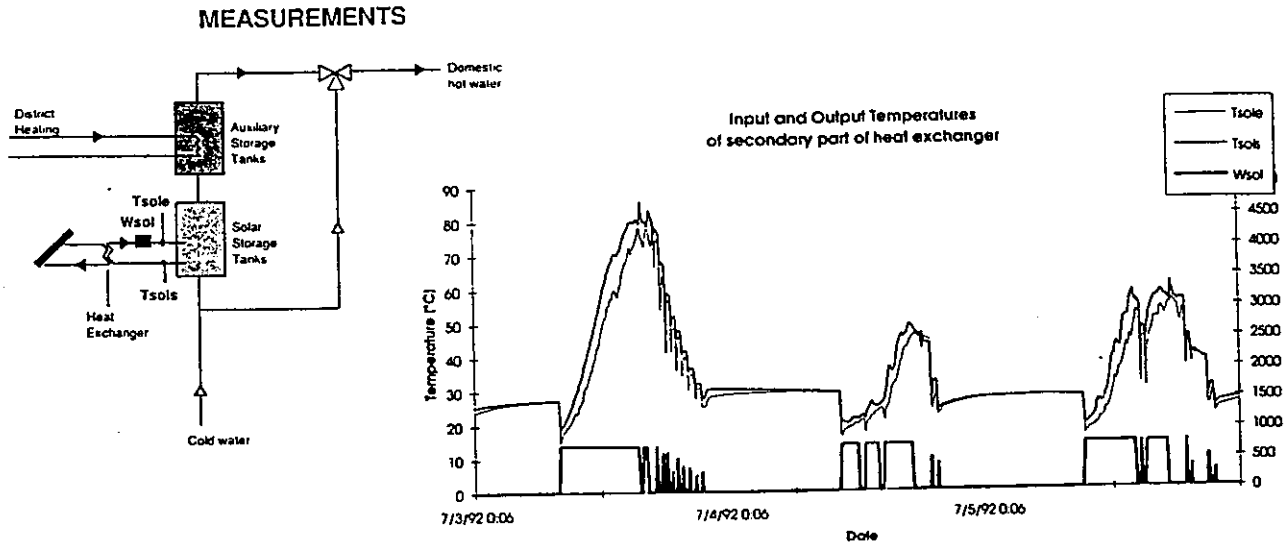

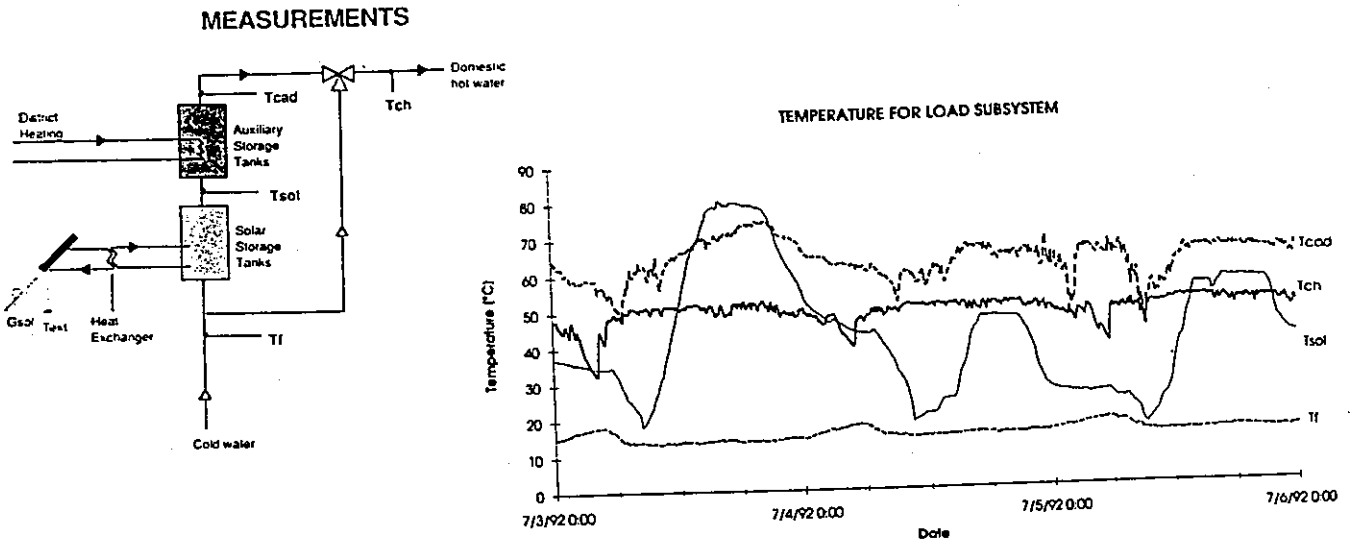

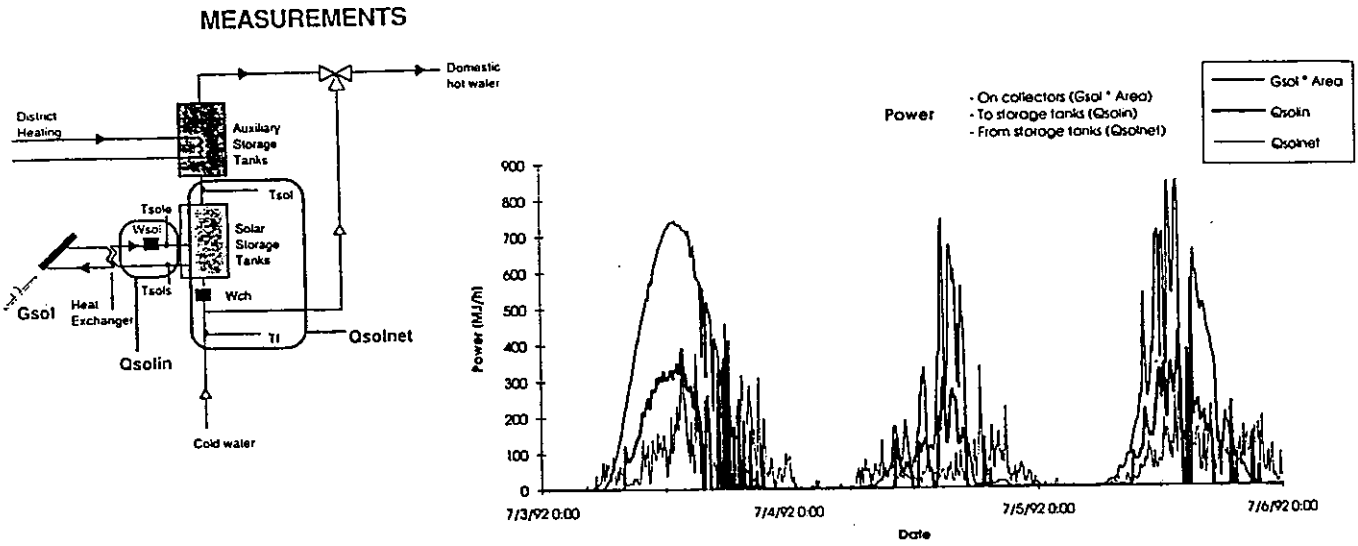
MEASUREMENTS
Domestic hot water
District Heating
Auxiliary Storage Tanks
Tsol
Tsole
Wsol
Solar Storage Tanks
Tsols
Wch
Gsol
Heat Exchanger
Qsolin
Qsolnet
Tl
Cold water
Power
- On collectors (Gsol * Area)
- To storage tanks (Qsolin)
- From storage tanks (Qsolnet)
Gsol * Area
Qsolin
Qsolnet
Power (MJ/h)
900
800
700
600
500
400
300
200
100
0
7/3/92 0:00
7/4/92 0:00
7/5/92 0:00
7/6/92 0:00
Date

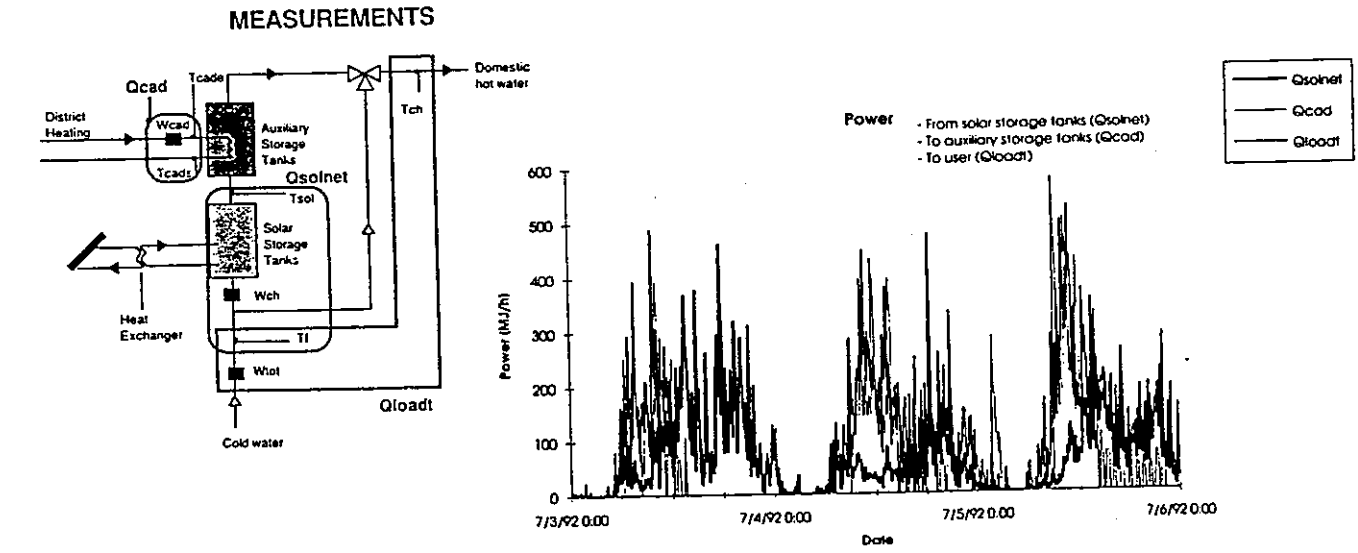
MEASUREMENTS
Qcad
Tcade
Domestic hot water
Tch
District Heating
Wcad
Tcads
Auxiliary Storage Tanks
Qsolnet
Tsol
Solar Storage Tanks
Wch
Heat Exchanger
Tl
Whot
Qloadt
Cold water
Power
- From solar storage tanks (Qsolnet)
- To auxiliary storage tanks (Qcad)
- To user (Qloadt)
Qsolnet
Qcad
Qloadt
Power (MJ/h)
600
500
400
300
200
100
0
7/3/92 0:00
7/4/92 0:00
7/5/92 0:00
7/6/92 0:00
Date

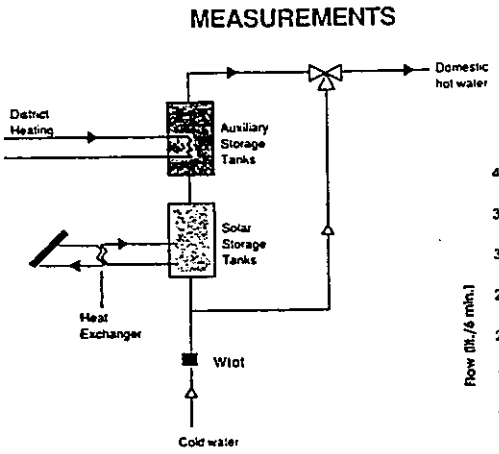
MEASUREMENTS
Domestic hot water
District Heating
Auxiliary Storage Tanks
Solar Storage Tanks
Heat Exchanger
Wlot
Cold water

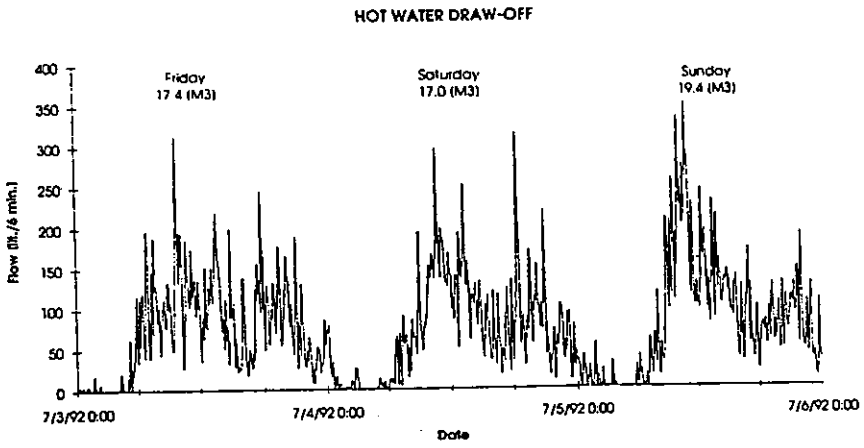
HOT WATER DRAW-OFF
Friday
17.4 (M3)
Saturday
17.0 (M3)
Sunday
19.4 (M3)
Flow (lit./6 min.)
400
350
300
250
200
150
100
50
0
7/3/92 0:00
7/4/92 0:00
7/5/92 0:00
7/6/92 0:00
Date

B.2 MEASUREMENT QUALITY TESTS

TEMPERATURES

Thanks to two temperature measurement devices installed at very close distances (10 cm) on the same pipe (see figure B.8), in-situ comparisons have been made during some days, for temperatures between 15°C to 70 °C. The test shows a mean bias of 0.02°C and a standard deviation of 0.015°C. The histogram of temperature differences of the two sensors is shown in figure B.9.

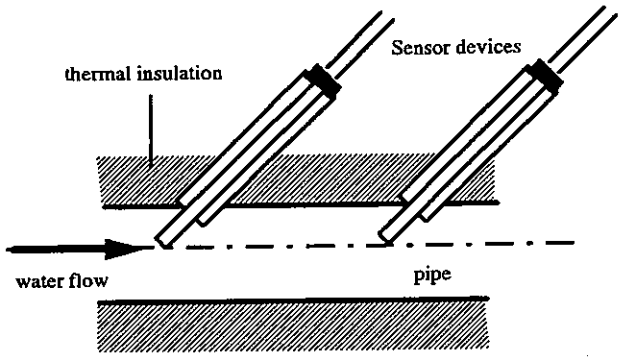

Figure B.8 In situ test of thermocouple sensors.

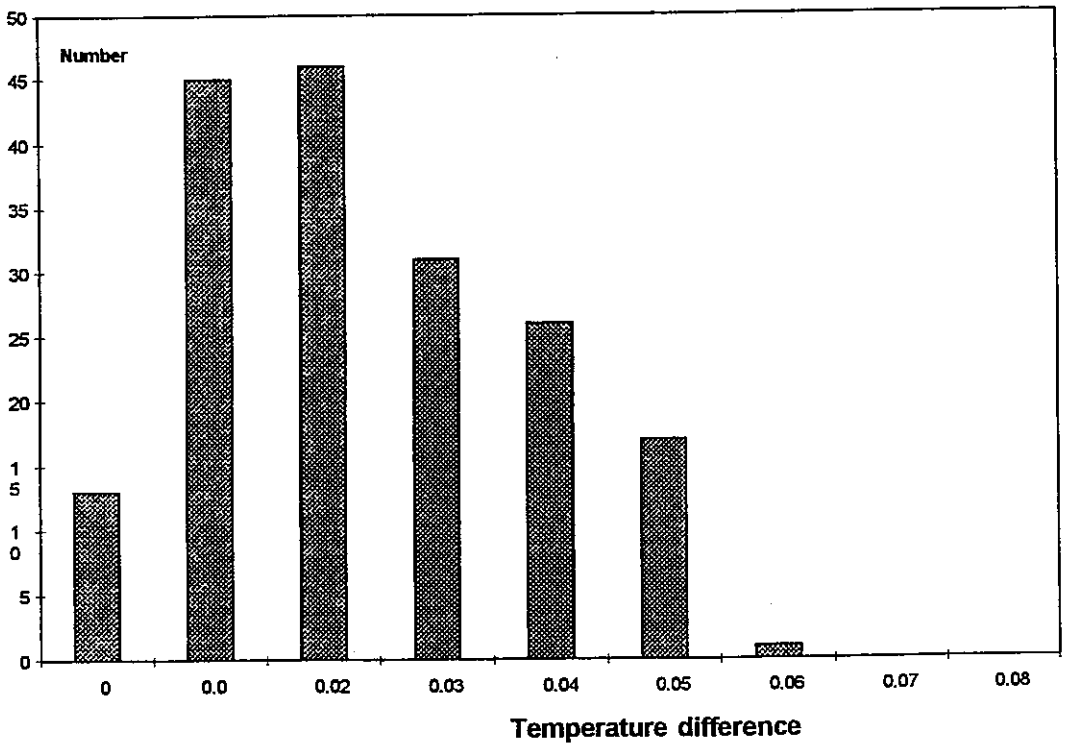

Figure B.9 temperature difference histogram

SOLAR RADIATION

Well calibrated solarimeters are used. The shadowband used for diffuse radiation measurement was removed during some days in order to compare the two solarimeters and to check the given precision (2% for the global radiation and 5% for the diffuse radiation measurements, including the shadowband effect).

FLOWMETERS

Closing a valve allows to compare two flowmeters (Wch and Wtot) because, in this situation, they measure exactly the same quantity. Figure B.10 shows the results obtained during a few days period and confirms the accuracy given by the manufacturer (±1%).

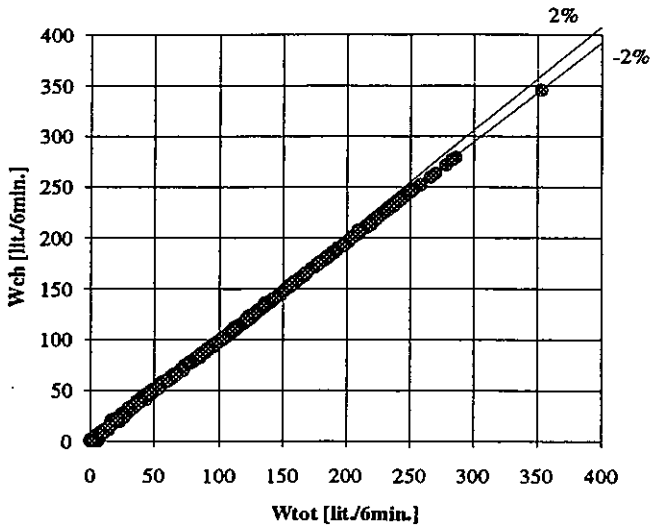

Fig B.10 Comparison between two flowmeters when they measure the same quantity (one valve is closed so they are in series).

HEAT FLOW

The hot water heat demand is computed twice :

. QloadT, using the total flow to the user and the temperature difference between the hot water after the mixing valve and the cold water,

. Qload, using the water flow through the tanks and the temperature difference between the hot water after the auxiliary tank (= before the mixing valve) and the cold water.

Figure B.11 gives the comparison in daily values for the reference year (09-92 - 08-93).

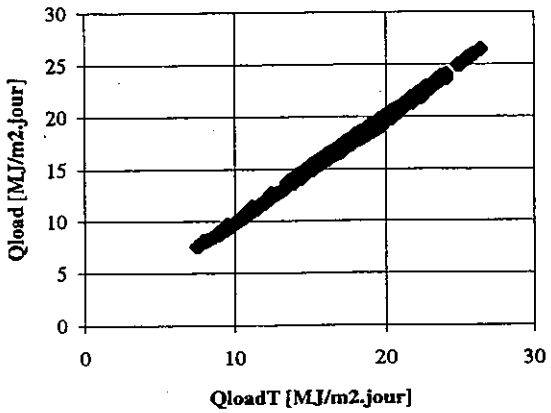

Figure B.11 comparison between the two independant measurements of heat demand QloadT and Qload. Daily values, from 09-92 to 08-93.

B.3 PERIODS OF MEASUREMENTS

The reference year is defined by the period 1/09/92 - 31/08/93. A complete year of data is available, based on 6 minutes interval except for the following periods, where the frequency of the data is one minute :

. from day 283 to day 292 1992 (8/10/92-17/10/92)
. from day 5 to day 20 1993 (5/1/93-20/1/93)
. from day 85 to day 109 1993 (25/3/93 - 19/4/93)
. from day 164 to day 179 1993 (13/7/93 - 20/7/93).

The integrity of this data is very high. Only 20 minutes of data have been lost and have been corrected by hand (the problem occured during nighttime).

C THEORY OF DYNAMIC FITTING

C.1. INTRODUCTION

The aim of this chapter is to try to explain, as simply as possible, the methodology of Dynamic Fitting (DF) procedure and compare this approach with more classical ones. This contribution proposes to be a positive criticism, in order to understand the DF method we have to work with rather than to use it blindly like a "magic black box".

Since no listings of the DF program are available, the documents used for this study are :

.Spirkl Thesis [C.1]
.Final Report of the IEA DST group, March 1992, [C.2],
.SDHWTest program manual [C.3].

We also refer to the very excellent book "Numerical Recipes in PASCAL" [C.4].

C.2 GENERAL PHILOSOPHY OF DF

DESCRIPTION

Figure C.1 compares the well-known methodology of DF and the standard/classical non linear fitting methodology, as described in ref [C.4], chapter 14, especially 14.4 : Nonlinear Models (page 572). The standard method is also successfully used in dynamic fitting, for example in buildings (see [C.5] and figure C.2).

Both approaches use the same general idea (available for non linear models) : start with a set of parameters, compute the errors between model and measures and minimize a function of these errors (more or less complex and called objective function) with a minimization algorithm. This algorithm changes the parameters in a way to decrease the value of the objective function at each step until reaching the minimum of this function. The Levenberg-Marquardt (or Marquardt) algorithm is the standard one for non linear models (see ref [C.4], chapter 14.4, page 574). The most reliable objective function when the model is perfect and the measurement errors are normally distributed is the sum of the squared errors (least square fit). When measurement errors are not normally distributed (outlier points or systematic errors), the objective function has to be changed. To do that needs at least some statistical justifications.

The only difference between DF and the classical approach is the definition of the objective function, defined by the two boxes named "F" and "IS" in DF papers,

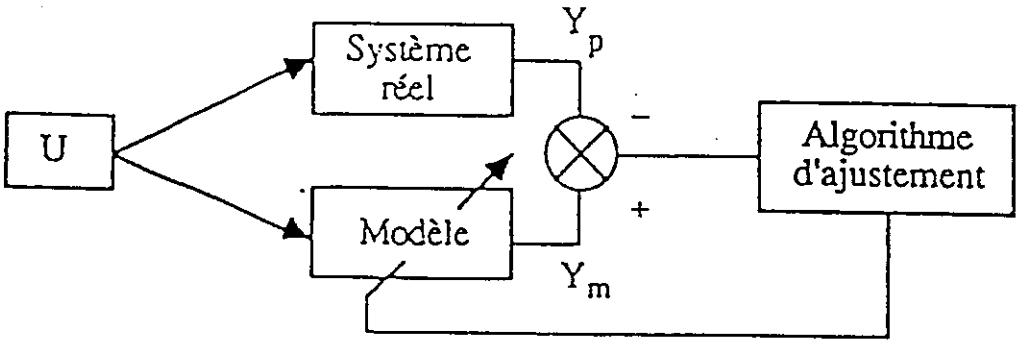

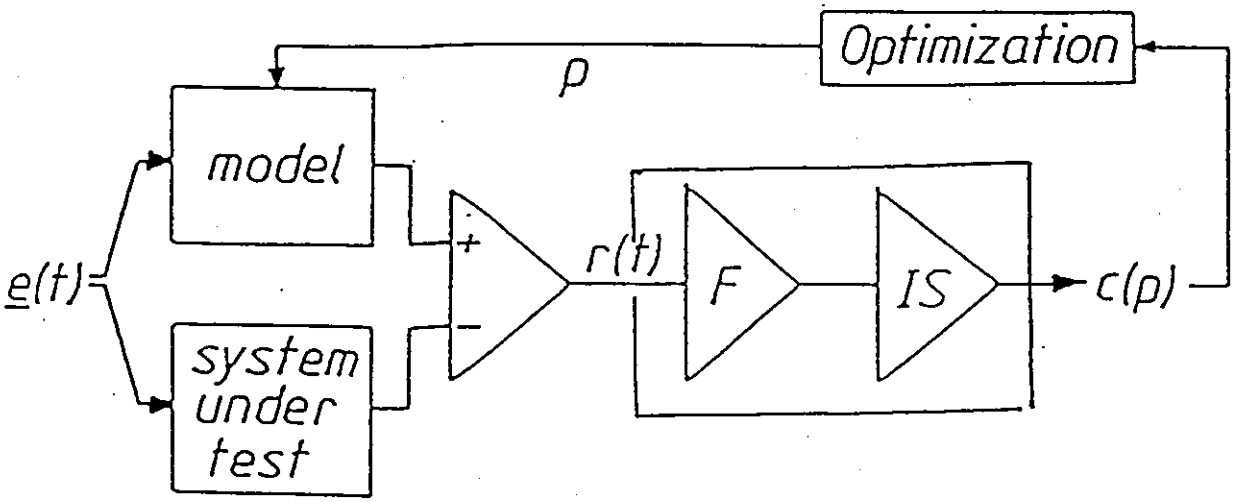

During the experiment, the input e is applied to the system under test. Its measured output η is compared with the modelled output y depending on the parameters p. The integral of the square (IS) of the filtered (F) residue r gives a measure $C(p)$ of the goodness of the fit. An optimization procedure is used to determine $\hat{p}$, the value of p for which $C(p)$ reaches its minimum.

Figure C:1 Standard methodology (from [C.5]) and SDF methodology comparison.

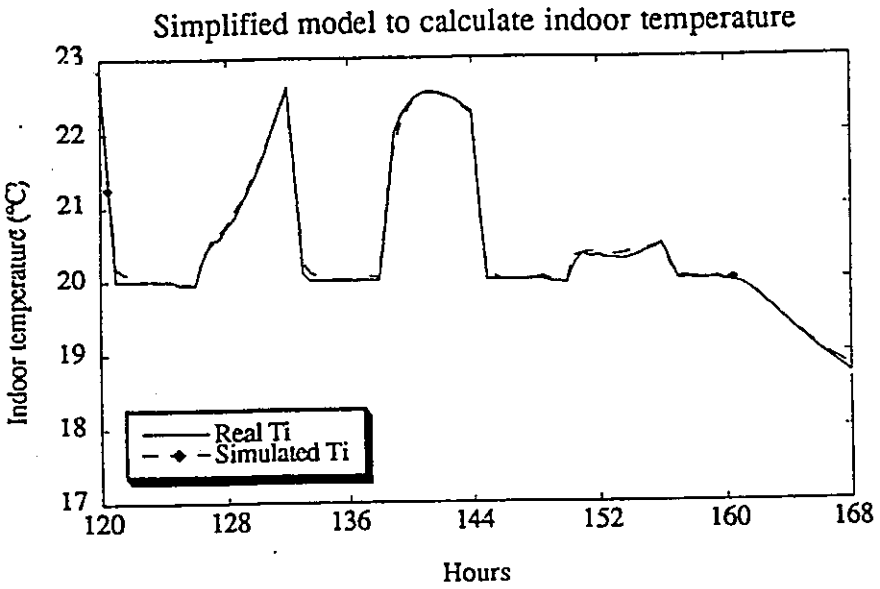

Figure 2- a : Validity of the simplified model for temperature variations in the cooling case Set point 20°C between 0-6 h and 12-18h.

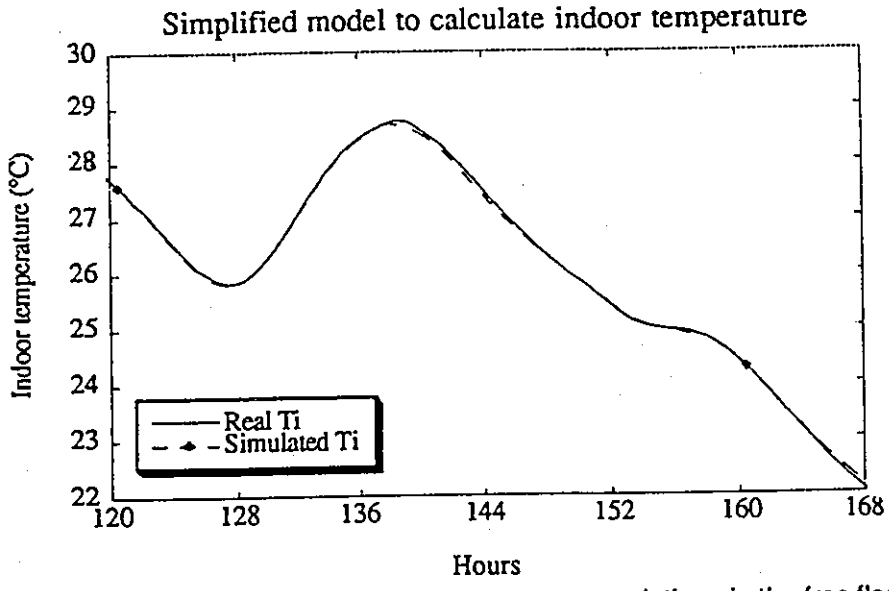

Figure 2- b : Validity of the simplified model for temperature variations in the free floating case

Figure C.2. Dynamic fitting of internal temperature of a building using standard method (from [C.5]).

which are the "integral of the square (IS) of the filtered (F) residue". Let us describe what is inside these boxes.
Rather than minimize the sum of the squared errors, DF minimizes the sum of the filtered squared Discrete Fourier Transform coefficients of the errors. For each set of parameters in minimization algorithm, the DF program :

. computes the errors between model and measurement,
. computes the Discrete Fourier Transform (DFT) of this error data set,
. applies a low-pass filter to the squared coefficients of the DFT,
. computes the sum of these filtered squared coefficients which replaces the sum of the squared errors used in the classical Marquardt algorithm.

This definition of the objective function is the originality of the DF methodology.
Let us develope the three last points.

DISCRETE FOURIER TRANSFORM (DFT)

DFT is well described in ref [C.4], chapter 12, page 422. It is a mathematical operation which transforms a set of N data into another set of N data in the frequency space. For the cosine transform, which is used in the 1.19 version of SDF program, we have : (see page 442 of [C.4])

$$Fk = \sum_{J=0}^{j=N-1} fj*\cos(pi*j*k/N)$$

where fj, j = 0,..,N-1 is the data array,
Fk, k = 0,..,N-1 is the Discrete cosine Fourrier Transform coefficient array.

Figure C.3 shows the five first basic functions used by the cosine DFT.

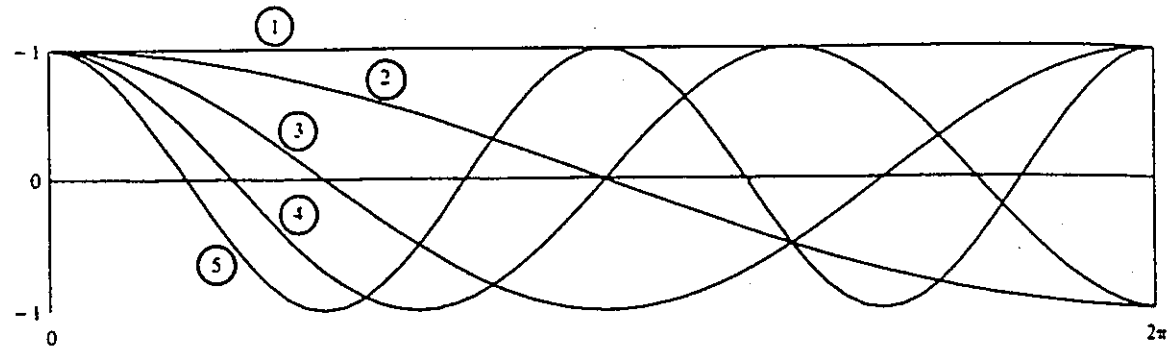

Figure C.3 : First basic functions used by the cosine Fourier Transform. (from [C.4])

Be careful not to confuse Discrete Fourier Transform with Fourier series(used for continuous and periodic functions) and Fourier transform (used for continuous and **not** periodic functions). The Fourier series transforms the function in a sum of sine and cosine with an infinite number of **discrete** frequencies (harmonics). The Fourier transform also transforms the function in a sum of sine and cosine but with an infinite number of **continuous** frequencies (from zero to infinite).

FILTERING THE ERRORS

When DF filters the errors in the frequency domain to obtain the objective function, it gives more importance for the errors of low frequencies, corresponding to the errors with a systematic behaviour. For example, it is easy to see that the first coefficient Fo (frequency equal to zero) represents the mean bias of the fit . Increasing the weight of this low frequency part in the objective function could avoid too high systematic errors, which would be given by a least square fit. **In other words, with DF, we could obtain a worse fitting in the sense of least square, but more reliable parameters because they lead to less biased errors, for example for the daily energy.** This part is linked with "robust estimation", described in page 590 of [C.4].

MINIMIZING THE "INTEGRAL (IN FACT THE SUM) OF THE SQUARE OF THE FILTERED RESIDUE ".

It is equivalent to minimize the sum of the filtered square of the DFT coefficients of the errors and the sum of the square of the filtered errors (demonstration similar that for the Parseval theorem, page 425 of [C.4] and [C.7]). So it is not necessary to rebuild the filtered error signal.

C.3 ABOUT DF METHODOLOGY

Because the Discrete Fourier Transform is very time consuming (with a N data set, it needs N*N operations) and because DF uses DFT once per iteration, we think that DF uses Fast Fourier Transform (Ref [C.4] , chapter 12.1, page 427). This algorithm uses only N*log2N operations instead of N*N, allowing a gain of time of N/log2N. But, to be applied, this algorithm strictly implies :

.1) sampled data, i. e. with constant time interval

.2) the number of data must be a power of 2 : $N = 2^n$.

The first condition is generally observed in monitored data. But, it is not clear if the preprocessing of SDHW Data program used by DF conserves this condition.

The second condition is more complex. DF manual never tips this point, so people generally use an input data file with a number of data not equal to a power of 2

The response was given in the 2.2 DFP manual [C.6], where we can read :

« the cosine transorm....is a fast transform for a power of two (2^N) of equidistant points. Hence before the cosine transform the data are transformed - conserving energy- to 2^N equidistant intervals «

C.4 CONCLUSIONS

In conclusion, the DF methodology is original by the objective function used in the minimization algorithm. This objective function uses Fourier transform of the residue in order to decrease systematic errors and decrease the influence of transient errors (due to measurement devices or due to the model). These errors are caracterized by low frequencies in the Fourier space. Other methods exist ([C.4], page 590), allowing to minimize the importance of outlier data, and are called "robust methods". All these methods, including DF, are very time consuming, so people generally prefer to use them only if necessary and only after a first determination of parameters with non robust but faster algorithm, such as the Marquardt algorithm using least square.

So, the best way would be:

. first to apply a non robust method, such as Dynamic Fitting but without Fourier transform and without low pass filter, in order to get a set of parameters. Then, a visual test of the errors (versus time or its distribution) allows to determine if a more robust algorithm is necessary. We feel that, in most cases when using collector models with a capacity term, this will be not necessary. The Marquardt algorithm is relatively easy to program or it is easy to obtain the code (see [C.4]).

. to apply, if necessary and only after the first step, a robust algorithm of minimization. These algorithms are generally based on other objective functions, like the sum of absolute error or more exotic functions. DF could be a candidate, but other methods have to be considered and compared.

Such an approach has the advantage of pushing people to avoid using dynamic fitting like a black box and allows to separate methodology aspects (is dynamic fitting useful for testing solar collectors?) and computing aspects (which is the best/faster/more reliable algorithm to do this?).

REFERENCES

[C.1] Spirkl Thesis, München University, Mai 1989.
[C.2] Final report of the IEA DST Group, march 1992.
[C.3] SDHWTest progam manual, version 1.19b, from DIN
[C.4] Press and al, Numerical Recipes in Pascal, Cambridge University Press, 1989.
[C.5] Bacot, "Energetique des bâtiments", PYC, 1988 (in French), or Richalet, paper distributed during the Lyon's meeting of European Pascool Program, november 1992
[C.6] W. Spirkl, private communication
[C.7] J. GIL, « determination des parametres physiques d'un champ de capteurs par un test de courte durée », travail de diplome de physicien, Geneva University, 1993.

D DYNAMIC SYSTEM TEST APPLIED TO IN-SITU DATA OF A LARGE SOLAR DOMESTIC HOT WATER SYSTEM

In this chapter, we present the results of the fits performed by DFP (Dynamic Fitting program with the built in P_ model) applied for every month of the year and compare the results obtained making an annual prediction to the real one. In fact, we presently dispose of a complete set of data (in-situ) for a whole year. The period taken here for the monthly or yearly analysis goes from September 1992 to August 1993.

This will show the potentiality of the method to make an annual prediction and to see if seasonal bias are important.

This work has the particularity to being, to our knowledge, the first to compare the results from the dynamic fitting methodology to a full year measurements performed over a large system (200 square meters) working in real conditions (i.e. in situ data).

Dynamic System Testing means here (in this chapter) the application of the DFP package (Dynamic fitting with P_model) to our data. The data correspond to the preheat system (see figure A.1).

D.1 COMMENTS ABOUT THE P_MODEL

The Dynamic fitting procedure has been commented previously in chapter C. The P_model is described in the manual of Dynamic System Testing (ref. [C.3]). The documentation for this model is available but not the software implementation.

In the P_model, the storage is modelled using a plug flow model similar to the so-called TYPE 38 Algebraic Tank Model in the simulation program TRNSYS. In this model, the capacity of solar collectors is neglected, and only the heat capacity of the storage is taken into account.

The parameters for the P_model are the following:

A_C*	[m2]	Effective collector area $A_C^* = A_C F_R^*(\tau\alpha)$, where F_R* is the heat removal factor of the collector loop, Ac the physical area,
u_C*	[W/(Km2)]	Effective collector loop heat loss coefficient (normalized to Ac*).
U_S	[W/K]	Total storage heat loss coefficient.
C_S	[MJ/K]	Total storage heat capacity.
f_{aux}	[-]	Fraction of the storage volume used for auxiliary heating.
D_L	[-]	Mixing constant, describing mixing effects during cold water inlet.
S_C	[-]	Stratification parameter (for storage loading).

We will briefly explain here what these parameters could take into account for our system:

Collector parameter A_C* , called the effective collector area includes collector area, the effective transmission - absorption product ($\tau\alpha$), effective heat removal factor F_R* of the collector loop and the mean transfer coefficient for the heat exchanger. Also the mean

value of the incident angle modifier $K_{(\tau\alpha)}$, the mutual shadow between collectors and shadow coming from obstacles (as the elevators rooms) are included.

The collector loop heat loss parameter u_C* that will take into account the losses from the collectors, the pipes and the external heat exchanger. The dependency of heat losses on the temperature is lumped in this parameter. As we do not measure wind velocity, these effects are also lumped in the parameter u_C*.

The power given by the solar loop to the store is modelled by the following equation:

$$P_C = A_C*[G_t-u_C*(T-T_{ca})]$$

where P_C is the collector loop power, Gt the solar irradiance in the collector plane, T the **store** temperature, and T_{ca} the external ambient temperature.

The storage heat loss parameter US will take into account the heat losses from the four solar storages and the pipes connecting them. Thermal bridges exist where valves are placed.

The storage parameter Cs will take into account the heat capacity of the solar storages, maybe excluding the dead zone at the botton of the storage and including the water contained in the pipes between the input of the storages and the place of the temperature sensor.

RUNNING DFP

Some choices have to be made before the fit can be run:
- the skip time
- the length of the periods
- averaging time of data
- the values for the filters

Additionally some other choices such as:
- the kind of data file (compressed or not)
- the options for the Plug Flow Model
- to solve manually the problem of the convergence

can be made.

THE COMMAND FILE

The command file used with each data file is the following:

```
**************************************************************************
* Command File to fit the monthly data
**************************************************************************
*Resuls in RESULTS
FileName,RESULTS\dfan%1
```

```
*Options pour le Plug Flow Model.
Model,Aux,Off
Model,WindCollector,Off
Model,LoadHeatExchanger,Off
Model,DrawOffMix,On
Model, SolarStratification,Off

NumOfLocMin,10
*Monthly data files in DAT, Skip of 3 days
Read,DAT\dfp%1.d3,SKIP=72

* Filter constants 4 hours, 1.6MJ/K
FilterConst,4,1.6E6

Fit
```

And the fits have been called by the following instruction:

```
df_p cgoan %1 /B /F /trace
```

where cgoan is the name for the command file, and %1 is to take the corresponding month file of data.

The explanation for the different options in this command file is given below.

THE SKIP TIME:

To choose the skip time we have run the program "SkipSDHW". For this, we have taken the parameters that were found in a previous fit using data for one month, plus a week of skip time. From the resulting graphics, we have found that, in all the cases, less than two days of skip time was necessary. We can note that in our system, the total solar storage volume is withdrawn more or less 4 times per day. We have decided to give 3 days of skip time for every file in order to assure a good "forgetting" of the initial conditions of the system.

THE FILTER:

Following the manual (ref. [C.3]), a filter is introduced to damp the influence of transients. The program uses a constant filter coefficient tf, and a time variant filter coefficient t. We have fixed the value of Cf as explained in the manual (in our case the value is 1,6*10^6 [J]), but we do not fully understand the significance of the filter and we do not know which value we must attribute to the filter tf.

In order to check the influence of the filter on the results, we have run the same fit changing the value of the filter time tf. The values of the parameters seem not to change very much, but their errors increase (except for US) with the value of the filter (figure D.1). As expected, the value of the objective function decreases when the filter increases (figure D.2). The variances calculated, making the sum of the squared errors (from the files f1), increase with the filter (figure D.3). This is due to the objective function used by DFP, as seen in chapter C (theory of Dynamic fitting) : »with DFP, we could obtain a

worse fitting in the sense of least square, but ....(it) leads to less biased errors, for example for the daily energy ». If an annual prediction (with STP) is made and compared with the real one, the difference decreases, as expected, when the filter time increases (figure D.4).

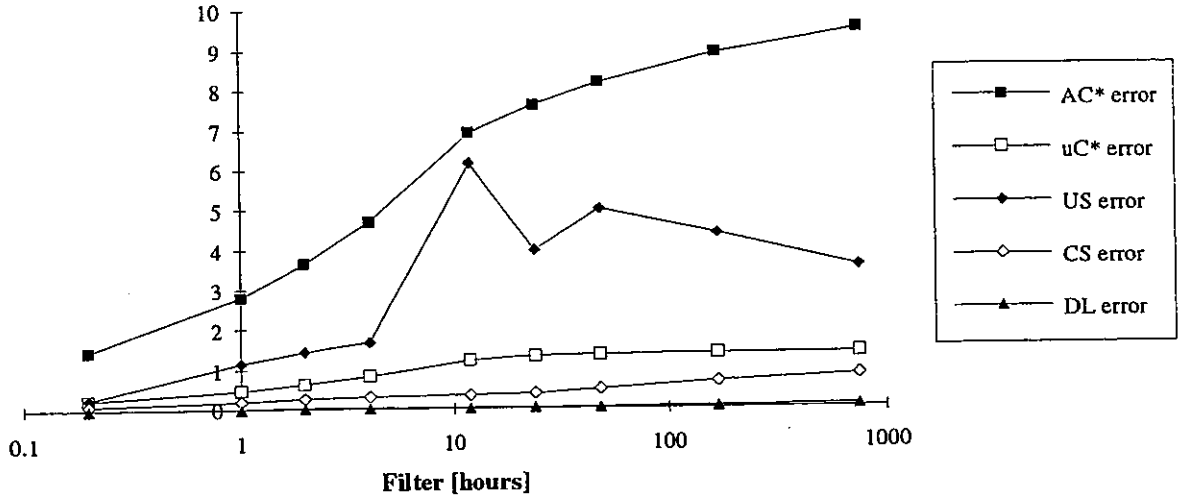

Figure D.1:Parameter errors versus filter time, units : m ², W/K m², W/K, J/K, - .

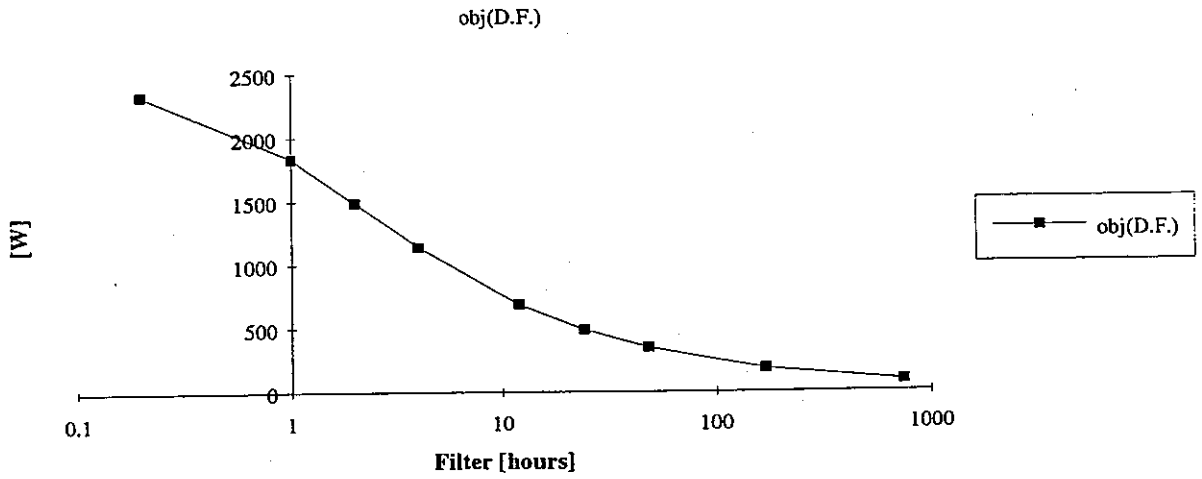

Figure D.2: Objective function versus filter time

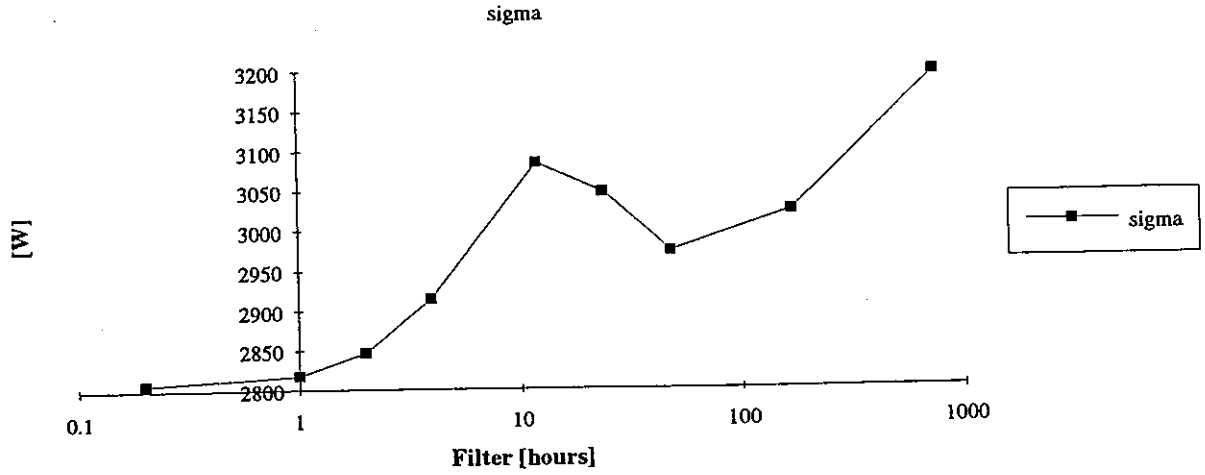

Figure D.3: Standard deviation (square root of the variance) versus filter time.

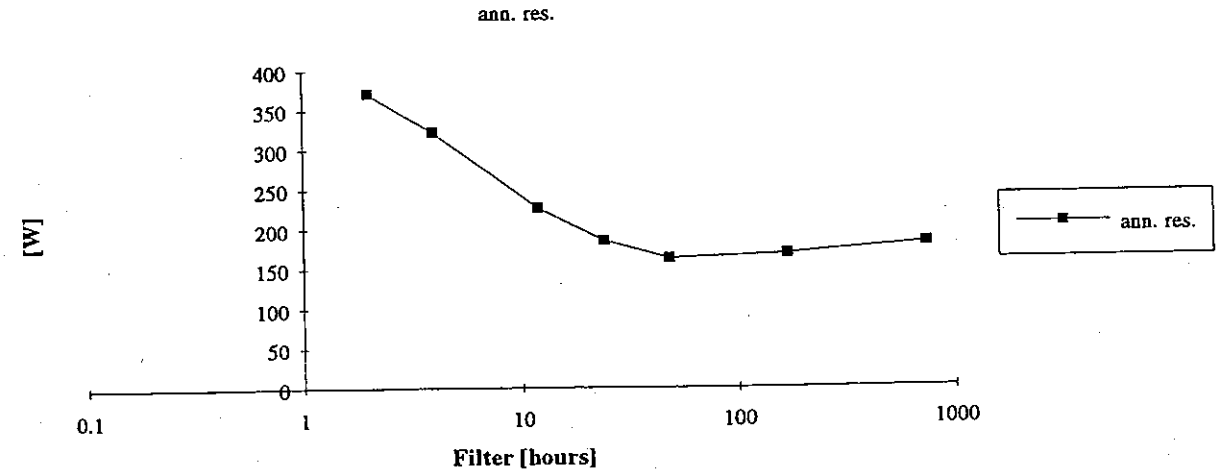

Figure D.4: Annual prediction residue (bias) versus filter time

From all this, it is difficult to obtain a criteria to attribute a value to this filter. Finally we have decided to set the filter tf to 4 hours as recommended (or imposed) by the draft proposal ISO 9459, Part 5(ref. [D.1]). At least with this value, our results can be compared with others.

We have also noted that the time for the calculations is slightly increased when the filter is small. In fact, many frequencies (even more than the number of data available to fit !!!) are taken into account.

DATA FILES :

We have the possibility of using two kind of data files for the fit with DFP:
- the data files as we have produced (i.e. 6 minute averaged data taken every 10 seconds),
- the processed data files resulting from the run of the program "SDHWP".

In order to check if any differences exist in the results, we have compared the fit between a data file and a file processed by "sdhwp". We have not found important differences between them. So, we decided to work with the processed data files (i.e.: files with extension "d3" by default) because the time for the calculations is somewhat reduced using the latter.

OPTIONS FOR P_MODEL:

Some options are implemented in the P_Model, and it is the responsibility of the user to choose the good ones. For our system, the following options were set for the model:

Model,Aux,Off
Model,WindCollector,Off
Model,LoadHeatExchanger,Off
Model,DrawOffMix,On
Model, SolarStratification,Off

Because no auxiliary heater is integrated in the solar tanks, the Aux option is set to Off.

The effects of the wind over covered collectors in Geneva are very slow, so the option WindCollector is set to Off.

As no internal heat exchangers exist in the solar tanks the option LoadHeatExchanger is set to Off.

The option drawOffmix is set to On in order to evaluate the mixing of cold water inside the store.

About the option Solar Stratification, some comments must be added:
Our system has an external heat exchanger, and following the paragraph B.3.2 of the manual a parameter Sc different from 0 must be used. As we did not understand how equation B.5 of the DFP manual is taken into account in equation B.3, we have tried many fits with and without SolarStratification option. With this option ON, one parameter more must be fitted, and we noticed that the calculation time was increased, leading to not very different values for the other parameters. The value found for this parameter is equal to 0, equivalent to the SolarStratification Option set to OFF

We have preferred to continue working with Sc=0. For example, the following results (from a month data file : September 92) shows that Sc is not very well determined and is very close to 0. In addition, for this example, one could conclude (from the objective function value) that the option OFF models our data better.

Results for the option SolarStratification ON

AC*	uC*	US	CS	DL	SC	objective
[m²]	[W/K/m²]	[W/K]	[MJ/K]	[-]	[-]	[W]
104	5.526	0.3184	17.19	0.08485	0	541.3
2.5	0.349	0.465	0.13	0.00657	0.007	

Results for the option SolarStratification OFF

AC* [m²]	uC* [W/K/m²]	US [W/K]	CS [MJ/K]	DL [-]	objective [W]
107.5	6.121	0	17.22	0.0838	537.89
1.77	0.296	0.405	0.128	0.00642	

LENGTH OF THE PERIOD:

We have performed different fits with data files having different lengths of periods. We have begun first by taking a period of 10 days (where the first 3 days are skipped) and we have increased the length by four day steps until a period containing 58 days has been reached. We have stopped here for two reasons:

- The amount of memory needed by a file (compressed) containing data for 62 days is too big to be handle by the DFP program. The following error message is given by the program:

<Esc> Error. Memory exceeded.
STOP: Memory exceeded

- Over this length, the « classical » methods can obtain the information needed to predict the annual energy for a given system with a relatively good accuracy.

The results coming from this test give us some information about the length of the period needed to obtain good results. But, of course these conclusions are restricted for the considered period and the climatic conditions of Geneva.

All the files containing the data begin on May first 1993, and take the last 3 days of the month of April as data for the skipped time. The table 1 shows the results from the different fits.

Length (days)	AC*	AC* error	uC*	uC* error	US	US error	CS	CS error	DL	DL error	obj(D.F.)
10	130.0	8.5	10.7	1.2	0.045	3.69	17.6	0.48	0.0343	0.0166	704.7
14	128.5	8.0	10.0	1.2	0.000	5.39	17.07	0.43	0.0392	0.0174	851.8
18	123.0	6.6	9.3	1.1	0.001	3.69	17.25	0.37	0.4152	0.0155	866.7
22	118.5	6.2	8.2	1.0	0.022	2.30	17.08	0.40	0.4813	0.0182	1073.1
26	116.9	5.4	8.0	0.9	0.000	2.42	17.00	0.34	0.4919	0.0151	1002.9
30	114.1	5.2	7.6	0.9	0.000	2.90	16.75	0.32	0.0517	0.0159	1079.6
34	112.1	4.7	7.5	0.8	0.000	2.04	16.58	0.31	0.0491	0.0152	1137.2
38	111.1	4.4	7.4	0.8	0.000	1.54	16.54	0.29	0.0478	0.0140	1141.3
42	110.4	4.0	7.2	0.7	0.000	1.34	16.44	0.27	0.0488	0.0134	1162.7
46	110.9	4.0	7.5	0.7	0.000	1.75	16.45	0.25	0.0453	0.0123	1174.8
50	111.2	3.8	7.5	0.6	0.000	1.57	16.54	0.25	0.0452	0.0114	1135.2
54	109.8	3.5	7.3	0.6	0.026	1.85	16.46	0.23	0.0453	0.0109	1138.3
58	109.6	3.4	7.3	0.6	0.000	1.49	16.41	0.22	0.0453	0.0104	1108.8

Table D.1: The principal results are condensed here for the fits with different lengths of periods (starting May 1st 1993).

As expected, the errors for the parameters decrease when more data is available for the fit (see figure D.5), but surprisingly the objective function increases (figure D.6). These results are not very coherent. Then, we have performed the corresponding long term performances.

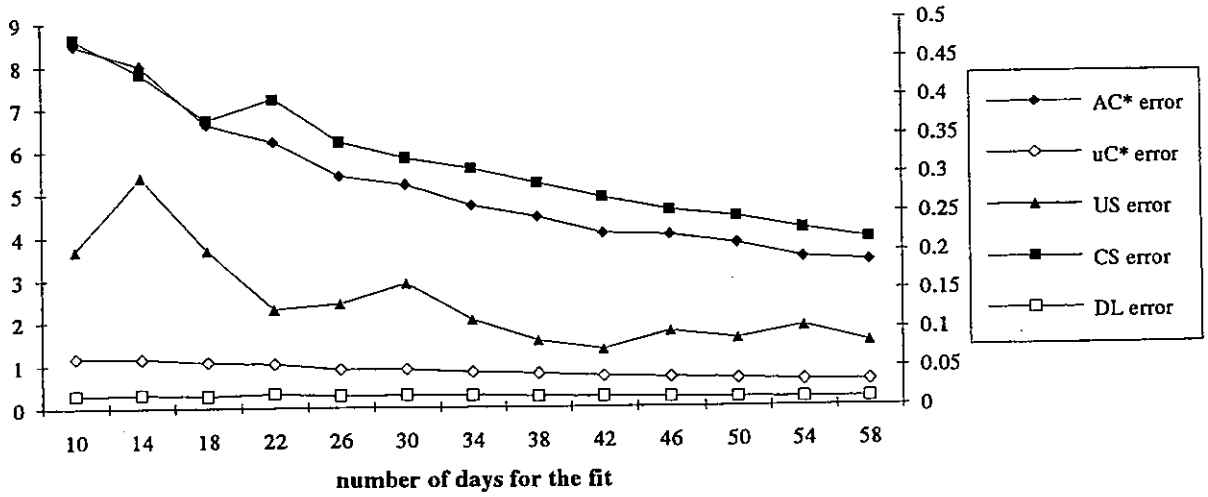

Figure D.5 : This figure shows the errors in the parameters against the number of days used in the fit.

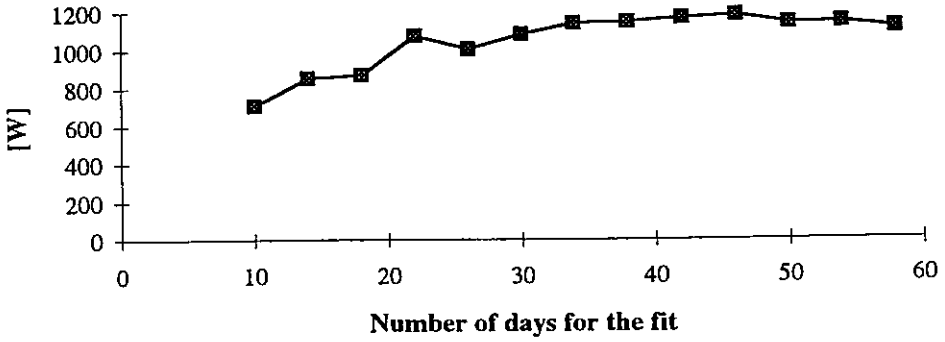

Figure D.6: This figure shows the values for the objective function given by DFP against the number of days used for the fit.

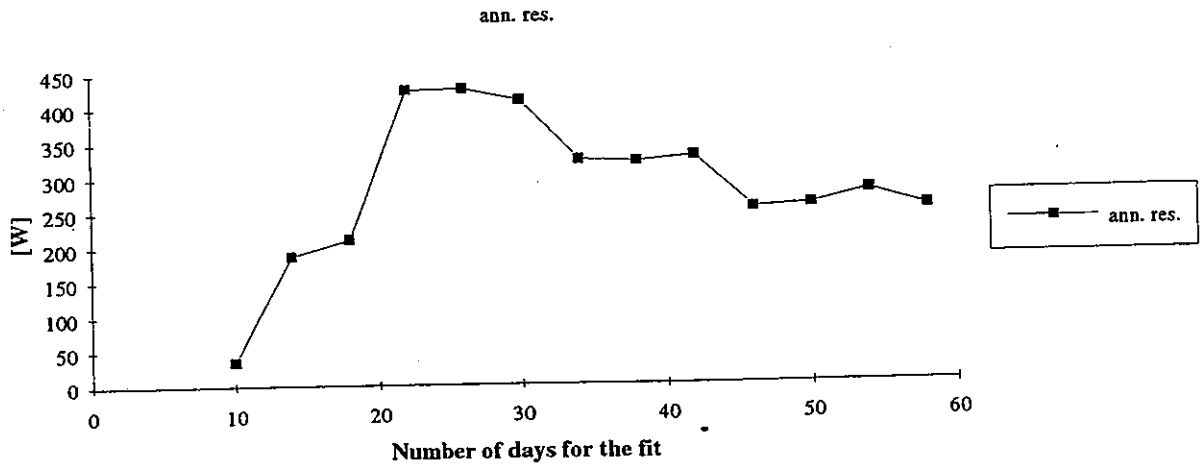

Figure D.7: Error of the annual prediction using the program STP.

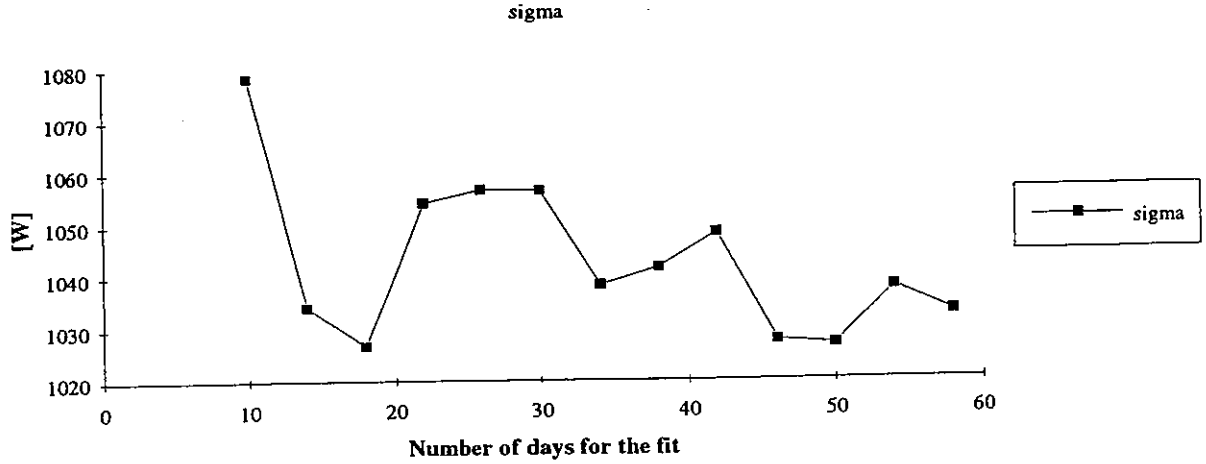

Figure D.8 : Standard deviation (square root of the variance) of STP predictions versus the measured values for different period lengths to obtain the parameters.

The long term prediction, as carried out here (with STP as described above), shows that it can be dangerous to take only the predicted annual energy as a criterion to judge the results obtained from a particular fit (figure D.7). But, as expected, the standard deviation calculated over the whole year (i.e. the square root of the sum of the squared errors) slowly decreases when the number of days for the fit is increased (figure D.8).

STEP AVERAGED DATA

It is important to know how will be the time step for average our data. This question was crucial for us because our goal was to collect data over the complete year. Then, storing very closed data asks for a big amount of memory and this complicates the analysis of data (searching for possibly errors and others). But in the other hand data taken as short as possible should give more information about the dynamics of the system

In this sense we have performed some fits taking data for 1 month, but taking different steps. We have begun from 2 minutes averaged data until 3 hours averaged data.

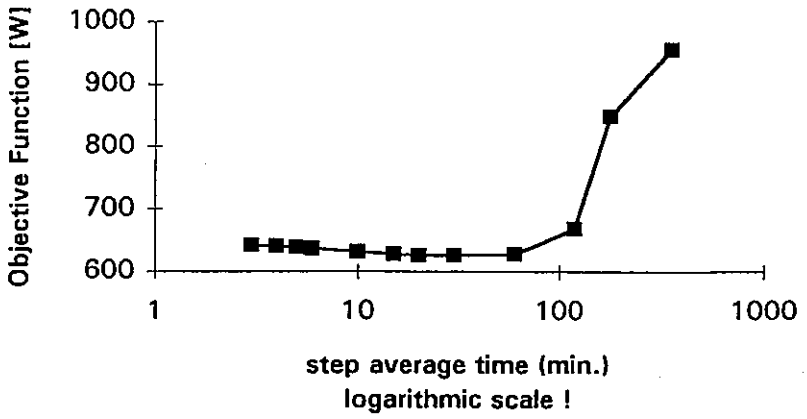

Figure D.9 Objective function versus step average time

We can see in the figure D.9 that the lowest objective function is given for the files containing 20 or 30 minutes averaged data.

With respect to the values of parameters we obtain interesting results :

data step, mn	Ac*, m²	Uc*, W/K.m²	Us, W/K	Cs, MJ/K	DL,-
2	110.4	6.58	0.017	17.1	0.075
3	110.2	6.58	0.004	17.1	0.075
4	110.0	6.51	0	17.1	0.076
5	110.1	6.53	0	17.0	0.077
6	110.4	6.58	0	17.1	0.077
10	110.3	6.54	0	17.0	0.078
15	111.8	6.76	0	17.1	0.076
20	110.7	6.55	0	17.0	0.078
30	111.5	6.61	0	17.1	0.082
60	108.5	6.03	0	16.8	0.084
120	108.7	5.99	0	16.3	0.071
180	104.0	4.78	0	16.1	0.069
360	92.1	2.47	0	13.9	0.013

Table D.2 : parameter value versus time step

The values of the parameters do not change too much with the time step, untill the time step is as high than 30 minutes. Higher time steps lead to different parameters (Ac*, Uc* Cs and DL decrease).

D.2 PROBLEMS WITH THE STOP CRITERIA IN DFP

We have applied DFP to the data that we obtained from our Large Solar Domestic Hot Water System (200 square meters of collectors and 4 cubic meters of solar storage). We began by choosing a sequence of 10 days (3-07-1992 to 13-07-1992). We have taken the estimated values of the parameters as initial values hoping that they would converge quickly to the final parameters. We retried the fit in order to check the convergence and we surprisingly obtained, at this point, another set of parameters. Then we have continued this same procedure again and again, until the set of parameters seemed stable: many cycles are needed to obtain stable parameters (nearly 1 day of computation with a PC 486, 33 MHz). The figure D.10 shows the values of the parameters AC* (effective collector area) and uC* (effective collector loss coefficient) against the cycle of the procedure, and the figure D.11 shows the errors for these parameters.

We can see from figures D.10 and D.11 that the values of the parameters overlap if we take into account their errors. Then, the first value obtained could be acceptable. But, some other results (see for example the figure D.12 for a 10 day sequence : 3/7/92-13/7/92) show that the values found in the first cycles with their error do not overlap the last ones found (with their respective errors). Note that for every cycle we use exactly the same sequence with the same filter time constant and the same skip time.

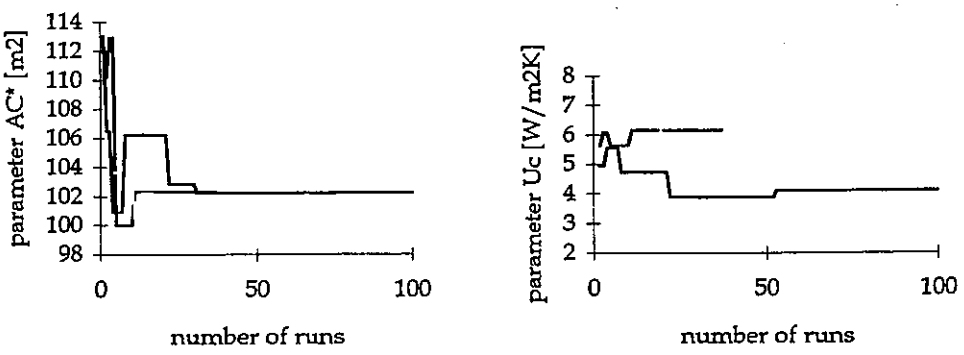

Figure D.10. The left hand figure shows the values found by DFP for the parameter AC* (effective collector area) against the number of runs (fit again with the values found in the precedent fit). The right hand figure shows the values for the parameter Uc* against the run. We have used here the version 1.19 for the fit. A sequence of 10 days (3-07-1992 to 13-07-1992) has been used with a skip time of 1 day. The command "NumOfLocMin" is set by default.

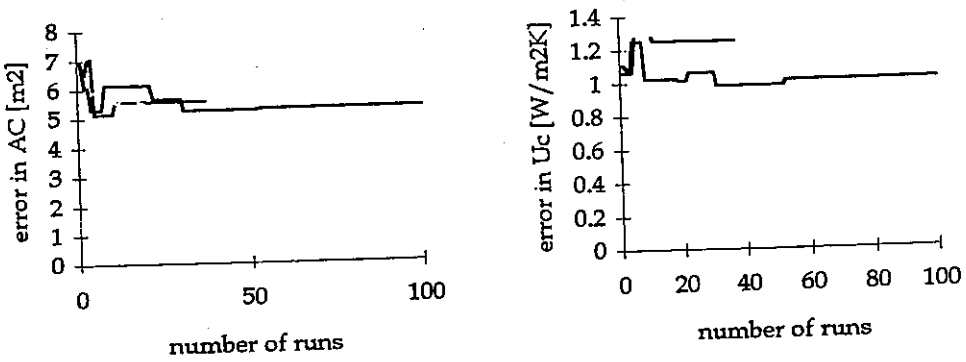

Figure D.11 These figures show the errors for parameters AC* and Uc* plotted in D.10.

We do not believe in the existence of many minima near the solution (see figure D.13). Rather, we think that the global minima can not be very well defined and the use of an adequate finding criteria could solve this problem. The algorithm used in DFP to find the minima stops too soon (i.e. not really in the minima). In fact, Dynamic Fitting finds a set of parameters that satisfies, but not those which optimise the fit. Something like when you take your car to go to the movie and you search for a parking place, you will take the first place you will find near from the movie but not the best one (i.e. in front of the movie).

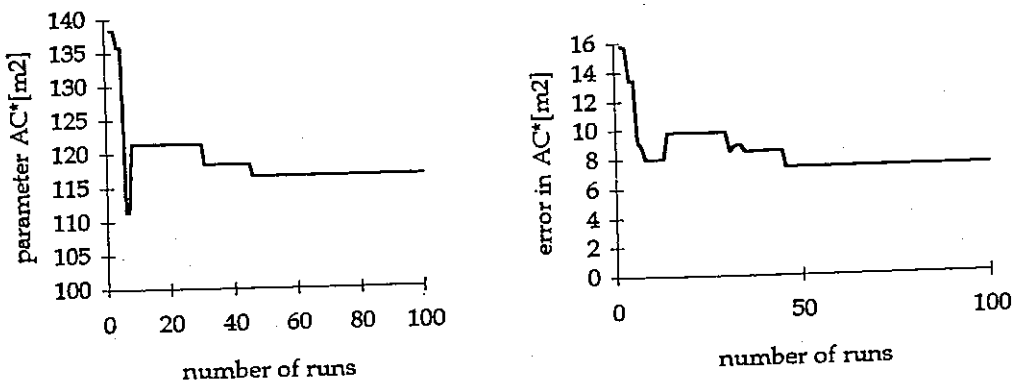

Figure D.12. The left hand figure shows the values for the parameter AC* (effective collector area) against the number of runs, and the right hand figure shows the errors for this parameter. We have used here the version 2.1 for the fit. A sequence of 20 days (3-07-1992 to 23-07-1992) has been used with a skip time of one day. The command "NumOfLocMin" is set by default. The expected value for the parameter AC* (i.e. the initial parameter for the first cycle) is 160 [m2].

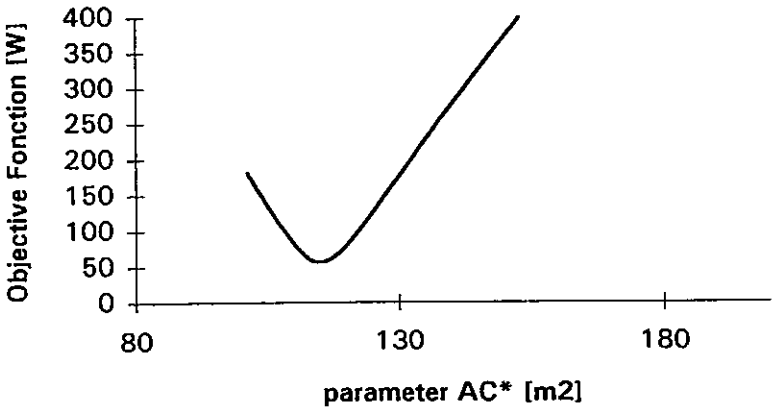

Figure D.13 Objective function evolution near the minimum value, for one parameter.

Therefore the algorithm to find the minima has to be revised.

D.3 MONTHLY FITS

We have partitioned the year in monthly periods for practical reasons. Apparently such a period is enough to give results that will not greatly change with additional data. Taking smaller periods, increases inversly proportionnally the time for the calculations and the compilations of the results without giving more information. Dividing the year in periods of one month is enough to show the influence coming from different seasons.

We have decided to give the same length to every set of data. It means that for some months some days are picked from the precedent month, for example the month corresponding to February takes the last days of January to complete the data. Each month-file contains 34 days, where the first 3 days are to be skipped. Then, data from 31 days is effectively used for the fit.

The results for the parameters and the accuracy are presented in the figures D.14 to D.18.

As said before, each fit has been repeated many times until the final results do not change at least the last 3 times.

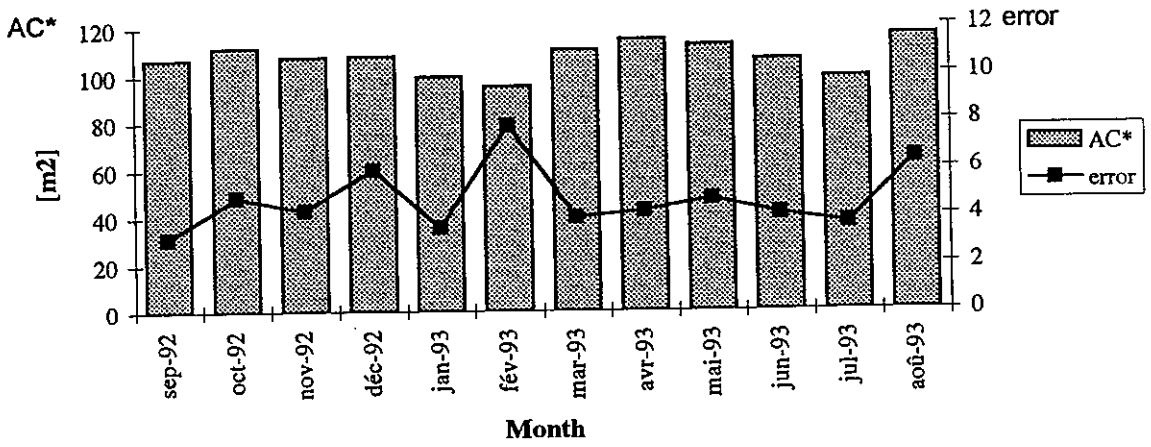

Figure D.14: Values for the parameter AC* (and its error) of the P_Model in function of the month used for the fit.

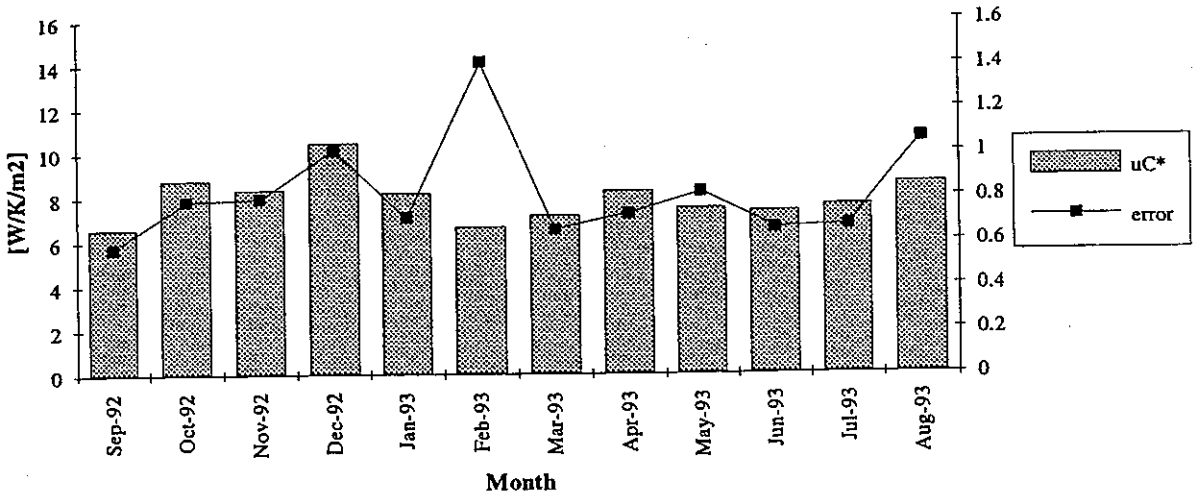

Figure D.15: Values for the parameter Uc* (and its error) of the P_Model in function of the month used for the fit.

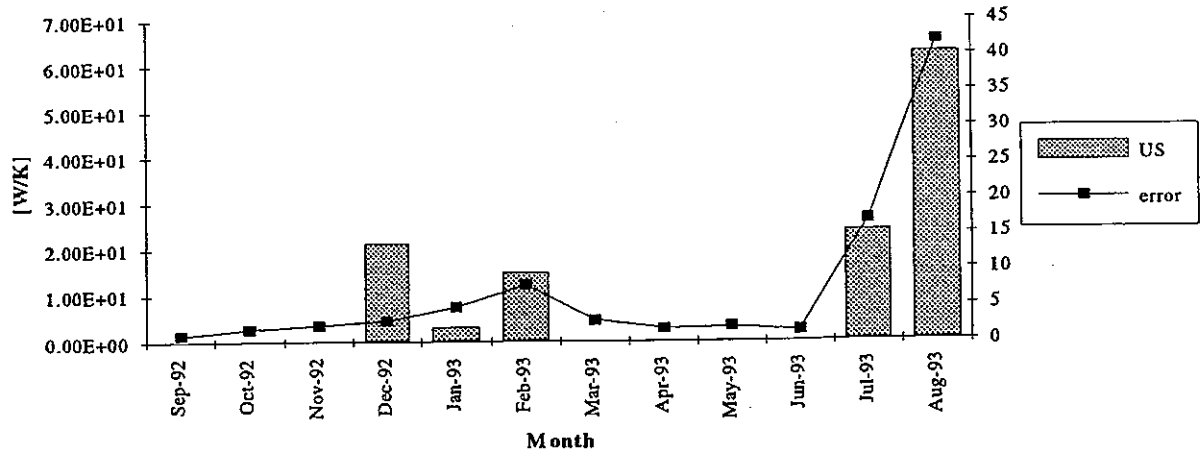

Figure D.16: Values for the parameter US (and its error) of the P_Model in function of the month used for the fit.

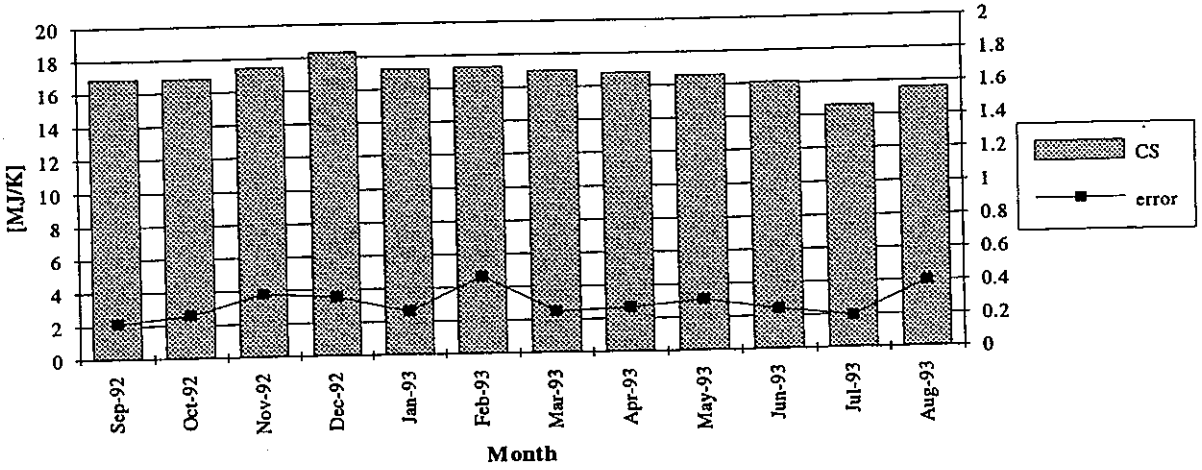

Figure D.17: Values for the parameter Cs (and its error) of the P_Model in function of the month used for the fit.

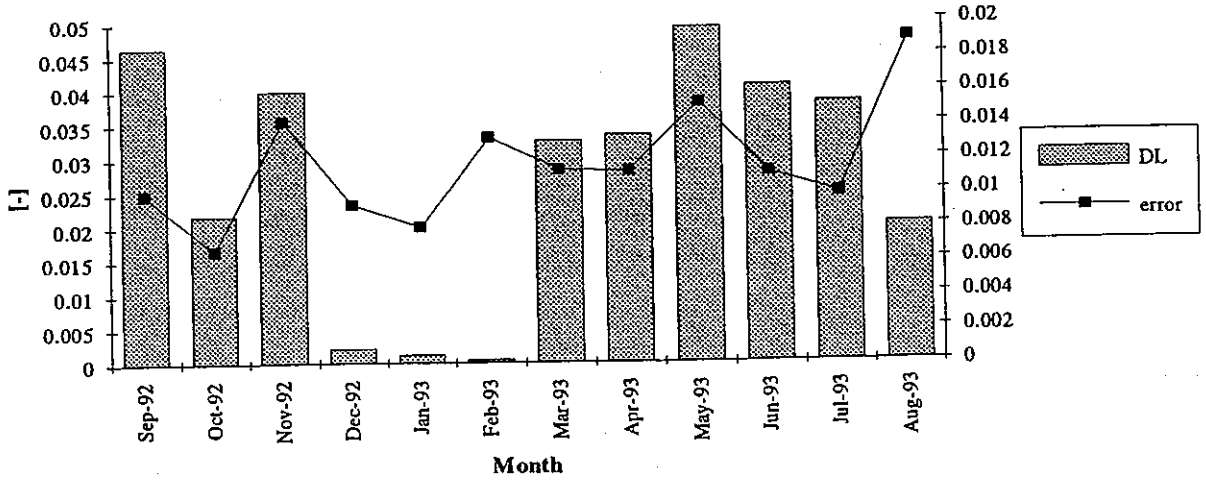

Figure D.18: Values for the parameter DL (and its error) of the P_Model in function of the month used for the fit.

For the comparison with the annual results, we have used a big file containing data for one year. This file contains data averaged per hour. We have failed to work with an annual file containing data averaged per 6 minutes because the memory needed was too big. But we have checked, making short term predictions over a period of 2 months, that this does not have any importance.

Here, the annual data file is not processed by the sdhwp program. To make the comparisons, we have used the Short Term Prediction program STP, because the program intended to make Long Term Predictions (LTP) does not allow to take all the inputs as measured. For example, the program for the Long Term Prediction does not allow for seasonal variations of the load. With our measurements, we have noticed that the variations for the load are important, a factor of 2.5 between winter and summer.

Then, the syntax used is the following:

STP monthfile.dfr annualfile.dat resultsfile /SKIP=72

where:
monthfile.dfr is the result from a fit using a data file for a given month
annualfile is the annual data file, with data averaged per hour

We can see (figure D.19) that the annual predictions for the different months are good (always less than 7%). Moreover, as we can expect, the prediction is smaller for the winter months: it can be the result from the shadows in the collectors and effects of angle incidence

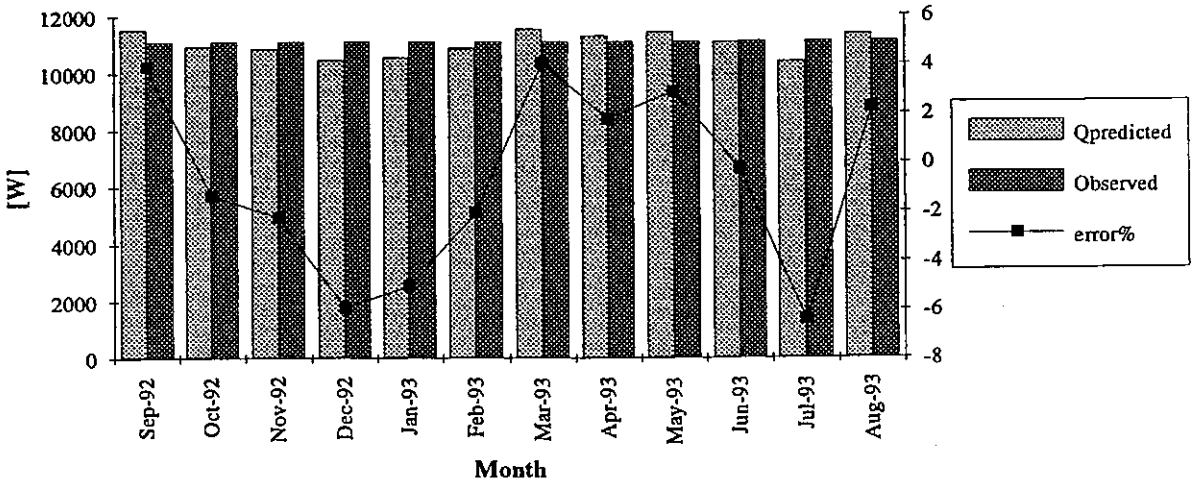

Figure D.19: This figure shows the predicted and the observed energies (and the error or residual) obtaining with the parameters resulting from fits using monthly data.

But looking at the values of the parameters (figures D.14 to D.19) we can see that the parameters deduced from the fits are not very stable. From our point of view, a method must not only predict the total energy given by a system, but must also give values that characterise the system (realistic values for the parameters) in order to give the possibility of making improvements. That seems not to be the case here. For example, the Ac* value was expected to be close to 150 m² - including the 0.9 factor due to the external heat exchanger- instead of the 110 m² found. A very strong correlation (>0.9) exists between the parameters AC* and UC* (see the correlation matrix for example for the month september 92 given below). These parameters are very difficult to uncorrelate when having in-situ data, and we must work with it. But this correlation could be due also to the simplicity of the collector model (no capacity effect in collector loop, collector temperature equal to solar tank temperature,..). The next chapter tries to answer this point.

AC* [m²]	uC* [W/K/m²]	US [W/K]	CS [MJ/K]	DL [-]	objective [W]
107.2	6.08	8.753E-8	17.22	0.08472	538
1.79	0.302	0.555	0.128	0.00648	

Cross correlation matrix:

1.0000000	0.9207149	-0.0160852	0.3755030	-0.2265588
0.9207149	1.0000000	-0.0291968	0.2432650	-0.4459741
-0.0160852	-0.0291968	1.0000000	-0.0062803	0.0093966
0.3755030	0.2432650	-0.0062803	1.0000000	0.2911014
-0.2265588	-0.4459741	0.0093966	0.2911014	1.0000000

Table D.3 Results from September 92 data.

REFERENCE

[D.1] ISO 9459 , proposed draft

E. DYNAMIC FITING OF SUBSYSTEMS

It is very useful to have an all-system model, particulary if it is very general, but this generality leads to a certain imprecision in some particular systems. One of the reasons we have performed "subsystem tests" is because a general model (the P_model in this case) failed to give the correct parameters characterising the system we have studied (a large solar domestic hot water system), as described in the previous chapters.

As we have commented previously, two goals are searched: to obtain parameters characterising the system and to predict the yearly energy gain of the system. However there is a little difference with regards to a whole system testing. It can include in the fit system failures that comes from the pump controller (regulation), and will include this in the yearly prediction.

Here, the system is split into two subsystems : the collector loop and the solar tanks. The Matched Flow Collector Model MFC (ref. E.1) simulates the solar loop and the P_model (ref. D.1) used just as storage model to simulate the four solar storages.

E.1 SOLAR LOOP WITH MFC

APPLYING DF

The Matched Flow Collector Model is intended to model the thermal performance of a flat plate collector cooled by a fluid. It is based on a plug flow model that accounts for:
- the heat capacity of the collector and the fluid
- the transport time of the fluid trough the collector

This second feature is very important for our solar field as we will explain later.
The model can also take into account for
- the temperature dependence of the collector U- value
- the incidence angle of various solar radiation components

To perform this we dispose of the following data (see figure E.1):
- The meteorological data (solar irradiation and external temperature).
- Temperatures just before the heat exchanger in the solar loop.
- Flow measurements in the secondary loop.
- Power given by the heat exchanger, calculated (with the respective temperature sensors and flow meter) every 10 seconds and then averaged over one or six minutes.

Applying this model to our data we have found that here it is very important to have short time steps to average the data. In fact, we have found that using the same data, where the only difference is that one file has 6 minutes averaged data and the other file has one minute averaged data, we can find different results for the values of parameters.

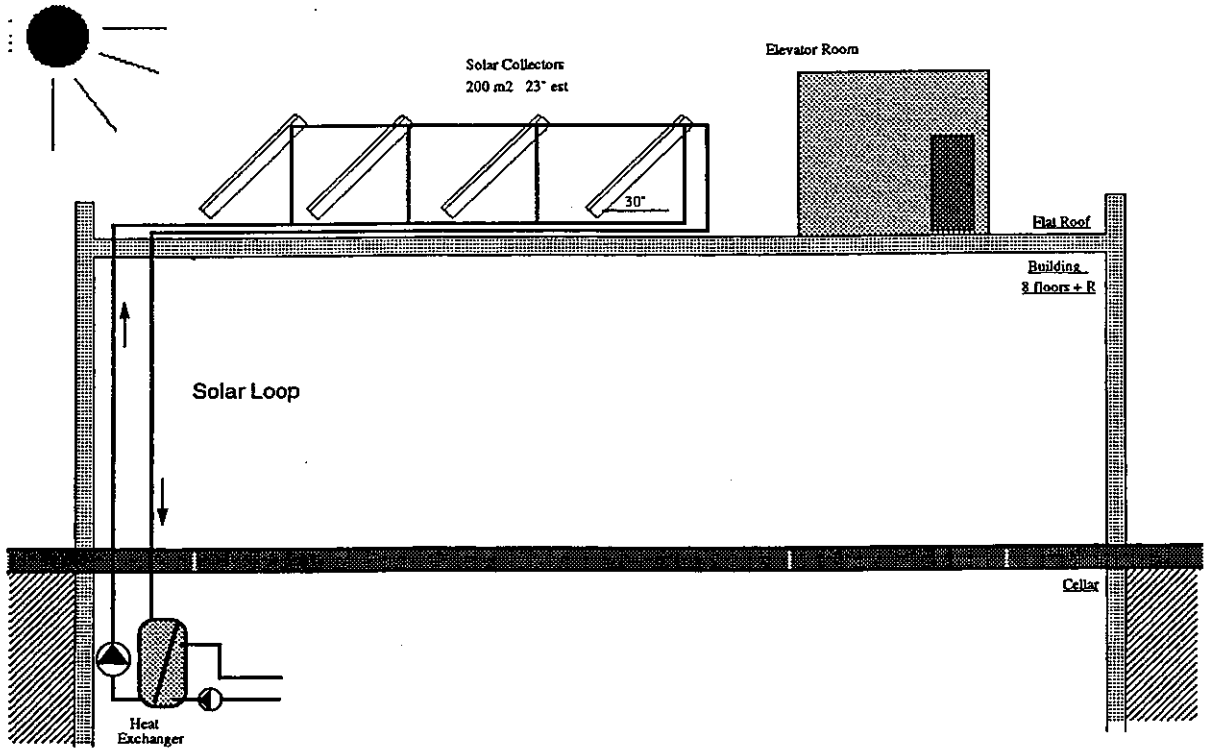

Fig E.1 : collector loop subsystem

The following lines show the results for a file containing data averaged by minute. Here 10 days have been used in one data file for a spring period (26 mars 1993- 4 Avril 1993).

```
* OUTPUT\MFC003

\Results DF 2.3á Jan 94 @Copyright InSitu running 14.04.1994 18:35:38
\Value,Parameters,"Ceff=30.5 n0=0.685 a1=5.62 a2=1.31 Obj=5501"
* External model temp\MFC_DF  MFC,1.0b,93-06-24
Transform method..... Cosine
Numerical precision..... 1
Time base..... 1
Filter type..... Gaussian, tf=300
            Name   mode  t_start  t_skip   t_end nFreq      Size
        TYPE14.DAT   Mean      360   86760  864001  4096  241..2399
    Ceff       n0       a1       a2 objective
 [kJ/K.m2]      [-] [W/K.m2] [cW/K2.m2]      [W]
   30.45   0.8163    3.607      1.4    11952
    1.34   0.0173    0.669     1.75
Cross correlation matrix:
 1.0000000  0.4071677  0.1174954  0.0105788
 0.4071677  1.0000000  0.6597894 -0.4157682
 0.1174954  0.6597894  1.0000000 -0.9213990
 0.0105788 -0.4157682 -0.9213990  1.0000000
```

COMPARISON WITH EXPECTED VALUES

Values for the collector parameters are available from two sources :

. A) Using a non linear least square fit program LSFIT, developped in Geneva (annexe 3), the parameters of collector loop have been found. The collector model used is the GAP model (ref [E.2]) with a capacity term :

$$\dot{q} = F_u\eta_0\overline{G} - 2F_u^3\frac{K_2}{U_{ech}}\left(\overline{T}_{fl\text{-}stk} - \overline{T}_a\right)\overline{G} - F_u^3K_2\left(\overline{T}_{fl\text{-}stk} - \overline{T}_a\right)^2 - F_uK_1\left(\overline{T}_{fl\text{-}stk} - \overline{T}_a\right)$$
$$-\frac{F_u^3\eta_0^2}{U_{ech}^2}\overline{G}^2 - F_uC_{eff}\left(1 - 2F_u^2\frac{K_2}{U_{ech}}\left(\overline{T}_{fl\text{-}stk} - \overline{T}_a\right)\right)\frac{T_{fl\text{-}stk}^{fin} - T_{fl\text{-}stk}^{init}}{\Delta t}$$

with the F_u factor (dimensionless) given by :

$$F_u = \frac{1}{1+(K_1/U_{ech})} = \frac{1/K_1}{1/K_1 + 1/U_{ech}}$$

where .

$T_{fl\text{-}stk}$ Mean temperature of fluid, tank side of heat exchanger (HX), given by the average of input and output temperature of HX (Tsole et Tsols) :

$$T_{fl\text{-}stk} = \frac{T_{sole} + T_{sols}}{2}$$

$T_{fl\text{-}stk}^{fin}$ Fluid temperature at the beginning of the period.
$T_{fl\text{-}stk}^{init}$ Fluid temperature at the end of the period.
$\dot{q}$ Power given by the collectors through HX [W/m^2].
G Solar radiation on collector field [W/m^2].
Ta Mean external temperature [°C].
η_0 Optical efficiency of collector field [-].
K1 Heat loss factor of collector field, including plumbing [W/m^{2}K].
K2 Temperature dependance of K1 [W/m^{2}K^2].
Uech Heat transmission of the heat exchanger [W/K].
Ceff Heat capacitance of the solar loop (including plumbing) [J/m^{2}K].
Δt one hour.

Hourly data of the total reference year are used with the criteria:
- pump ON during 60 minutes
- from 10 to 13 hours (in order to minimize the Incidence angle modifier effect)
- no self shading from one collector row to the next.

B) the officiel ISO test done at Rapperswill. The parameters obtained are valid for one collector, without plumbing and without optical obstructions.

The results are given in the table E.2.

	eta0	k1	k2	kexch	Ceff	sigma
	[-]	[W/m2K]	[W/K2m2]	[kW/K]	kJ/m2K	[W/m2]
GAP + LSFIT	0.83	5.81*	-	7.2	31.5	25
MFC + DF	0.82	3.6*	0.014	-	30.5	60
ISO test for collector	0.87	4.6	-	10 **	33***	
P-model + DFP	0.55	3	-	-	-	

* including plumbing (estimated to 1.8 [W/m^{2}K]).
** from manufacturer
*** computed from plan and in situ survey

Table E.2 : parameter values comparison.

As one can easily see on table E.2, the agreement is excellent between the different evaluations, taking into account that the parameter definitions are not exactly the same. The results obtained with the P_model (see par.D) are very different from all the other. Another point is to be mentionned : the correlation between optical efficiency and heat loss factor has decreases when a subsystem analysis is made (0.66 instead of 0.9).

E.2 SOLAR STORAGE WITH P_MODEL

To perform this, we have proceeded in the following way:

- We give in the column corresponding to the solar irradiation, the power measured after the external heat exchanger.
- We give in the column corresponding to the external temperature, the ambient temperature of the storage's rooms.
- We fix the parameter AC* to 1 and the parameter uc* to 0.

The identified parameters are (see par.D) :

. the heat loss factor of the solar tank Us, including the associated plumbing,
. the heat capacitance of the solar tanks Cs,
. the mixing factor Dl.

The data periods are one month, from september 92 to april 93. The data frequency is 6 minutes. The fit is repeated 8 times. The results are given in figure E.2.

month	Us (W/K)	Cs (MJ/K)	Dl (-)	obj (W)	dUs	dCs	dDl
sep-92	19.6	17.07	0.06	317	1.87	0.06	0.003
oct-93	31.3	16.85	0.02	153	1.4	0.05	0.001
nov-92	31.2	16.52	0.02	98	0.7	0.05	0.001
dec -92	28.9	16.74	0.01	82	0.5	0.05	0.001
jan-93	31.7	16.76	0.02	148	1	0.05	0.001
fev-93	30.5	16.87	0.02	198	1.2	0.06	0.002
mar-93	27.6	16.95	0.04	357	2.5	0.06	0.003
avr-93	27.8	16.88	0.06	329	2.7	0.06	0.003

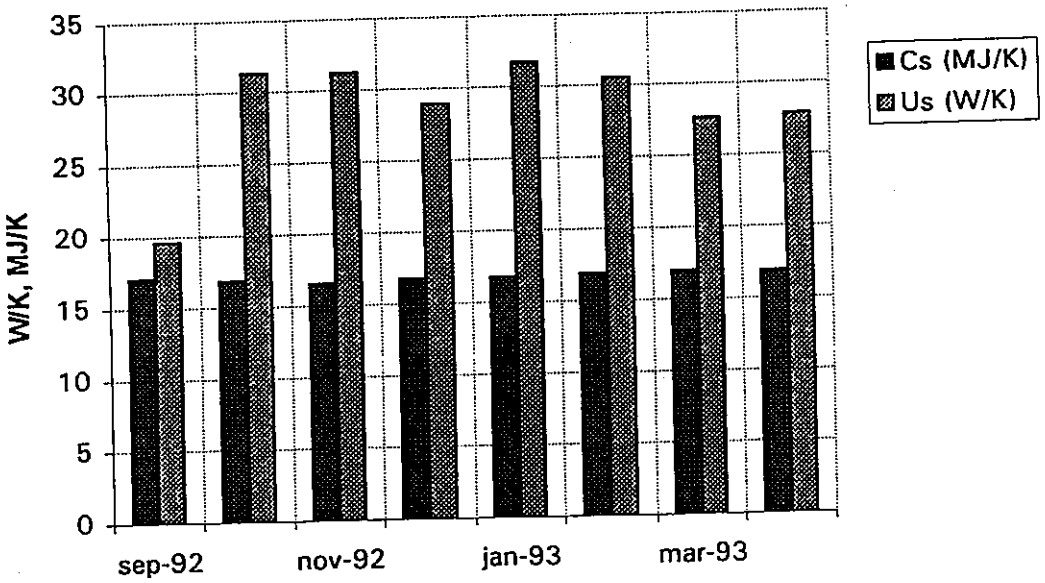

Figure E.2. Solar storage parameters from different monthly fits

F. TESTS OF DIFFERENT ALGORITHMS APPLIED TO DIFFERENT INSTALLATIONS

In this chapter, we test 3 different « dynamic fitting » programs to 3 different installations in order to evaluate the advantages of the DF program, specially the use of the filter and of the Discrete Fourrier Transform in the objective function.

F.1 THE 3 PROGRAMS

The 3 programs used are :

. DF (Dynamic Fitting), developed by the University of München (described in chapters C and D),

.LSFIT (Least Squares FIT), developped by the Geneva University, based on ref [C.4] and described in Annexe 3,

.SIMPLEX, available from MATLAB® library software.

OBJECTIVE FUNCTIONS

Two types of Objective Function (FO) have to be minimized :

. the sum of squared errors between model and measures (LSFIT and SIMPLEX)
. the filtered sum of squared errors between model and measures (DF), this needs to apply the (fast) discrete Fourrier transform to the residues (i. e. : at each step of the algorithm used to find the minimum of the FO) and then to apply a gaussien filter to the coefficient.

MINIMUM ALGORITHMS

Two algorithms are used to find the minimum of the FO :

. the Levenberg-Marquardt algorithm (DF and LSFIT), an improved gradient method (see chapter C and annexes),

. the SIMPLEX algorithm. This method has a geometrical naturalness. As mentionned in ref [C.4], page 326: « the downhill simplex method requires only function evaluations, not derivatives. It is not very efficient in terms of the number of function evaluations that it requires. ...However the downhill simplex method may frequently be the *best* method to use if the figure of merit is « get something working quickly » for a problem whose computational burden is small »

F.2 LARGE IN SITU COLLECTOR FIELD, MFC MODEL AND LSFIT PROGRAM

The data are exactly the same as those used in paragraph E.1, we only identify the parameters of the MFC model with our LSFIT program. The output of the program is :

```
NON LINEAR LEAST SQUARES ESTIMATION
A MINIMA has been found in  4 iterations.
Tolerance in the variation of chisquare : TOL= 1.0E-0003
Value of epsilon for the derivatives : EPS= 1.0E-0004

The sigma has been fixed to 1, the estimated standard deviation is given lower

Ninitial[1] = 500   Nfinal[1] = 10080
Total number of points used in the fit : 9581

The initial parameters are :
    Ceff       n0       a1
[kJ/K.m2]      [-]  [W/K.m2]
   32.7353     0.7114     6.7160

The parameters found and the value of chisquare are:

    Ceff       n0       a1
[kJ/K.m2]      [-]  [W/K.m2]
   31.8695     0.8129     5.1352

The following is the cross correlation matrix
the standard deviations are in the diagonal:
   Ceff     n0        a1
1.051284 0.21719  0.10863    Ceff
 0.21719 0.022823 0.93203     n0
 0.10863 0.93203  0.58841     a1
estimated sigma = 5987.1[W]
```

The parameters are very close to those obtained when using DF program, as seen in the table F.1, except for the heat loss factor K1. Note that the parameters found for MFC model and GAP model are very similar when identified with the standard least squares fit using Marquardt-Levenberg algorithm, in spite of the very different approach for the two models. In addition, the GAP model includes the external heat exchanger and has to identify a value for the heat transfer coefficient; the MFC model is applied before the external heat exchanger and then works with the temperature of the solar loop. The same number of parameters are identified, the heat loss coefficient is supposed constant in the GAP model (K2 set to zero).

MODEL + PROGRAM	eta0	k1	k2	kexch	Ceff	st. dev.
	[-]	[W/m2K]	[W/K2m2]	[kW/K]	kJ/m2K	[W/m2]
MFC + DF	0.82	3.6*	0.014	-	30.5	60
MFC + LSFIT	0.81	5.13*	-		31.9	30
GAP + LSFIT	*0.83*	*5.81**	-	*7.2*	*31.5*	*25*

* including plumbing (estimated to 1.8 [W/m^{2}K]).

Table F.1 : parameter values comparison for Comte Geraud collector field.

F.3 ITR TEST, MFC COLLECTOR MODEL, THREE PROGAMS

The data have been kindly sent by U. Frei and N. Findlater and correspond exactly to those described in ref [F.1]. The outdoor test facility built on the roof of the School Of Engineering in Rapperswil is used. The trackers allow a great deal of flexibility in test procedures. The temperature entering collectors is controlled by heating and cooling devices. The inlet temperature is varied as a function of time (here, a sine wave) to produce continuously varying conditions.
The data from 1 day are processed and correspond to sequence RF2_813 in ref [F.1]. The tested collector is single glazed, fin and tube absorber, 7 parallel tubes with manifolds. The day is « variable».

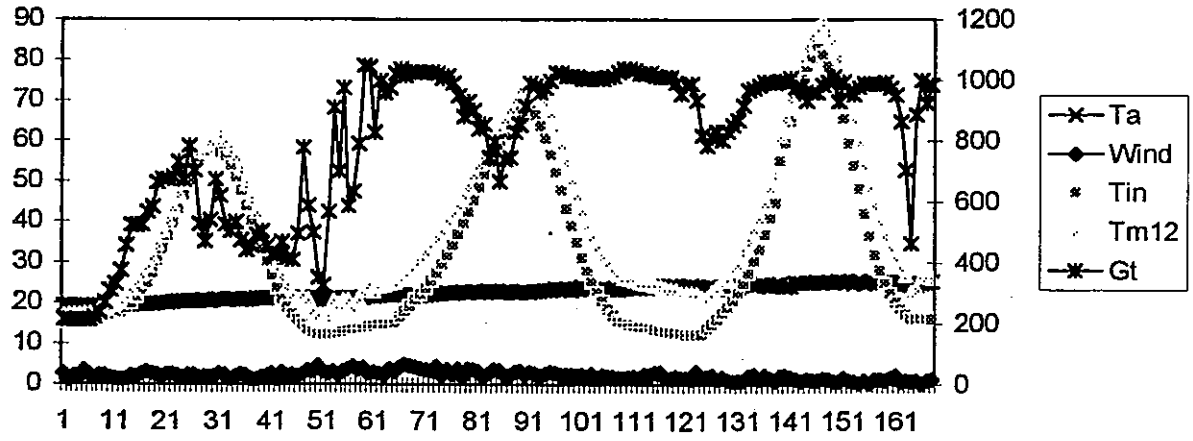

Figure F.1 : experimental conditions of sequence RF2_813, cf ref [F.1]

We reprocess the data with the MFC model and DF program. using the same conditions as given in ref [F.1] : skip time = 7500s and filter constant of 600 s. The result of DF are :

\Results DF V1.19á Feb 1992 (W. Spirkl) running 08.01.1993 11:26:44
\Value,Parameters,"Ceff=0.548 n0=0.783 a1=4.86 a2=0 Obj=0.163"
* External model \isakson\sim\exe\LE2DF_cv Per f'rsta f'rs"k med DF 1.19
Transform method..... Cosine

```
Numerical precision..... 1
Time base..... 1
Filter type..... Gaussian, tf=600
            Name   mode t_start  t_skip   t_end nFreq      Size
      RF2_813.MET   Mean   32400   39900   53010  256    63..167
    Ceff       n0       a1       a2 objective
 [kJ/K.m]      [-] [W/K.m2] [cW/K2.]      [C]
   0.548   0.7835    4.861        0  0.16334
   0.092  0.00572    0.661    0.453
Cross correlation matrix:
 1.0000000  0.0416418 -0.0669718  0.0644079
 0.0416418  1.0000000 -0.8035524  0.8628733
-0.0669718 -0.8035524  1.0000000 -0.9887565
 0.0644079  0.8628733 -0.9887565  1.0000000
```

These numbers are exactly the same as those given in ref [F.1].
The same set was processed with LSFIT and the output of the program is :

```
CONSTRAINED NON LINEAR LEAST SQUARES ESTIMATION
External Model in \isakson\sim\exe\LE2DF_cv.exe
Data in file RF2_813.met
A MINIMA has been found in  2 iterations.
Tolerance in the variation of chisquare : TOL= 1.0E-0003
Epsilon value for the derivatives : EPS= 1.0E-0004

The sigma has been fixed to 1, the estimated standard deviation is given lower

Ninitial[1] = 62   Nfinal[1] = 168
Total number of points used in the fit : 107

The initial parameters were :
   Ceff      n0      a1      a2
 [kJ/K.m2]     [-] [W/K.m2] [cW/K2.m2]
  0.5480  0.7835  4.8614  0.0000

The parameters found are:
   Ceff      n0      a1      a2
 [kJ/K.m2]     [-] [W/K.m2] [cW/K2.m2]
  0.5433  0.7833  4.8577  0.0000

The following is the cross correlation matrix
the standard deviations are in the diagonal:
  Ceff    n0    a1    a2
 0.0956  0.0347 -0.0551  0.0579   Ceff
 0.0347  0.0058 -0.8051  0.8636    n0
-0.0551 -0.8051  0.6713 -0.9885    a1
 0.0579  0.8636 -0.9885  0.4598    a2

Standard deviation =  0.08124[C]
```

Finally, the SIMPLEX-MATLAB program gives also good numbers when the initial parameters are not too far from the best ones, as shown in table F. 2. But, this method does not give any indication about errors on the parameter estimation.

program	Ceff kJ/m².K	ETA0 -	a1 W/m².K	a 2 cW/m².k²
DF	0.548±0.09	0.784±0.006	4.86±0.66	0±0.45
LSFIT	0.543±0.09	0.783±0.006	4.82±0.67	0.004±0.46
SIMPLEX	0.535	0.785	4.29	0.34

Table F.2 : estimated parameters from a the one day sequence RF2_813 (ref[F.1]) with 3 methods of Dynamic fitting.

As can be seen in table F2, the three methods give the same results. The fact that the SIMPLEX method works indicates that the data are very uncorrelated thanks to the sine wave and the solar tracker. Of course, more complete methods giving the error on the parameter estimation are preferable.

F.4 STUTTGART DATA, P_MODEL, THREE PROGAMS

The data have been sent by Th. Pauschinger, from the Institut für Thermodynamik und Wärmetechnik (ITW) of the Stuttgart University, ref [F.2]. The system under test is a typical forced circulation system with a 7.2 m² selective flat-plate collector and a 500l storage with an immersed heat exchanger at the bottom and an electrical auxiliary heater for the upper third of the storage, see ref [F.2]. Six sequences are available but we only present the results of sequence called « number 10 »; the other sequences leading to the same conclusions.

The sequence 10 was done from June 17 to June 24. The P_model is used for the entire system (see chap. D), 8 parameters have to be identified with the 3 programs tested.

The output of DFP is :

```
* RESULTS\SEQ10

\Results DF_P 2.3á Jan 94 @Copyright InSitu running 24.05.1994 08:36:54
\Value,Parameters,"AC*=5.48 uC*=9.74 US=4.52 CS=2.22 faux=0.566 DL=0.052 SC=0.00266 uC*v=0.0152
Obj=8.38"
* SDHW Plug Flow Model (V 2.1, Jun 1992)
Transform method..... Cosine
Numerical precision..... 1
Time base..... 3600
Filter type..... Gaussian, tf=4, CF=2E5
            Name   mode t_start  t_skip   t_end nFreq      Size
        DAT\SEQ10.D3   Mean      0  7.9083  192.04  256  372..1120
   AC*    uC*     US     CS   faux     DL     SC   uC*v objective
  [m²] [W/K/m²  [W/K] [MJ/K]    [-]    [-]    [-] [J/K/m3      [W]
  5.48  9.742  4.522  2.217 0.5658 0.05202 0.00266 0.01525    8.3787
 0.171  0.476    0.6 0.0884  0.023 0.0167 0.0413  0.249
Cross correlation matrix:
 1.0000  0.3656 -0.3771 -0.3223  0.2039  0.7347 -0.5970  0.1492
 0.3656  1.0000 -0.7251  0.3243 -0.1926  0.3985  0.1500 -0.6399
-0.3771 -0.7251  1.0000 -0.1621  0.0090 -0.5135  0.0303  0.1652
-0.3223  0.3243 -0.1621  1.0000 -0.7994  0.0306  0.7874 -0.6132
 0.2039 -0.1926  0.0090 -0.7994  1.0000 -0.1935 -0.6027  0.5472
 0.7347  0.3985 -0.5135  0.0306 -0.1935  1.0000 -0.1951 -0.0963
-0.5970  0.1500  0.0303  0.7874 -0.6027 -0.1951  1.0000 -0.4557
 0.1492 -0.6399  0.1652 -0.6132  0.5472 -0.0963 -0.4557  1.0000
```

The results of LSFIT are :

```
CONSTRAINED NON LINEAR LEAST SQUARES ESTIMATION
External Model in c:\iss2.3b\ds_p.exe
Data in file DAT\seq10.d3
A MINIMA has been found in 12 iterations.
Tolerance in the variation of chisquare : TOL= 1.0E-0003
Epsilon value for the derivatives : EPS= 1.0E-0004

The sigma has been fixed to 1, the estimated sigma is given lower

Ninitial[1] = 371   Nfinal[1] = 1121
Total number of points used in the fit : 751

The initial parameters were :
    AC*      uC*       US       CS      faux       DL       SC     uC*v
    [mý]  [W/K/mý]    [W/K]    [MJ/K]     [-]      [-]      [-] [J/K/m3]
  6.0000   8.0000   3.5000   2.2000   0.5800   0.1000   0.0000   0.2000

The parameters found are:

    AC*      uC*       US       CS      faux       DL       SC     uC*v
    [m²]  [W/K/m²]    [W/K]    [MJ/K]     [-]      [-]      [-] [J/K/m3]
  5.4788   9.4273   3.8977   2.2076   0.5745   0.0489   0.0000   0.4082

The following is the cross correlation matrix
```

the standard deviations are in the diagonal:

AC*	uC*	US	CS	faux	DL	SC	uC*v	
0.07130	0.24083	-0.11075	0.29813	-0.20747	0.36211	-0.75832	-0.15810	AC*
0.24083	0.11832	-0.19316	0.26455	-0.01158	-0.05047	0.02060	-0.54884	uC*
-0.11075	-0.19316	0.12459	-0.21087	0.09212	-0.29829	0.07180	-0.26516	US
0.29813	0.26455	-0.21087	0.02662	-0.61155	0.22168	-0.04926	-0.30594	CS
-0.20747	-0.01158	0.09212	-0.61155	0.00910	-0.45680	-0.05589	0.03191	faux
0.36211	-0.05047	-0.29829	0.22168	-0.45680	0.00635	0.05240	0.05363	DL
-0.75832	0.02060	0.07180	-0.04926	-0.05589	0.05240	0.01041	0.09151	SC
-0.15810	-0.54884	-0.26516	-0.30594	0.03191	0.05363	0.09151	0.08024	uC*v

The SIMPLEX program is not able to find the minimum of the least squares objective function, the number of parameters is too high : this method is clearly not efficient enough for a real case of system testing.

The table F.2 compares the parameters found :

Program	Ac* m^2	Uc* $W/K:m^2$	Us W/K	Cs MJ/K	faux	DL	SC	Uc*v J/K.m3
DFP	5.48	9.74	4.5	2.22	0.566	0.052	0.00266	0.0153
LSFIT	5.48	9.43	3.90	2.21	0.575	0.0489	0	0.408
ref [F.2]	5.52	10	3.91	2.21	0.578	0.0537	0	-

Table F.2 : Identified parameter comparison for the sequence 10 of Stuttgart data.

The two programs DFP and LSFIT give very comparable results, except for the heat loss factor where a small difference appears. The numbers given in the original paper by Th. Pauschinger using DFP are not the same as ours, obtained with the same program and the same data. This could be due to the convergence problem (we repeat each fit many times until the final results do not change at least the last 3 times).

F.5 CONCLUSIONS

These tests show the potentiality of dynamic fitting but also the fact that the exact objective function definition is of minor importance. In fact, the complexity of the objective function used by DF is not usefull, even for real cases with a lot of transcients, and leads both to time consuming and to superfluous mathematics.

REFERENCES

[F:1] Application of dynamic fitting to solar collector tests, U. Frei and N. Findlater, Expert meeting of IEA task XIV , Hameln, August 1992.

[F.2] Short report : application of the new draft of ISO 9459, Part 5 on a typical forced circulation solar domestic hot water system, Th. Pauschinger, Expert meeting of IEA task XIV , Arolla, August 1993 and Sevilla, january 1994.

G GENERAL CONCLUSIONS

We give here the more important conclusions.

We want to stress that the idea to use dynamics models to characterise solar systems is very good. Undoubtedly the time needed to characterise a system can be considerably decreased, and in addition in-situ test can be treated without requiring stationnary conditions.

The conclusions we present here come from the fits we have performed with our data (in-situ data). We have also used data kindly furnished by Thomas Pauschinger (system outdoor data) and Nigel Findlater & Ulli Frei (collector outdoor data). We have used to perform the fits the DF package (Munich University) and standard Least Squares (self programmed). Finally we have used different dynamic models where the principals are: P_model (system model) and MFC_model (collector model).

Our general conclusions are the following:

About the Estimator

We do not fully agree with the mathematical developement used. More precisely, we do not have found clear statistical or mathematical foundations to the objective function used by DF.

For all the performed tests, we have found that standard least squares yield good results for the parameters (in addition they are close those obtained by DF). Theoretical foundations are more satisficient than "it is good because it works", and will explain why and when it does not work.

We feel that it is not very wise to use a statistical package without having a background in this field. Moreover, a good knowledge in this field will yield to improve the utilisation of statistics and the optimisation of data collection.

About the search Method (the algorithm)

The fact that we use non linear models in the parameters forces to use an iterative algorithm. DF and LSFIT use the same approach, i.e. the Levenberg- Marquardt algorithm. But in addition DF performs some random jumps (the number is given by the NumOffLocMin option, the default being 5). These random jumps are dangerous because if you repeat your search several times with exactly the same conditions, you can converge to different results if you are dealing with a not very nice problem.

In addition we have found that the criterion that DF uses to stop the iterative procedure is not adequate to guarantee that a minimum has been found. For example, with P_Model and our data we have found that DF (=DFP) stops many times near the global without reaching it. The stop criteria is in fact a very difficult problem and needs some improvements in the DF program.

About the Models

In our work we have employed the P_model as a system model. With different periods of the year and time averages going from 2 minutes to 1 hour, we have found some problems to fit our data. We think that the first term in the equation of the P_model is not detailed enough to describe the collector parameters for all the systems for the following reasons:

. a system that has a collector inertia comparable to the storage inertia is not well explained by this model

. analysing the equation we can see that it will be very difficult to decorrelate the thermal loss collector parameters uc* and the thermal loss storage parameter US. The thermal loss storage coefficient is deduced from the storage temperature, and this same temperature is used for the collector thermal loss.

We have also employed this model as a Storage Model (see chapter E for the details). In addition, we have also worked with the MFC as collector model.

About the data

We have noticed that beside other problems arising when measuring in-situ is the fact that we do not have any way to vary the inputs in order to decorrelate the data.

About the possibility to use DFP for large systems

Even if dynamic fitting seems promising to check solar systems in a short period, we are not totally convinced by the DFP (DF with P_model) capability to test large systems. We have obtained very good results for the long term prediction **but the values of the physical parameters of the system obtained by DFP are not correct, rendering the in situ diagnostic very difficult or even wrong**. We think that a subsystem analysis is preferable because it is the only way, up to now, to obtain reliable values for the parameters. This subsystem analysis can use DF program with a good external collector model for the collector field subsystem and the DFP package for the storage tank subsystem, as seen in chapter E. However such an approach requires a heavier instrumentation.


IEA
INTERNATIONAL ENERGY AGENCY
Solar Heating & Cooling Programme